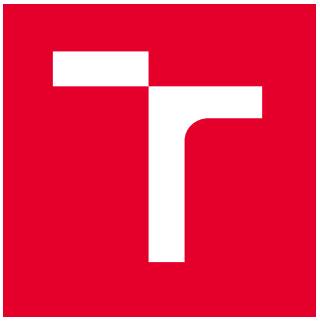

BRNO UNIVERSITY OF TECHNOLOGY

VYSOKÉ UČENÍ TECHNICKÉ V BRNĚ

FACULTY OF CHEMISTRY

FAKULTA CHEMICKÁ

INSTITUTE OF FOOD SCIENCE AND BIOTECHNOLOGY

ÚSTAV CHEMIE POTRAVIN A BIOTECHNOLOGIÍ

VALORIZATION OF LIGNIN ISOLATED FROM AGRICULTURAL WASTE

ZHODNOCOVÁNÍ LIGNINU IZOLOVANÉHO ZE ZEMĚDĚLSKÉHO ODPADU

DOCTORAL THESIS

DIZERTAČNÍ PRÁCE

AUTHOR — **Ing. Pavel Vostrejš**

AUTOR PRÁCE

SUPERVISOR — **prof. Ing. Adriána Kovalčík, Ph.D.**

ŠKOLITEL

BRNO 2025

BRNO UNIVERSITY OF TECHNOLOGY
FACULTY OF CHEMISTRY

Doctoral Thesis Assignment

Number of thesis:	FCH-DIZ0262/2024	Academic year: 2024/25
Institute:	Institute of Food Science and Biotechnology	
Student:	**Ing. Pavel Vostrejš**	
Study programme:	Biophysical Chemistry	
Study field:	no specialisation	
Head of thesis:	**prof. Ing. Adriána Kovalčík, Ph.D.**	

Title of Doctoral Thesis:

Valorization of Lignin Isolated from Agricultural Waste

Doctoral Thesis assignment:

1. To determine the antioxidant properties of lignin from agricultural waste, specifically grape seeds, rose hip seeds, plum shells, and cherry shells, and compare them with industrial lignin. Subsequently, the aim is to evaluate the impact of lignin on thermal and mechanical properties of polyhydroxyalkanoates (PHA) when used as an active green additive.
2. To measure the changes in molecular weight and dispersity of lignin modified using the fungi Fomitopsis pinicola, Lenzites betulina, and Phanerochaete chrysosporium, and to assess the resulting
3. To evaluate the impact of different solvent systems and their combinations on the formation of lignin nanoparticles, and to characterize the nanoparticles with a focus on their antioxidant and antimicrobial properties.
4. To systematically evaluate the adhesion properties of lignin based nanoparticles with polyelectrolytes on gold. The aim is to prepare lignin-based thin films with antioxidant and antimicrobial activities.

Deadline for Doctoral Thesis delivery: 18. 4. 2025

Doctoral Thesis is necessary to deliver to a secretary of institute in the number of copies defined by the dean. This assignment is part of Doctoral Thesis.

Ing. Pavel Vostrejš Student	prof. Ing. Adriána Kovalčík, Ph.D. Head of thesis	prof. RNDr. Ivana Márová, CSc. Head of institute

In Brno, 1. 9. 2024

prof. Ing. Michal Veselý, CSc.
Dean

Abstract

Lignin, the most abundant natural aromatic polymer and a major byproduct of paper production, holds significant potential as a renewable alternative to fossil-based raw materials. However, its inherent chemical heterogeneity poses considerable challenges for downstream processing. This PhD thesis focuses on isolating lignin from agricultural wastes using the soda pulping method, with particular emphasis on achieving high antioxidant activity. Among the various lignin sources, grape seed lignin exhibited the highest antioxidant properties and was subsequently used to modify polyhydroxyalkanoate (PHA) cryogels. Incorporation of 1% lignin enhanced the thermal stability and antioxidant capacity of the cryogels. Further, lignin samples were subjected to biotechnological modification using white-rot fungi. Although this treatment did not reduce the molecular weight, it resulted in a slight improvement in antioxidant properties. Lignin nanoparticles (LNP) were then prepared from the various lignin types, with an aqueous tetrahydrofuran (THF) solution proving to be the most effective. Surface modification was investigated by fabricating ultrathin films using QCM-D layer-by-layer assembly, with the highest LNP adsorption achieved using poly-L-lysine. These films exhibited both antioxidant and antimicrobial functionalities. Overall, this study demonstrates that lignin isolated from agricultural residues can be processed and further modified, highlighting its potential for integration into sustainable, high-performance materials.

Keywords

Lignin, nanoparticles, lignin ultrathin films, polyhydroxyalkanoates, cryogels, agriculture waste, white rot fungi, antioxidant activity, antimicrobial activity

Abstrakt

Lignin je nejrozšířenější přírodní aromatický polymer a hlavní vedlejší produkt při výrobě papíru. Lignin má významný potenciál jako obnovitelný zdroj alternativní k fosilním surovinám. Jeho přirozená chemická heterogenita však představuje značnou výzvu pro zpracování. Tato dizertační práce se zaměřuje na izolaci ligninu ze zemědělských odpadů metodou soda rozvlákňování s důrazem na dosažení vysoké antioxidační aktivity. Z porovnávaných typů ligninu vykazoval nejvyšší antioxidační aktivitu lignin získaný z hroznových semen, který byl následně použit, k modifikaci polyhydroxyalkanoátových (PHA) kryogelů. Začlenění 1 % ligninu zvýšilo tepelnou stabilitu a antioxidační kapacitu kryogelů. Dále byly vzorky ligninu biotechnologicky modifikovány pomocí hub s bílou hnilobou. Ačkoli tato úprava nesnížila molekulovou hmotnost, vedla k mírnému zlepšení antioxidačních vlastností. Z různých typů ligninu byly poté připraveny ligninové nanočástice (LNP), přičemž nejvhodnější analyzované rozpouštědlo byl vodný roztok tetrahydrofuranu (THF). Úprava povrchů byla zkoumána přípravou ultratenkých filmů pomocí QCM-D "layer-by-layer" metodou a nejvyšší adsorpce LNP bylo dosaženo použitím poly-L-lysinu. Tyto filmy vykazovaly jak antioxidační, tak antimikrobiální aktivitu. V souhrnu tato studie ukazuje, že lignin izolovaný ze zemědělských odpadů lze zpracovat a dále upravovat, což zdůrazňuje jeho potenciál pro integraci do udržitelných, pokročilých funkčních materiálů.

Klíčová slova

Lignin, nanočástice, ultratenké filmy z ligninu, odpad ze zemědělství, houby s bílou hnilobou, polyhydroxyalkanoáty, kryogely, antioxidační aktivita, antimikrobiální aktivita

VOSTREJŠ, Pavel. Valorization of Lignin Isolated from Agricultural Waste. Online, doctoral Thesis. Adriána KOVALČÍK (supervisor). Brno: Brno University of Technology, Faculty of Chemistry, 2025. Available at: https://www.vut.cz/en/students/final-thesis/detail/169457.

DECLARATION

I declare that my doctoral thesis was worked out independently and that the used references are quoted correctly and fully. The content of the above mentioned thesis is considered a property of BUT Faculty of Chemistry and all commercial uses are allowed only if approved by both the supervisor and the dean of the Faculty of Chemistry, BUT.

……
Student‘s signature

ACKNOWLEDGEMENT

The greatest thanks undoubtedly belong to my supervisor Prof. Adriána Kovalčík PhD, members of our team, Ing. Nicol Černeková and Ing. Radim Stříž, and colleagues Ing. Michal Kalina PhD, doc. Vojtěch Enev PhD, Leona Kubíková, Ing. Jan Hajzler PhD and Ing. Matěj Březina PhD. Special thanks go to my favourite colleagues from the Institute of Food Chemistry and Biotechnology, without whom my studies would have been significantly more difficult and far less enjoyable. Last but certainly not least, I want to thank my partner Karolína for endless encouragement, patience, and support.

CONTENT

1. INTRODUCTION

Global oil consumption has reached approximately 4.5 billion metric tons per year. Despite growing awareness of climate change and environmental pollution, most everyday products continue to be produced from fossil fuels. This reliance on non-renewable resources is unsustainable, particularly as the impacts of climate change, resource depletion, and pollution become increasingly apparent. In response, biobased and biodegradable materials have emerged as promising alternatives to reduce dependence on fossil resources, decrease greenhouse gas emissions, and mitigate environmental burdens associated with landfilling and marine pollution.

Among the renewable materials available, lignin stands out as one of the most promising candidates. As the second most abundant biopolymer on Earth, after cellulose, and the most abundant renewable aromatic polymer, lignin is produced in large quantities as a byproduct of pulping and biorefinery processes. However, its complex and heterogeneous structure poses significant challenges for processing and conversion into high-value products. Despite these challenges, lignin offers unique advantages compared to conventional oil-based materials, as its natural antioxidant, antimicrobial, and UV-shielding properties can be exploited in a range of applications, from food packaging and medical devices to sustainable building materials.

This PhD thesis aims to contribute to the advancement of sustainable material development by focusing on the isolation of lignin from selected agricultural wastes and evaluating its properties for various applications. Special attention is given to lignin-rich residues from grape and rose hip seeds, as well as plum and cherry shells, byproducts that are typically discarded but may serve as valuable feedstocks. The extracted lignin is analysed with an emphasis on solubility and antioxidant properties and is compared with commercial lignin samples. Furthermore, the work explores the preparation of lignin nanoparticles from these sources, which, with their defined size and regular shape, extend lignin’s potential for high-tech applications such as surface modification.

In addition, the thesis describes the fabrication of porous materials based on polyhydroxyalkanoates (PHA) without the use of halogenated solvents and their modification through blending with grape seed lignin. The study also investigates the biotechnological modification of lignin using white-rot fungi that produce lignolytic enzymes capable of cleaving lignin bonds, which is an alternative to chemical modifications of the lignin structure.

Overall, this thesis expands the understanding of lignin’s potential in sustainable material development by addressing both its processing challenges and inherent advantages. By exploring lignin from underutilized agricultural residues and testing novel strategies for its conversion and application, this work supports the transition toward bio-based solutions and a broader circular economy.

.

2. THEORETICAL SECTION

2.1 Biological function of lignin

Lignin is a natural, heterogeneous polymer primarily found in the secondary cell walls of vascular plants. These plants are distinguished by the presence of xylem tissue, which facilitates the transport of water and minerals [1]. The xylem is composed of cells known as tracheids and tracheae, whose secondary cell walls contain lignin. This lignin provides mechanical strength, water resistance, and structural cohesion, and it also contributes to resistance against biodegradation [2]. Together with hemicelluloses, lignin fills the spaces between cellulose bundles, giving lignocellulose its composite structure (Figure 1). Lignin is also present in cells of the conducting phloem and sclerenchyma tissue, which serve as the mechanical support of plants [3]. Since tree wood consists largely of xylem and secondary phloem tissues, lignin is abundantly present in plant biomass.

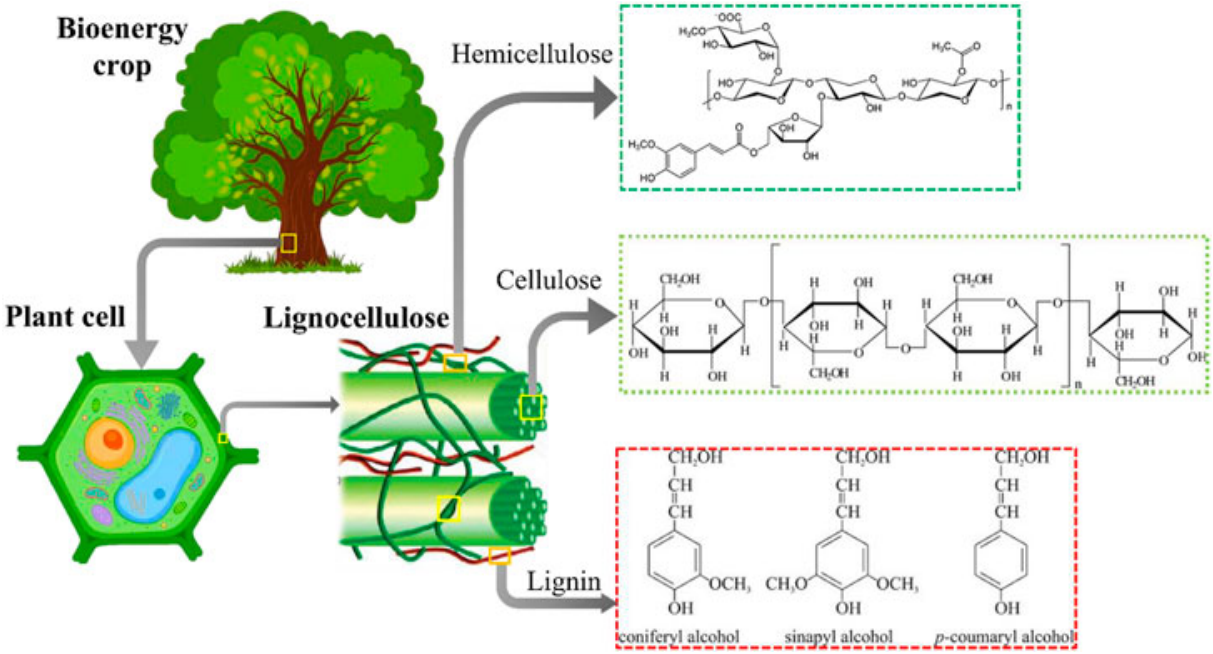

Figure 1 Schematic illustration of the lignocellulosic composition of wood, highlighting its main components: cellulose and hemicellulose as carbohydrate polymers, and lignin as an aromatic polymer [4].

The definition of lignin encompasses several criteria. Lignin is composed of phenylpropane units, known as monolignols, which are interconnected by carbon-carbon bonds, as well as ether and ester linkages. Although compounds such as lignans also meet these criteria, lignans differ from lignin in their low molecular weight [5]. A distinctive feature of lignin is its lack of optical activity, despite having multiple chiral centers. This results from the random formation of bonds between monolignols during lignin biosynthesis, which occurs via a radical mechanism independent of specific enzyme catalysts. Consequently, lignin forms a racemic mixture, a characteristic unusual for biopolymers. The structural heterogeneity of lignin also explains the challenge microorganisms face in degrading it, as the irregular primary structure makes it difficult for specific enzymes to evolve for its breakdown.

2.2 Structure and biosynthesis of lignin

Lignin is synthesized from three main precursors: p-coumaryl, coniferyl, and sinapyl alcohols (Figure 2). These precursors are produced in the cytoplasm through the shikimate and cinnamic acid pathways before being transported to the cell wall, where polymerization (lignification) occurs via a radical mechanism [6].

Lignification begins with the enzymatic dehydrogenation of monolignols, forming phenoxy radicals stabilized by resonance. This radical formation is catalysed by oxidative enzymes such as peroxidases and laccases. The resulting monolignol radicals undergo coupling reactions, leading either to the formation of dimers or further polymerization with growing lignin oligomers, ultimately generating a complex polymer with diverse intermolecular linkages [7].

Incorporation of phenylpropanoid precursors into the lignin structure gives rise to three main subunits: p-hydroxyphenyl (H), guaiacyl (G), and syringyl (S) (Figure 3). The relative abundance of these subunits varies depending on plant species, cell type, and environmental conditions. Conifers predominantly contain G subunits, while deciduous plants have a mixture of G and S subunits. In contrast, grasses incorporate all three subunits.

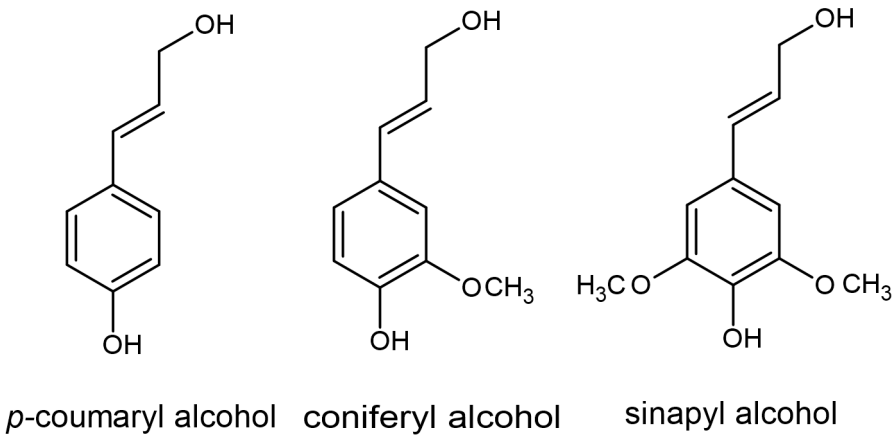

Figure 2 Structure of lignin phenylpropanoid precursors – monolignols

Unlike carbohydrates or proteins, lignin does not have a uniform primary structure with a single type of linkage. Instead, its subunits are irregularly interconnected, resulting in a highly complex and heterogeneous polymer [5]. Each plant species possesses specific regulatory mechanisms that influence lignin biosynthesis and allow for adaptation to environmental conditions. Due to this complexity, lignin cannot be accurately represented by a single structural formula.

Understanding the relationship between lignin's structure and its physicochemical properties is crucial for its effective utilization. The foundational concepts of lignin structure were first proposed in the 1950s by Erdam [8] and Freudenberg [9] but research into its structural details remains ongoing [5].

An exception among lignin types is catechyl lignin (C-lignin), a linear homopolymer composed exclusively of caffeyl alcohol units. It has been identified in the seed coats of *Vanilla planifolia* and several species within the Cactaceae family[10]. Compared to typical G/S

lignins, C-lignin exhibits a lower molecular weight, likely due to the reduced polymerization efficiency of caffeyl alcohol relative to guaiacyl or syringyl units. Structural analysis via all-atom molecular dynamics simulations has shown that C-lignin possesses a denser and more rigid three-dimensional structure. Owing to its uniform composition and well-defined linkages, C-lignin is considered a promising feedstock for biorefinery applications, especially for the production of high-value chemicals such as catechol, which serves as a precursor in pharmaceutical synthesis [11].

2.3 Lignin bonds

The basic structure of lignin consists of monolignol units interconnected by various C–C and C–O–C linkages, the presence of which has been confirmed through studies analysing lignin degradation products [6, 12]. The β-O-4 bond (aryl-propyl alcohol-β-aryl ether) is the most abundant linkage in lignin, comprising up to 65% of all bonds in hardwoods (Table 1). Notably, all three monolignol-derived subunits (H, G, and S) can participate in this type of bond formation [13].

Among carbon-carbon bonds, the most prevalent is the β-5 linkage, which connects the β-carbon of a phenylpropanoid unit to the fifth carbon of the aromatic ring in another subunit, forming the phenylcoumaran structure (Figure 3, structure B). This structure primarily exists in the trans conformation. While β-5 linkages are relatively rare in hardwoods, they occur more frequently in softwoods.

Other common lignin interunit linkages include α-O-4, 5-5, β-β′, 4-O-5, and β-1 bonds, each contributing to the complex and heterogeneous nature of lignin's polymeric structure.

Table 1 Common lignin interunit linkages and their relative abundance in hardwoods and softwoods [6]**.**

Linkage type	Substructure	Percentage content	
		Softwood	Hardwood
β-O-4	Phenylpropane β-aryl ether	45-51	60-65
β-5	Phenylcumaran	9-15	6
5-5‘	Biphenyl	9-11	2-5
α-O-4	Phenylpropane α-aryl ether	6-8	6-8
β-1	1,2-diarylpropane	7-10	7-10
4-O-5	Diphenyl ether	3-8	6
β-β′	Resinol	3	2-6

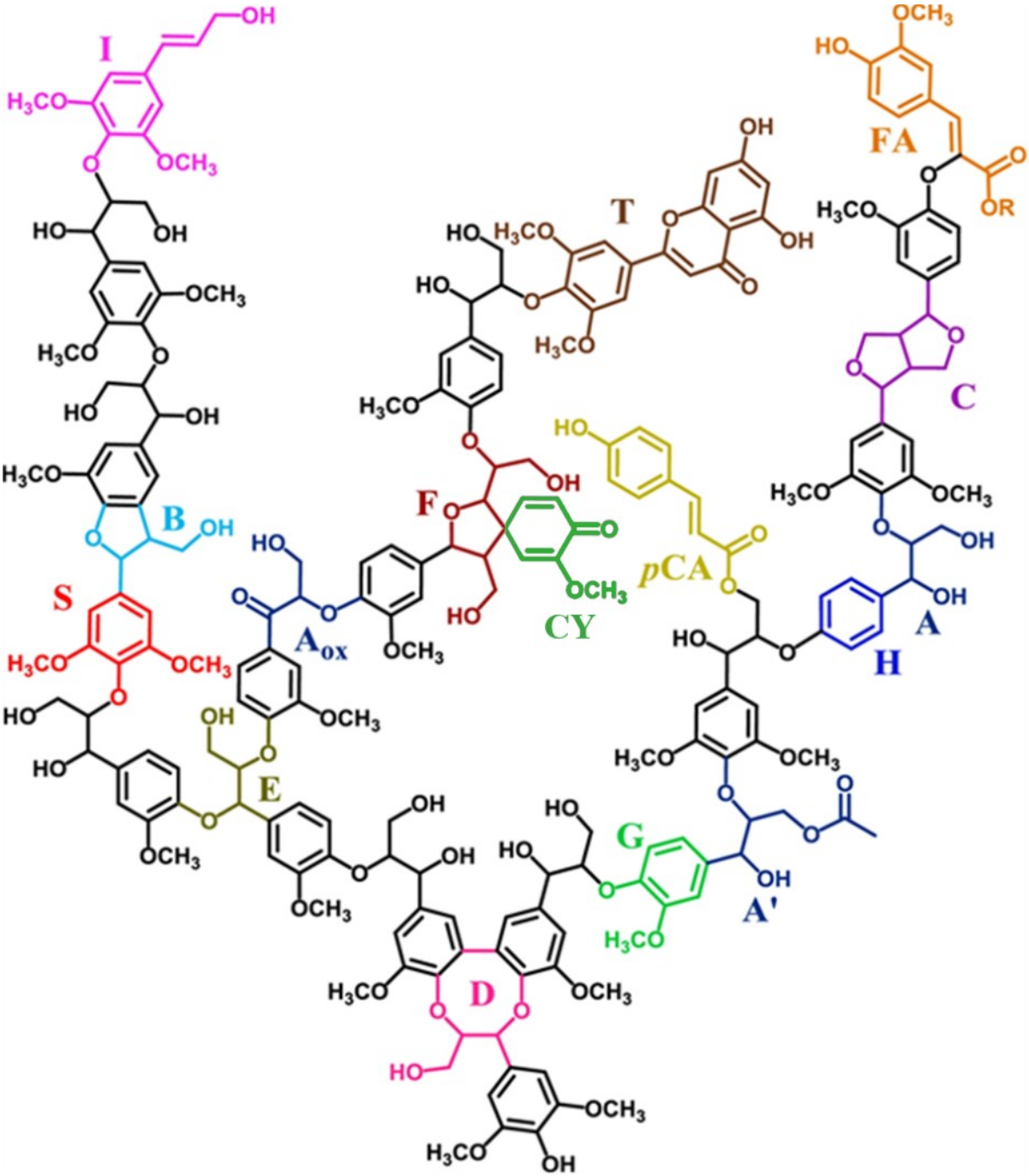

Figure 3 Representative lignin model illustrating the most frequently occurring structures and interunit linkages. G: guaiacyl unit; S: syringyl unit; A: β-O-4′alkyl-aryl ether; A′: β-O-4′alkyl-aryl-ether γ-acylated; Aox: β-O-4′alkyl-aryl-ether Cα- oxidized; B: phenylcumaran; C: resinol; D: dibenzodioxocin; E: α,β-diarylether; F: spirodienone; I: cinnamyl alcohol (or aldehyde); T: tricin; pCA: p-coumarate; FA: ferulate (R = H or arabinose) [14].

2.4 Function groups in lignin

Lignin contains various functional groups, including aliphatic hydroxyl, phenolic hydroxyl, carbonyl, carboxyl, methoxyl, and sulfonic groups [7]. The abundance of these groups influence lignin's chemical reactivity and overall properties. Moreover, functional groups play a crucial role in lignin modification and the development of high-value-added products.

A significant number of aliphatic and aromatic hydroxyl groups are present in lignin, with their content varying depending on the lignin isolation method. The determination of aliphatic hydroxyl content can be influenced by residual carbohydrates, which must be removed prior to analysis. Several techniques are used to quantify hydroxyl groups, including spectrophotometric methods in the UV region [15]. This approach relies on the differential absorption of phenolic units at 300 and 350 nm. Another widely used method is the modified Folin–Ciocalteu assay [16].

Additionally, hydroxyl group content can be assessed via conductometric or potentiometric titration [17], as well as Fourier transform infrared spectroscopy (FT-IR), which requires prior acetylation of hydroxyl groups. The presence of acetylated hydroxyls is then identified by characteristic absorption peaks at 1745 and 1765 cm^{-1} [18]. Nuclear magnetic resonance (NMR) spectroscopy is another precise technique for hydroxyl quantification [19].

Lignin also contains significant amounts of carbonyl and carboxyl groups. However, while carbonyl groups naturally occur in native lignin, carboxyl groups are predominantly formed during lignin degradation or chemical isolation processes. Carbonyl groups can be present as conjugated aldehydes or ketones on the propyl side chains, or as part of cyclohexadienone structures (Figure 3) [13]. Among the available analytical techniques, NMR spectroscopy is the most accurate and widely used method for determining both the type and abundance of carbonyl groups.

2.5 Lignin carbohydrate complex

In lignocellulosic biomass, lignin is closely associated with polysaccharides, forming the lignin–carbohydrate complex (LCC). The exact nature of this complex remains an area of active research, as native lignocellulose cannot be analyzed without some degree of structural alteration, making it difficult to precisely identify the linkages between lignin and carbohydrate components [20].

Harsh isolation conditions, such as high temperature, pressure, or extreme pH, can promote the formation of covalent bonds between lignin and carbohydrates. However, substantial evidence suggests that covalent linkages, particularly between lignin and hemicellulose, exist even in the native state [13, 21].

The primary types of covalent bonds linking lignin to carbohydrates include glycosidic, ether, and ester bonds [22], which are typically found at the α-carbon position and the C-4 position of the aromatic ring Figure 4 [21]. The most common interactions occur between lignin and hemicelluloses, such as xylan and glucomannan. The specific carbohydrate composition and the distribution of different types of linkages vary depending on the botanical origin of the biomass. Unlike hemicellulose, cellulose primarily interacts with lignin via hydrogen bonding, further contributing to the complexity of the LCC structure [23].

The presence of covalent linkages within the LCC plays a crucial role in lignin's biological functions. The rigid nature of lignin enhances the mechanical strength of the LCC system, while also contributing to microbial resistance and water repellency [21]. Although lignin is more

hydrophobic than cellulose, it remains significantly less hydrophobic than plant waxes due to the presence of hydroxyl and methoxyl groups. Water resistance in lignocellulose is primarily attributed to the cross-linked structure of the LCC, which limits swelling in aqueous environments. A higher degree of cross-linking results in increased hardness but also greater brittleness, as observed in nutshells [5].

Due to the complex structure and strong interactions within the LCC, isolating and separating its individual components remains a significant challenge. Efficient biorefinery strategies must be carefully designed to effectively process these complex substrates [22].

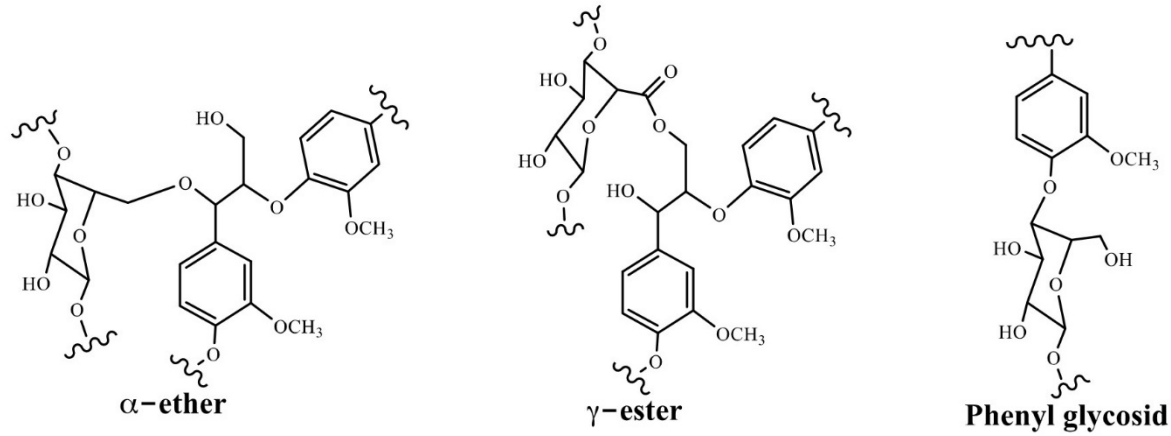

Figure 4 Common types of covalent bonds between lignin and polysaccharides [5]**.**

2.6 Lignin extraction methods

The extraction of lignin from lignocellulosic biomass is technically challenging due to its inherent resistance to chemical and biological degradation [24]. In nature, certain bacteria and wood-decaying fungi, including soft-rot, brown-rot, and white-rot fungi, possess the ability to degrade lignin within the LCC. A comprehensive overview of wood-degrading microorganisms has been provided by Asina *et al.* [25]. This microbial degradation is facilitated by ligninolytic enzymes, primarily laccases and peroxidases [26]. However, due to the complex and irregular structure of lignin, its biodegradation is relatively slow.

Lignin can also be extracted using various chemical processes that disrupt the bonds within the LCC, separating lignin from cellulose and hemicellulose. These extraction methods can be broadly classified into two main categories. The first category, delignification, involves dissolving lignin while leaving cellulose and hemicellulose in the solid phase [27]. The dissolved lignin is subsequently precipitated as a solid or recovered in the form of depolymerized lignin oil. The second category relies on the hydrolysis and dissolution of cellulose and hemicellulose, leaving lignin as an insoluble residue. Although these methods are not commonly used in industry, they serve analytical purposes, such as determining the total lignin content in a sample. The total lignin fraction measured using this approach is referred to as Klason lignin [28].

Industrial delignification processes are primarily employed in the paper and pulp industry, yielding technical lignin. These processes, collectively known as pulping methods, include the

Kraft process, sulfite pulping, soda pulping, and organosolv processes, which together account for the vast majority of lignin production (Figure 5).

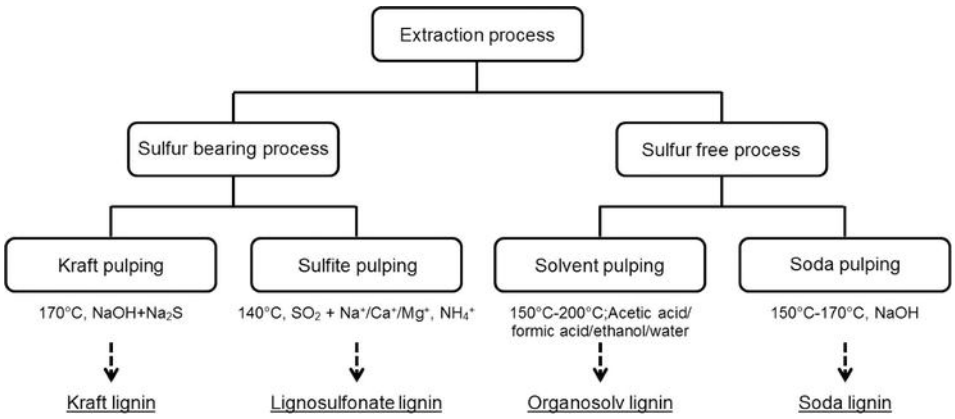

Figure 5 Classification of basic lignin isolation methods based on the use of sulfur compounds [29]**.**

2.6.1 Kraft lignin

The Kraft pulping process is the dominant method used in the pulp and paper industry. This process extracts the largest quantity of lignin, producing up to 14 million tons per year. However, the majority of this lignin is utilized as an energy source within the pulp production cycle, with only approximately 256,000 tons of Kraft lignin being marketed annually [30]. The main advantages of Kraft lignin include its high purity and relatively consistent properties across different batches, provided that it originates from the same type of wood.

Kraft lignin is obtained through the Kraft process, in which lignocellulosic biomass is boiled at temperatures up to 170 °C in an alkaline solution known as white liquor, which consists of NaOH and Na_2S [31]. The presence of HS^- ions in the white liquor enhances lignin solubility and promotes its depolymerization, while cellulose and hemicellulose remain largely insoluble. The resulting liquid containing dissolved lignin is referred to as black liquor.

Lignin can be further isolated from black liquor by acidification, which induces its precipitation. However, during this process, sulfur is incorporated into the lignin structure in the form of thiol groups, which may pose challenges if sulfur-free lignin is required for specific applications. The structure of Kraft lignin is classified as condensed lignin, meaning that it contains a high proportion of strong C-C bonds between lignin units due to condensation reactions occurring during pulping. This extensive condensation limits its depolymerization into smaller compounds [32]. Additionally, the Kraft process significantly cleaves aryl ether bonds, leading to a high content of phenolic hydroxyl groups. Under oxidative conditions, quinones, catechols, and carboxyl groups can also form [33].

A key advantage of Kraft lignin is its low ash and carbohydrate content (Table 2), which is achieved due to the high efficiency of the Kraft pulping process. A comprehensive review of current Kraft process modifications can be found in the work of Kienberger *et al.* [34].

Table 2 Characterisation of different types of technical lignin [29, 35]

Lignin type	Isolation conditions	Ash content (%)	Sugar content (%)	Sulfur content (%)	Molecular weight (kDa)	Poly-dispersity	Purity
Kraft	Alkaline	0.5-3.0	1.0-2.3	1.0-3.0	25	2.5-3.5	High
Lignosulfonates	Acidic	4.0-8.0	-	2.5-8.0	150	4.2-7.0	Low
Soda	Alkaline	0.7-2.3	1.5-3.0	0	15	2.5-3.5	Medium
Organosolv	Acidic	1.7	1.0-3.0	0	5	1.5	High

2.6.2 Lignosulfonate

Lignosulfonate is obtained through sulfite pulping, which is conducted at 130–180 °C in an aqueous solution of sulfite or bisulfite salts of sodium, magnesium, calcium, or ammonium. Several modifications of the sulfite process exist, operating under acidic, alkaline, or neutral conditions [36].

During sulfite pulping, both lignin-polysaccharide bonds and inter-unit lignin linkages are cleaved. However, the most significant reaction is sulfonation of the lignin aliphatic chain (

Figure 6), which determines the final properties of lignosulfonate. Sulfonation involves the incorporation of negatively charged sulfite or bisulfite ions into the lignin structure. Regardless of pH conditions, α-positions in the lignin structure undergo sulfonation, forming benzyl sulfonate. The presence of sulfonate groups significantly increases water solubility and prevents reprecipitation of lignin onto cellulose fibers [37].

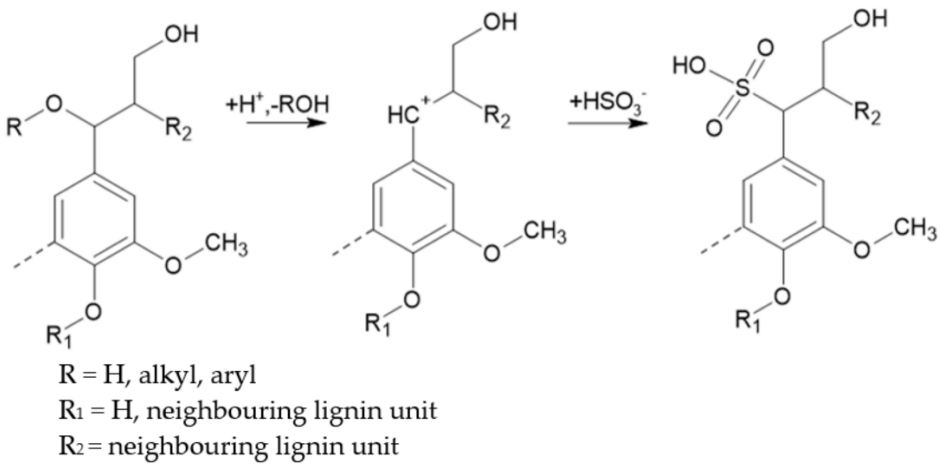

Figure 6 Mechanism of the lignin sulfonation reaction during acid sulfite pulping [38]**.**

Lignosulfonate can be extracted from spent pulping liquor using ultrafiltration, solvent extraction, or precipitation. The molecular structure of lignosulfonates varies depending on the isolation conditions. For example, sodium sulfite tends to produce longer-chain lignin, while calcium sulfite leads to a more compact structure [32]. In general, lignosulfonate is characterized by a high molecular weight, broad polydispersity, high ash content, and a sulfur content of up to 8%.

With the introduction of the Kraft process, the significance of sulfite pulping has declined, and it now accounts for less than 10% of industrial lignin production. However, lignosulfonate remains the most commercially available form of lignin, as most Kraft lignin is burned for energy within the pulping process [30].

2.6.3 Soda lignin

The soda process is the oldest method for pulping lignocellulosic biomass and is primarily used today for processing non-wood raw materials and agricultural waste, such as sugarcane bagasse, flax, straw, husks, and press residues [39]. Soda pulping operates similarly to the Kraft process, but without sodium sulfide (Na_2S). Due to the absence of a strong nucleophile, alkaline depolymerization is less efficient. However, a major advantage of soda lignin is its lack of sulfur contamination, making it more suitable for further applications [40].

During soda pulping, biomass is treated with concentrated sodium hydroxide (NaOH) at high temperature (170 °C) and pressure (10 bar). Lignin dissolves, forming a black liquor, from which it can be recovered by precipitation with CO_2 or HCl. As the pH decreases, lignin becomes more hydrophobic and precipitates [41].

Under alkaline hydrolysis, ether inter-unit bonds in lignin are cleaved, leading to a low content of β-O-4 bonds. The reaction of β-O-4 and β-5 bonds with NaOH produces vinyl ether structures and p-hydroxyphenyl units (Figure 7) [42]. Vinyl ether units are unstable and tend to undergo condensation reactions, but at the same time, fragmentation reactions lead to lower molecular weight lignin fractions compared to other pulping methods. If soda lignin is extracted from non-wood biomass, it may contain a higher proportion of carboxyl groups than lignin derived from wood [41].

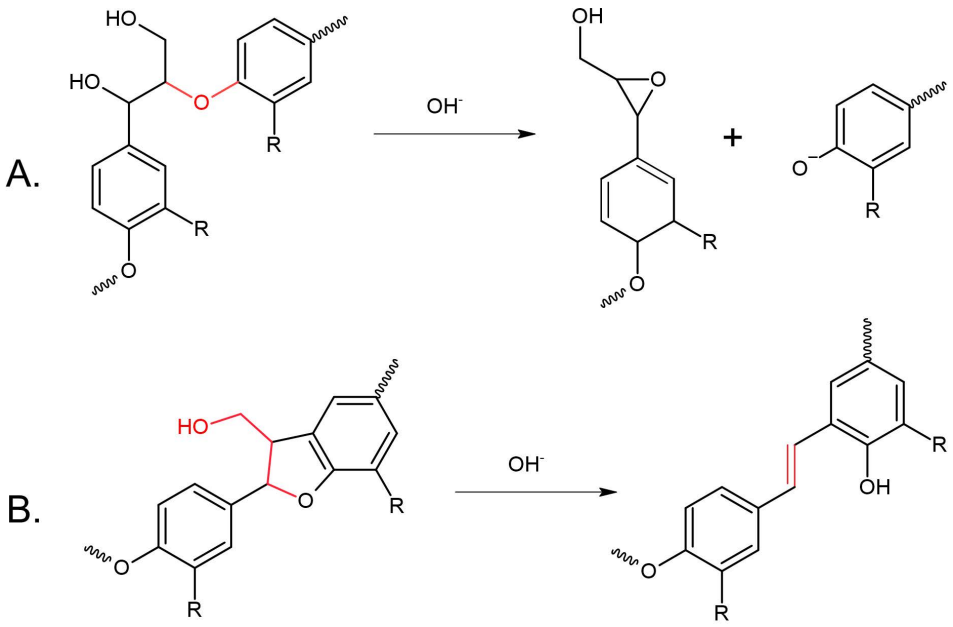

Figure 7 Reactions occurring during soda pulping: cleavage of β-O-4 (A) and β-5 (B) bonds under alkaline conditions [42]**.**

In alkaline conditions, NaOH also reacts with polysaccharides, leading to the dissolution of over 50% of hemicelluloses and 5–10% of cellulose into the black liquor [43]. Although soda pulping has a relatively low efficiency, its performance and selectivity can be enhanced by adding a strong oxidizing agent, such as anthraquinone [41]. Anthraquinone is thought to facilitate reductive cleavage of ether bonds while also minimizing carbohydrate degradation by acting as a redox mediator (quinone–hydroquinone cycle) [31, 44].

2.6.4 Organosolv lignin

The organosolv process enables the separation of lignocellulose into its main components: dissolved hemicellulose, solid cellulose, and precipitated lignin. This method yields highly pure lignin with less than 1% residual carbohydrates[40].

A variety of organic solvents are used in this process, including alcohols (methanol, ethanol, butanol), ketones (acetone), ethers (dioxane, tetrahydrofurfuryl alcohol), and polyols (glycerol, ethylene glycol) [45]. The process can also be catalysed using mineral acids (H_2SO_4, HCl, H_3PO_4) or organic acids (acetic, formic, oxalic acids) to enhance ether bond cleavage and the breakdown of LCC. However, these conditions can also promote condensation reactions, leading to the formation of new carbon-carbon bonds. Conventional organosolv pulping is typically carried out at 100–250 °C for 30–90 minutes, using aqueous solutions of organic solvents at varying concentrations.

For effective delignification, the solvent mixture should have a Hildebrand solubility parameter of approximately 23 ± 2 $MPa^{1/2}$, which corresponds to lignin's solubility parameter. This value represents the total intermolecular forces within a substance and is commonly used to predict solvent-polymer interactions. A substance dissolves in a given solvent when their solubility parameters are sufficiently close [46]. The Hildebrand parameter is critical in lignin dissolution, as the solvent mixture facilitates both the diffusion of catalysts or reagents through the polysaccharide matrix and the extraction of soluble lignin fragments into solution[47].

The key advantages of the organosolv method include its sulfur-free process, preventing sulfur contamination of the lignin, and the production of low molecular weight lignin (~5 kDa) [48]. However, despite the potential for solvent recovery due to the low boiling points of many organic solvents, organosolv pulping is not widely used. This is primarily due to its high energy demands, as well as the technical challenges associated with corrosion risks in process equipment. Currently, organosolv lignin is commercially available on a pilot scale [30].

It is important to note that technical lignins differ structurally from native lignin in plants due to chemical modifications during isolation. As a result, their properties also deviate from those of native lignin [32, 49].

2.7 Lignin properties

2.7.1 Antioxidant properties

Lignin belongs to the class of polyphenols, which are known for their antioxidant activity. This property arises from its molecular structure, which has been extensively studied in relation to

antioxidant mechanisms. It is widely accepted that free phenolic hydroxyl groups, methoxy groups, aliphatic hydroxyl groups, and double bonds in the side chains contribute to lignin's antioxidant activity [41]. In contrast, carbonyl groups in the aliphatic chain have a negative effect [50]. The relative contribution of these structural features to antioxidant activity follows the order proposed by Nsimba *et al.* [51], with phenolic hydroxyl content being the most critical determinant [52].

Hydroxyl groups act as proton donors for free radicals and are stabilized through quinone resonance structures (Figure 8). The detailed mechanism of antioxidant reactions has been described in literature [53].

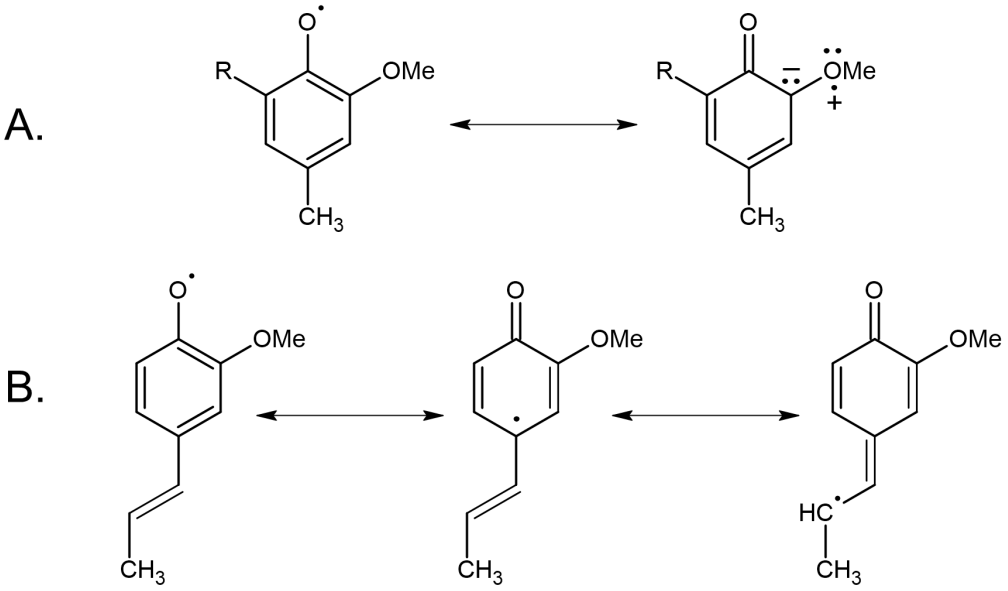

Figure 8 Resonance stabilization of the phenoxy radical by the ortho methoxy group (A) and conjugation with C=C bonds in the side chain (B) [54]**.**

Studies confirm that total polyphenol content correlates with antioxidant activity [55], but it is not the only determining factor. Other influential parameters include structural heterogeneity, molecular weight, purity, and polydispersity of lignin [56, 57]. Contamination with hemicelluloses negatively affects antioxidant activity, as hydrogen bonding between hemicellulose and lignin's hydroxyl groups reduces the availability of free hydroxyls [40]. The extent of hemicellulose contamination is strongly influenced by isolation conditions. For example, acid purification steps in a study by García *et al*. [55] educed the hemicellulose content but also decreased the total polyphenol content and antioxidant activity.

Another key factor is molecular weight [58]. Lignin with lower molecular weight exhibit higher antioxidant activity, primarily due to the formation of additional hydroxyl groups during depolymerization. Conversely, condensation reactions negatively impact antioxidant properties.

Technical lignin displays variable physicochemical properties, and extraction methods significantly influence their antioxidant potential, even when the same substrate is used [55, 59,

60]. Moreover, lignin obtained from different raw materials, such as sawdust and agricultural residues, exhibit different antioxidant behaviours due to structural variations [61].

The pH of lignin precipitation during extraction also affects its antioxidant activity. For example, a study comparing Kraft lignin and lignosulfonate extracted at different pH values showed that Kraft lignin exhibited the highest antioxidant activity at pH 6, whereas lignosulfonate reached its peak at pH 2. While both lignin ultimately achieved similar antioxidant levels, their activity varied by up to 35% depending on pH [62].

Studies on lignin fractionation reveal that increased solubility correlates with reduced antioxidant activity. This trend is attributed to a decrease in phenolic hydroxyl and methoxy group content, both of which stabilize free radicals [60].

Antioxidant activity of lignin has attracted significant interest in various fields, particularly as a natural additive. Potential applications include: i) food industry – protection against lipid oxidation [63], ii) cosmetics and pharmaceuticals – formulations for oxidative stress reduction, iii) polymeric materials – slowing down oxidation or photodegradation in polymer composites.

Lignin's role in polymer stabilization has been investigated in blends with polypropylene and polyethylene [64, 65]. In biopolymers, its effects have been studied in mixtures with starch [66], poly-3-hydroxybutyrate (P3HB) [67, 68] and polylactic acid (PLA) [57, 69]. Research suggests that incorporating small amounts of lignin (<10%) optimizes antioxidant performance without compromising material properties.

Free radicals pose a threat to cellular integrity, leading to DNA damage. Studies have shown that lignin prevents DNA strand breaks induced by H_2O_2 [70]. Additionally, lignin-based biomaterials are being explored for scaffold fabrication in tissue engineering [71]. However, while higher lignin concentrations enhance antioxidant effects, they can also induce cytotoxicity. Thus, it is essential to balance lignin concentration and biocompatibility for safe medical applications.

2.7.2 Antimicrobial properties

Lignin's antimicrobial activity is closely linked to its molecular structure, particularly the composition of its side chains and functional groups. The presence of double bonds in the α, β positions of the side chain, as well as methyl groups in the γ position of phenolic fragments, likely contributes to its antimicrobial properties [72, 73]. In contrast, the presence of carbonyl, carboxyl, and hydroxyl groups on the side chain reduces antimicrobial efficacy [74]. However, the available literature does not provide definitive conclusions regarding lignin's antimicrobial activity, and further detailed research is needed to better understand the properties of different lignin types.

A study on lignin obtained as a by-product from bioethanol production reported no antimicrobial activity against Gram-negative bacteria (tested on *Escherichia coli* a *Salmonela enteritidis*) [75]. However, this lignin exhibited inhibitory effects against Gram-positive bacteria (*Listeria monocytogenes* and *Staphylococcus aureus*) and yeasts (*Candida lipolytica*). The most significant effect was observed against *S. aureus*, with a minimum inhibitory concentration (MIC) of 1.25 $mg \cdot mL^{-1}$.

Similar findings were reported for demethylated lignin, which demonstrated antimicrobial activity against *S. aureus* in a study focused on lignin-based polyurethanes [72]. In another study investigating lignin for textile applications, lignin isolated from sugarcane bagasse showed antimicrobial effects against *Staphylococcus epidermidis*, with MIC and minimum bactericidal concentration values of 4.10 mg/mL and 8.19 mg/mL, respectively [76].

While lignin has often been considered effective only against Gram-positive bacteria, likely due to their lack of an outer membrane, some exceptions have been reported. Lignin extracted from oil palm fruit pomace exhibited antimicrobial activity against both Gram-positive (*Bacillus subtilis* and *S. aureus*) and Gram-negative (*E. coli* and *Salmonella typhimurium*) bacteria [77].

The effects of lignin on yeasts and fungi remain inconsistent. In one study, lignin from oil palm fruits showed no inhibitory effect against the yeast *Candida albicans* or the fungus *Aspergillus niger* [77]. However, another study demonstrated that lignin isolated from apple wood inhibited *A. niger* by slowing fungal growth and altering colony morphology [78]. A strong inhibitory effect was also observed against *Saccharomyces cerevisiae*. A comprehensive review of lignin's antimicrobial properties can be found in [72].

Beyond its intrinsic antimicrobial effects, lignin can be chemically modified to enhance its bioactivity. One of the most studied approaches involves combining lignin with antimicrobial agents, such as silver nanoparticles [79]. This combination has shown high antimicrobial efficacy, with the mechanism of action attributed to silver nanoparticles binding to sulfur atoms in membrane proteins, leading to cell membrane damage and loss of function [74]. The effectiveness of lignin-silver nanoparticle composites has been confirmed in multiple studies [80–82].

2.8 Strategy for Lignin Utilization

Currently, approximately 1.65 megatons of commercial technical lignin are produced annually, excluding the portion used for energy generation [83] (Figure 9). As the demand for sustainable materials grows, research and industrial efforts focus on utilizing lignin in two main ways.

The first approach involves using lignin as a macropolymer in the production of polymer composite materials, where it enhances mechanical strength, thermal stability, antimicrobial and antioxidant properties, or biodegradability. It has been studied in blends with conventional polymers such as polypropylene [84], polyethylene [85], polystyrene [86], polyurethanes [87], and acrylonitrile butadiene styrene [88], as well as with bioplastics like starch [89], PHA [90–93], and PLA [94, 95]. Additionally, macropolymer lignin can serve as a substitute for phenol in phenol-formaldehyde resins [96, 97]. However, a key drawback of macropolymer lignin is its variability in properties, which depends on both the feedstock and the isolation method.

The second approach involves processing lignin within a biorefinery system, enabling its conversion into valuable chemicals, fuels, and functional materials.

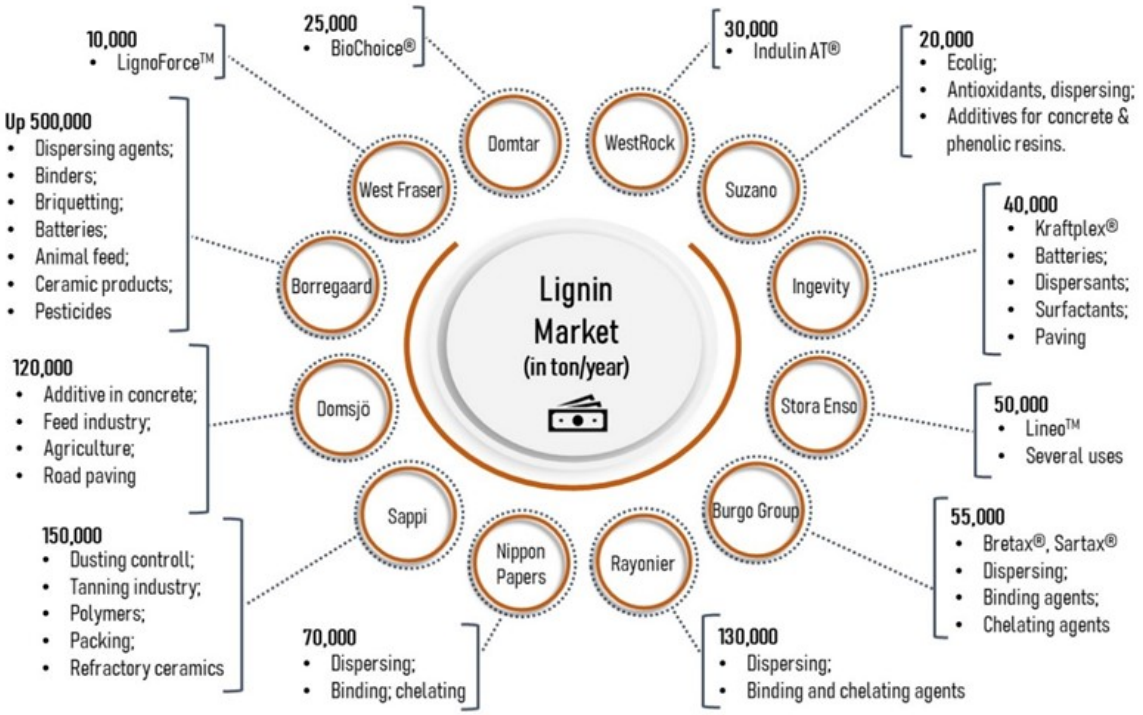

Figure 9 Overview of commercial lignin producers and their applications [98]**.**

2.8.1 Lignin biorefinery

Lignin biorefinery involves the depolymerization of lignin into low-molecular-weight compounds [99]. Due to its abundance and unique aromatic structure, lignin is considered one of the most promising biopolymers for the production of high-value chemicals. However, effective lignin valorization requires breaking down the complex macromolecular structure into more uniform oligomeric and monomeric aromatic compounds, which can then be processed into commercially valuable products [100] (Figure 10).

Currently, lignin depolymerization is pursued through two main approaches: thermochemical and biochemical methods (Figure 11). Thermochemical methods include hydrolysis, pyrolysis, gasification, hydrogenolysis, and chemical oxidation [101]. These techniques offer high efficiency and short reaction times but require harsh conditions, which are both costly and often lead to non-selective degradation of lignin bonds. In contrast, biochemical methods operate under mild reaction conditions and achieve greater specificity through enzymatic hydrolysis. However, their efficiency remains significantly lower compared to thermochemical approaches.

In thermochemical methods, lignin is first dissolved in organic solvents and then depolymerized at high temperatures and pressures, often in the presence of metal catalysts. Noble metal catalysts such as ruthenium (Ru), rhodium (Rh), palladium (Pd), and platinum (Pt) are commonly used [102]. Redox catalysts play a crucial role in stabilizing lignin fragments by suppressing repolymerization and the formation of condensed lignin structures, thereby increasing the overall yield of monomers.

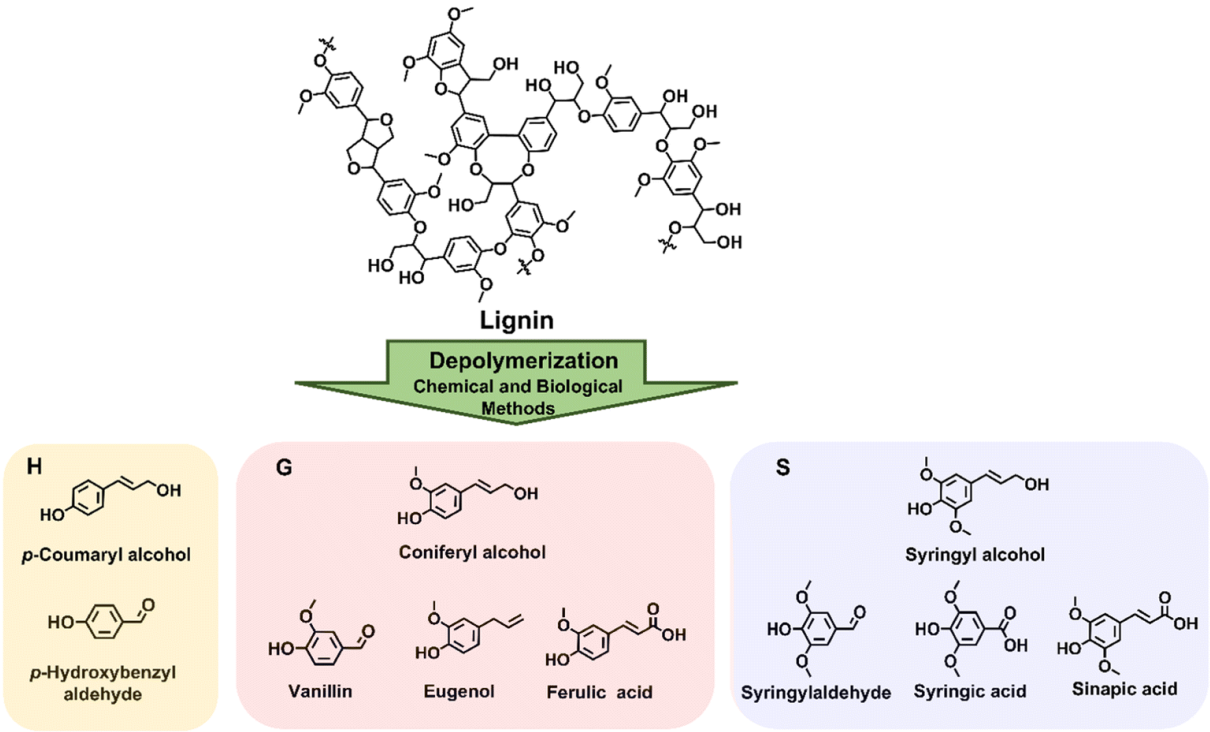

Figure 10 Schematic representation of lignin depolymerization into high-value, low-molecular-weight compounds. The products are categorized based on their originating monolignols [103].

Biochemical methods for lignin degradation rely on wood-degrading fungi and certain bacteria. Although bacteria are generally less efficient in lignin decomposition than fungi, they have been widely studied due to their greater environmental adaptability, shorter growth cycles, and ease of genetic modification [104]. Bacterial species capable of degrading lignin include *Actinomycetales, α-Proteobacteria* a *γ-Proteobacteria* [105].

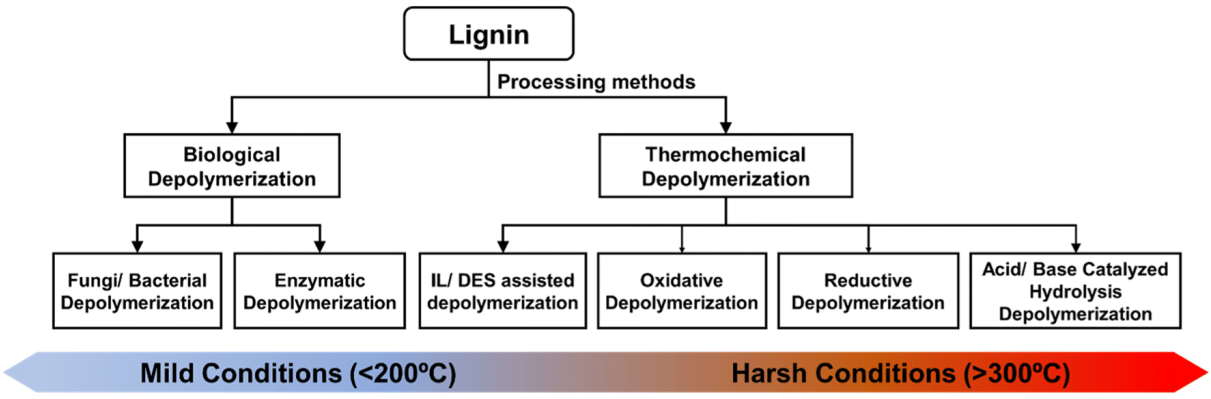

Figure 11 Schematic classification of basic lignin depolymerization methods [103]

Among fungi, white-rot, brown-rot, and soft-rot fungi are the primary decomposers involved in natural wood decay [106]. White-rot fungi, belonging to *Basidiomycetes*, are the most efficient lignin-degrading microorganisms in nature and, so far, the only known species capable of completely degrading lignin [107].

Microorganisms utilize enzymes to degrade lignin and LCC. These enzymes are classified as metalloproteins, primarily peroxidases and laccases. Unlike ligninolytic peroxidases, which

require hydrogen peroxide as an electron acceptor, laccases use molecular oxygen, releasing only water as a byproduct. This mechanism offers advantages for potential applications in lignocellulosic biorefineries due to its simplicity and lack of peroxide dependence [108].

Laccase

Laccase, a polyphenol oxidase belonging to the multi-copper oxidase family, has a molecular weight ranging from 60 to 70 kDa [109]. It consists of approximately 500 amino acid residues and features three copper-binding sites [110]. These sites include four copper ions: a single type I Cu^{2+} (T1Cu), a single type II Cu^{2+} (T2Cu), and two type III Cu^{2+} (T3Cu). These ions form three-dimensional copper clusters that serve as active centers with specific configurations (Figure 12) [106].

Laccase has low redox potentials and can oxidize phenolic and non-phenolic compounds, generating reactive radicals. The enzyme's activity is pH-dependent, with optimal activity occurring at acidic pH values [111]. Laccase-catalysed reactions follow a redox mechanism in which electrons are sequentially transferred between the four copper atoms. The three active centres facilitate electron transfer from the substrate to oxygen molecules, ultimately reducing oxygen to water [112].

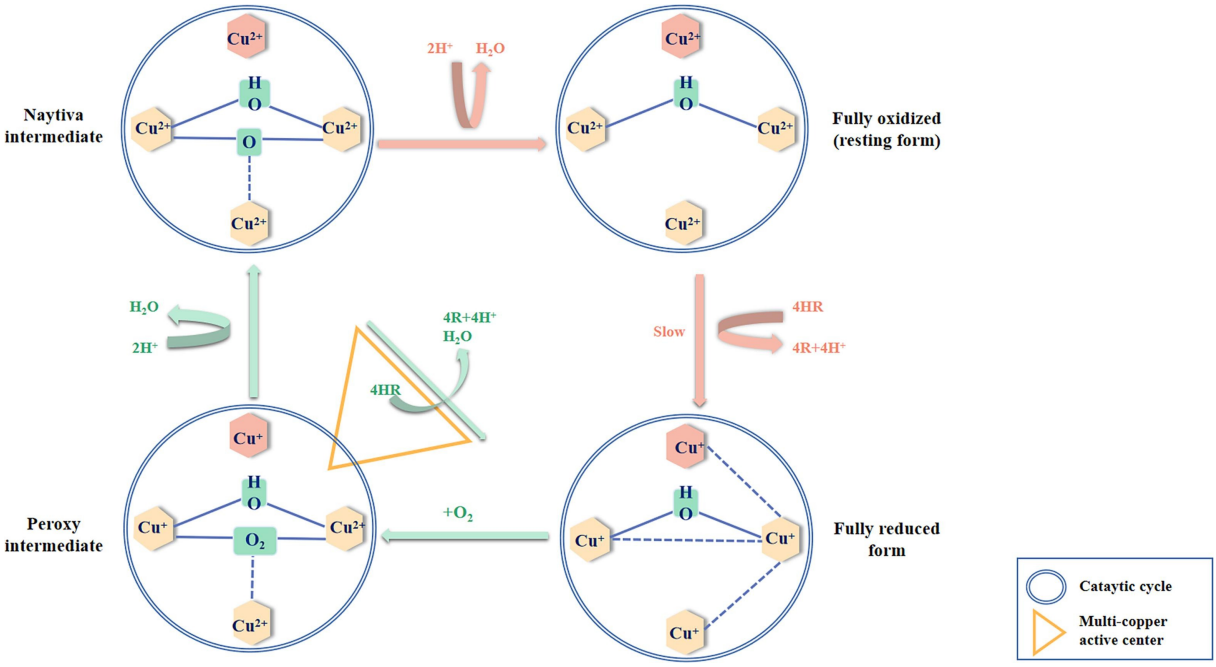

Figure 12 Laccase-catalysed reactions mechanism of lignin oxidation [106].

Laccase can degrade both phenolic and non-phenolic lignin compounds, with oxygen serving as the final electron acceptor [113]. The oxidation of phenolic substrates generates phenoxy radicals, which act as unstable intermediates. These radicals promote oxidative cleavage at the Cα position, cleavage of alkyl-aryl bonds, and breakdown of Cα-Cβ bonds, contributing to lignin depolymerization [114].

Lignin peroxidase

Lignin peroxidase (LiP) is a hydrogen peroxide-dependent glycoprotein with a heme prosthetic group and a molecular weight of approximately 38–43 kDa [115, 116]. Compared to laccases and manganese peroxidase, LiP exhibits a significantly higher redox potential, enabling it to oxidize non-phenolic aromatic compounds even in the absence of a mediator. The reaction catalysed by LiP is illustrated in Figure 13A [111].

Lignin peroxidase mediated lignin degradation generally consists of one oxidative and two reductive steps. In the first step, the ferric ion Fe^{3+} in the active site is oxidized, forming a compound I (LiPI) oxo-ferryl intermediate, while hydrogen peroxide is simultaneously reduced to water [117].

In the second step, LiPI is reduced by a substrate (S), which donates one electron, generating a compound II intermediate (LiPII) containing Fe^{4+}, and free radical ($S^{\cdot}$). In the final step, LiPII is further reduced by a second substrate molecule, restoring LiP to its resting ferric oxidation state and completing the oxidation cycle [106, 118].

At low substrate concentrations and in the presence of excess hydrogen peroxide, compound II can be irreversibly converted into an inactive enzyme form due to LiP's high reactivity with peroxide [119]. However, inactivation can be prevented by the presence of aromatic stabilizers such as veratryl alcohol or tryptophan.

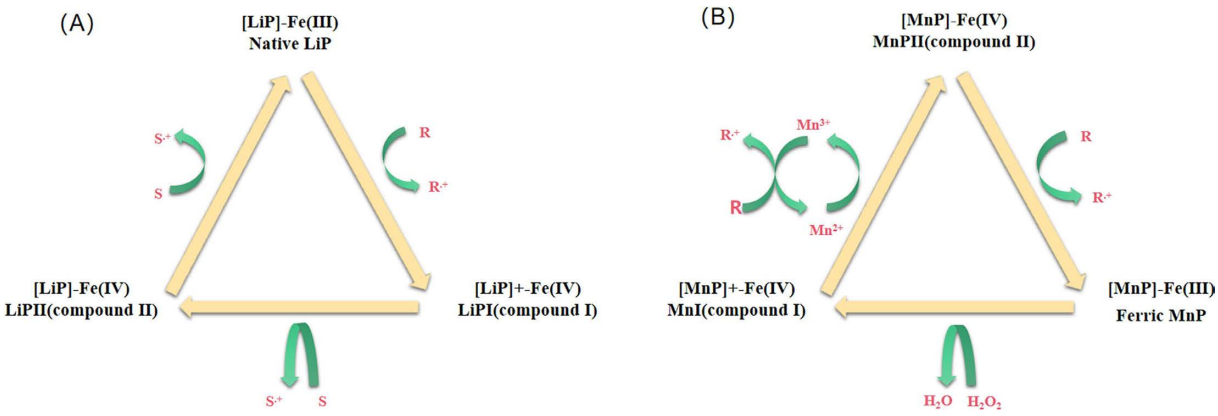

Figure 13 Mechanism of the lignin depolymerization process as mediated by lignin peroxidase (A) and manganese peroxidase (B) [106]**.**

Manganese-dependent peroxidase

Manganese-dependent peroxidase (MnP) is a glycosylated heme-containing oxidase with a molecular mass of approximately 40–50 kDa. It is the most commonly produced lignin-modifying peroxidase, secreted by nearly all wood-degrading basidiomycetes and some bacteria [111]. Structurally, MnP shares similarities with LiP, but it differs in its manganese ion content, heme propionate, and side chains. Unlike other peroxidases, MnP exclusively relies on a one-electron oxidation mechanism involving Mn^{2+} as the primary substrate [120]. MnP requires an acidic pH range for optimal function.

In the first step of the catalytic cycle, hydrogen peroxide reacts with MnP in its Fe^{3+}, leading to the formation of MnP compound I and the release of one water molecule (Figure 13B). In the second step, Mn^{2+} is oxidized to Mn^{3+} in the presence of chelators such as oxalate or malonate, forming MnP compound II. These chelators stabilize Mn^{3+} and enhance enzyme activity [121].

The Mn^{3+} chelator acts as a diffusible oxidant for phenolic compounds, allowing oxidation to occur beyond the enzyme's active site. This oxidation process generates phenoxy radical intermediates, which subsequently lead to the cleavage of lignin bonds and the formation of various degradation products [111].

Lignin bioconversion

The enzymatic cleavage of lignin's complex structure enables its bioconversion into valuable products such as vanillin, *cis,cis*-muconic acid, microbial lipids, PHA, furfural, and other industrially relevant compounds [114, 122].

One of the most important products derived from lignin bioconversion is vanillin (4-hydroxy-3-methoxybenzaldehyde). Vanillin is widely used in the cosmetics, pharmaceutical, and food industries, as well as in battery technology [122, 123]

Traditionally, vanillin is obtained from natural plant sources or synthesized chemically, but its biosynthesis from lignin offers a cleaner and more sustainable alternative. During lignin metabolism, vanillin can be released through depolymerization or synthesized from ferulic acid via microbial catalysis[124].

Many microorganisms have demonstrated the ability to convert lignin into vanillin; however, the yields remain limited. Therefore, genetic modification is often required to optimize this bioconversion. Vanillin can be produced using various bacterial strains as well as fungi such as *Phanerochaete chrysosporium* [125].

Cis, cis-muconic acid (*Cis, cis*-MA) is a dicarboxylic acid primarily used in the production of polymers, including nylon, polyurethane, and polyethylene terephthalate [114]. Conventionally, *Cis, cis*-MA is synthesized chemically from petroleum-based feedstocks. However, an environmentally friendly alternative involves lignin bioconversion via microbial catalysis.

Lignin-derived aromatic compounds can be directly converted into *Cis, cis*-MA through microbial metabolism. Additionally, intermediates from glucose metabolism (e.g., 3-dehydroshikimate) can be redirected toward *Cis, cis*-MA production through genetic modifications. The use of transgenic bacteria is often necessary to enhance this bioconversion process [126, 127].

Similarly, other dicarboxylic acids, such as pyridine-2,4-dicarboxylic acid and pyridine-2,5-dicarboxylic acid, can be synthesized using engineered microorganisms [114].

Lignin can also be bioconverted into microbial lipids, which are produced by oleaginous microorganisms through the catabolism of aromatic compounds. Specific fungi can convert lignin into fatty acids, including palmitic acid, oleic acid, and tetracosanoic acid [128–130].

These microbial lipids have various applications, such as biodiesel production, which can also be achieved using bacterial strains capable of lignin metabolism [131–133].

Certain bacteria producing lignolytic enzymes can biotransform lignin into PHA via the β-ketoadipate pathway [134, 135]. Additionally, lactic acid can also be derived from lignin through microbial fermentation [136].

Furfural is another valuable product obtained from lignin bioconversion. It serves as a precursor for various industrial chemicals, including methylfuran, tetrahydrofuran, furfuryl alcohol, dihydropyran, furoic acid, and tetrahydrofurfuryl alcohol [122].

Lignin-carbohydrate complexes are also relevant in the bioethanol industry, where white-rot fungi are used in biomass pretreatment to enrich fermentable carbohydrate content. This process enhances sugar availability for microbial fermentation, improving bioethanol yields [137, 138].

Other aromatic compounds derived from lignin deconstruction, such as phenylpropanols and propylphenols, have limited direct applications [139]. However, they can be further converted into fundamental chemical industry feedstocks, including benzene, toluene, and xylene.

Currently, the high production costs of lignin-derived aromatic compounds hinder their competitiveness with petroleum-based alternatives. However, process optimization could improve cost efficiency. For instance, combining lignin-derived benzene with bioethylene (which can be obtained from bioethanol) could enable biorefinery-based styrene production. Given that the global styrene market reached approximately $60 billion in 2024 [140], such advancements could significantly enhance the economic feasibility of lignin valorisation.

2.8.2 Lignin nanoparticles

The formation of spherical, well-defined lignin nanoparticles (LNP) addresses many of the limitations that hinder the efficient and widespread use of macromolecular lignin [141]. As a result, lignin nanoparticle production has become an intensely studied area over the past decade. Lignin particles are classified based on their size, with nanoparticles ranging from 1 to 100 nm, while submicron particles fall within the range of 100 to 1000 nm.

Compared to macroscopic, irregular lignin particles, nanoparticles offer a well-defined morphology (Figure 14), allowing for better control over their properties, which is otherwise difficult to achieve with heterogeneous geometries [142]. One of the major breakthroughs in LNP production was the discovery that chemical derivatization of lignin is not necessary when an appropriate organic solvent system is available. The choice of solvent plays a crucial role in ensuring safety, recyclability, and economic feasibility. Furthermore, studies have confirmed that lignin nanoparticles do not exhibit cytotoxic effects, as demonstrated by both *in vitro* [143] and *in vivo* [144] experiments.

The isolation of lignin nanoparticles and microparticles is generally less energy-intensive than conventional chemical synthesis processes [142]. This is primarily due to surface energy considerations, particularly when synthesis methods involve reactions with high enthalpy, such as covalent bond formation or reduction processes. The regularity of nanoparticle shape plays a crucial role in determining the behaviour of colloidal systems. Studies have shown that

morphology significantly influences key aspects such as flow properties, agglomeration tendencies, and packing efficiency, all of which are important for optimizing colloidal formulations and improving processability in various applications.

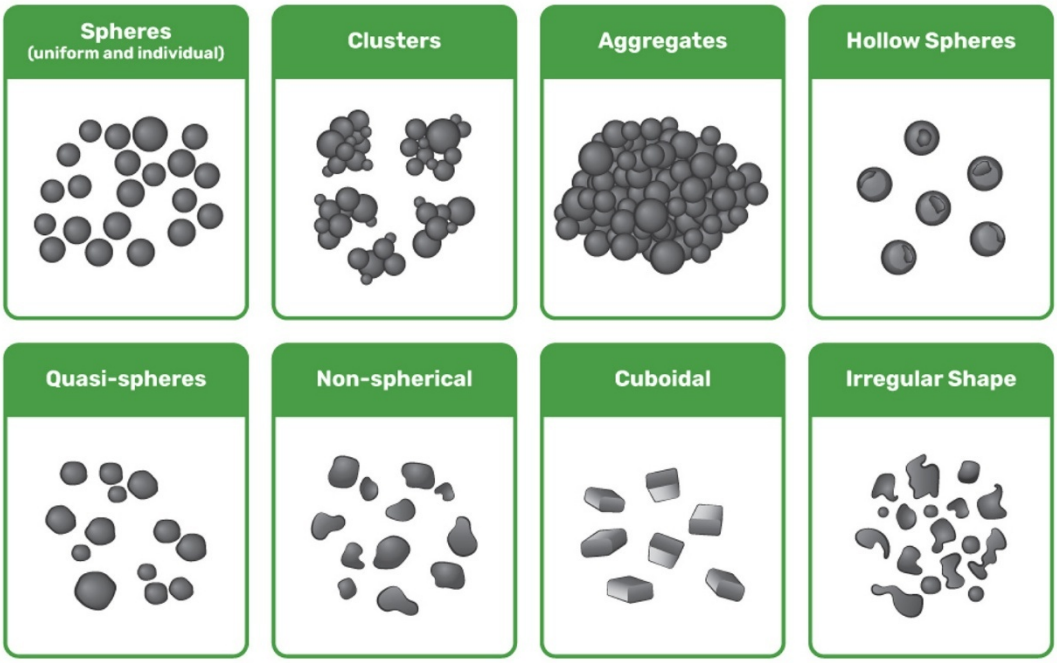

Figure 14 Representation of the different shapes of LNP [145]**.**

Preparation of lignin nanoparticles

Methods for preparing nanoparticles can be categorized into two main approaches: dry and wet preparation. Dry spherical lignin particles can be obtained by controlled drying of lignin dissolved in a solution. One example is the method of controlled evaporation of atomized lignin droplets using an aerosol flow reactor [146]. In this approach, dissolved lignin is atomized into droplets and carried by a heated gas stream, leading to solvent evaporation. Once formed, the particles are cooled in an air stream and subsequently fractionated by size [147].

Another method for producing dry lignin particles involves spray drying, which creates spherical particles from a concentrated colloidal lignin solution. However, the resulting particles typically have an average size of 230 nm [148]. In contrast to these methods, uncontrolled drying, such as using a hot air dryer, leads to the formation of irregular, aggregated, and heterogeneous microparticles.

The second approach to preparing spherical nanoparticles involves wet methods, which are summarized in Figure 15. The most commonly used method is precipitation, where lignin is first dissolved in an organic solvent, such as tetrahydrofuran [149], dimethylsulfoxide [150], dimethylformamide [151] or acetone. Lignin is then precipitated by adding a non-solvent, typically water. In this non-solvent environment, lignin tends to form spherical particles to minimize its contact area with the surrounding solution.

This process differs from lignin precipitation from black liquor by acidification, where protonation of charged groups prevents electrostatic stabilization, leading to cross-linking and

the formation of irregular structures [142]. In contrast, nanoprecipitation methods yield lignin nanoparticles that remain stable for several months.

The morphology and structure of nanoparticles depend on multiple parameters, including the lignin type, its source, solvent properties, and nanoparticle formation conditions. Factors such as the rate of non-solvent addition, the method of mixing, final solvent concentration, and pH all influence the final particle characteristics [152].

The molecular weight of lignin also affects nanoparticle formation [153]. It is assumed that

high-molecular-weight lignin molecules precipitate first, acting as nucleation sites onto which other molecules aggregate. The final nanoparticle surface is typically composed of low-molecular-weight lignin fragments, often enriched with hydrophilic functional groups such as carboxyl or sulfonic groups [154].

Studies investigating the effect of solution pH on nanoparticle formation have shown that particle size decreases linearly with increasing pH from 3 to 6. This trend is expected, as the deprotonation of carboxyl groups increases surface charge, promoting electrostatic stabilization [155].

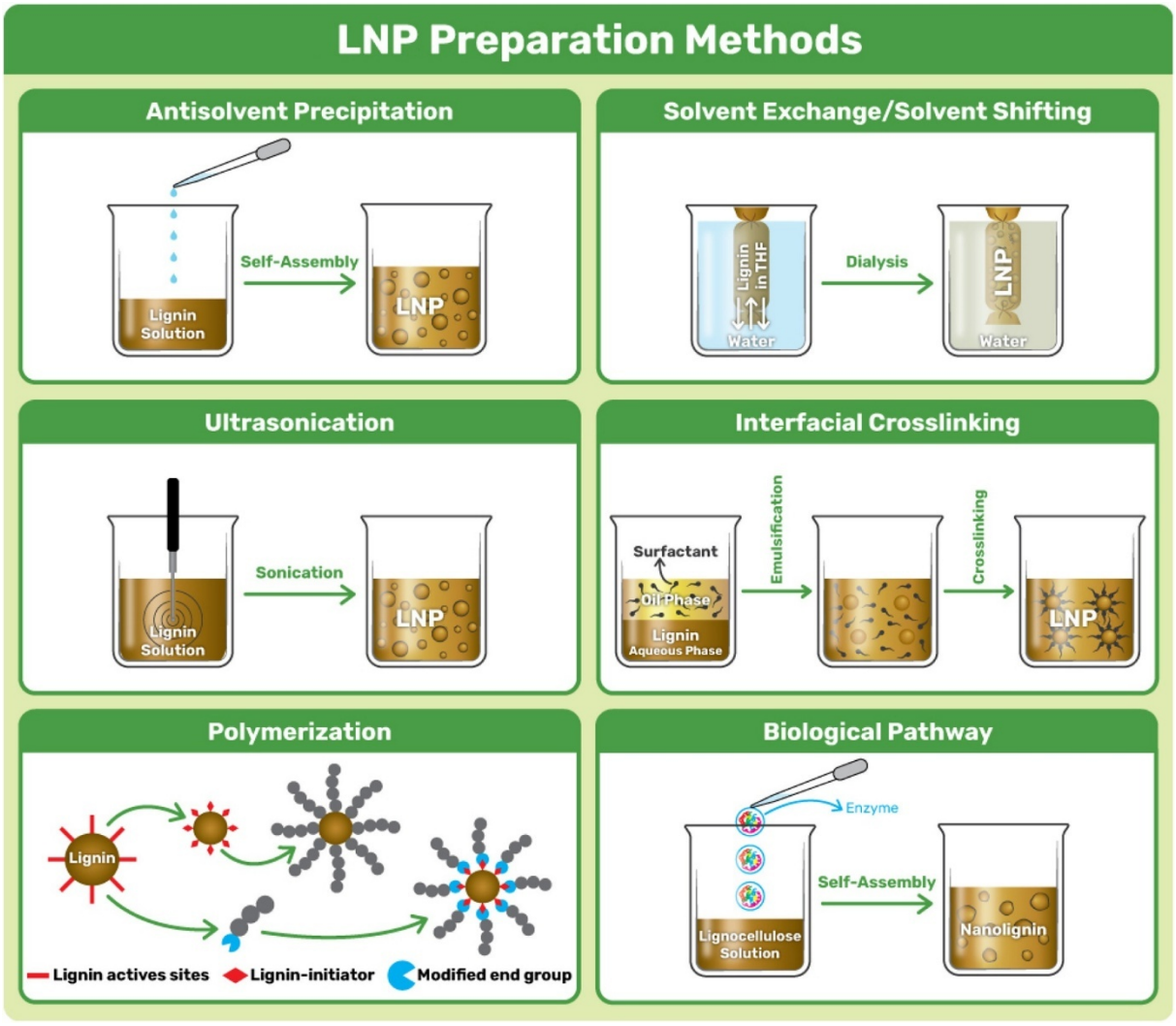

Figure 15 Overview of lignin nanoparticles preparatin method (LNP, Lignin nanoparticles) [145].

A related technique, known as solvent exchange or solvent shift, involves dissolving lignin in an organic solvent and then precipitating it using a non-solvent, typically water [156]. Unlike the precipitation method, where a non-solvent is added to the lignin solution, in solvent exchange, dissolved lignin is placed in a dialysis membrane. Lignin nanoparticles then form slowly during the dialysis process.

Lignin nanoparticles can also be prepared using ultrasound, which suspends lignin in an aqueous solution [157]. A key advantage of this method is that it eliminates the need for toxic organic solvents, making it more environmentally friendly. However, because ultrasound generates particles with broad size distributions, this method is not ideal. A modified approach combines ultrasound with the solvent exchange method, eliminating the need for dialysis while improving particle uniformity [158].

Another technique, interfacial crosslinking, involves emulsifying lignin, typically in an oil-in-water system [159]. In this process, lignin is dispersed in the oil phase using ultrasound or vigorous mixing, and colloidal lignin particles are stabilized with a surfactant. The resulting microcapsules are then crosslinked using agents such as epichlorohydrin or 1,6-dibromohexane.

Polymerization-based methods involve activating lignin's functional groups, allowing it to react with targeted compounds to form copolymers. For example, 2-(dimethylamino)ethyl methacrylate has been used to produce amphiphilic copolymers with highly branched structures, featuring a hydrophobic main chain and cationic hydrophilic arms. These copolymer particles have been investigated for gene transfection applications [151, 160]. Similarly, electrospinning has been employed to produce microfibrils from lignin and poly(methyl methacrylate) [161].

Lignin nanoparticles can also be obtained via microbial degradation. Enzymes or microorganisms, such as bacteria and fungi, can break down lignin into nanoparticles. One approach involves treating lignocellulosic material with a mixture of cellulases and pectinases, yielding cuboidal particles ranging from 20 to 100 nm in size [162]. Another study demonstrated the degradation of coconut fibers by the fungus *Aspergillus*, successfully producing nanoparticles with an average size of 200 nm [163]. Similar results were obtained using laccase enzymes from *Trametes hirsuta* and *Melanocarpus albomyces*, which facilitated the preparation of Kraft lignin nanoparticles stabilized through surface and intraparticle crosslinking.

Emerging Applications of Lignin Nanoparticles

The application of LNP is a relatively recent area of research that has received growing attention due to their versatility and sustainability. Several comprehensive reviews have addressed LNP, highlighting their broad application potential and the prospects of lignin as a high-value renewable material [145, 164–168]. Lignin offers numerous advantages for industrial applications due to its low toxicity, adaptability and abundance. Its key benefits include wide availability, cost-effectiveness, and alignment with the growing demand for biologically based and sustainable materials. The general applications of LNP are summarized in Figure 16.

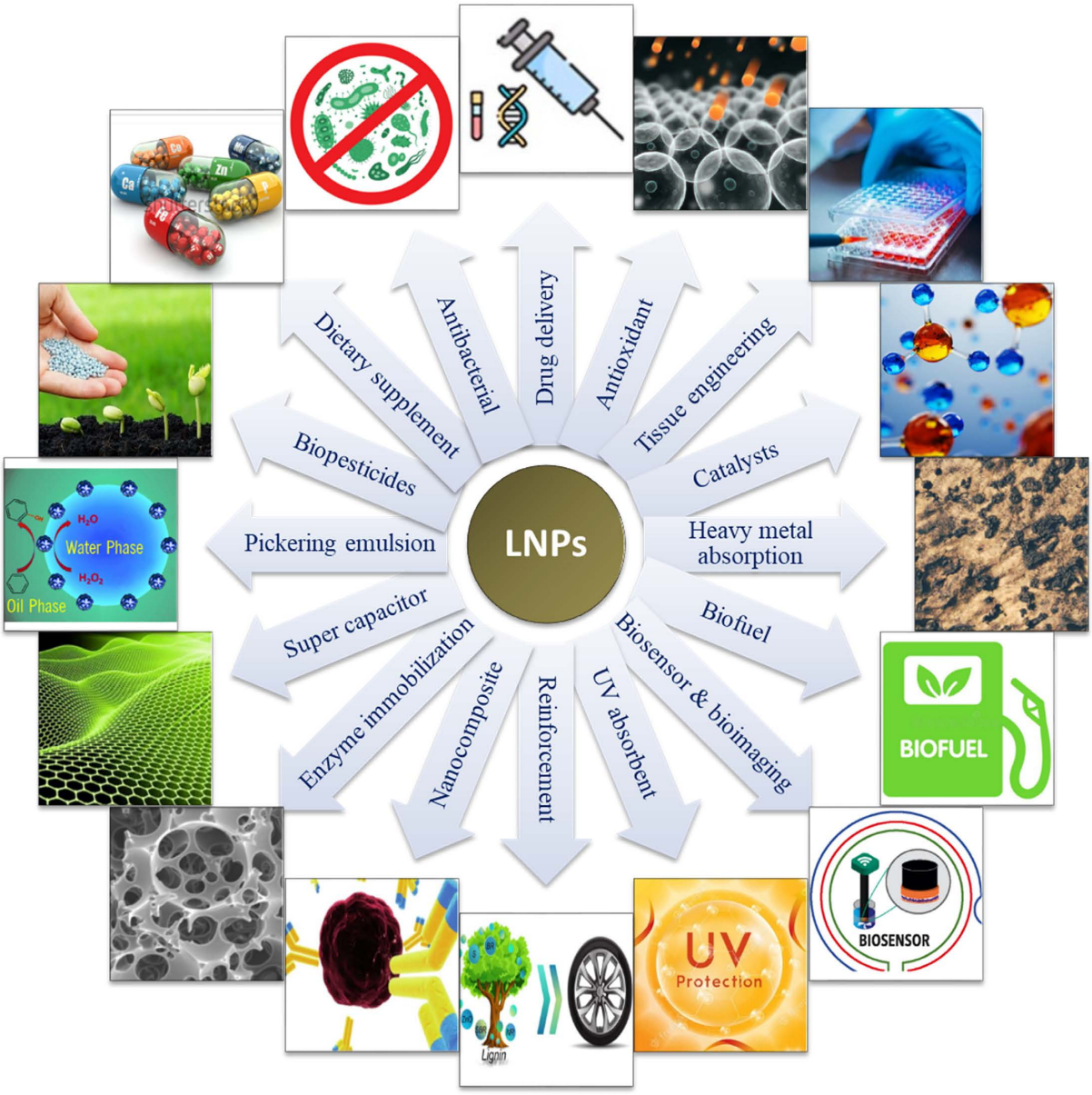

Figure 16 Overview of various applications of lignin nanoparticles (LNP) [167].

LNP are being intensively studied for biomedical applications, where their antioxidant properties and ability to encapsulate a range of active compounds make them particularly attractive. Among the most promising uses is drug delivery [169–171], in which LNP can protect therapeutic agents and enable their controlled release. Typically, hydrophobic compounds are encapsulated within the hydrophilic shell of LNP [172, 173]. Beyond drug delivery, LNP also exhibit antimicrobial [174, 175] and anti-inflammatory properties [176], supporting their use in wound healing [177], and tissue engineering [178]. Their natural origin and modifiable surface chemistry enable further functionalization for targeted delivery or enhanced bioactivity. Together, these properties make LNP a sustainable and versatile platform for developing advanced medical materials.

Another potential application of LNP is enzyme immobilization, where they serve as solid, insoluble support matrices for enzymes [179]. The use of free enzymes in continuous industrial

processes often results in poor stability, reusability, and efficiency. Immobilization helps overcome these limitations by enhancing enzyme stability and performance. LNP offer advantages such as high surface area, strong adsorption, and the presence of various functional groups that enable multi-site enzyme attachment, improving catalytic activity [180]. Due to their biocompatibility and versatility, lignin-based supports are particularly attractive for enzyme immobilization.

Several immobilization strategies have been applied with LNP, including adsorption, entrapment, cross-linking, and layer-by-layer (LBL) strategy [181]. A range of enzymes, such as lipase [182, 183], phospholipase D [184], tyrosinase [185], laccase [186],glucose oxidase and horseradish peroxidase [187], have been successfully immobilized using LNP. These systems also show potential for biosensor development.

LNP are also under investigation in sustainable agriculture, particularly as carriers in nano-fertilizers [188]. They may serve as renewable, slow-release carriers for nutrients. [189], as well as delivery systems for nano-biocides and nano-pesticides. LNP have been used for the gradual release of essential oils with biocidal activity [190]. which could reduce the reliance on conventional fertilizers and pesticides and mitigate their environmental impacts in intensive farming.

Environmental decontamination is another relevant application. LNP can be employed in the fabrication of absorbents for capturing hazardous compounds such as heavy metals from wastewater [191, 192] or for the removal of dye pollutants [193, 194].

2.9 Lignin and polyhydroxyalaknoates

Polyhydroxyalkanoates are a group of microbial biopolymers produced by specific strains of bacteria. These are polyesters accumulated in the form of intracellular granules when in the presence of an excess of carbon and other nutrients deficient conditions. The primary biological function of PHA is the storage of carbon and energy [195].

The advantage of polyhydroxylacanoates lies, among other things, in their diversity of structure, which results in different properties of the resulting materials and consequently different possibilities of use. In general, however, PHA are biobased, biodegradable, biocompatible, gas barrier and have hydrophobic character. These unique properties also imply a variety of applications, including disposable bioplastics, animal feed, biofuels, 3D printing and smart materials usages, as well as biomedical applications specially tissue engineering [196, 197].

PHAs are associated take with some obstacles, which is necessary to overcome, these being limited solubility where toxic halogenated solvents dominate or the poor mechanical properties of P3HB, the basic representative of PHA. For high-value applications, PHA can be modified using a variety of strategies (Figure 17). These are mainly chemically based modifications such as grafting [198, 199] even directly using lignin [200], epoxidation [201, 202] and others. The second group is biological modification, which mainly focuses on modifying the structure of produced PHA by changing the culture medium, either by feeding the culture with functional

group containing substrates or co-adding two substrates in culture medium. By these methods and of course by using recombinant strains, it is possible to produce a variety of copolymers such as poly-3-hydroxybutyrate-*co*-3-hydroxyvalerate (PHBV) [203, 204], poly-3-hydroxybutyrate-*co*-3-hydroxyhexanoate (PHBH) [205–207], poly-3-hydroxybutyrate-*co*-4-hydroxybutyrate (P3HB-*co*-4HB) [208, 209], which have very interesting properties.

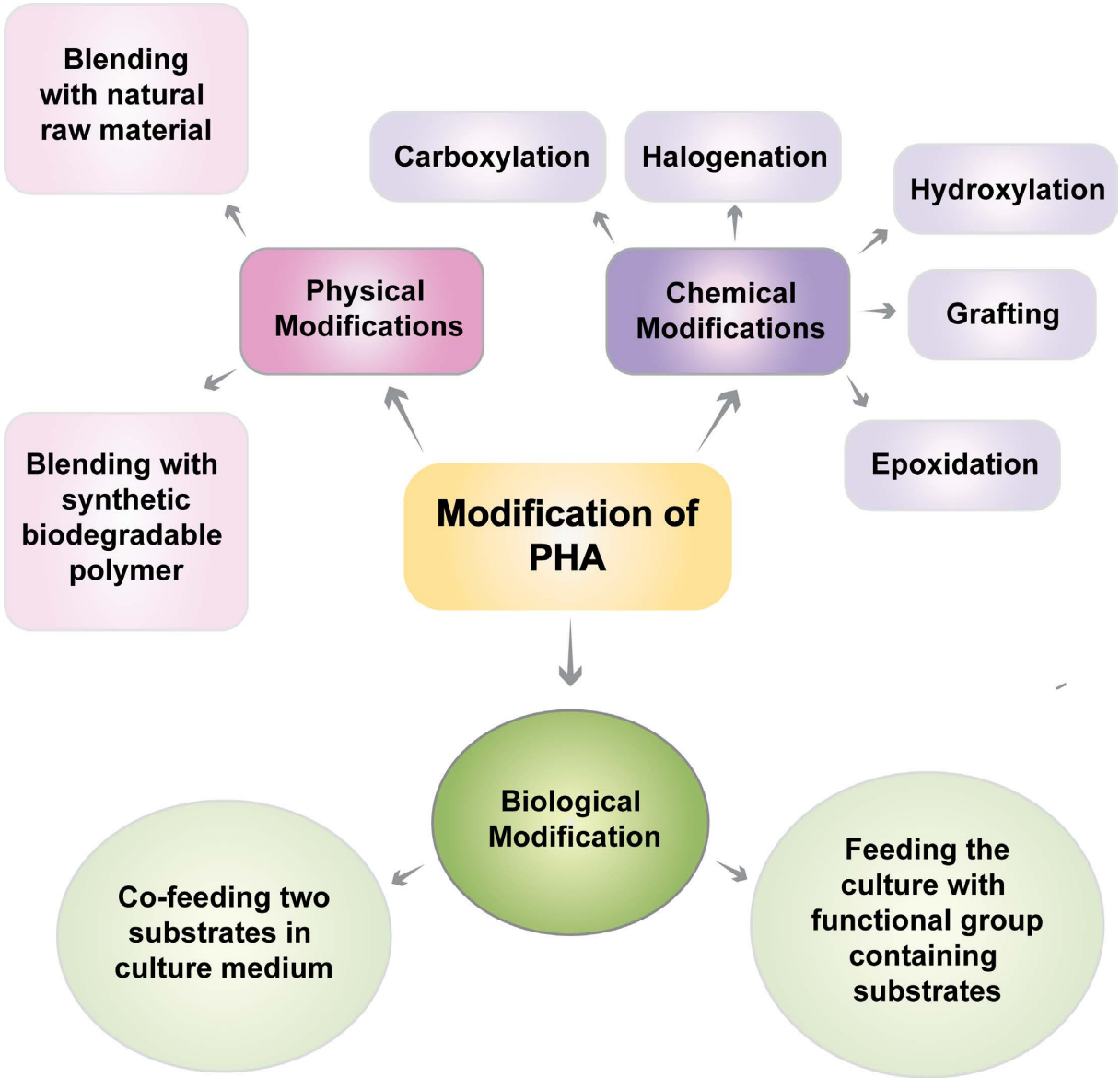

Figure 17 Comprehensive scheme of PHA modification approaches [210].

Last but not least, it is possible to use physical modifications to modify the properties of PHA, which include blending PHA with other polymers and substances. This category also includes PHA blending with lignin and lignocellulose materials. Thanks to intra- and intermolecular hydrogen bonds in lignin contributes to its thermoplastic characteristics, good thermal stability, and the ability to act as a thermoset substance at high temperatures [211].

A frequently used method for blending PHA with lignin is extrusion [93, 212–216]. The advantage of this method is mainly the avoidance of toxic solvents that are used to dissolve PHA, but again care must be taken with the thermal degradation of PHA. Using extrusion, it

has been possible to prepare a compostable material of lignin and PHA improve thermostability [93, 212], and even extruded filaments have been used for 3D printing [214]. However, it has also been described that mixtures containing more than 50% lignin were already very brittle [214, 217], on the other hand, it should be noted that the combination of PHA with 50% lignin is very high compared to other methods. Furthermore, the biodegradability was reduced [213], since lignin is a very complex compound, and its biodegradation is possible only with ligninolytic enzymes.

Another possible method of blending PHA with lignin is solution casting [90, 218, 219]. Using this method, thin films can be prepared by evaporating the solvent. It was described that the resulting material had improved thermal, mechanical and gas barrier properties, have antioxidant activity and UV shielding properties due to the presence of lignin.

A thin composite film of PHA and lignin can be prepared by hot pressing [220]. P3HB has a high degree of crystallinity, and it has been shown that lignin in P3HB blends, prevents the formation of massive PHB spherulitic crystallites, hence inhibiting secondary crystallization. Lignin enhances the formation rate and number of PHB spherulites while decreasing their size.

Another method described for processing is the Pickering emulsion approach [221]. Using it, it was possible to create an emulsion of LNP in water phase and P3HB dissolved in chloroform (water phase). Using hot compression, it was then possible to prepare thin films which, thanks to the lignin, showed no light transmission in the UV region, i.e. protection against light radiation was achieved. Furthermore, the material showed a widened melt-processing window which could help for the processing of P3HB.

3. AIMS

This PhD thesis explores various aspects of lignin processing, modification, and application. The research is based on four central hypotheses and focuses on the following objectives.

1) **Hypothesis:** Lignin isolated from plant seeds using soda pulping exhibits high antioxidant properties.
    - **Aim:** To determine the antioxidant properties of lignin from agricultural waste, specifically grape seeds, rose hip seeds, plum shells, and cherry shells, and compare them with industrial lignin. Subsequently, the aim is to evaluate the impact of lignin on thermal and mechanical properties of polyhydroxyalkanoates (PHA) when used as an active green additive.
2) **Hypothesis:** Enzymatic modification of lignin alters the molecular weight and dispersity of lignin, potentially influencing its antioxidant and antimicrobial properties.
    - **Aim:** To measure the changes in molecular weight and dispersity of lignin modified using the fungi *Fomitopsis pinicola*, *Lenzites betulina*, and *Phanerochaete chrysosporium*, and to assess the resulting antioxidant and antimicrobial properties.
3) **Hypothesis:** Derivatizing lignin into nanoparticles enhances its applicability in various fields.
    - **Aim:** To evaluate the impact of different solvent systems and their combinations on the formation of lignin nanoparticles, and to characterize the nanoparticles with a focus on their antioxidant and antimicrobial properties.
4) **Hypothesis:** Lignin nanoparticles can form thin films suitable for surface modification of various materials.
    - **Aim:** To systematically evaluate the adhesion properties of lignin based nanoparticles with polyelectrolytes on gold. The aim is to prepare lignin-based thin films with antioxidant and antimicrobial activities.

4. EXPERIMENTAL SECTION

4.1 Materials

4.1.1 Chemicals

Sodium hydroxide (Lach-ner, Czech Republic)

Viscozyme® L (Sigma Aldrich, Germany)

HCl 37% (Lach-ner, Czech Republic)

Ethanol UV-VIS, (Lach-ner, Czech Republic)

Dimethyl sulfoxide 99.9 % (Carl Roth GmbH, Germany)

ABTS, (2,20-azino-bis(ethylbenzthiazoline-6-sulfonic acid) (Sigma Aldrich, Germany)

Trolox (6-hydroxy-2,5,7,8-tetramethylchroman-2-carboxyl acid) (Sigma Aldrich, Germany)

Folin-Ciocalteu reagent (Penta, Czech Republic)

Galic acid monohydrate (Loba biotech GmbH, Austria)

n-hexane 99 % (Carl Roth GmbH, Germany).

Na_2CO_3 anhydrous (Lach-ner, Czech Republic)

LiBr (Carl Roth GmbH, Germany)

KBr (Carl Roth GmbH, Germany)

Ammonium acetate (Thermo Fisher Scientific, USA)

Potassium sodium tartrate (Lach-ner, Czech Republic)

Glucose (Lach-ner, Czech Republic)

Ammonium tartrate (Lach-ner, Czech Republic)

Thiamine (Alfa Aesar GmbH, Germany)

KH_2PO_4 (Lach-ner, Czech Republic)

$CoCl_2 \cdot 6\ H_2O$ (Lach-ner, Czech Republic)

$CaCl_2$ (Lach-ner, Czech Republic)

NaCl (Lach-ner, Czech Republic)

$MgSO_4 \cdot 7\ H_2O$ (Lach-ner, Czech Republic)

$MnSO_4 \cdot H_2O$ (Lach-ner, Czech Republic)

$FeSO_4 \cdot 7\ H_2O$ (Lach-ner, Czech Republic)

$ZnSO_4 \cdot 7\ H_2O$ (Lach-ner, Czech Republic)

$CuSO_4 \cdot 5\ H_2O$ (Lach-ner, Czech Republic)

H_3BO_3 (Lach-ner, Czech Republic)

H_2O_2 30% p.a. (Lach-ner, Czech Republic)

Malt extract (Carl Roth GmbH, Germany)

Potato dextrose broth (HiMedia, India)

Nutrient broth with 1% Peptone (HiMedia, India)

2,6-dimethoxyphenol (DMP) (Merck Life Science, Germany)

Veratryl alcohol (Merck Life Science, Germany)

Ethylenediaminetetraacetic acid (EDTA) (Lachn-ner, Czech Republic)

Malonic acid (Riedel de Haën, Germany)

Poly(allylamine hydrochloride) (PAH) Mw 50,000 $g \cdot mol^{-1}$, lot #283223 (Sigma Aldrich, Germany)

Poly-L-lysine (PLL) 0.1 % (w/v) solution, lot #P8920 (Sigma Aldrich, Germany)

Poly(diallyldimethylammonium chloride) (PDM) Mw 200,000-350,000 $g \cdot mol^{-1}$, lot #409022, (Sigma Aldrich, Germany)

Polyethyleneimine (PEI) ethoxylated solution lot #423475 (Sigma Aldrich, Germany)

Lignin Alkali 471003 (Merck Life Science, Germany)

Lignin Organosolv (Reference sample)

Lignin Indulin AT (Ingevity, USA)

Poly-3-hydroxybutyrate (P3HB) EDW 2394 (TianAn, China)

Poly-3hydroxy-*co*-4-hydroxybutyrate (P3HB-*co*-4HB), (Yield10 Bioscience, USA)

Tetracycline hydrochloride, Code No: BIT0150 (Apollo Scientific, United Kingdom)

4.1.2 Biological sources

Plant raw materials

- Grape pomace (*Vitis vinifera*) variety Sauvignon Blanc harvested at autumn 2018, Mikulov region
- Rose hip (*Rosa canina*) harvested at autumn 2021, Blansko region
- Cherry stones (*Prunus avium*) harvested at autumn 2022, Blansko region
- Plum stones (*Prunus domestica*) harvested at autumn 2021, Kroměříž region

Microorganisms

- *Escherichia coli* (CCM 7395)
- *Micrococcus luteus* (CCM 1569)
- *Serratia marcescens* (CCM 8587)
- *Fomitopsis pinicola* (DSM 3521)
- *Lenzites betulina* (DSM 4954)
- *Phanerochaete chrysosporium* (CCM 8074)

4.1.3 Equipment

Hydrothermal Autoclave (ENSECO s.r.o., Slovakia)

Spectrum™ Labs Spectra/Por™ 1 6-8 kD MWCO (Spectrum Chemical Mfg. Corp., USA)

Gerhardt Soxtherm, SOX 412 (C. Gerhardt GMBH & CO. KG, Germany)

Chamber furnace LE 05/11 (LAC, Czech Republic)

Nicolet iS5 spectrometer (Thermo Fisher Scientific, USA)

Programmable rotator Biosan Multi Bio RS-24 (Biosan SIA, Latvia)

Elemental analyzer Euro Vector 3000 (EuroVector, Italy)

ELISA reader BioTek Elx808 (BioTek, USA)

Centrifuge Z 32 HK (HERE Labortechnik GmbH, Germany)

Zetasizer Ultra (Malvern Pananalytical Ltd, UK)

Quartz Crystal Microbalance E4 (Q-Sense, Sweden)

Tosca™ 400 atomic force microscope (Anton Paar, Austria)

Drop shape analyzer DSA100 (Krüss GmbH, Germany)

RSA-G2 Solids Analyzer (TA Instruments, USA)

TGA Q50 (TA Instruments, USA)

DSC Q2000 (TA Instruments, USA)

BET Surface area analyzer NOVA 2200e (Quantachrome Instruments, USA)

UV-VIS Spectrophotometer U-3900H (Hitachi, Japan)

Laboratory vibrating mill (Okresní podnik služeb Přerov, Czechoslovakia)

Polaron SC 7640 sputter coater (Laughton, United Kingdom)

JEOL JSM-7600 Field-Emission Scanning Electron Microscope (Akishima, Japan)

4.2 Lignin isolation and characterisation

4.2.1 Fractionation of fruit seeds

Pretreatment

The study utilized grape and rose hip seeds as well as plum and cherry stones, as specified in Section (4.1.2). Grape and rose hip seeds were separated from dried grape pomace and rose hips, which were dried at 40 °C for 5 days, and then ground using a vibrating mill. Plum and cherry stones were carefully broken with a hammer to avoid damaging the seeds contained inside. The seeds were then manually separated, and the remaining stone material was ground using a vibrating mill.

Oil extraction was performed using n-hexane in a Soxtherm extraction system at 180 °C for 3 hours. To remove soluble carbohydrates, as well as portion cellulose and hemicellulose, an enzymatic treatment with Viscozyme was applied. Specifically, 1 mL of Viscozyme was added per 100 g of defatted raw material in 1000 mL of distilled water, and the mixture was stirred at 37 °C for 24 hours [222]. The resulting mixture was then filtered, washed with distilled water, and the solid phase obtained was subsequently dried at 50 °C overnight.

Lignin extraction

The isolation process was adapted from the biorefinery soda pulping method [223] and gradually improved. Initially, the isolation was carried out using a reflux apparatus in an oil bath. Later, a hydrothermal autoclave was employed to enhance the process.

The isolation process was carried out using the following protocol (Figure 18). The dried material was placed in the hydrothermal autoclave and 1.5 M NaOH solution was added (15 mL per 1 g). The autoclave was heated to 121 °C per 1 hour, then cooled. The slurry was filtered through a Büchner funnel and washed with distilled water. The solid fraction was returned to the autoclave along with a 1.1 M NaOH solution in the same ration. The autoclave was then heated to 155 °C for 1.5 hours and cooled again. The resulting solution was again filtered under reduced pressure and washed with distilled water. Lignin was precipitated from the liquid phase by heated to 50 °C and concentrated HCl was added slowly dropwise with constant stirring until the pH reached neutrality. The solution was then transferred to an ice bath, where HCl was added dropwise until pH reached 2. The precipitated lignin was separated by centrifugation, washed multiple times with distilled water, and further purified by dialysis in a Spectra/Por® 1 tubing with a MWCO of 6–8 kDa against distilled water for 4 days. The final product was then freeze-dried.

Klason Lignin

Klason lignin method was used to characterize the biological lignin sources and to compare their yields [224].

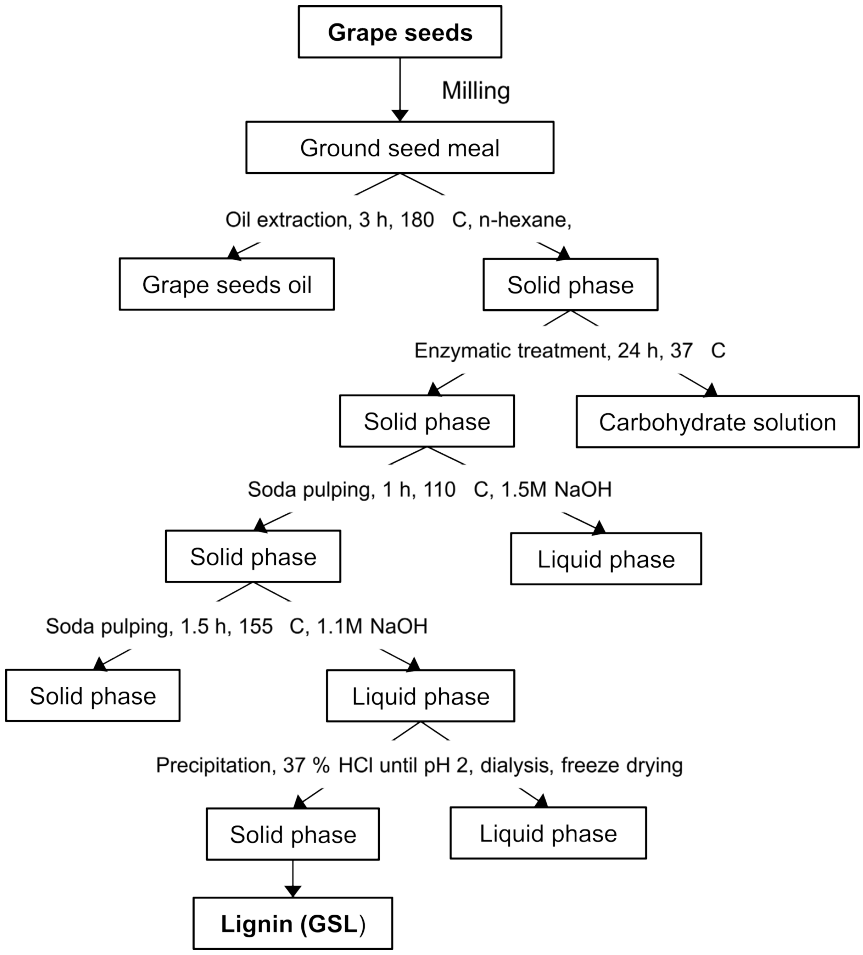

Figure 18 Lignin isolation process. Schematic representation of the lignin isolation process using grape seeds as an example.

4.2.2 Lignin characterisation

FT-IR

FT-IR spectroscopy was used to determine the presence of the functional groups employing a Nicolet iS5 spectrometer. The FT-IR spectra were recorded using KBr tablets in the range of 4000-400 cm^{-1}, at 4 cm^{-1} resolutions, using 64 scans. KBr tablets were prepared using a solid mixture of 1.5 wt% of dry samples and KBr in a Lab Tools press at a pressure of up to 10 MPa. The KBr infrared grade spectrum was used as the background for DRIFT (Diffuse Reflectance Infrared Fourier Transform Spectroscopy) measurement. The raw absorption DRIFT spectrum was evaluated without artificial processing.

Elemental composition

The elemental composition was determined using a CHNS analyser (Euro Vector 3000) with a combustion program set to 980 °C. Pure oxygen was used as the combustion gas, and pure helium served as the carrier gas [68]. The resulting gaseous products (N_2, CO_2, H_2O, and SO_2) were detected by a thermal conductivity detector. A reference standard sample, sulfanilamide, was used for calibration. The oxygen content was calculated by difference, and the values were corrected for ash and moisture content.

Antioxidant Activity

The antioxidant activity of lignin samples was assessed using the $ABTS^{\cdot+}$ radical decolorization assay, commonly referred to as the Trolox Equivalent Antioxidant Capacity (TEAC) method. Trolox (6-hydroxy-2,5,7,8-tetramethylchroman-2-carboxylic acid) served as the standard, and results were expressed in milligrams of Trolox equivalents per gram of lignin [51]. The reaction mixture consisted of 1 mL of $ABTS^{\cdot+}$ radical solution and 10 μL of lignin sample dissolved in 0.1% (w/v) DMSO. Absorbance was measured at 734 nm at the start of the reaction (A_0) and after 10 minutes (A_{10}).

Total Phenolic Content

The total phenolic content (TPC) of lignin samples was determined using the Folin–Ciocalteu spectrophotometric method. Samples were dissolved in 0.1% (w/v) DMSO, and the TPC was expressed as gallic acid equivalents (mg GAE per g lignin) [55]. During the reaction, polyphenols in the sample were oxidized by the F–C reagent in an alkaline environment, forming a blue complex. The intensity of this complex was quantified spectrophotometrically at 750 nm [225].

Molecular weight

The molecular weight and polydispersity of lignin samples were determined using size exclusion chromatography (SEC, Infinity 1260, Agilent Technologies) coupled with multi-angle laser light scattering (Dawn Heleos II, Wyatt Technology) and a differential refractometer (Optilab T-rEX, Wyatt Technology). Lignin samples were dissolved in 0.2% (w/v) DMSO with 0.1% LiBr to minimize sample aggregation. The solutions were filtered through a nylon syringe filter (pore size 0.45 μm) before analysis, with no further treatment [226].

Solubility

Solubility was also expressed using Hansen solubility parameters (HSP) [227]. Lignin samples were subjected to analysis using 29 solvents, in concentration 1 $g \cdot L^{-1}$ of lignin samples. The mixture was shaken for 24 hours at room temperature using Biosan multirotator and subsequently classified by visual inspection into "good" or "bad" solvents. Obtained data were filled into spreadsheet developed and described by Ríos and Ramos [228]. This useful tool was used to calculate Hansen parameters of lignin samples and necessary to create a graphical treatment in the form of Hansen spheres. A very useful tool of this spreadsheet is the solvent blends calculator, which can estimate whether the tested mixture of solvents can dissolve the given sample and, above all, propose the optimal ratio of solvent blends.

For selected lignin samples, solubility was also determined quantitatively. A 50 $g \cdot L^{-1}$ sample was prepared using a specific solvent and stirred with a magnetic stirrer at room temperature for 24 hours. The solution was then filtered under reduced pressure using filter paper with a particle retention range of 2–3 μm. The volume of the filtrate was recorded. Solution was evaporated, dried, and weighed. The solubility was expressed as a percentage of the solute dissolve in a given volume of solvent according to equation (1):

$$Solubility\ \% = \frac{m_f}{m_s} \cdot 100 \quad \textbf{(1)}$$

Where m_s is original sample weight and m_f is weight of dried filtrate.

Nuclear magnetic resonance

High-resolution Nuclear magnetic resonance (NMR) spectra were obtained using a Bruker Avance III HD spectrometer equipped with a 5 mm cryoprobe operating at 14 T and maintained at 40 °C in deuterated dimethyl sulfoxide (DMSO-d6). Proton and carbon chemical shifts were referenced to tetramethylsilane. One-dimensional ^{1}H (600 MHz) and ^{13}C (150 MHz) NMR spectra as well as two-dimensional ^{1}H-^{13}C heteronuclear single quantum coherence (HSQC) spectra were recorded to assign ^{1}H and ^{13}C chemical shifts. HSQC spectra were acquired with a spectral width of 0–12 ppm ^{1}H and 0–210 ppm ^{13}C, using 2048 points in F2 dimension, and 256 increments in F1 (zero-filled to 4K x 1K points) with 128 transients. Data were processed using Bruker and MestReNova software, and chemical shifts (δ) are reported in parts per million (ppm).

4.3 Polyhydroxyalkanoates solid blocks

4.3.1 Preparation of PHA solid blocks

PHA solid blocks were prepared from P3HB and blend of P3HB and P3HB-*co*-4HB in ration 1:1. A specific PHA was dissolved in DMSO at a concentration of 5–10 wt% at temperature 115 °C and continuously stirred.

The resulting solution was poured into a Petri dish and allowed to cool and solidify over two days. Subsequently, the solidified block underwent solvent exchange with distilled water, with the water replaced twice daily for 4 days. Afterward, the solid block was lyophilized to obtain the final product.

Optionally, lignin (dissolved in DMSO at 20 wt%) and mixed bacterial cellulose (50 wt%) according to the described procedure [229] were added to the hot PHA solution. Note that the biotechnological production of bacterial cellulose was beyond the scope of this thesis.

4.3.2 Characterisation of PHA solid blocks

Mechanical properties

The mechanical properties of the material were evaluated using dynamic mechanical analysis (DMA). This technique monitors the viscoelastic response of a material subjected to oscillatory stress. The method separates the viscoelastic response into two components of the complex modulus of elasticity (E*): storage modulus (E′) and the loss modulus (E″), such that (equation (2):

$$\mathrm{E}^{*} = \mathrm{E}' + \mathrm{iE}'' \quad \textbf{(2)}$$

The modulus of elasticity is determined from deformation curves in the region where the stress (σ) exhibits a linear dependence on strain (ε). In this region, Hooke's law applies, which states that deformation is directly proportional to the applied stress (equation (3)

$$\sigma = E \cdot \varepsilon \rightarrow E = \frac{\varepsilon}{\sigma} \quad \textbf{(3)}$$

Hooke's law describes the elastic deformation of materials under small forces, where the deformation is reversible once the load is removed.

The measurements were conducted in a three-point bending mode, which is suitable for stiff materials. This mode was selected due to the material's characteristics and the practical limitations of clamping in other measurement modes.

To identify the material's linear viscoelastic (LVE) range (Figure 19A), an amplitude sweep test was performed as the initial step. This test is crucial for determining the range within which primarily elastic (reversible) deformation occurs, ensuring Hooke's law is applicable. During the test, a very low strain is applied, which is gradually increased (Figure 19B) [230]. At low strain levels the storage and loss moduli E′ and E″ exhibit constant values, indicating the LVE plateau. The LVE range is particularly relevant as it allows for the accurate determination of mechanical properties without compromising the sample's structural integrity.

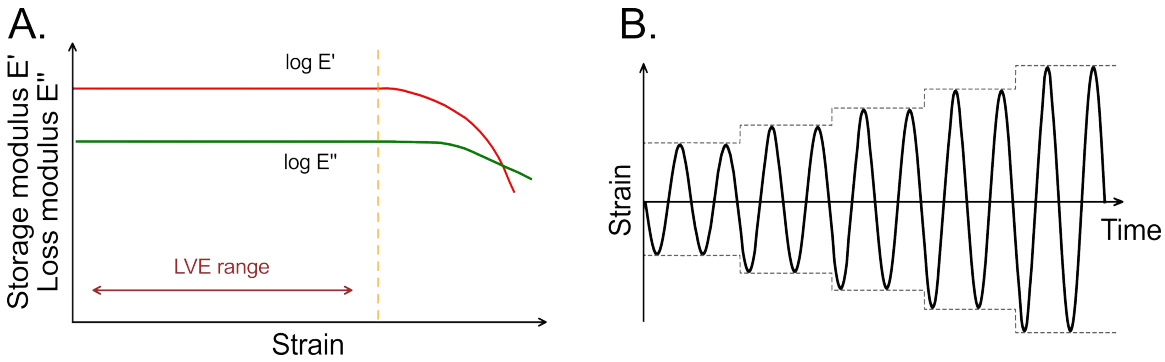

Figure 19 Amplitude sweep test. Linear viscoaleastic range of E′ and E″ in the low stress region (A) and applied stress profile during the test (B). LVE range – Linear viscoelastic range.

Amplitude sweep tests were conducted at a constant temperature (26 °C) and frequency, varying the applied strain amplitude within the range of $1 \cdot 10^{-3}$% to 1%. The geometry span for the three-point bending was chosen 25 mm, and the samples, with dimensions of 31 mm × 5.9 mm × 1–2 mm, were stamped using a punch and press (Figure 20).

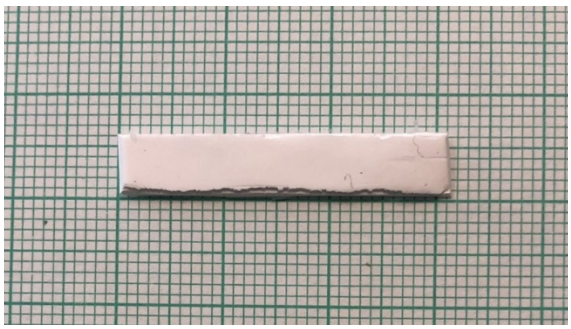

Figure 20 Stamped test specimen of P3HB for DMA on graph paper

Following the amplitude sweep, a time-dependent measurement was conducted. Samples were exposed to the selected strain for 5 minutes to evaluate whether irreversible deformations occurred over time.

Thermogravimetry

Thermogravimetric analysis (TGA) experiments were performed by TGA Q50 (TA Instruments, USA) by the non-isothermal method. Approximately 5 mg of the sample was sealed in an aluminium pan and heated from 25 °C to 400 °C with a heating rate of 10 °C·min^{-1} with an airflow of 30 mL·min^{-1}.

Differential scanning calorimetry

DSC experiments were performed using a DSC Q2000 under a nitrogen atmosphere to prevent oxidative degradation. The calibration performed using high-purity indium. Samples of about 10 mg were hermetically sealed in aluminium pans. Thermal transitions and the material's response to temperature changes were investigated using a non-isothermal protocol [231]. The experiments involved a three-step heating and cooling cycle with a heating/cooling rate of 10 °C·min^{-1}and a nitrogen gas flow of 60 mL·min^{-1}:

First heating from 25 °C to 190 °C

Isothermal hold for 1 min

Cooling from 190 °C to -40 °C

Isothermal hold for 1 min

Second heating from -40 °C to 190 °C

Melting temperature (T_m) and enthalpy of melting (ΔH_m) were determined from the endothermic peaks. The crystallization temperature (T_c) and enthalpy of crystallization (ΔH_c) were measured from the exothermic peak during the cooling cycle.

Scanning electron microscopy

The micromorphology of PHA solid blocks was examined using a JEOL JSM-7600 Field-Emission Scanning Electron Microscope. Prior to imaging, samples were coated with gold using a Polaron SC 7640 sputter coater. Images were captured at an accelerating voltage of 1 kV and a magnification of 15,000×.

Specific surface area

Measurements were conducted on a NOVA 2200e analyser. The specific surface area (S_{BET}), pore volume (V_p), and pore size distribution of freeze-dried samples were analysed through nitrogen adsorption–desorption using the Brunauer–Emmett–Teller (BET) method. Measurements were conducted on a NOVA 2200e analyser. Prior to analysis, the samples were degassed at 50 °C for 24 hours.

Density

Density of cryogels were analysed by pycnometer standard method ASTM D792-98, Method B. The density was calculated using equation (4):

$$\rho_S = \frac{m_S}{V_S} = \frac{m_S}{\frac{m_{H_2O} - m'_{H_2O}}{\rho_{H_2O}}} \quad \textbf{(4)}$$

Where ρ_s is density of measured sample, V_s is volume of measured solid object, m_s is weight of measured sample, m_{H_2O} is weight of water in pycnometer without sample and m'_{H_2O} is weight of water in pycnometer when sample is inside.

Water contact angle

The wettability of the cryogels was investigated by determining the static water contact angle (WCA) using the sessile drop method with a drop shape analyser Krüss DSA100. For each measurement, a droplet of deionized water (~2.3 µL) was deposited onto the surface, and images were recorded for 1 minute and averaged.

Antioxidant properties

The antioxidant properties of PHA gryogels were analysed using the ABTS·+ radical scavenging assay, as described in Chapter 4.2.2 with minor modifications. Approximately 25 mg of sample was immersed in 3 mL of ABTS·+ radical solution, and absorbance was recorded after 10 minutes.

4.4 Lignin nanoparticles

4.4.1 Preparation lignin nanoparticles

Colloidal lignin nanoparticles were prepared following a previously described antisolvent precipitation method [149]. Lignin powder was dissolved in an organic solvent or solvent mixture overnight. The solution was filtered through a syringe filter with a 0.45 µm nylon membrane to remove insoluble components.

The filtered lignin solution was rapidly poured into vigorously stirred deionized water (750 rpm), inducing precipitation and the formation of LNPs. The volume of water was selected so that, after adding the lignin solution, the water-to-organic solvent ratio in the final mixture was 75:25. The resulting dispersion was purified by dialysis for 4 days using Spectra/Por® 1 tubing (MWCO 6–8 kDa) against deionized water.

4.4.2 Properties of lining nanoparticles

Dynamic light scattering and zeta potential

The particle size distribution, Z-average particle sizes, polydispersity, and zeta potential of LNP were determined using a Malvern Pananalytical Zetasizer Ultra, employing dynamic and electrophoretic light scattering. Measurements were conducted at a laboratory temperature

(25.0 ± 0.1 °C). All reported data represent the average values from three independent experiments.

Stability assessment

The stability of LNP was evaluated by measuring the Z-average particle size and zeta potential at regular intervals over 40 days. Additionally, the effect of pH on nanoparticle aggregation was investigated.

Scanning electron microscopy

The micromorphology of LNP was examined using a JEOL JSM-7600 Field-Emission Scanning Electron Microscope (FESEM). A dispersion of LNP at a concentration of approximately 1 $g \cdot L^{-1}$ was deposited onto a silicon wafer and allowed to air-dry at room temperature. Images were captured with an accelerating voltage of 5 kV and a magnification of 50,000×.

Antimicrobial, antioxidant activity and TPC

The antibacterial activity of lignin was tested against the Gram-positive bacterium *Micrococcus luteus* and the Gram-negative bacterium *Escherichia coli*, both obtained from the Czech Collection of Microorganisms (Masaryk University, Brno, Czechia). Bacterial cultures were grown in Nutrient Broth supplemented with 1% peptone (Table 3) under sterile conditions.

Table 3 Nutrient Broth composition

Peptone	10 $g \cdot L^{-1}$
Beef extract	10 $g \cdot L^{-1}$
NaCl	5 $g \cdot L^{-1}$

Inhibition of bacterial growth in case of lignin samples was monitored through the broth dilution method by measuring the turbidity at 630 nm. In the beginning of each trial, the inoculums were diluted to final absorbance 0.1. 50 µL of the lignin sample was added to 150 µL of diluted bacterial suspension in suitable growth medium to the wells of a sterile 96-well microtiter plate. The turbidity change was analysed at 0 and 24 hours, using ELISA reader BioTek Elx808 (BioTek, USA). Diluted inoculum with the addition of 50 µL of distilled water was used as a blank. Plates were incubated at the optimal temperatures for bacterial growth.

Antioxidant activity and TPC of LNP were determined following the protocol described in chapter 4.2.2.

4.5 Biotechnological lignin modification

4.5.1 Fungi cultivation

The typical submerged batch cultivation for lignin modification by the studied fungi was carried out in 100–500 mL Erlenmeyer flasks, with a cultivation medium volume of 50–250 mL.

Fomitopsis pinicola was cultivated at 25 °C, *Lenzites betulina* at 30 °C, and *Phanerochaete chrysosporium* at 32 °C. Various media suitable for each microorganism were tested as production media (Table 4), with thiamine added aseptically after sterilization. The detailed compositions of Mineral medium I and II are described in tables 5–8. Malt extract and Potato dextrose broth were enriched with thiamine at a concentration of 0.1 $g \cdot L^{-1}$. The static cultivations were carried out for 14 or 30 days, during which, or at the end of the cultivation period, samples were collected to determine enzyme activity.

Table 4 Overview of cultivation media for fungi

Microorganism	Cultivation medium
Fomitopsis pinicola	Mineral medium I
	Malt extract
Lenzites betulina	Mineral medium I
	Potato dextrose broth
Phanerochaete chrysosporium	Mineral medium II

Table 5 Mineral medium I [232]

Glucose	10.00 g / 5.00 g
Ammonium tartrate	0.53 g
Thiamine	0.10 g
KH_2PO_4	7.23 g
$MgSO_4 \cdot 7H_2O$	4.97 g
$CaCl_2$	0.36 g
NaCl	0.22 g
$MnSO_4 \cdot H_2O$	0.13 g
$CoCl_2 \cdot 6H_2O$	0.04 g
$FeSO_4 \cdot 7H_2O$	0.22 g
$ZnSO_4 \cdot 7H_2O$	0.02 g
$CuSO_4 \cdot 5H_2O$	0.03 g
H_3BO_3	0.02 g
Water	1000 mL

Table 6 Mineral medium II [233]

Basal III medium	100 mL
Trace element solution	60 mL
Water	840 mL
Glucose	10 g
Thiamin	0.1000 g
Ammonium acetate	0.1542 g
Potassium sodium tartrate	0.2363 g

Table 7 Basal III medium [233]

Trace element solution	100 mL
KH_2PO_4	20 g
$MgSO_4$	5 g
$CaCl_2$	1 g
Water	900 mL

Table 8 Trace element solution [233]

$MgSO_4$	3 g
$MnSO_4$	0.5 g
NaCl	1 g
$FeSO_4 \cdot 7H_2O$	0.1 g
$CoCl_2$	0.1 g
$ZnSO_4 \cdot 7H_2O$	0.1 g
$CuSO_4$	0.1 g
H_3BO_3	10 mg
Water	1000 mL

4.5.2 Enzymatic activity assay

During cultivation, samples were taken daily, and the activity of lignolytic enzymes was determined. The collected samples were centrifuged for 10 minutes at 15,650 rcf and 4 °C. The resulting supernatant was used for the spectrophotometric determination of enzyme activity [234]. Changes in absorbance were recorded at 1-minute intervals during the measurement. Enzyme activity was defined as the amount of enzyme catalysing substrate conversion, indicated by an increase in absorbance over time, and was calculated using equation (5).

$$EA = \frac{\Delta A}{\varepsilon \cdot l} \cdot \frac{V_t}{V_e} \cdot \frac{1}{t} \cdot 10^6 \quad \textbf{(5)}$$

Where

EA	enzyme activity ($\mu mol \cdot min^{-1} \cdot L^{-1}$; $U \cdot L^{-1}$)
ΔA	change in absorbance during measurement (-)
ε	molar absorptivity ($L \cdot mol^{-1} \cdot cm^{-1}$)
l	cuvette thickness (1 cm)
V_t	total volume in the cuvette (µl)
V_e	volume of enzyme in the reaction mixture (µl)
t	time of reaction (min)

Laccase activity

Laccase activity was measured using ABTS as the substrate [235]. The measurement was monitored at 415 nm. The reaction mixture consisted of 900 µL of 0.1 M sodium acetate buffer (pH 4.5), 50 µL of supernatant and 50 µL of 10 mM ABTS. The reaction was initiated by adding the substrate. The extinction coefficient (ε = 36000 $L \cdot mol^{-1} \cdot cm^{-1}$) was used for activity calculation.

Lignin peroxidase activity

Lignin peroxidase activity was determined using veratryl alcohol as the substrate [236]. The reaction was monitored at 310 nm. The reaction mixture consisted of 775 µL of 100 mM tartrate buffer (pH 3), 50 µL of 54 mM H_2O_2, 150 µL of supernatant, and 25 µL of 25 mM veratryl alcohol. The reaction was initiated by adding veratryl alcohol. The extinction coefficient (ε = 9300 $L \cdot mol^{-1} \cdot cm^{-1}$) was used for activity calculation.

Manganese-dependent peroxidase activity

The activity of manganese peroxidase was determined using 2,6-dimethoxyphenol (DMP) as the substrate [237]. The reaction was monitored at 469 nm. Two different reaction mixtures were prepared for the assay (Table 9), and the reaction was initiated by the addition of DMP. The enzyme activity was calculated as the difference in activity between mixtures I and II, using equation (5) and an extinction coefficient (ε = 49,600 $L \cdot mol^{-1} \cdot cm^{-1}$) [238].

Table 9 MnP assay reaction Mixture Components

Reaction mixture	I (µl)	II (µl)
65.8 mM malonate buffer (pH 4.5)	760	760
10 mM H_2O_2	40	40
20 mM $MnSO_4$	50	-
20 mM EDTA	-	50
Supernatant	100	100
20 mM DMP	50	50

4.5.3 Lignin modification and characterisation

For the lignin biotechnological modification trials, lignin was added at a concentration of 2 $g \cdot L^{-1}$ to obtain a sufficient quantity of product for subsequent analyses. In the first batch, lignin was added to the culture medium and inoculated with a specific fungal strain. A mineral cultivation medium with a reduced glucose concentration (5 $g \cdot L^{-1}$) was used. After a 14-day incubation period, the modified lignin was filtered, washed thoroughly with water, centrifuged at 3,130 rcf for 3 minutes, and freeze-dried. Fresh lignin was then introduced into the medium for the second batch.

Antioxidant properties, TPC, FT-IR and molecular weight of modified lignin were determined as described in Chapter 4.2.2. Antimicrobial activity was analysed following the procedure outlined in Chapter 4.4.2. Since lignin nanoparticles were required for antimicrobial testing, they were prepared accordingly.

4.6 Lignin ultrathin films

Ultrathin lignin films were prepared using quartz crystal microbalance with dissipation monitoring (QCM-D). For films preparation, grape seeds LNP were used alongside four different polyelectrolytes (PEs), see Figure 21.

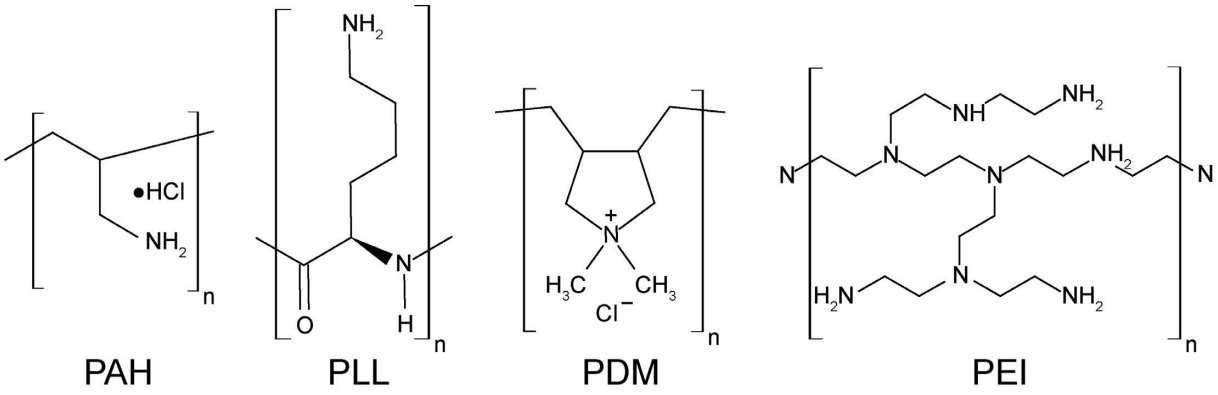

Figure 21 The structure of polyelectrolytes used for LBL adsorption experiments: polyallylamine hydrochloride (PAH), poly-L-lysine (PLL), polydiallyldimethylammonium chloride (PDM) and polyethyleneimine (PEI)

4.6.1 QCM-D

The QCM-D instrument enables the simultaneous measurement of changes in resonance frequency (Δf) and energy dissipation (ΔD), which occur due to mass adsorption on a piezoelectric crystal's surface [239]. The dissipation parameter reflects energy losses during the crystal's oscillation and depends on the material's viscoelastic properties. This allows the characterization of molecular layers formed on the sensor during adsorption.

For rigid adsorbed layers fully coupled to the crystal's oscillation, the frequency shift (Δf) relates to mass change (Δm) via the Sauerbrey Equation (6):

$$\Delta m = C\frac{\Delta f_{\mathrm{n}}}{n} \tag{6}$$

where C is the Sauerbrey constant (-17.7 ng·Hz^{-1}·cm^{-2} for a 5 MHz crystal), n is the overtone number (e.g., 1, 3, 5), and Δf (Hz) represents the observed frequency shift [240].

For soft film not fully coupled to the crystal's oscillation, the Sauerbrey relation no longer applies due to energy dissipation occurring within the film during oscillation. Dissipation (D) is defined as equation (7):

$$D = \frac{E_{\mathrm{diss}}}{2\pi E_{stor}} \tag{7}$$

where E_{diss} is the energy dissipated, while E_{stor} represents the stored energy in one oscillation cycle. During adsorption, changes in dissipation (ΔD) and frequency (Δf) were recorded over time, with the third overtone (Δf_3, ΔD_3) were analysed.

4.6.2 Lignin nanoparticles-polyelectrolytes LBL assembly

For the layer-by-layer (LBL) assembly lignin nanoparticles, 4 negatively charged PEs (polyallylamine hydrochloride (PAH), poly-L-lysine (PLL), polydiallyldimethylammonium chloride (PDM) and polyethyleneimine (PEI)) and gold crystals as substrates were used. The PEs were dissolved at 0.1 wt% in 100 mM NaCl and Milli-Q water, and the pH-value adjusted with 1 M HCl or NaOH. QCM-D Q sense model E4 and gold sensor surfaces (QSX-301) were used. The sensors were rinsed with Milli-Q-water in the assembled QCM-D cells for

20 minutes, followed by the PE solution for approximately 20 minutes, and rinsed again with Milli-Q water to remove loosely bound molecules for another 20 min. For the second layer, sensors were rinsed with the LNP solution (concentration 1 $g \cdot L^{-1}$) and rinsed again with Milli-Q water, each for 20 min. Layer three and four followed in the same manner (Figure 22). In all cases the flow rate was 0.1 $mL \cdot min^{-1}$.

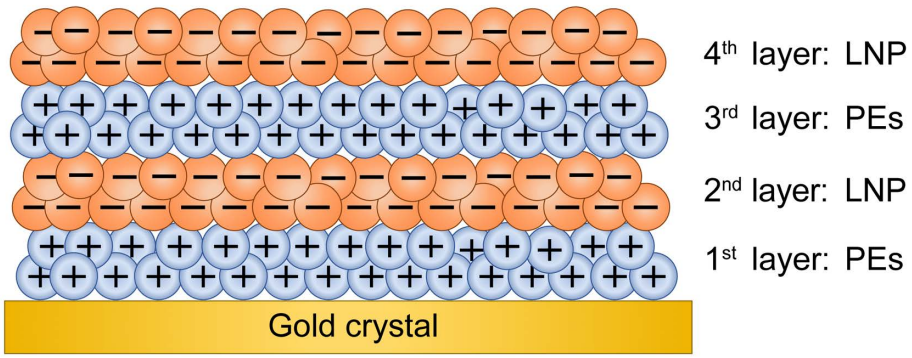

Figure 22 Scheme of the LBL assembly process using LNP and specific polyelectrolytes, each applied in two consecutive layers onto a gold crystal. The LBL assembly is facilitated by the electrostatic attraction between the oppositely charged molecules in the layers. This structure was prepared for and analysed using a QCM-D experiment.

4.6.3 Atomic force microscopy

Atomic force microscopy (AFM) images were collected in tapping mode with a Tosca™ 400 atomic force microscope utilizing silicon cantilevers (AP-ARROW-NCR) from Nanoworld AG with a resonance frequency of 285 kHz and a force constant of 42 $N \cdot m^{-1}$. Image processing and calculation of root mean square roughness (RMS) were performed with Gwyddion v2.59 software.

4.6.4 Water contact angle

Water contact angle of the LBL assembly was analysed similar as described in chapter 4.3.2.

4.6.5 Antioxidant activity of LBL assembly

Antioxidant activity of prepared LBL assembly was analysed following the protocol described in chapter 4.2.2 with slight modifications. The gold crystal was immersed in 2 mL of ABTS solution, ensuring complete submersion. The previously described $ABTS^{\cdot+}$ assay was then performed, and the change in absorbance was determined at time 0 and 10 minutes.

4.6.6 Antimicrobial activity of LBL assembly

Antimicrobial activity of prepared LBL assembly was analysed following the protocol described in chapter 4.4.2. The coated gold crystals were added to 4 mL of diluted inoculum with final absorbance of 0.1. Turbidity changes were measured at 600 nm using an ELISA reader at 0 and 24 hours. A diluted inoculum containing a sterile gold sensor crystal was used as a blank.

5. RESULTS AND DISCUSSION

5.1 Agricultural waste lignin isolation

Agricultural waste, particularly grape and rose hip seeds, along with plum and cherry shells, was utilized as raw material for lignin extraction. This approach aligns with upcycling principles, aiming to convert waste into valuable products. These annual plant materials are known to have a high lignin content [241], making them promising sources of lignin with unique properties, such as antioxidant and antimicrobial activities [242–244]. Notably, plum and cherry endocarp biomass and grape seeds can be readily sourced from the well-established fruit processing industries, offering advantages in feedstock supply chain stability and logistics.

Currently, plum and cherry kernels are of significant interest due to their high oil content and bioactive compounds, which have various applications [245, 246]. In contrast, I focus in this study on the shells (endocarp), the hard outer layer of the stone that encases the seed, which have limited value-added applications. Significantly, plum production reached approximately 12.5 million tons, and cherry production was around 2.96 million tons globally in 2023, highlighting the abundant availability of these materials [247].

For rose hips, oil extraction is primarily focused on the seeds, which are valued for their nutritional and cosmetic properties [248]. Grape seeds, on the other hand, are rich in bioactive compounds. Grape seed oil is widely used in nutrition, and the seeds themselves can also serve as a food supplement [249]. According to the International Organization of Vine and Wine, global grape production was approximately 77 million tons in 2022 [250], with seeds accounting for around 5% of the total weight [251]. This represents a significant amount of material that could be utilized for further processing, supporting sustainable and circular economy practices.

The first step in processing of all raw agricultural waste material was oil extraction using *n*-hexane. This step was essential to prevent contamination of the isolated lignin by fatty acids while simultaneously obtaining valuable seed oil. The oil yields from grape and rose hip seeds were significantly higher compared to those from plum and cherry shells (Figure 23A), primarily due to differences in sample pretreatment tailored to plant anatomy. For plums and cherries, the kernels were separated from the shells. These kernels, rich in nutrients, support seed growth, while the shells, being low in oil, contribute little to extraction yields. In contrast, the kernels of grape and rose hip seeds are extremely small, making their separation impractical. The oil extraction yields achieved align with reported values, with grape seeds yielding 10–17% [252, 253] and rose hip seeds yielding 5.5% [254].

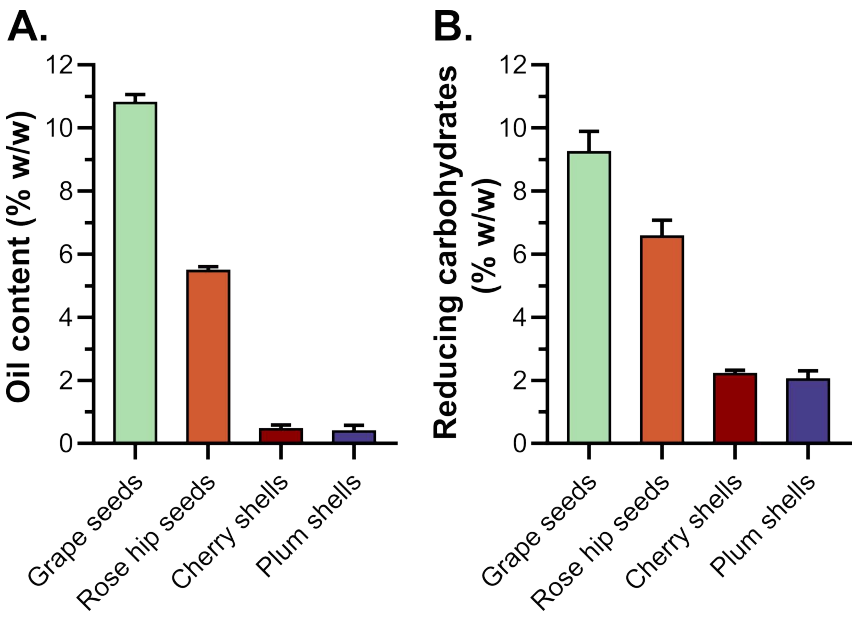

Figure 23 Yield of oil and reducing carbohydrates during pretreatment steps

Agricultural waste also represents a potential source of carbohydrates that can serve as a low-cost carbon source for biotechnological production [255, 256]. Therefore, pretreatment including carbohydrate extraction was incorporated into the process. This step was particularly important given the relatively low efficiency of soda pulping, as it helps minimize cellulose and hemicellulose contamination in the isolated lignin. To enhance carbohydrate yields, enzymatic hydrolysis was employed [257]. This strategy offers two key advantages: it facilitates the extraction of more valuable carbohydrates and simultaneously improves lignin accessibility within LCC. As shown in Figure 23B, reducing carbohydrate content was quantified after hydrolysis. The highest yield was obtained from grape seeds, reaching up to 10% w/w. In contrast, cherry and plum stones provided significantly lower yields, approximately 2% w/w. This discrepancy is attributed to differences in sample mechanical pretreatment, as explained in the previous paragraph.

Following the pretreatment steps, lignin was isolated using the soda pulping method, which is particularly suitable for non-wood lignocellulosic materials. Although this method may have a lower efficiency compared to the Kraft process, it offers a significant advantage: the resulting lignin is sulfur-free. This absence of sulfur compounds is beneficial for subsequent material applications, as it preserves the lignin's native phenolic hydroxyl groups, thereby maintaining its inherent antioxidant properties [258, 259].

The isolation yield is presented in Figure 24B. The highest yield was recorded for plum shells (35.5 ± 3.0% w/w), followed closely by cherry shells, which were only 2% lower. Conversely, the lowest yield was obtained from rose hip seeds, at 10.4 ± 0.9% w/w. These results exhibit an inverse trend compared to oil and carbohydrate yields, which was expected, as plum and cherry shells are more compositionally homogeneous and contain higher lignin levels, as determined by the Klason lignin method (Figure 24A). Lignin content here refers to the sum of acid-soluble and acid-insoluble lignin fractions. The high lignin content in these fruit wastes highlights their potential as an interesting source for lignin isolation [260]. However,

the relatively low yield of grape seeds lignin (GSL) and rose hips lignin (RHL) extraction indicates potential for optimization and presents a challenge for further research.

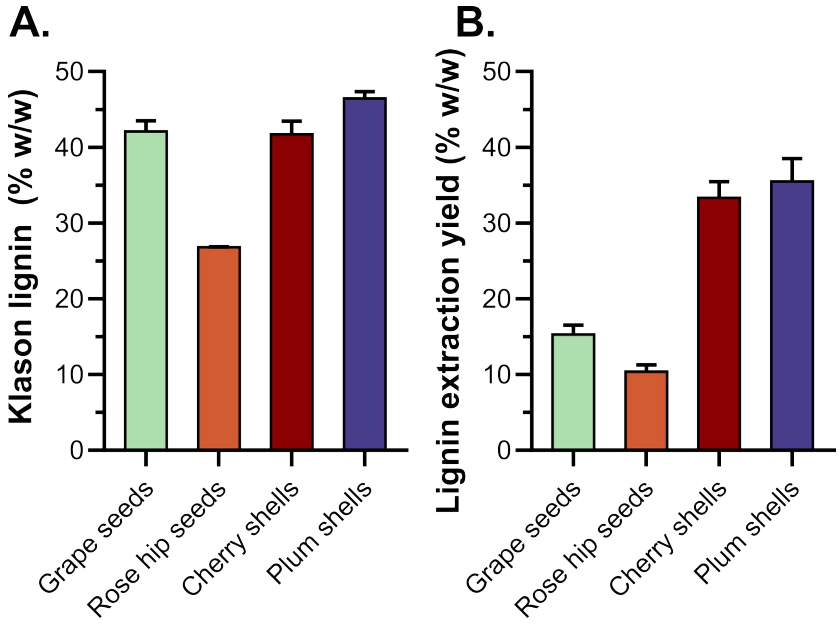

Figure 24 Lignin content in agricultural waste expressed as Klason lignin (A) and lignin extraction yield of soda pulping method.

5.2 Lignin characterisation

5.2.1 FTIR

The structural composition of the isolated lignin samples was studied using FT-IR spectroscopy, with commercial alkali, kraft, and organosolv lignin samples included for comparison. The FT-IR DRIFT spectrum (Figure 25) confirmed several characteristic spectral features of lignin, according to [261–266]. A broadband of around 3400 cm^{-1} corresponds to the stretching vibration of the hydroxyl groups in phenolic and aliphatic structures. The bands between 3000 cm^{-1} and 2850 cm^{-1} are attributed to asymmetric and symmetric C–H stretching in $–CH_2–$ groups. The peak at 1710 cm^{-1} is assigned to C═O stretching vibrations in non-conjugated ketones, carbonyl, and ester groups. Additionally, the band at 1624 cm^{-1} is associated with C═O conjugated to the aromatic ring and eventually to aliphatic carboxylates. The skeletal vibrations of C═C stretching in aromatic rings are represented by peaks at 1598 cm^{-1}, 1514 cm^{-1}, and 1423 cm^{-1}, while deformation vibrations of the $–CH_2–$ and $–CH_3$ groups are observed at 1463 cm^{-1}.

The region below 1300 cm^{-1} is more complex due to overlapping signals from lignin and carbohydrate components however, characteristic lignin features could still be distinguished. Signals specific to guaiacyl units were detected, with notable bands at 1269 cm^{-1} and 1220 cm^{-1}, corresponding to C–O stretching in guaiacyl aromatic methoxyl groups [267]. Additionally, a peak associated with syringyl units was observed at 1125 cm^{-1} attributed to aromatic C–H in-plane deformation.

Typically, lignin spectra exhibit a peak around 1030 cm^{-1}, attributed to aromatic C–H in-plane deformation and C–O stretching in primary alcohols. However, in the soda lignin samples, this peak was shifted to 1045 cm^{-1} likely indicating contamination with hemicellulose, such as xylan [268]. Hemicelluloses often display absorption bands in the 1030–1050 cm^{-1} range, corresponding to C–O and C–C stretching and C–OH bending vibrations. This assumption is further supported by the high intensity of this peak, which is also characteristic of xylan. The observed shift and increased intensity suggest overlapping contributions from lignin and hemicellulose components.

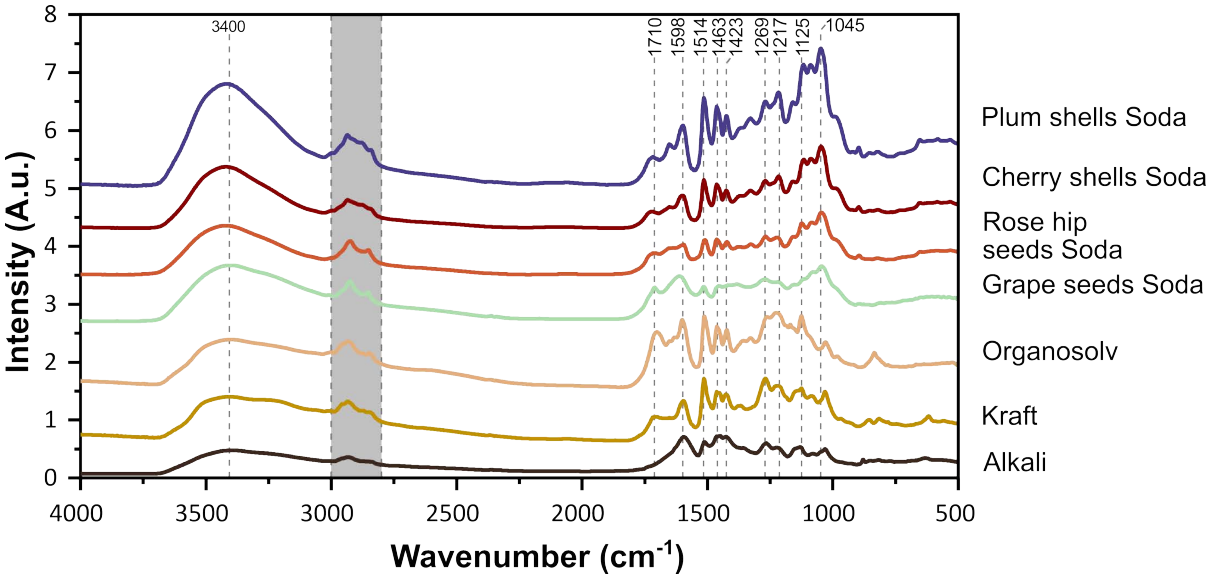

Figure 25 FT-IR DRIFT spectrum of lignin samples.

5.2.2 Elemental analysis

Elemental analysis was another method used for lignin characterization, revealing some unexpected results, most notably the absence of sulfur in all samples, including kraft lignin, which typically contains sulfur groups due to the kraft pulping process (Figure 26). Sodium sulfide, used in the process, generates HS^- nucleophilic anions in an alkaline environment [31]. These anions not only enhance lignin solubility but also incorporate sulfur in the form of thiol groups [269]. However, this result can be explained by the use of Indulin AT, a commercial kraft lignin derived from pine, which is highly purified and unsulfonated. Similarly, the alkali lignin sample is declared to have a low sulfonate content. The remaining lignin samples lack sulfur compounds due to the principle of their isolation process.

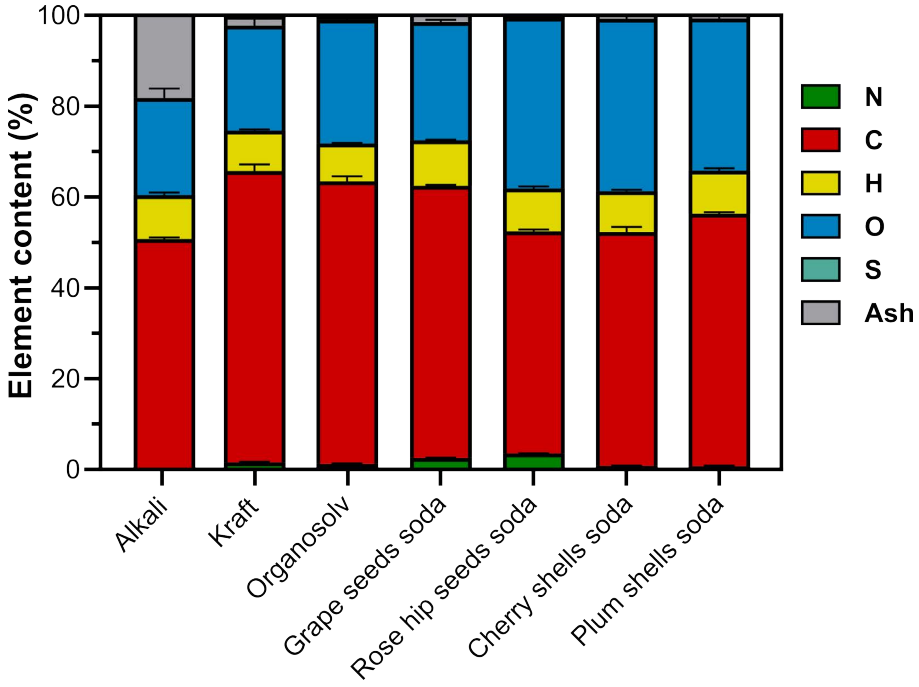

Figure 26 Elemental composition of lignin samples. N – Nitrogen; C – Carbon; H – Hydrogen; O – Oxygen; S – Sulfur. Alkali lignin contain high amount of ash and grape and rose hip seeds lignin contain higher amount of nitrogen caused probably by protein contamination.

Another notable observation is the high nitrogen content in GSL and RHL. This is likely due to the pretreatment method, as the seeds (embryos) were not removed from the grape seeds or rose hips for practical reasons. Consequently, the samples may have been more contaminated with proteins [270]. The alkali lignin sample also exhibited a notably high ash content, likely attributable to its high residual ions content, as the alkali lignin solution had a pH of 11 when dissolved in water.

Finally, the elemental composition of the other samples aligns well with typical values reported in the literature [271, 272]. Exact data are shown in the Table 10.

Table 10 Elemental composition of lignin samples

Lignin sample	N	C	H	S	O	Ash
Alkali	0.09 ± 0.01	50.71 ± 0.34	9.63 ± 0.56	0	21.41 ± 2.11	18.16 ± 2.13
Kraft	1.59 ± 0.17	64.13 ± 1.49	8.90 ± 0.31	0	23.13 ± 1.56	2.25 ± 0.03
Organosolv	1.23 ± 0.11	62.28 ± 1.09	8.28 ± 0.13	0	27.31 ± 1.20	0.90 ± 0.18
Grape seeds soda	2.58 ± 0.09	59.89 ± 0.26	10.04 ± 0.16	0	26.07 ± 0.46	1.42 ± 0.04
Rose hip seeds soda	3.60 ± 0.03	48.84 ± 0.48	9.50 ± 0.40	0	37.62 ± 0.62	0.44 ± 0.05
Plum shells soda	0.79 ± 0.10	51.57 ± 1.12	8.95 ± 0.34	0	37.98 ± 1.09	0.71 ± 0.05
Cherry shells soda	0.76 ± 0.14	55.56 ± 0.35	9.50 ± 0.57	0	33.49 ± 0.56	0.69 ± 0.03

5.2.3 Antioxidant activity and polyphenol content

Antioxidants play a critical role by preventing oxidation reactions caused by oxidative stress, reactive oxygen species, and related agents [273]. This protective function is essential for safeguarding living organisms and biological tissues from oxidative damage. Similarly, polymer materials such as polypropylene and polyethylene are prone to oxidative degradation, where antioxidants can also provide valuable protection.

Numerous studies have investigated the antioxidant activity of different lignin types, including Kraft lignin [274–277], organosolv lignin [55, 274, 277–280], soda lignin [55, 279, 281, 282], and alkali lignin [283]. However, the diversity of methods used to assess antioxidant activity, and the varying units of expression make it challenging to directly compare results across studies. Comparisons are more reliable when samples are analysed under consistent conditions.

From the comparison of the results of commercial lignin samples analysed in this work (Figure 27A), it is evident that Kraft lignin exhibited the highest antioxidant activity, reaching 738.9 ± 28.4 mg Trolox per gram of lignin. This enhanced performance could be attributed to using highly purified Kraft lignin (Indulin AT) in the study, rather than conventional Kraft lignin. The notable antioxidant activity of Indulin AT has also been reported previously [277]. Organosolv lignin displayed slightly lower antioxidant activity, while alkali lignin exhibited the lowest value of 393.4 ± 40.9 mg Trolox per gram. These findings highlight the variability in antioxidant performance among lignin types, which could be influenced by their structural differences and the presence of specific functional groups.

Significant differences were observed in the antioxidant activity of Soda lignin samples derived from agricultural waste. The highest activity was recorded for GSL, reaching 847.7 ± 51.0 mg Trolox per gram of lignin. This result aligns with the natural abundance of antioxidants in grape seeds, including flavonoids – group of phenolic pigments. Key compounds such as catechin and epicatechin, which polymerize to form proanthocyanidins, are highly effective antioxidants [284, 285]. Additionally, grape seeds contain gallic acid, its esters, and their polymers, collectively known as hydrolysable tannins. These compounds may not have been fully removed during GSL isolation, likely contributing to the high antioxidant activity observed in this case.

In contrast, lignin from plum and cherry shells exhibited moderate antioxidant activity, while rose hip seed lignin showed the lowest activity, reaching only 242.4 ± 14.7 mg Trolox per gram of lignin.

As shown in Figure 27, the antioxidant activity results exhibit a strong correlation with the total phenolic content (TPC) values. This correlation is expected, as the TPC method relies on a redox mechanism to quantify total phenols in the sample, aligning with the redox–based detection principle of the $ABTS^{\cdot+}$ assay. Thus, the TPC results validate the findings from the $ABTS^{\cdot+}$ assay.

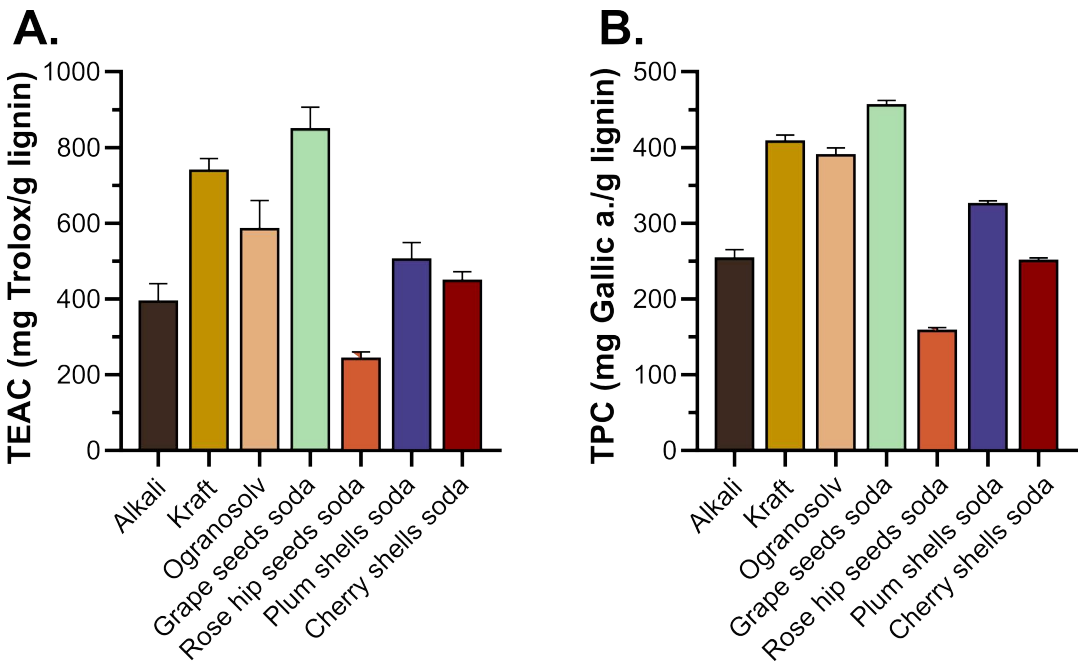

Figure 27 Comparison of Antioxidant activity expressed as Trolox equivalent (TEAC) (A) and Total phenolic content (TPC) (B). The results correlate with each other, which is usual for lignin, and point to the best antioxidant values of lignin isolated from grape seeds.

5.2.4 Molecular weight

The number-average molecular weight (Mn), weight-average molecular weight (Mw), and polydispersity index (PDI) of lignin samples were determined through size exclusion chromatography It is important to note that these molecular weight values are considered apparent ($M_{w_{app}}$), as two correction steps were required to account for lignin absorption and fluorescence in the MALLS data. According to Zinovyev *et al*. [286], both phenomena can cause significant overestimation of Mw. Fluorescence becomes more prominent at longer elution times, compounding the overestimation. To address this, data from the early portion of the MALLS chromatogram were fitted with an exponential model and extrapolated to later elution times, yielding corrected apparent ($M_{w_{app}}$) values (Table 11).

Kraft lignin displayed the lowest Mw, which aligns with previous findings for Indulin AT [287–289]. Because molecular weight can influence antioxidant activity [290], this relatively low Mw may help explain the high antioxidant activity observed for Kraft lignin, whereas alkaline lignin with the highest Mw exhibited the lowest antioxidant activity. Differences among agricultural waste lignin samples were not substantial, particularly with regard to Mn. Furthermore, molecular weight may play a role in determining the size of lignin nanoparticles [291].

Table 11 Molecular weight of lignin samples

Lignin sample	Mw (kDa)	Mn (kDa)	PDI (kDa)
Alkali	19.50 ± 0.50	17.77 ± 0.70	1.10 ± 0.02
Kraft	6.01 ± 0.57	1.95 ± 0.35	3.11 ± 0.26
Organosolv	12.33 ± 0.16	1.86 ± 0.13	6.65 ± 0.37
Grape seeds soda	12.98 ± 0.62	3.56 ± 0.11	3.67 ± 0.29
Rose hip seeds soda	12.19 ± 0.23	3.71 ± 0.64	3.33 ± 0.51
Plum shells soda	10.19 ± 0.13	3.12 ± 0.06	3.27 ± 0.10
Cherry shells soda	8.59 ± 0.42	3.71 ± 0.11	2.32 ± 0.18

5.2.5 Solubility

The solubility of lignin is a crucial parameter in its characterization and can be evaluated using Hansen solubility parameters (HSP). This method allows for identification of suitable solvents for lignin and can be graphically represented. The solubility screening results summarized in (Table A1).

Using spreadsheet available at [292], I generated HSP spheres (Figure 28) to visually represent solubility. Among the tested samples, organosolv lignin exhibited the highest solubility in the screening test, resulting in the largest sphere radius, which represents the distance to the outermost good solvent. However, due to the inclusion of several "false positive" solvents, classified as good solvents despite not actually dissolving the lignin, organosolv lignin had a lower fit accuracy compared to Kraft and grape seed soda lignin.

In contrast, grape seed lignin had the lowest solubility and correspondingly the smallest sphere radius. Alkali lignin was unique in being the only sample soluble in water, while simultaneously showing low solubility in most organic solvents. This limited solubility reduced the model's reliability, with a fit accuracy of only 13%. The complete solubility of Alkali lignin in water is unusual for lignin and can be attributed to the high pH (~12) of the solution, suggesting the presence of hydroxide ions (OH^-), likely originating from residual alkali compounds in the sample.

The obtained HSP data were used to select appropriate solvents for subsequent experiments, optimizing both time and resource consumption. The potential of HSP for obtaining specific lignin fractions has been explored in the work of Leuken *et al.* [293].

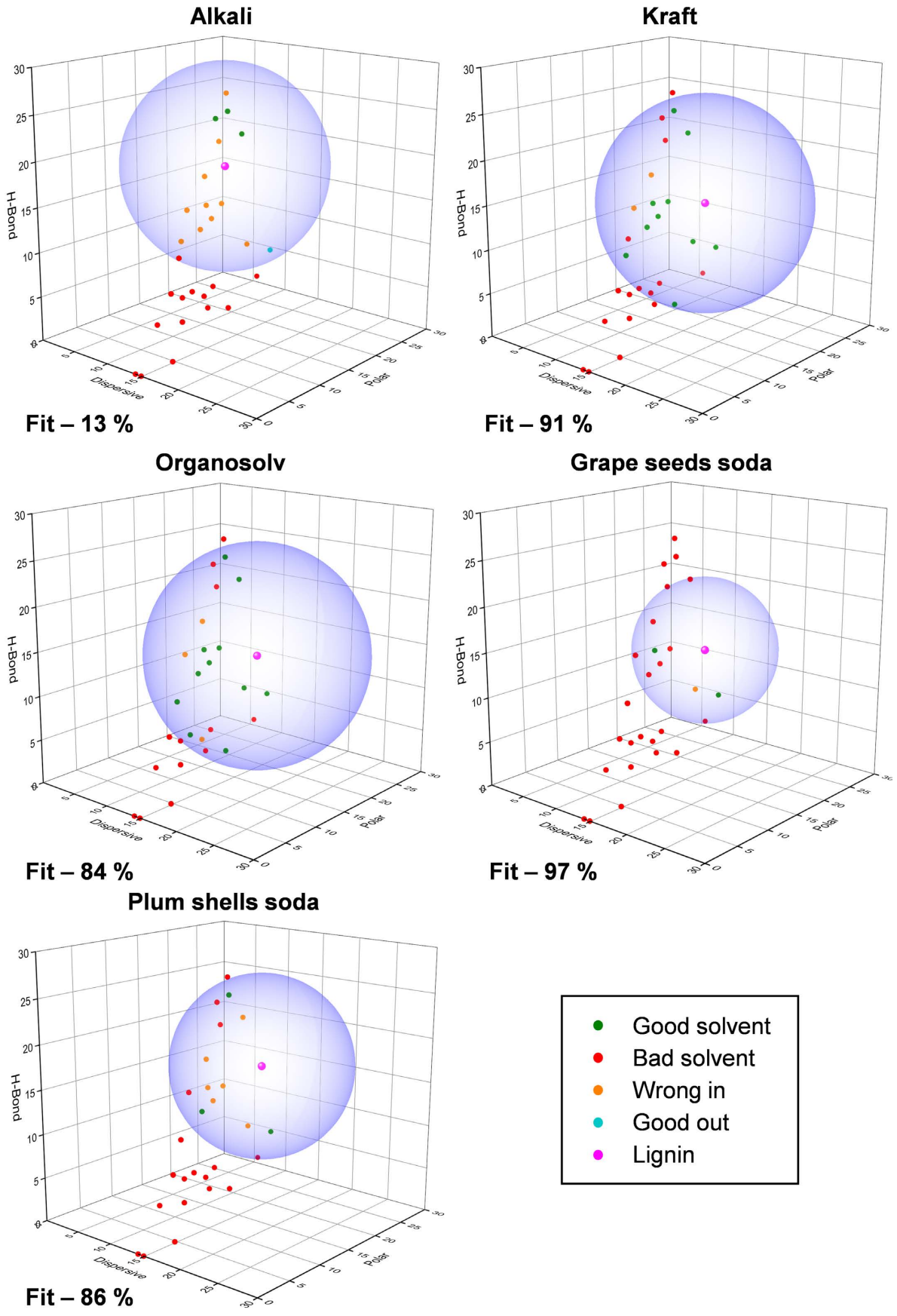

Figure 28 HSP spheres of lignin samples. Units for dispersion forces δ_D, polar interactions δ_P and hydrogen bonding δ_H are $MPa^{0.5}$. Fit values represent model fit accuracy.

Despite its usefulness, the Hansen solubility method has limitations. Firstly, it is a qualitative rather than a quantitative approach, which may introduce inaccuracies. However, using a large number of solvents helps mitigate this issue. Secondly, the method requires a wide range of organic solvents for testing, making it essential to evaluate whether its application is justified in a given context [294].

To further assess lignin solubility, samples were quantitatively analysed using pre-selected solvents and their aqueous mixtures. Figure 29 shows that DMSO was the best solvent, achieving up to 100% solubility for organosolv and plum stone soda lignin. DMSO is widely recognized as an effective solvent for lignin [295]. Another highly effective solvent was an aqueous mixture of THF, which dissolved more than 90% of Kraft, organosolv, and grape seed soda lignin. In contrast, water was the poorest solvent, as lignin is generally insoluble in neutral water, as previously discussed. Overall, the results indicate that aqueous mixtures of organic solvents were generally more effective than pure organic solvents, as the presence of water adjusted the solubility parameters of the mixture to better match those of lignin. This trend was also predicted using the HSP spreadsheet.

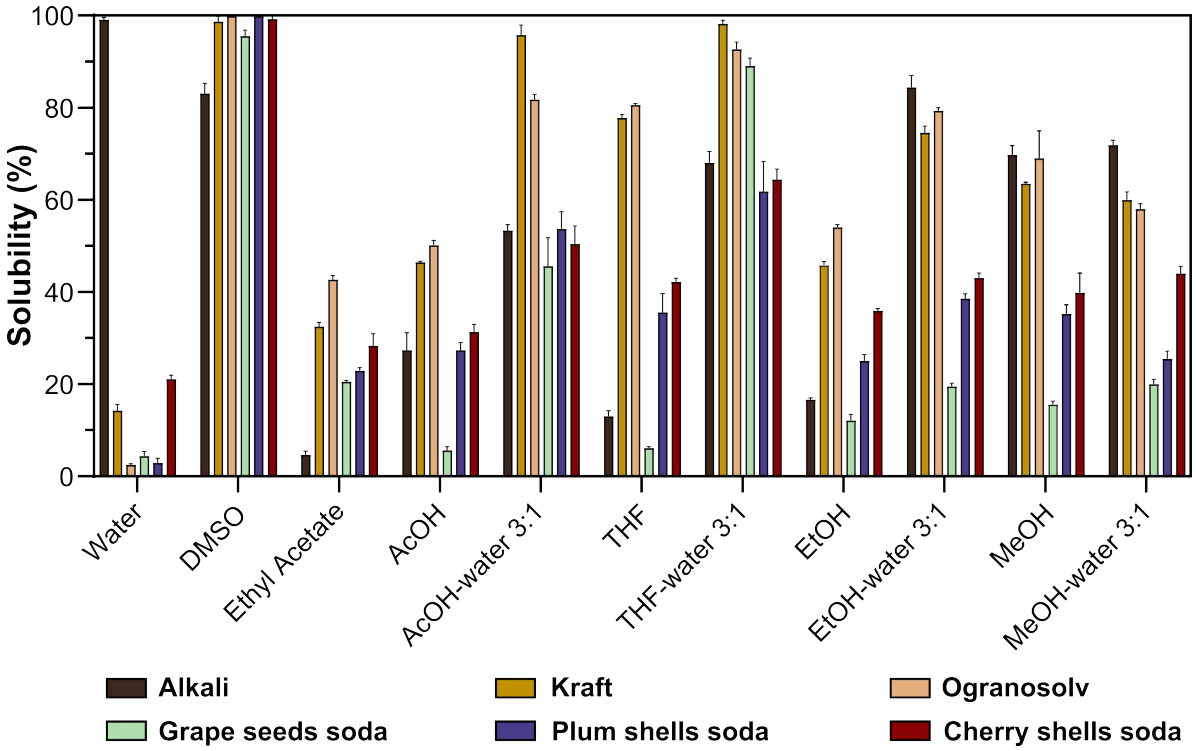

Figure 29 Comparison of lignin solubility in organic solvents and their aqueous mixtures

5.3 PHA solid blocks

Due to their favourable properties, PHA are considered highly promising bio-based materials for a wide range of applications. This study builds on our previous work, which explored the blending of PHA with GSL, two bio-based and biodegradable materials, for the preparation of thin films intended for active food packaging. These films exhibited antioxidant activity attributed to the presence of GSL [90].

In contrast to that research, the current study focuses on the modification of PHA using GSL and bacterial cellulose (BC), another bio-based and biocompatible polymer, to develop porous materials aimed at medical applications. This shift in application leverages the inherent biocompatibility of both PHA and BC. It is important to highlight that developing a composite material based on hydrophobic PHA and hydrophilic BC presents significant challenges.

To the best of my knowledge, while studies on PHA/BC composites exist, they primarily involve materials prepared through dissolution in chloroform, a highly toxic and environmentally hazardous solvent [296–299]. In contrast, this work presents a method for preparing a porous composite without the use of halogenated solvents. Although halogenated solvents are considered the gold standard for processing PHA, their toxicity significantly limits the broader adoption of PHA-based materials.

5.3.1 Dynamical mechanical analysis

The mechanical properties of PHA solid blocks were evaluated using dynamic mechanical analysis (DMA). The three-point bending method was selected as the most suitable approach for testing the prepared porous cryogels, which could not be shaped into other geometries.

Initially, the viscoelastic properties of PHA samples with varying ratios of PHA to DMSO were tested to determine the formulation with the most favourable properties. A range of 5-10 wt% PHA in DMSO was examined, determined by the solubility of P3HB in DMSO and its capacity for solidification (Figure 30A). Samples containing 5 wt% PHA in DMSO exhibited brittleness, while those with 10 wt% were too viscous in a liquid state, presenting challenges for handling. Based on these observations, a 7.5 wt% PHA concentration was identified as having the optimal balance of properties, and this ratio was used for all subsequent analyses.

PHA cryogels exhibited an E’ modulus in the range of tens of MPa, approximately an order of magnitude larger than the values measured for polyvinyl alcohol (PVA)/cellulose nanofibers (CNF) aerogels [300]. However, porous materials based on CNF [301], PLA [302], and PVA reinforced by cellulose nanocrystals [303] achieved E’ modulus in the order of GPa.

PHA solid blocks were subsequently modified using three approaches: 1) the addition of BC, 2) the addition of GSL and 3) the combination of BC and GSL.

The crystalline structure of P3HB contributes to its rigidity and mechanical strength. Conversely, bacterial cellulose, a fibrous hydrophilic polymer, could impede the mobility of P3HB polymer chains when blended, particularly during the cooling and crystallization phases. This restriction in chain mobility may hinder the polymer from achieving its optimal physical state, resulting in a softer material with a reduced storage modulus (Figure 30B). In contrast,

for the mixture of crystalline P3HB and amorphous P3HB-*co*-4HB, the E' modulus decreased only slightly. Furthermore, the additional modification of the PHA blend with BC did not exhibit any adverse effects on the storage modulus.

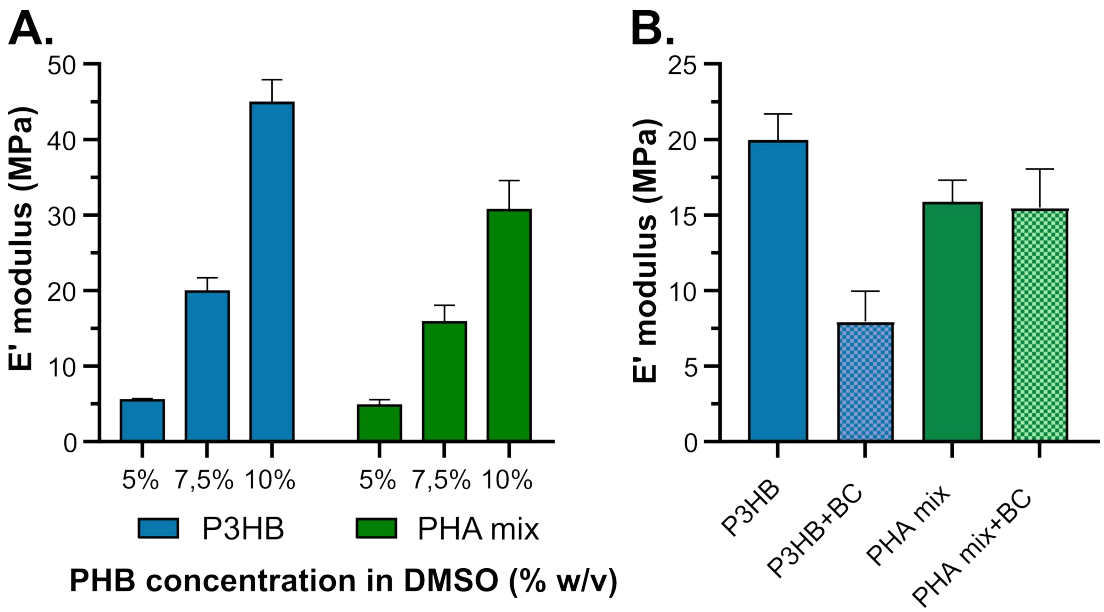

Figure 30 Storage modulus of PHA solid blocks. A) comparison of different concentration of PHA samples in DMSO. B) comparison of modification of solid blocks with bacterial cellulose.

For the second modification of P3HB cryogels, GSL was used. The premise was that GSL could act as a nucleating agent, reducing the energy barrier for nucleation and crystal growth, increasing the density of crystallization centres, and resulting in smaller crystals [93, 95]. This, in turn, positively impacts the viscoelastic properties of the material. A similar effect was previously observed in our earlier study [90], where PHA films with lower GSL concentrations exhibited improved mechanical performance.

In the case of P3HB cryogels, the most pronounced effect was observed with the addition of 1 wt% GSL, which increased the E' modulus to 23.50 ± 4.34 MPa, compared to 19.89 ± 1.80 MPa for neat P3HB (Figure 31A). These findings are consistent with our previous work [90], as well as studies on PHBV [93] lignin/sugar-based polyurethane films [304], and PVC composites [305], where the addition of lignin similarly enhanced mechanical properties.

However, increasing the GSL content further led to a slight reduction in the E' modulus, likely due to phase separation and interfacial incompatibility, which represent ey challenges in the lignin/polymer blend [306, 307]. The impact of GSL addition on PHA blends was limited, and except for 1 and 5 wt% GSL, it decreased the E' modulus (Figure 31B). As a result of the negative effects observed with 10 wt% GSL, this option was not further evaluated.

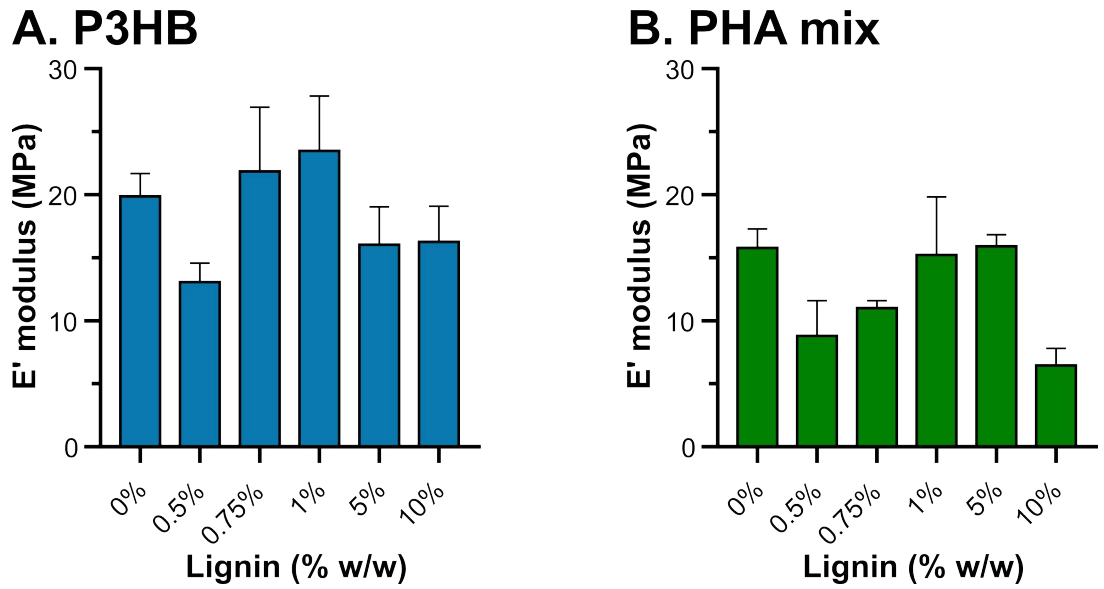

Figure 31 Comparison of storage modulus of P3HB cryogels modified by GSL (A) and PHA blends modified by GSL (B).

The third type of modification combined the previous approaches, involving the addition of both BC and GSL to P3HB and PHA blend. In this modification, the P3HB variant with BC and lignin showed a positive effect in all tested cases (Figure 32A). The most significant improvement was observed with 0.5 wt% GSL, where the E' modulus increased to 13.80 ± 2.09 MPa, compared to P3HB+BC, which had an E' modulus of 7.95 ± 2.00 MPa.

Conversely, for the PHA mix with BC, a significant effect on the E' modulus was only observed with the addition of 0.5 wt% GSL, which had a negative impact (Figure 32B). In all other cases, no significant changes were detected.

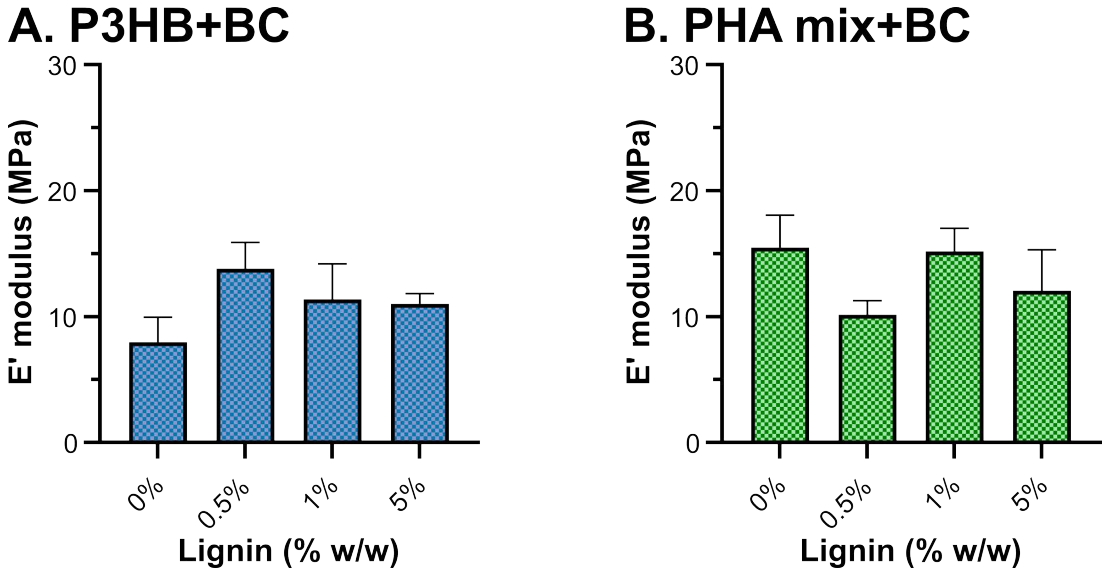

Figure 32 Comparison of storage modulus of composite cryogels based on P3HB and BC, modified by GSL (A) and PHA blends with BC modified by GSL (B).

5.3.2 Differential scanning calorimetry

Thermal properties of mixed PHA cryogels were analysed by non-isothermal differential scanning calorimetry in nitrogen atmosphere. The measured data of P3HB clyogels are summarized in Table 12 and for PHA blends in Table 13. The records of the first heating and cooling cycle are shown in Figure 33, where the thermograms of P3HB and modified samples are compared.

Table 12 DSC data of P3HB and their bacterial cellulose and grape seeds lignin blends

Sample	1st heating scan				Cooling scan	
	T_{m1} (°C)	ΔH_{m1} ($J \cdot g^{-1}$)	T_{m2} (°C)	ΔH_{m2} ($J \cdot g^{-1}$)	T_c (°C)	ΔH_c ($J \cdot g^{-1}$)
P3HB	138.0	7.8	173.5	80.8	100.0	64,63
P3HB+ 0.5% GSL	137.5	20.0	173.0	102.0	105.1	65.4
P3HB+ 1% GSL	140.7	5.9	173.5	82.4	96.9	62.9
P3HB+ 5% GSL	139.0	8.5	172.6	76.5	100.5	57.9
P3HB+ 10% GSL	138.0	7.9	172.1	63.9	98.2	53.5
P3HB+BC	140.0	6.0	171.6	70.3	102.0	60.5
P3HB+BC+ 0.5% GSL	141.3	16.6	173.9	84.9	95.8	62.5
P3HB+BC+ 1% GSL	140.4	9.6	172.9	73.8	93.4	58.7
P3HB+BC+ 5% GSL	139.9	12.1	172.3	86.3	100.5	66.1

Table 13 DSC data of PHA blends with bacterial cellulose and grape seeds lignin

Sample	1st heating scan				Cooling scan	
	T_{m1} (°C)	ΔH_{m1} ($J \cdot g^{-1}$)	T_{m2} (°C)	ΔH_{m2} ($J \cdot g^{-1}$)	T_c (°C)	ΔH_c ($J \cdot g^{-1}$)
PHA mix	138.3	14.5	174.0	79.8	92.3	59.8
PHA mix+ 0.5% GSL	137.8	4.0	171.9	44.4	81.9	20.6
PHA mix+ 1% GSL	138.2	1.1	172.8	41.9	72.7	32.2
PHA mix+ 5% GSL	136.8	5.8	171.3	39.5	83.4	27.3
PHA mix+ 10% GSL	134.1	3.8	172.1	19.0	65.8	14.8
PHA mix+BC	139.7	7.1	171.5	45.7	73.4	22.7
PHA mix+BC+ 0.5% GSL	146.6	1.8	171.1	36.0	72.1	18.3
PHA mix+BC+ 1% GSL	142.3	2.0	170.0	38.0	81.6	19.6
PHA mix+BC+ 5% GSL	140.9	1.3	172.1	33.4	80.0	21.5

During the first heating cycle all tested PHA cryogels showed double melting behaviour. The double melting peak indicates the presence of crystallites with different morphology and thermal stability [308]. Sample of P3HB showed first small melting peak at 138 °C and a broad

doble melting peak at 173.5 °C demonstrating the melting-recrystallization-melting process [309, 310]. Subsequently, P3HB crystallized back at 100 °C during the cooling cycle.

Modification by blending with amorphous P3HB-*co*-4HB did not influence the melting processes during first heating cycles, but the crystallization kinetics of the PHA blend was modified due to the presence of amorphous P3HB-*co*-4HB. The blend crystallized with the lower value of the enthalpy ΔH_c and at lower temperature than unmodified P3HB, large peak of PHA blends indicated slower crystallization kinetics [308].

In case of modification cryogels by addition of BC, was not recorded significant effect on thermal properties of P3HB cryogels. On the contrary, in case of PHA blends, BC decreased the enthalpy of melting as well as enthalpy and temperature of crystallization, that mean that crystallization was slower.

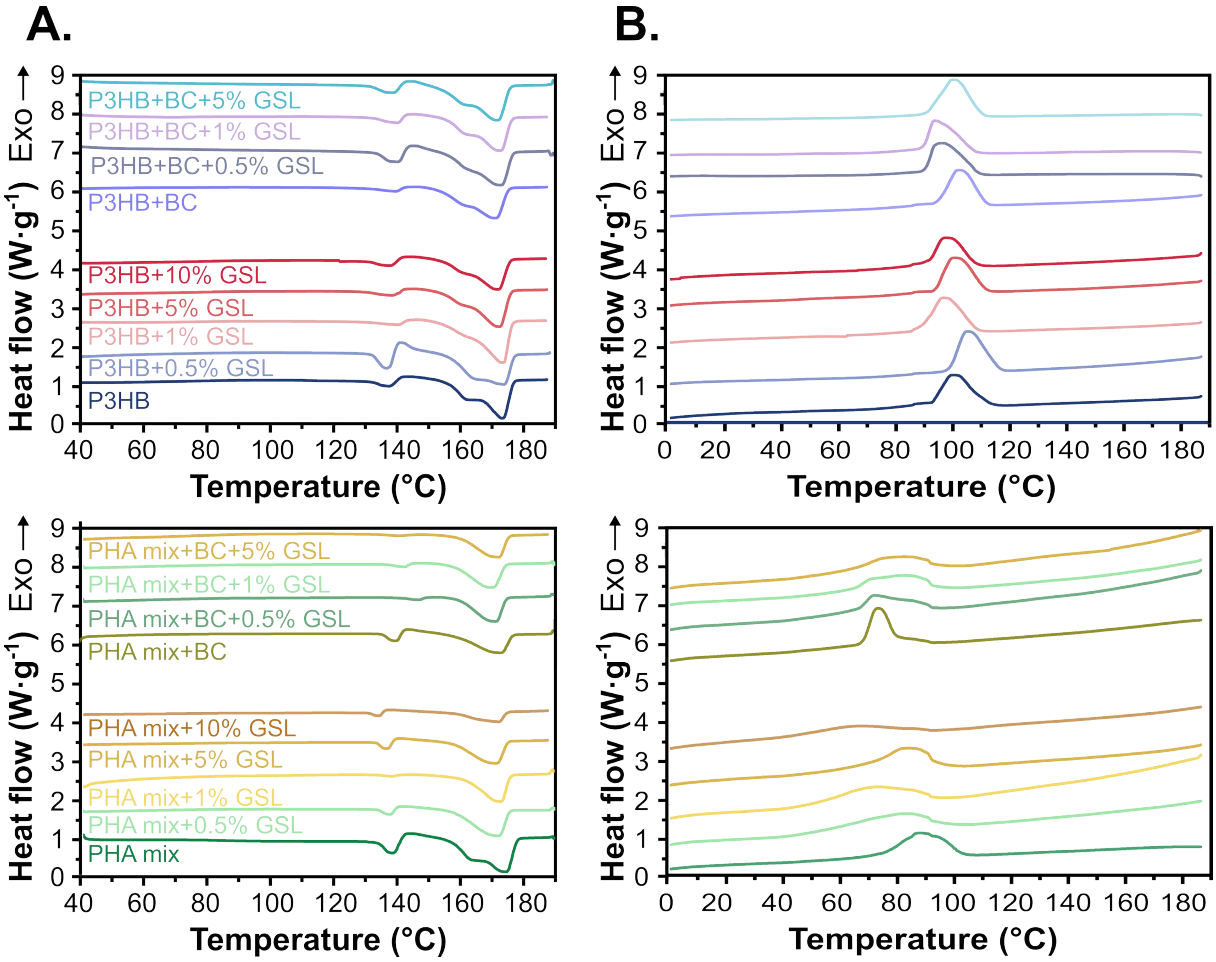

Figure 33 DSC thermograms of first heating (column A) and cooling (column B) cycles of P3HB and PHA blends. The colours of the curves in column A correspond to the samples in column B.

In case of modification by GSL there were not observed clear effect to cryogels. Described effect of lignin in polymers as nucleating agent [93, 95, 311, 312], results in a higher value of Tc and lower ΔH_c and therefore faster crystallization. However, in this study described effect was not observe, T_c was not definitely shifted to higher temperature. The reason may be that solidification of hot dissolved P3HB and blends into a gel form was very slowly and more nucleating centres did not affect the solidification process.

It is important to mention that P3HB belong to the short-chain-length PHA, they are semi-crystalline stiff polymers with a high degree of crystallinity and brittleness. The glass transition temperature (T_g) is related to the amorphous phase of the material [313], which causes that it was not possible to detect the value of T_g by DSC technique.

5.3.3 Thermogravimetric analysis

The thermal degradation of PHA cryogels and modified cryogels was analysed using thermogravimetric analysis (TGA). All samples exhibited a single decomposition step (Figure 34, 35) attributed to polymer chain scission and the volatilization of degradation products [91]. The thermal decomposition mechanism of P3HB is described in detail in the literature [213]. The onset temperature (T_{onset}), temperature of maximal degradation (T_{max}) and the residual mass at 400 °C (m_{rest}) reported in Table 14. The modification of P3HB cryogel with BC slightly decreased T_{onset} by approximately 3.6 °C. In contrast, the PHA blend and BC modified PHA blend exhibited significantly higher T_{onset} values, with increases of about 22.5 °C, 25.2 °C, respectively, compared to unmodified P3HB.

Table 14 The thermal properties of P3HB and its blends analysed by TGA

Sample	T_{onset} (°C)	T_{max} (°C)	m_{rest} 400 °C (%)
P3HB raw	232.5	285.7	0.4
P3HB	203.1	269.1	1.9
P3HB+BC	199.5	256.5	1.0
PHA raw	229.8	292.3	5.0
PHA mix	225.6	280.2	0.1
PHA mix+BC	228.3	287.0	2.6

The addition of GSL lignin to PHA cryogels caused a notable shift in both T_{onset} and T_{max} to higher temperatures across all analysed variants. This enhancement in thermal stability is likely due to the inherent properties and degradation mechanism of lignin [314, 315]. As a natural polyphenolic polymer, lignin contains aromatic structures that impart high thermal resistance. During thermal decomposition, lignin forms a stable char layer, which can act as a protective barrier, reducing the rates of heat transfer and oxygen diffusion [85, 316, 317]. This barrier effect may shield the polymer matrix from rapid degradation. Furthermore, interactions between lignin and the polymer matrix, such as hydrogen bonding, may improve the overall thermal stability by enhancing cohesive forces within the composite.

For the P3HB + 10% GSL sample, lignin particles may have agglomerated or clump together, leading to non-uniform dispersion within the P3HB matrix. These agglomerates could create weak points in the composite, thereby diminishing the effectiveness of the char barrier and potentially accelerating degradation in localized areas.

The observed increase in m_{rest} values can be attributed to the thermal decomposition behaviour of lignin. Lignin undergoes decomposition in three stages, with only the first two

steps completed at 400 °C. As a result, higher lignin content corresponds to a greater m_{rest} value [213].

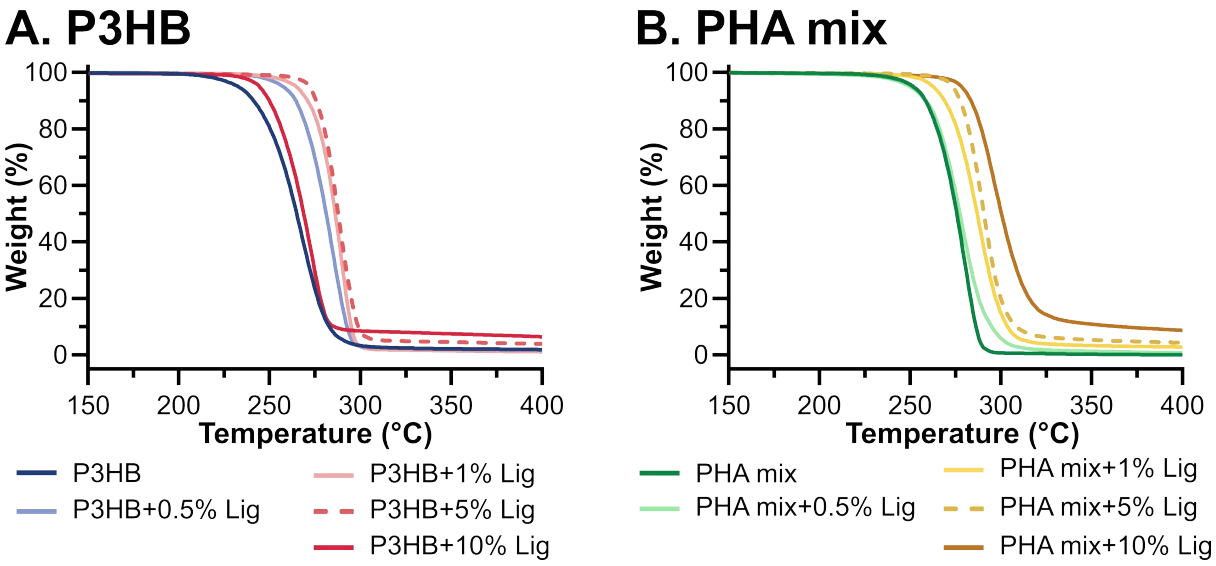

Figure 34 Weight of the samples as a function of temperature obtained by TGA for P3HB and PHA blends

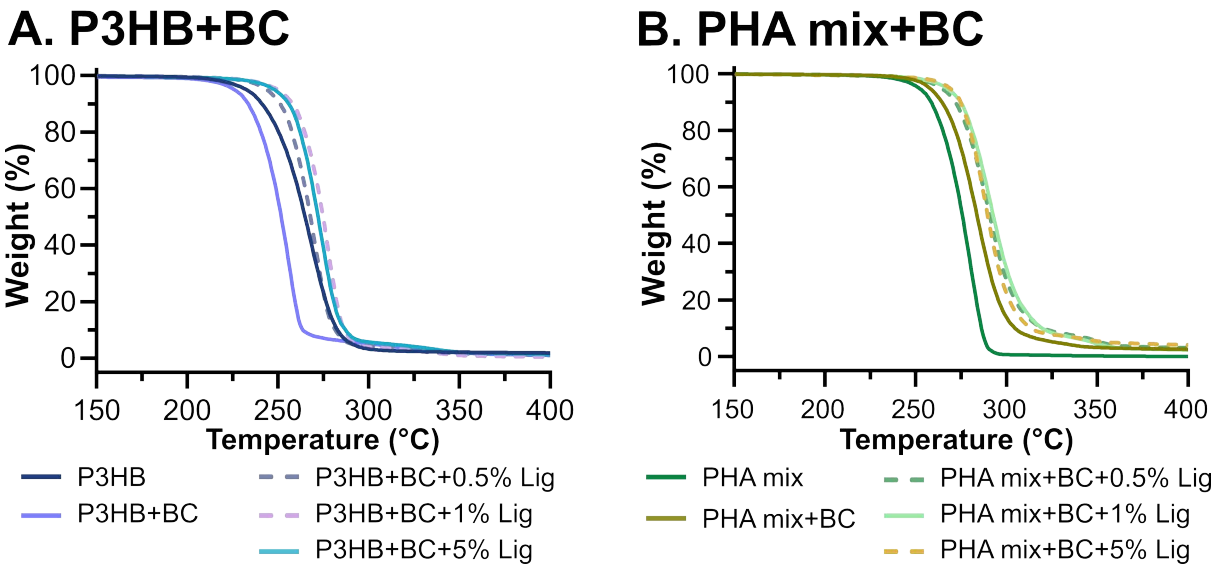

Figure 35 Thermograms of P3HB (A), PHA blends (B) and their modification by BC+grape seeds lignin.

These effects of lignin on the thermal properties of PHA cryogels are consistent with findings from previously published studies [93, 307, 317]. Similar improvements in thermal stability have also been reported for other porous materials, such as lignin-graphene aerogels [318, 319].

5.3.4 Morphology of PHA solid blocks

The surface morphologies of cryogels prepared from P3HB and modified samples were investigated by SEM (Figure 36). Similarly, SEM images of PHA blends and modified cryogels are shown in the Figure 37.

The morphology samples prepared from P3HB and P3HB modified by GSL (Figure 36A and B) differed only slightly. Due to the high solubility of lignin in DMSO and its small particle size at the applied concentration, lignin is difficult to distinguish in the SEM images. In contrast, samples containing bacterial cellulose (Figure 36C and D) exhibited a markedly different morphology. The images clearly show the characteristic fibres of bacterial cellulose, which are randomly arranged and visibly incorporated into the polymer structure.

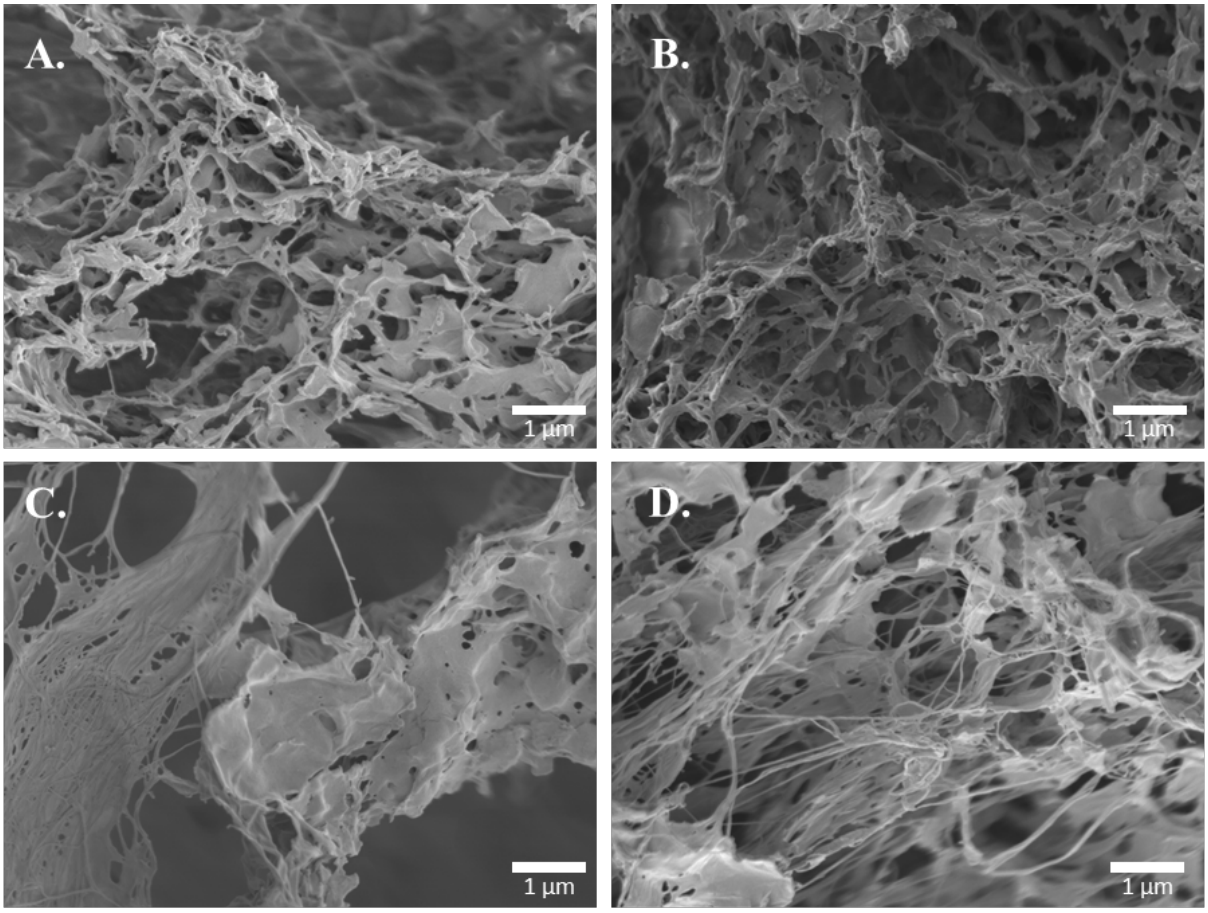

Figure 36 SEM pictures of P3HB cryogels. Pictures were obtained at an accelerating voltage of 1.00 kV, magnification 15,000 X, gentle Beam mode, WD 5-6mm. All pictures were taken using same conditions. (A) P3HB, (B) P3HB modified by GSL, (C) P3HB modified by BC, (D) P3HB modified by BC and GSL.

Figure 37 presents the morphology of PHA blends. Compared to neat P3HB, the pore size appears smaller and less frequent, a trend supported by BET analysis. The bacterial cellulose fibres are again clearly visible, while the small amount of lignin did not cause noticeable changes in the cryogel morphology.

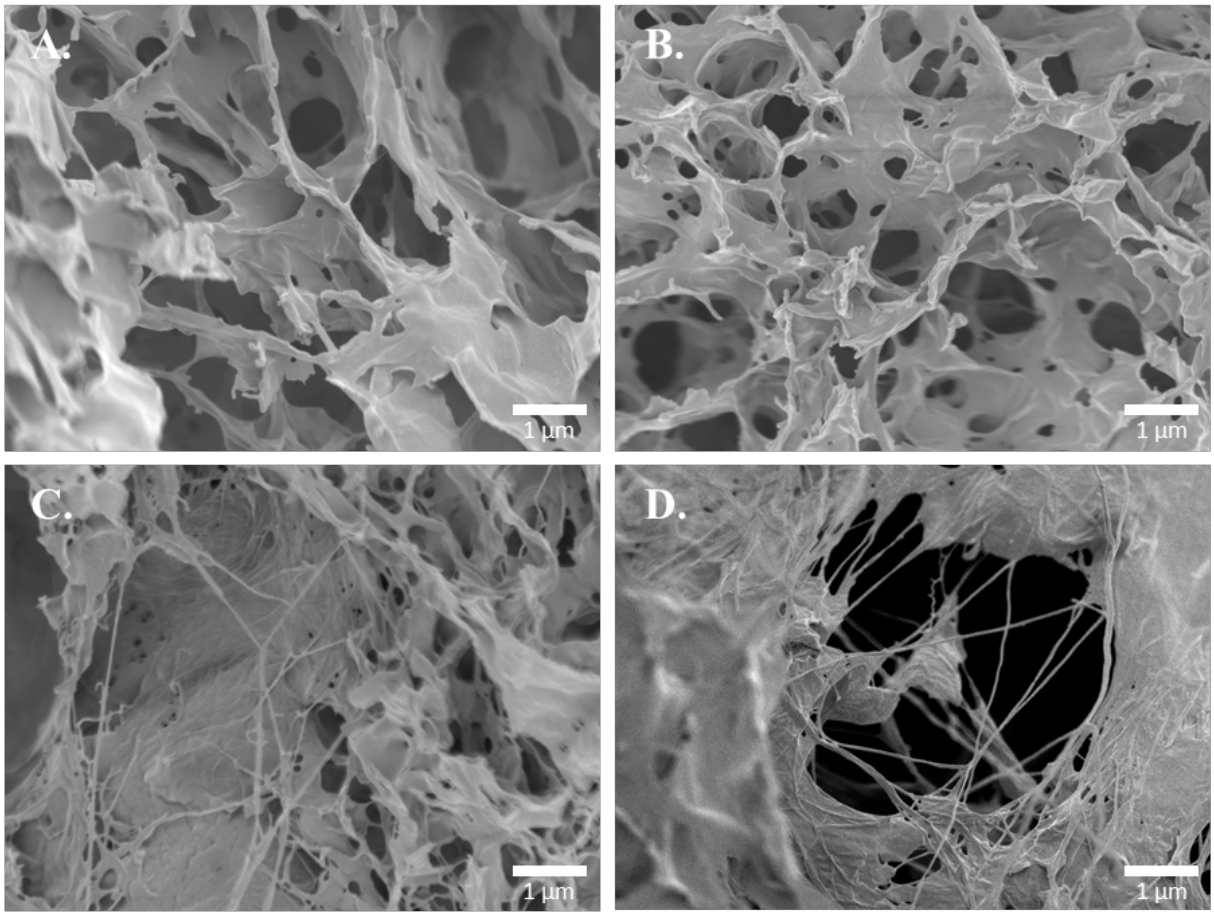

Figure 37 SEM pictures of PHA blend cryogels. All pictures were taken using same conditions: Magnification 15,000 X, 1.00 kV SEI, Gentle Beam mode, WD 2.6-5mm. (A) PHA mix, (B) PHA mix modified by GSL, (C) PHA mix modified by BC, (D) PHA mix modified by BC and GSL.

5.3.5 Surface area

Surface area was analysed using the Brunauer–Emmett–Teller (BET) method, with the results summarised in Table 15. Among the samples, unmodified P3HB exhibited the highest surface area, reaching up to 63.4 $m^2 \cdot g^{-1}$. However, incorporating bacterial cellulose into P3HB led to a reduction in both surface area and pore volume. In PHA blends, a significantly lower surface area and smaller pore sizes were observed, consistent with the structures visualized via SEM (Figure 36, 37).

Table 15 Porosity and density of PHA cryogels

Sample	Surface area ($m^2 \cdot g^{-1}$)	Pore volume ($mm^3 \cdot g^{-1}$)	Density ($mg \cdot cm^3$)
P3HB	63.41 ± 3.09	84.50 ± 8.50	106.31 ± 4.84
PHB+BC	51.46 ± 0.70	76.50 ± 4.50	81.05 ± 6.86
PHA mix	13.20 ± 1.67	13.00 ± 2.00	141.66 ± 7.89
PHA mix+BC	20.58 ± 2.92	23.50 ± 3.50	127.09 ± 5.43

In contrast, modifying PHA blends with BC resulted in an increase in both surface area and pore size, highlighting the influence of BC on the polymer matrix. These modifications also affected material density. Blending BC with both types of polymers increased the overall material volume while having minimal impact on weight, which aligns with expectations given the low density of used BC (0.25 ± 0.03 g cm^3 after freeze drying) [320].

The recorded specific surface areas are within the same range as similar materials based on Poly(3-hydroxybutyrate-co-3-hydroxyhexanoate) prepared using the same method [309]. However, the values are substantially higher than those of P3HB porous scaffolds fabricated via the salt leaching method [321] or PVA-cellulose nanofibrils aerogels [300], despite these materials having similar density ranges. For comparison, silica aerogels [322] and graphene aerogels [323, 324] have been reported to achieve surface areas exceeding 1000 $m^2 \cdot g^{-1}$.

These results provide a comprehensive characterization of our porous material, emphasizing the structural and textural impact of BC incorporation.

5.3.6 Water Interaction Analysis

Polyhydroxyalkanoates are inherently hydrophobic polymers, whereas exhibits a hydrophilic character. After overcoming challenges in combining these heterogeneous materials, I investigated how these modifications influenced the hydrophobic properties of porous PHA cryogels. Changes in hydrophobicity character were assessed by measuring WCA. The highest WCA was recorded for unmodified P3HB (131.0 ± 1.3°), confirming its hydrophobic nature. The measurement results are presented in Figure 38. Modifications via PHA blending and BC incorporation resulted in a decrease in WCA.

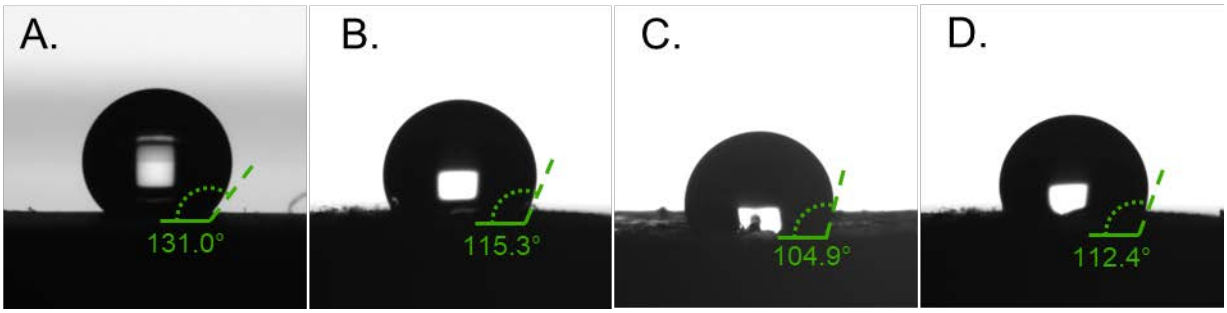

Figure 38 Sessile drop, water contact angle on P3HB (A), P3HB modified by BC (B), PHA blend (C) and PHA blend modified by BC (D)

5.3.7 Antioxidant properties

In addition, the antioxidant properties of PHA cryogels modified with GSL were assessed to determine whether the antioxidant potential of GSL was successfully transferred to the cryogels. As summarized in Figure 39, the results indicate that cryogels containing GSL exhibited dose-dependent antioxidant activity. Samples with 5 wt% GSL demonstrated an antioxidant capacity of approximately 25 mg Trolox equivalents per gram. The theoretical antioxidant activity, based on the GSL content in the samples, was estimated at ~80 mg Trolox equivalents per gram (5.2.3). The observed difference was expected and can be attributed to the partial loss of lignin during the cryogel preparation process, especially during the solvent

exchange, and also to the limited diffusion of the $ABTS^{\cdot+}$ solution into the cryogel matrix during measurement.

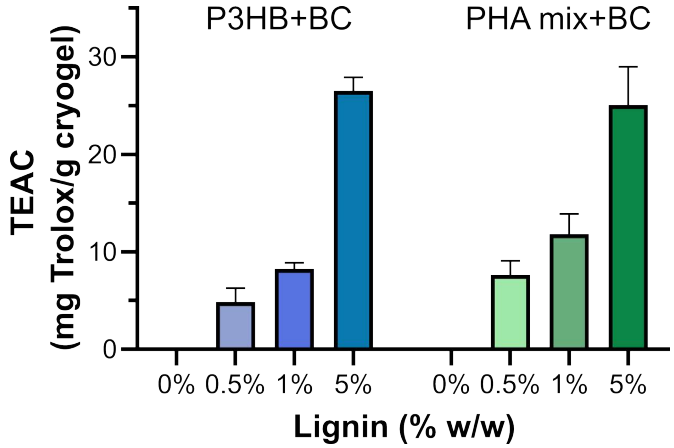

Figure 39 Antioxidant properties of P3HB and PHA mix cryogels modified with BC and GSL. TEAC – Trolox equivalent antioxidant activity.

5.4 Lignin nanoparticles

Lignin's large particle size, heterogeneity, poor dispersibility, and irregular morphology limit its potential as a high-value material [145]. One approach to overcome these challenges is the preparation of lignin nanoparticles (LNP), which serve as a promising and versatile green tool for various applications.

5.4.1 Assessment of the solution system for the preparation of LNP

Based on solubility results, several solvent systems were analysed for lignin nanoparticles preparation using the antisolvent precipitation method. Particle size was analysed by dynamic light scattering method and the results are at Figure 40. Particles smaller than 100 nm, which is considered as the limit for labelling as a "nanoparticle" [325]. LNP were prepared from specific lignin using DMSO, aqueous acetone (AcOH), THF and ethanol (EtOH) solvent systems. The other prepared particles bigger than 100 nm are classified as "sub-micro".

The smallest particles were obtained using aqueous AcOH as a solvent for Kraft lignin, these particles had 48.2 ± 4.7 nm. DMSO has proven to be another very good solvent for the preparation of LNP, that corresponds with the fact that DMSO is the best solvent for analysed lignin samples. LNP prepared from Kraft and organosolv lignin had Z-average 48.8 ± 6.6 and 50.4 ± 5.5 nm respectively. In contrary, alkali lignin proved to be unsuitable for the preparation of nanoparticles as only using DMSO produced particles that could be considered as nanoparticles, with a size of 99.4 ± 11.8 nm. Aqueous THF enabled nanoparticle formation from all lignin samples except Alkali lignin, confirming its suitability for LNP preparation. Furthermore, aqueous methanol (MeOH) did not work well, as no nanoparticles could be prepared.

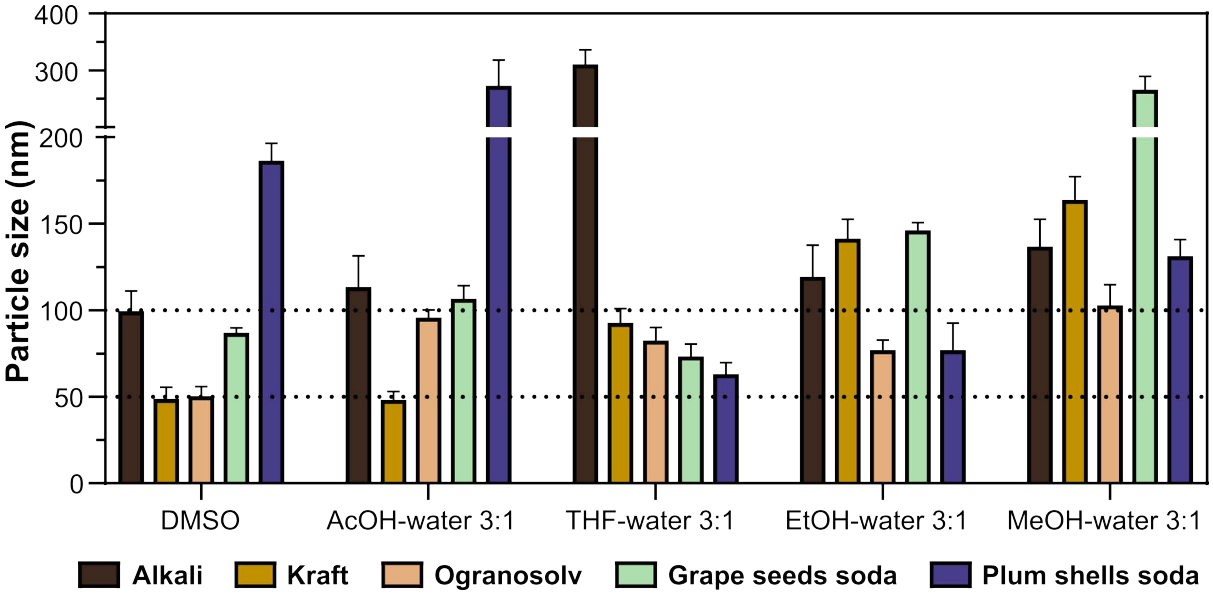

Figure 40 Comparison of different solvent systems and their impact to resulting nanoparticles side.

Preparation of LNP using different method is usual procedure, I focused on antisolvent aggregation method with dialysis because by another common method using rotary evaporator [326], I did not manage to prepare nanoparticles from grape seeds either plum shells soda lignin.

5.4.2 Characterization of lignin nanoparticles

When evaluating solvent systems for LNP preparation, DMSO, aqueous THF, and AcOH emerged as the most promising candidates. However, aqueous THF was ultimately selected for further use and analysis, as LNP solutions prepared with the other solvents proved unstable, exhibiting aggregation and sediment formation at the bottom.

Regarding lignin samples, I focused on grape seed-derived LNP for a detailed analysis, particularly due to their antimicrobial properties, which are discussed below. For comparison, Kraft and organosolv lignin were also included in the study.

Impact of preparation conditions on LNP

The properties of LNP were analysed as a function of the initial lignin solution concentration, specifically considering particle size, zeta potential, LNP yield, and pH (Figure 41). The results indicate that particle size increased with higher initial lignin concentrations, a trend observed across all lignin samples. This finding aligns with previous studies [291, 327–330].

Thus, by adjusting the initial lignin concentration, the resulting LNP size can be controlled. However, targeting smaller nanoparticles leads to a lower nanoparticle concentration in the final solution, as shown in Figure 41.

Additionally, LNP yield was assessed in relation to the initial lignin concentration. The results demonstrate a direct proportionality, indicating that when using the antisolvent precipitation method, the lignin solution is typically diluted by approximately fivefold.

In contrast to particle size, zeta potential remained largely independent of lignin concentration in most samples, with values around −25 mV for nearly all LNP formulations. Since a zeta potential below −30 mV is generally considered the threshold for colloidal stability [331], the prepared nanoparticles exhibited reasonable stability. However, Figure 42 confirms that the LNP maintained good stability over time.

As shown in the second column of the Figure 41, the pH of the solution decreased with increasing LNP concentration, even though the samples were dialyzed. This decrease in pH may be caused due to the acidic functional groups present in lignin. Lignin contains phenolic hydroxyl (-OH) and carboxyl (-COOH) groups, which can partially ionize in water, releasing protons (H^+) [332]. As the LNP concentration increases, more of these acidic groups are introduced into the solution, leading to a higher release of H^+ ions, which lowers the pH.

The stability of LNP over time in media with different pH values is an important factor influencing their potential applications. Therefore, I monitored the stability of LNP across a wide range of pH values. Studies on the effect of pH on nanoparticle stability generally indicate that LNPs remain stable within the pH range of 3-10 [216, 326, 330, 333–336]

Below pH 3, LNP tend to aggregate due to changes in surface charge. The carboxyl groups present in lignin are protonated predominantly at pH 3-6, while the hydroxyl groups on the aromatic core exhibit pKa values in the range of 7-10 [337], This results in a surface charge that stabilizes the nanoparticles by forming repulsive electrical double layers. However, under highly acidic conditions, the surface charge approaches the isoelectric point, leading to aggregation.

Most of the cited studies investigate nanoparticle stability as a function of pH only in the short term. In contrast, I monitored LNP stability over 40 days, confirming that the nanoparticles maintained stability throughout this period (Figure 42). Notably, organosolv LNP exhibited reduced stability at higher pH values. While long-term stability studies on lignin-based materials exist, they primarily focus on submicron lignin particles [328].

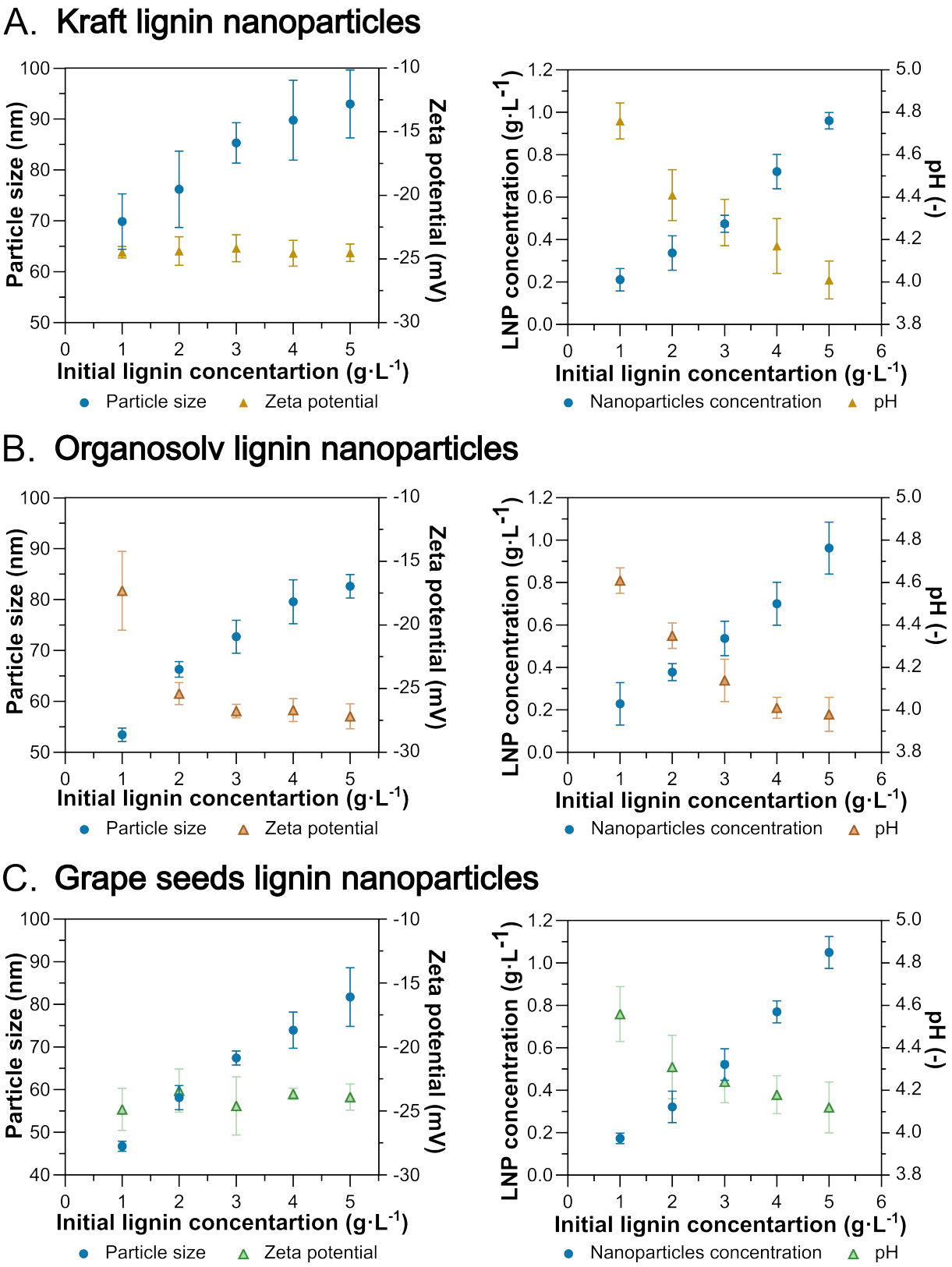

Figure 41 Dependency of LNP properties on initial lignin concentration. Kraft LNP (A), organosolv LNP (B) and grape seeds LNP (C).

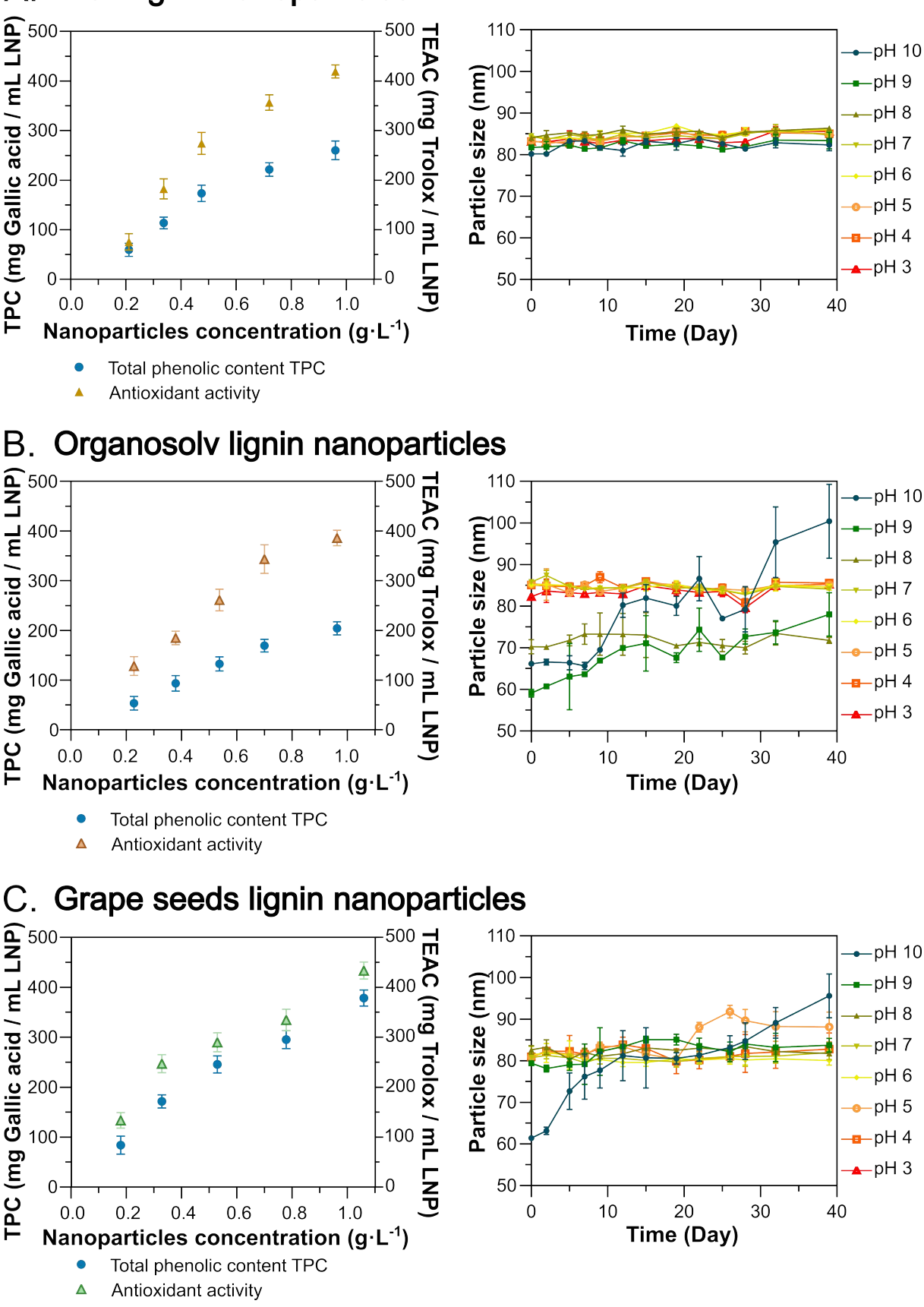

Figure 42 Total phenolic content, antioxidant activity and stability of LNP prepared from Kraft lignin (A), organosolv lignin (B) and grape seeds lignin (C).

Antioxidant activity and total phenolic content

The antioxidant activity of LNP was analysed as a function of LNP concentration (Figure 42). The results show that antioxidant activity increased with higher LNP concentrations, confirming the expectation that a more concentrated LNP solution would exhibit enhanced antioxidant properties. The relative antioxidant activity of different LNP samples corresponded to that of the initial lignin samples, following the trend: grape seed lignin > Kraft lignin > organosolv lignin (Figure 27). Although antioxidant activity has been widely studied [338–341], variations in analytical methods and result expression complicate direct comparisons between studies, as discussed in chapter 5.2.3. Antioxidant activity correlated with total phenolic content, supporting the validity of these results. This correlation can be attributed to the redox-based detection principle of the TPC method, as previously also discussed in chapter 5.2.3.

Lastly, the effect of stirring speed on particle size and zeta potential was examined over a range of 250-1250 rpm in 250 rpm increments. Literature suggests that very low stirring speeds may lead to larger particle sizes and zeta potential values closer to zero [174, 342]. However, within the tested range, no significant dependence of stirring speed on nanoparticle size or zeta potential was observed in this work.

Antimicrobial properties

Lignin, as a polyphenolic substance, is recognized for its biological activity and inherent antibacterial properties [174]. The antimicrobial effect of LNP prepared from various lignin sources were evaluated against both the gram-positive bacterium *Micrococcus luteus* and gram-negative bacterium *Escherichia coli*. As shown in Table 16, LNP prepared from grape seeds lignin exhibited a significant antimicrobial effect, with growth inhibition values exceeding 56 % for both bacteria. In contrast, a slight inhibitory effect was observed for organosolv LNP against *E. coli*, while nanoparticles prepared from Kraft lignin and plum shells soda lignin did not demonstrate any antimicrobial activity. These results underscore the unique properties of grape seed lignin nanoparticles, which motivated further investigation into their potential applications.

Table 16 Growth inhibition of lignin nanoparticle samples after 24 hours

Sample	Growth inhibition (%)	
	M. luteus	***E. coli***
Kraft lignin	nd	nd
Organosolv lignin	nd	12.5 ± 5.9
Grape seeds soda lignin	56.2 ± 15.8	56.7 ± 8.0
Plum shells soda lignin	nd	nd

The antimicrobial activity of lignin is primarily attributed to its phenolic structure. Previous studies have demonstrated that the biological activity of lignin is largely due to the presence of phenolic hydroxyl and methoxy groups [343]. Moreover, the presence of a double bond at the α, β positions of the side chain, together with a methoxyl group at the γ position, has been linked to enhanced efficacy against microorganisms [344]. The differences in antimicrobial

performance may also likely be related to the structural characteristics of the target bacteria; for instance, *M. luteus* features a thicker peptidoglycan layer [345], whereas *E. coli* has a more complex cell envelope with two concentric lipid bilayers [346].

Gao et al. [174] further investigated the antimicrobial mechanisms of LNP and reported, via SEM imaging, that bacterial cells exposed to LNP appeared distorted and deformed. By monitoring extracellular alkaline phosphatase activity, they proposed that the antimicrobial effects of LNP might involve different mechanisms for gram-positive and gram-negative bacteria. Their findings suggest that, in addition to causing external membrane disruption, LNP may also penetrate bacterial cells via endocytosis and disrupt intracellular processes.

Finally, it is worth noting that grape seed lignin also contains proanthocyanidins [347], compounds typical of grape-derived materials that possess antimicrobial properties [348, 349]. The presence of these bioactive compounds likely contributes to the enhanced antimicrobial activity observed in grape seed LNP.

Grape seeds LNP structure and morphology

The structure of grape seed LNP was characterized using scanning electron microscopy (SEM). Figure 43 clearly demonstrates that the nanoparticles exhibit a spherical morphology, which is a typical characteristic for LNPs prepared using THF [328, 342, 350]. Moreover, the SEM image conforms the particle size data obtained from DLS experiments.

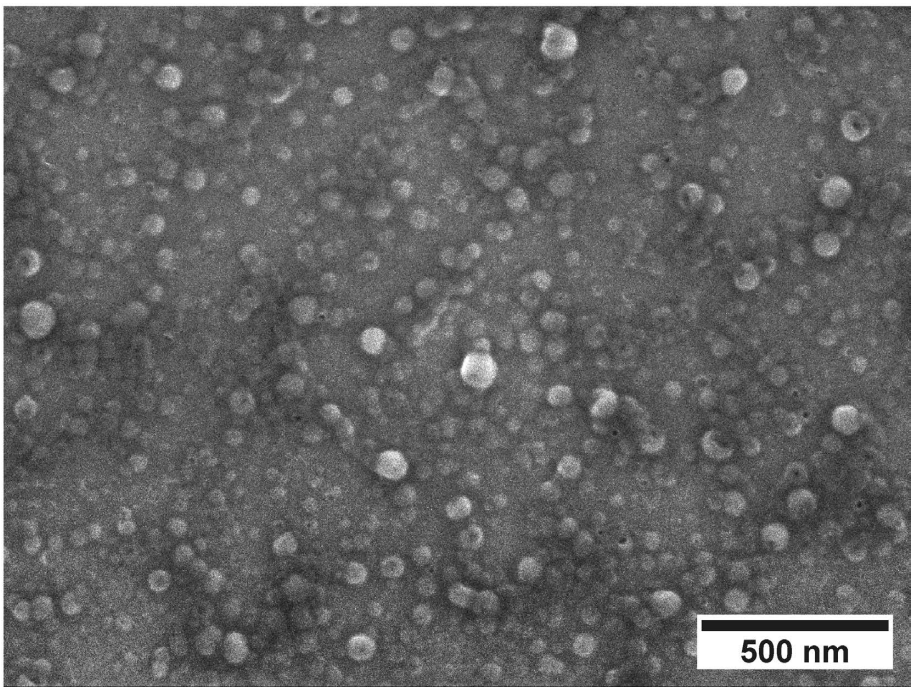

Figure 43 SEM of colloidal grape seed lignin nanoparticles prepared using aqueous mixture of THF. Picture was obtained at an accelerating voltage of 2 kV, a magnification of 50,000x, gentle beam mode and working distance 2.9 mm.

NMR

The 2D HSQC NMR experiments were conducted to elucidate the chemical structure of grape seeds lignin and its LNP. The chemical shifts of the cross-peaks and the respective assigned chemical structures are listed in Table 17 and illustrated in Figure 44.

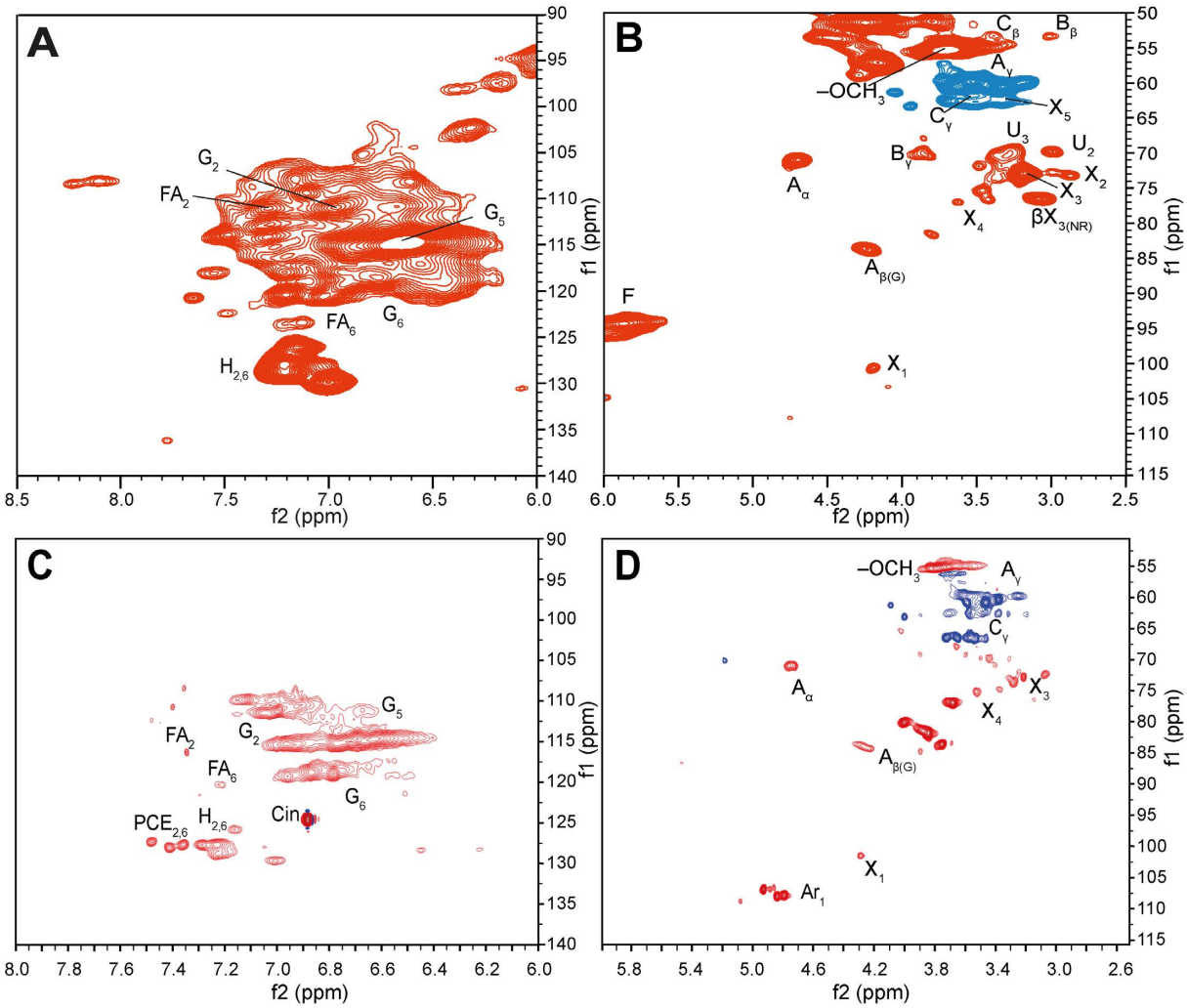

Figure 44 High-resolution 2D NMR HSQC spectra of grape seeds lignin (A, B) and grape seeds lignin nanoparticles prepared using aqueous THF (C, D). NMR spectra were collected at 14 T in dimethyl sulfoxide (40 °C), in the first column are shown aromatic parts (6–8.5 ppm for 1H / 90–140 ppm for 13C) and in the second column aliphatic parts (2.5–6 ppm for 1H / 50–115 ppm for 13C). Signals with positive phase (signals originating from methine and methyl groups) are in red, and signals with negative phase (resonances originating from methylene groups) are in blue.

The acquired 2D NMR spectra were compared with published spectra of grape seed lignin [351, 352], and lignin nanoparticles [353–355]. The spectra revealed characteristic linkages typical of lignin structures, including β-O-4 alkyl-aryl ethers (A), resinols (B) and phenylcoumarans (C) in the aliphatic region. In the aromatic region, signals corresponding to *p*-coumarates (*p*-CE), ferulates (*p*-FA), p-hydroxyphenyl units (H), guaiacyl units (G) were identified. The chemical structures of these compounds are illustrated in Figure 45. Notably, syringyl units were absent in the grape seed lignin spectra, which is consistent with previous studies [352, 356] and can be attributed to the botanical origin of the lignin.

Furthermore, the spectra indicated contamination with hemicellulosic compounds. Signals corresponding to β-(1→4)-D-xylopyranoside (X), α-D-glucuronic acid (U) and α-L-arabinofuranoside were observed, confirming the presence of LCC in the lignin fractions [357]. A comparison between the lignin and LNP spectra showed a reduction in signal intensity and overall spectral complexity in LNP, suggesting structural simplification during nanoparticle formation.

Additionally, it is important to consider that grape seeds are a rich source of proanthocyanidins [348]. These compounds are based on flavan-3-ol structures, with derivatives such as catechin and epicatechin. Previous studies have reported that grape seed lignin contains proanthocyanidins, and in 2D NMR spectra, signals from G-type lignin units can partially or completely overlap with characteristic procyanidin signals, making their identification more challenging [356]. These findings suggest that the material isolated from grape seeds is not pure lignin, as is typically the case with lignin extracted from wood sources, rather a mixture of lignin and polyphenols. This unique composition likely contributes to its distinctive properties. However, for simplicity, samples isolated from grape seeds are referred to in this work as grape seed lignin (GSL).

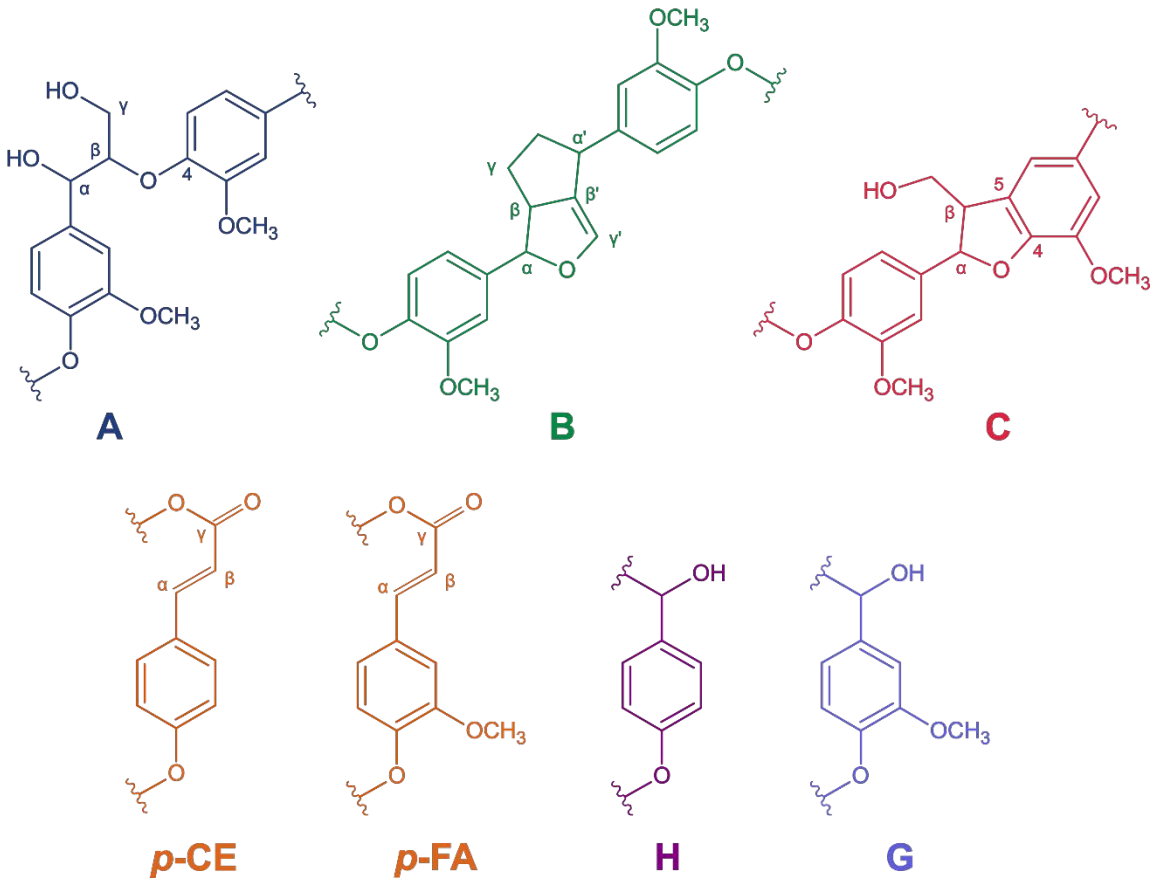

Figure 45 Main structures present in the grape seeds lignin: (A) β-O-4 alkyl-aryl ethers, (B) resinols, (C) phenylcoumarans, (*p*-CE) *p*-coumarates; (*p*-FA) ferulates; (H) *p*-hydroxyphenyl units, (G) guaiacyl units.

Table 17 Assignments of ^{13}C-^{1}H cross-signals in the 2D HSQC spectra of grape seeds lignin and LNP [358]

δ_C/δ_H (ppm)	Label	Assignments
53/3.1	B_β	C_β–H_β in resinol substructures (B)
53/3.5	C_β	C_β–H_β in phenylcoumarane substructures (C)
55/3.7	$–OCH_3$	C–H in methoxyls
60/3.5	A_γ	C_γ–H_γ in β-*O*-4′ substructures (A)
62/3.6	C_γ	C_γ–H_γ in phenylcoumaran (C)
63/3.4	X_5	C_5–H_5 in β-d-xylopyranoside
70/3.0	U_2	C_2–H_2 in 4-*O*-methyl-α-D-glucuronic acid
70/3.3	U_3	C_3–H_3 v 4-*O*-methyl-α-D-glucuronic acid
71/3.9	B_γ	C_γ–H_γ in resinol substructures (B)
71/4.7	A_α	C_α–H_α v β-O-4 unit (A)
73/3.0	X_2	C_2–H_2 in β-D-xylopyranoside
73/3.2	X_3	C_3–H_3 in β-D-xylopyranoside
75/3.5	X_4	C_4–H_4 in β-D-xylopyranoside
76/3.1	$\beta X_{3\ (NR)}$	(1→3)-β-D-xylopyranoside (Non-Reducing)
84/4.3	$A_{\beta(G)}$	C_β–H_β in β-*O*-4′ substructures linked to G and H units (A)
95/5.9	F	Flavonoids
100/4.2	X_1	C_1–H_1 in β-D-xylopyranoside
107/4.8	Ar_1	α-L-arabinofuranoside
110/7.0	G_2	C_2–H_2 in guaiacyl units (G)
110/7.4	FA_2	C_2–H_2 in ferulate (*p*-FA)
115/6.6	G_5	C_5–H_5 in guaiacyl units (G)
119/6.8	C_6	C_6–H_6 in guaiacyl units (G)
128/7.2	$H_{2,6}$	$C_{2,6}$–$H_{2,6}$ in H units (H)
123/7.1	FA_6	C_6–H_6 in ferulate (*p*-FA)
128/7.4	$PCE_{2,6}$	$C_{2,6}$–$H_{2,6}$ in *p*-coumarate (*p*-CE)

5.5 Biotechnological lignin modification

The aim of these experiments was to modify lignin biotechnologically using ligninolytic enzymes produced by white-rot fungi. The objective was to obtain low-molecular-weight lignin compounds with enhanced antioxidant properties, as ligninolytic enzymes can cleave both C–C and C–O bonds within the complex lignin structure [359].

One of the key challenges in this approach is that lignin biodegradation in nature occurs in native lignin. However, industrial processing subjects lignin to physical and chemical

treatments, resulting in technical lignin, which has a significantly altered chemical structure and should be considered a distinct substrate [360].

5.5.1 Screening of Ligninolytic Fungi and Enzyme Activity

Initially, three ligninolytic fungi *Fomitopsis pinicola*, *Lenzites betulina* and *Phanerochaete chrysosporium* were cultivated in appropriate culture media (chapter 4.5.1). The activity of key ligninolytic enzymes, specifically laccase, lignin peroxidase, and manganese-dependent peroxidase, was monitored throughout the experiments. Additionally, the potential induction of ligninolytic enzyme production by adding alkali lignin to the culture medium was investigated [361]. Screening results indicated that *Lenzites betulina* exhibited the highest enzymatic activity, making it the most promising candidate. Consequently, further studies focused on this fungus, particularly enzyme production in mineral cultivation media. The highest recorded enzyme activity values were for laccase: up to 350 $U \cdot mL^{-1}$, manganese-dependent peroxidase: up to 66 $U \cdot mL^{-1}$, lignin peroxidase: up to 8 $U \cdot mL^{-1}$ (Figure 46).

In contrast, *Phanerochaete chrysosporium* exhibited negligible activity (< 0.5 $U \cdot mL^{-1}$) for all studied enzymes (Figure 47). *Fomitopsis pinicola* exhibited lignin peroxidase activity comparable to *Lenzites betulina* but showed significantly lower activity for laccase and manganese peroxidase (Figure 48). Based on these findings, *Lenzites betulina* was selected as the most suitable fungus for the lignin modification assays. Previously published enzyme activity values varied widely, suggesting that culture conditions strongly influence enzyme production [361–364].

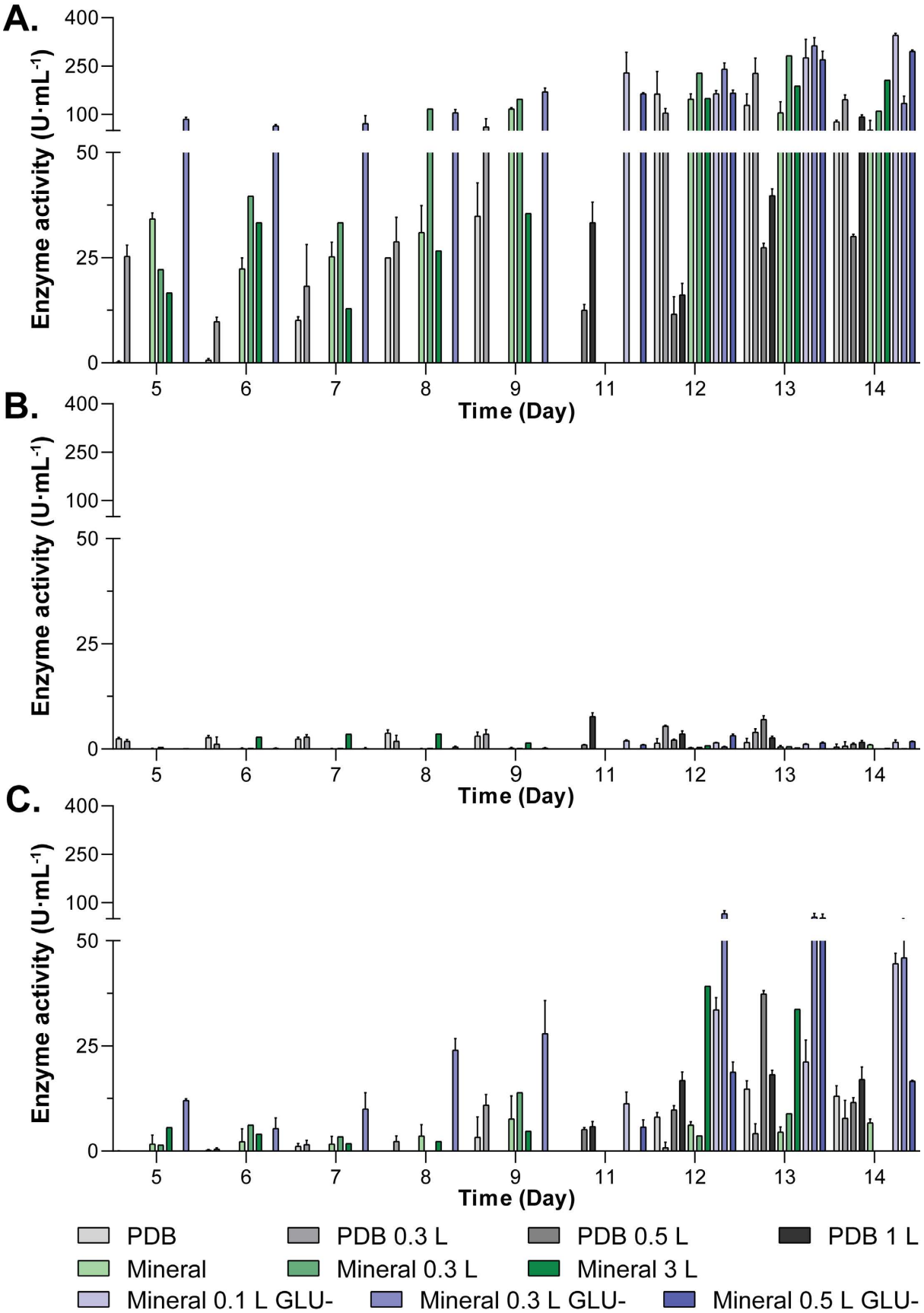

Figure 46 Enzyme activity of lignolitic enzymes produces by *Lenzites betulina.* Laccase (A), lignin peroxidase (B) and manganese-dependent peroxidase (C). PDB – Potato dextrose broth, GLU- stands for 5 g·L^{-1} glucose. 0.1 L, 0.3 L, 0.5 L, 1 L stand for lignin content in cultivation media in g·L^{-1}.

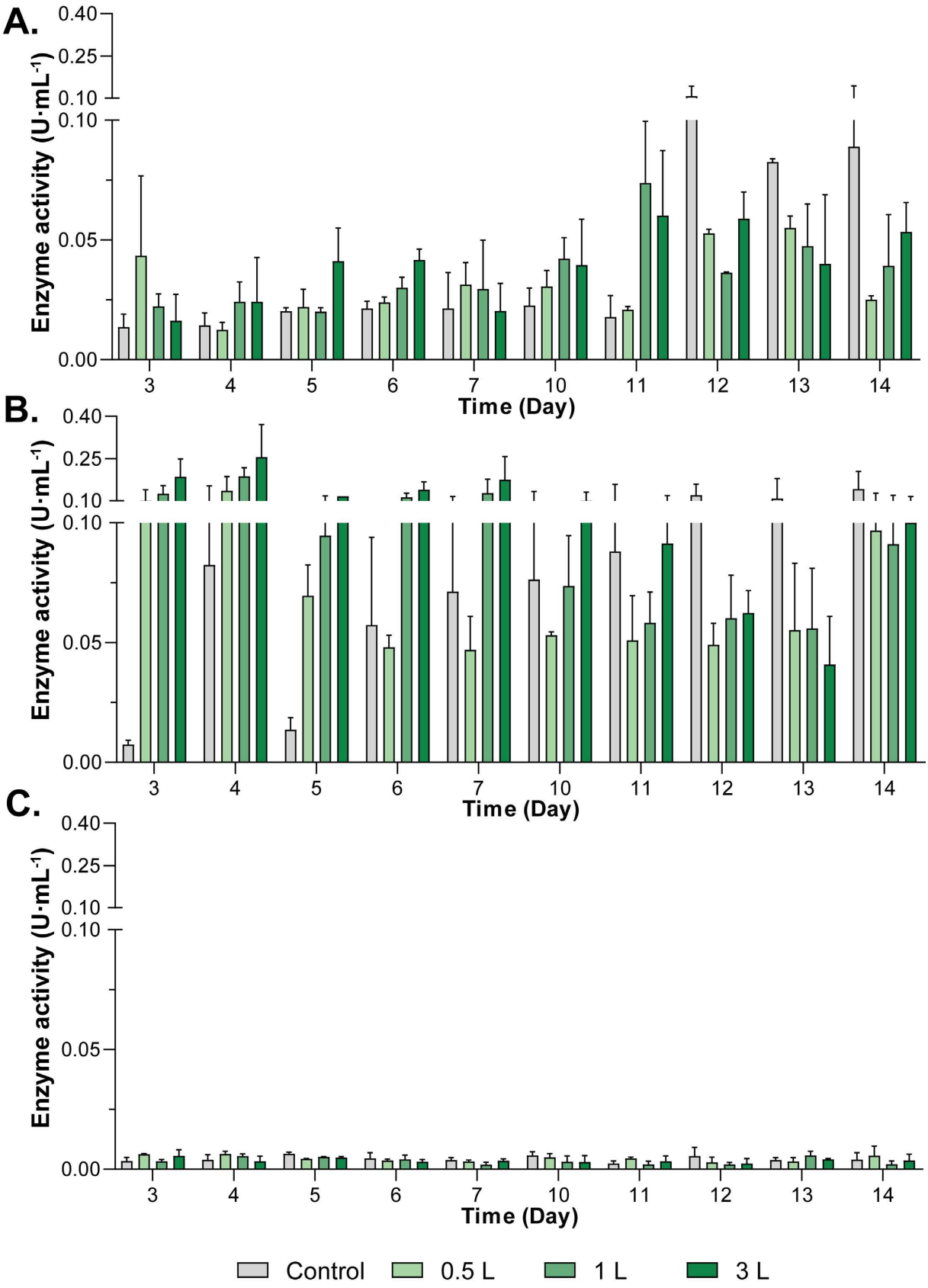

Figure 47 Enzyme activity of lignolitic enzymes produces by *Phanerochaete chrysosporium.* Laccase (A), lignin peroxidase (B) and manganese-dependent peroxidase (C). 0.5 L, 1 L, 3 L stand for lignin content in cultivation media in $g \cdot L^{-1}$.

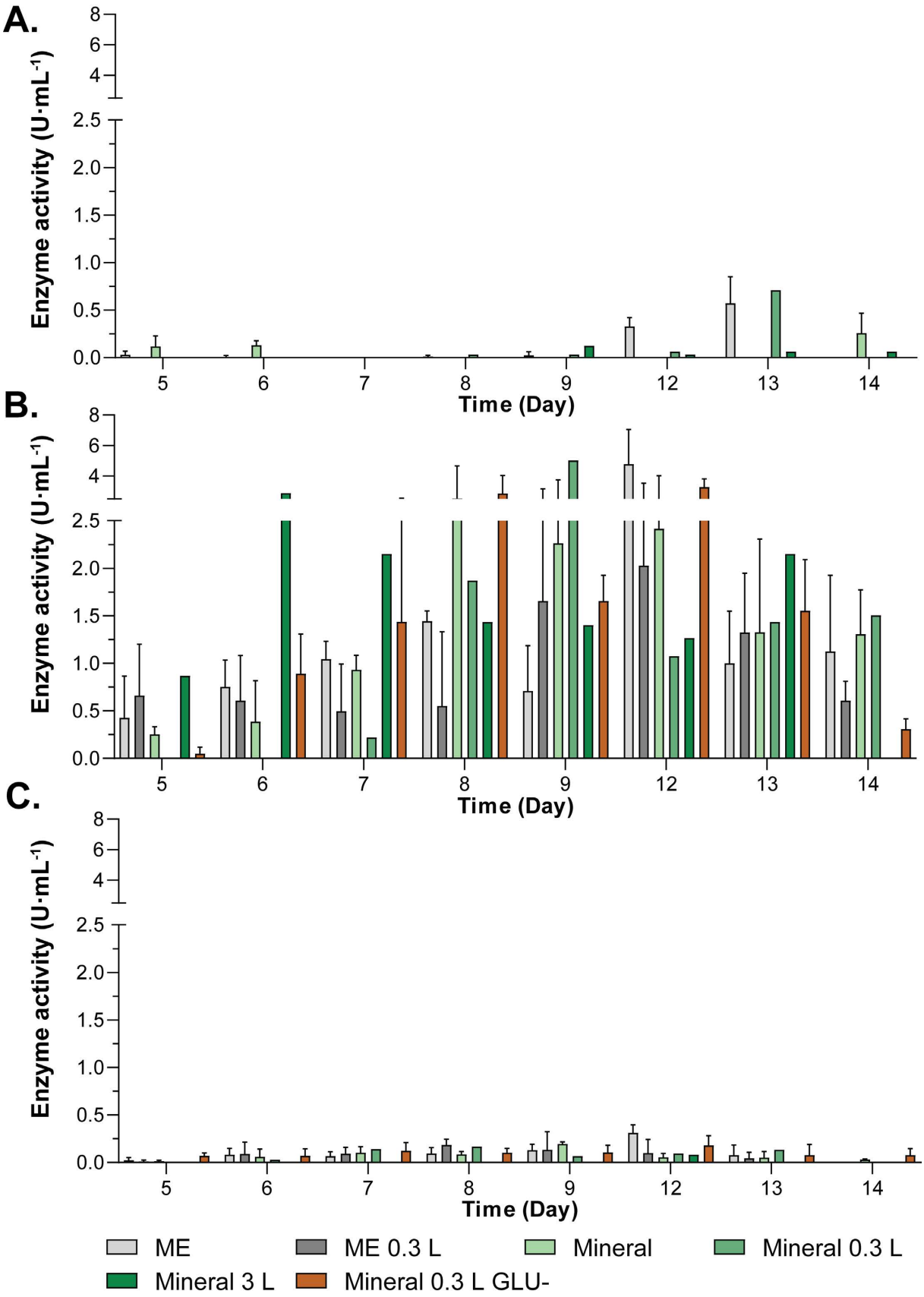

Figure 48 Enzyme activity of lignolitic enzymes produces by *Fomitopsis pinicola.* Laccase (A), lignin peroxidase (B) and manganese-dependent peroxidase (C). ME – Malt extract, GLU- stands for 5 g·L^{-1} glucose. 0.3 L, 3 L stand for lignin content in cultivation media in g·L^{-1}.

Selected fungi *Lenzites betulina* was subsequently used for biotechnological modification of lignin samples. Different lignin samples, Kraft, organosolv, grape seed soda, and plum shell soda lignin, were subjected to fungal treatment. Cultivation experiments were performed with 2 $g \cdot L^{-1}$ lignin, using a batch volume of 150 and 100 mL in 500 mL Erlenmeyer flasks. This setup maximized the surface area for fungal growth while preventing excessive dilution of the produced enzymes.

5.5.2 Antioxidant and antimicrobial properties of modified lignin

The effect of biotechnological modification on the antioxidant activity of lignin samples was analysed and compared to non-modified lignin. A comparison of results under different cultivation conditions is shown in Figure 49. According to the literature, an increase in antioxidant activity was expected [365], which was observed in the case of Kraft lignin (Figure 49A). This increase is likely due to the release of hydroxyl groups resulting from demethylation and depolymerization. The cleavage of the C–O bond in methoxyl groups can lead to demethylation, generating phenol hydroxyl-rich products with abundant ortho-hydroxy substitutions [366]. Additionally, the enzymatic cleavage of β-O-4’ bonds, the most abundant type of interunit linkage in lignin, occurred during laccase treatment, leading to lignin depolymerization [367].

For organosolv lignin, the increase in antioxidant activity was less pronounced. It was observed in some samples, but no decrease was detected (Figure 49B). In the case of grape seed and plum shell soda lignin, a slight increase in antioxidant activity was noted, though it was not statistically significant (Figure 49C).

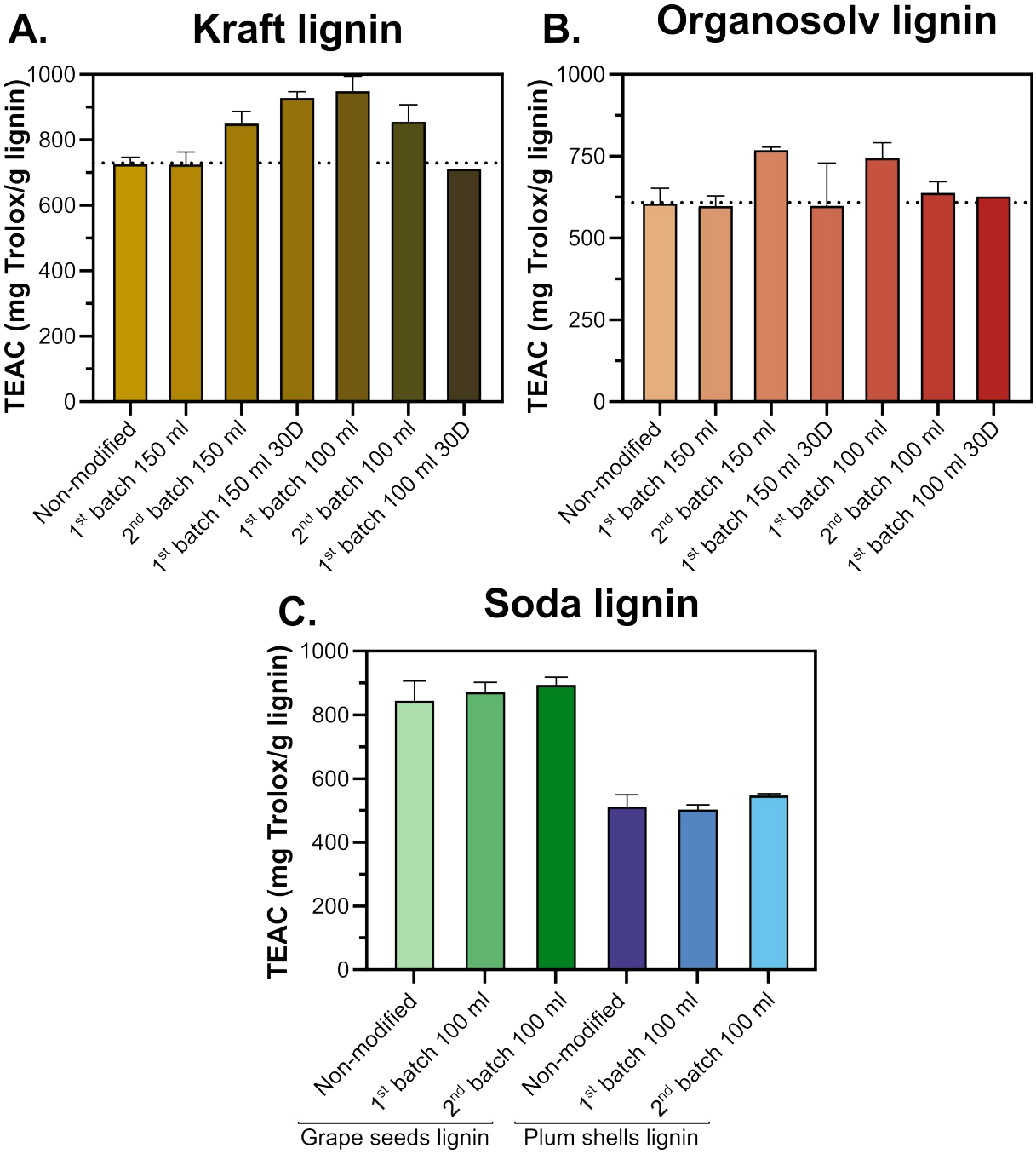

Figure 49 Comparison of Antioxidant activity expressed as Trolox equivalent (TEAC) of modified Kraft lignin (A) modified organosolv lignin (B) and modified grape seeds and plum shells soda lignin (C).

Regarding antimicrobial activity, only grape seed lignin and organosolv lignin exhibited antimicrobial properties, as described in chapter 5.4.2. To assess whether biotechnological modification influenced antimicrobial activity, treated samples were tested. However, none of the modified Kraft lignin, organosolv lignin, or plum shell soda lignin samples exhibited antimicrobial activity. Furthermore, for grape seed lignin, growth inhibition against *M. luteus* and *E. coli* decreased following modification (Table 18).

Table 18 Antimicrobial activity of modified grape seeds lingin

Sample	Growth inhibition (%)	
	M. luteus	***E. coli***
Grape seeds soda lignin (GSL)	56.2 ± 15.8	56.7 ± 8.0
Modified GSL: 1st batch	32.7 ± 0.7	37.2 ± 2.9
Modified GSL: 2nd batch	25.0 ± 5.0	53.6 ± 1.9

5.5.3 Molecular weight

Biotechnologically modified lignin samples were analyzed using size exclusion chromatography to determine their Mw, Mn and PDI (Table 19). Surprisingly, all samples exhibited an increase in molecular weight. The results suggest that rather than chain elongation leading to fibre formation, structural packing or aggregation occurred, as indicated by the low directive of the conformational diagram for the modified samples.

Table 19 Molecular weight and polydispersity of modified lignin samples

Lignin sample	Mw (kDa)	Mn (kDa)	PDI (kDa)
Kraft	6.01 ± 0.57	1.95 ± 0.35	3.11 ± 0.26
2nd batch 150 ml	10.65 ± 1.03	3.85 ± 0.75	2.83 ± 0.29
1st batch 150 ml 30 Days	11.86 ± 1.52	5.13 ± 0.52	2.31 ± 0.06
1st batch 100 ml	11.00 ± 0.15	4.72 ± 0.27	2.36 ± 0.12
2nd batch 100 ml	11.75 ± 0.25	5.81 ± 0.47	2.03 ± 0.12
Organosolv non-modified	12.33 ± 0.16	1.86 ± 0.13	6.65 ± 0.37
2nd batch 150 ml	20.29 ± 1.43	8.55 ± 0.67	2.40 ± 0.35
1st batch 150 ml 30 Days	10.51 ± 0.68	8.69 ± 0.75	2.39 ±0.28
1st batch 100 ml	18.82 ± 1.05	8.61 ± 0.35	2.23 ± 0.06
2nd batch 100 ml	21.30 ± 0.05	9.26 ± 0.63	2.31 ±0.15
Grape seeds non-modified	12.98 ± 0.62	3.56 ± 0.11	3.67 ± 0.29
1st batch 100 ml	45.99 ± 24.51	14.43 ± 9.02	3.59 ± 0.58
2nd batch 100 ml	47.13 ± 7.13	16.63 ± 6.63	3.24 ± 0.80
Plum shells non-modified	10.19 ± 0.13	3.12 ± 0.06	3.27 ± 0.10
1st batch 100 ml	9.77 ± 1.63	3.90 ± 0.30	2.50 ± 0.23
2nd batch 100 ml	11.63 ± 0.18	6.50 ± 0.20	1.80 ± 0.04

The observed increase in molecular weight is likely due to the dual activity of laccase enzymes, which are capable of both depolymerization and repolymerization [368]. Similar repolymerization behaviour has been also reported in chemical depolymerization techniques [369, 370].

The balance between polymerization and cleavage reactions is believed to depend on multiple factors, including: the structure and redox potential of the laccase enzyme, the structure and redox potential of the lignin substrate, the pH of the buffer used, The incubation temperature, and the solvent concentration [371, 372]. Despite advances in understanding lignin

transformation by laccases, the process remains poorly understood [373]. A significant obstacle in the valorisation of lignin is the tendency of lignin fragments, formed during oxidative cleavage, to repolymerize or condense into higher molecular weight species. This occurs via polymerization of radical intermediates, similar to the biosynthesis of lignin in plants [374, 375].

Radical depolymerization generates phenoxy radical intermediates that can undergo repolymerization, resulting in the formation of new diaryl-ether (4-O-5') and biphenyl (5,5') linkages [376]. In fungi, the enzyme cellobiose dehydrogenase, a flavin-dependent enzyme containing a heme cofactor, likely plays a role in preventing lignin repolymerization *in vivo* [377]. This enzyme has also been reported to act synergistically with fungal manganese peroxidase in the degradation of Kraft pulp lignin [378].

In this study, it is likely that both cleavage of the lignin structure, resulting in low-molecular-weight products, and repolymerization to high-molecular-weight products occurred. The low-molecular-weight products were not separable from the culture medium, while the high-molecular-weight products were readily isolated.

Addressing the issue of repolymerization remains a key challenge in lignin valorisation. One potential solution involves separating low-molecular-weight products using membrane filtration, although this approach is technically complex [379, 380]. Another general issue with repolymerization is the high heterogeneity of the resulting products. Narrowing the range of products to a lower number could improve their applicability and utilization [381].

5.5.4 FT-IR

Changes in the structural composition of the modified lignin samples were studied using FT-IR spectroscopy. The FT-IR DRIFT spectrum (Figure 50) shows changes in intensities of several peaks.

For plum shell soda lignin, generally was recorded reduction of all peak's intensity. The most pronounced decrease in peak intensity was 1714 cm^{-1}, which is assigned to C═O stretching vibrations in non-conjugated ketones, carbonyl, and ester groups.

In case of grape seeds soda lignin modification caused intensity reduction of peak 1714 cm^{-1} and increasing intensity of peak 1515 cm^{-1} which is associated with the skeletal vibrations of C═C stretching in aromatic rings. Intensity of peak 1045 cm^{-1} was reduced, this peak is attributed to hemicellulose. As was discussed previously this peak overlapped the peak 1030 cm^{-1}, which is assigned to C–O stretching in primary alcohols, which as an aliphatic hydroxyl would have negative effect on antioxidant activity [382].

In the organosolv lignin sample, the biotechnological modification led to a reduction in the intensity of the peak 1702 cm^{-1}, an increase in the intensity of the peak 1267 cm^{-1}. This signal corresponding to C-O stretching in the guaiacyl aromatic methoxyl groups, which may have just caused demethylation of the aromatic methoxyl groups leading to an increase in the concentration of aromatic hydroxyl groups responsible for the antioxidant activity. There was also a reduction in the intensity of the peak 1125 cm^{-1} assigned to the syringyl units.

Finally, increasing peak intensities of 1700 and 1126 cm^{-1} were observed for the Kraft lignin sample, while the peak intensities of 1270 a 1030 cm^{-1} decreased, which probably contributed to the increase in antioxidant activity and confirmed the results from $ABTS^{\cdot+}$ assay.

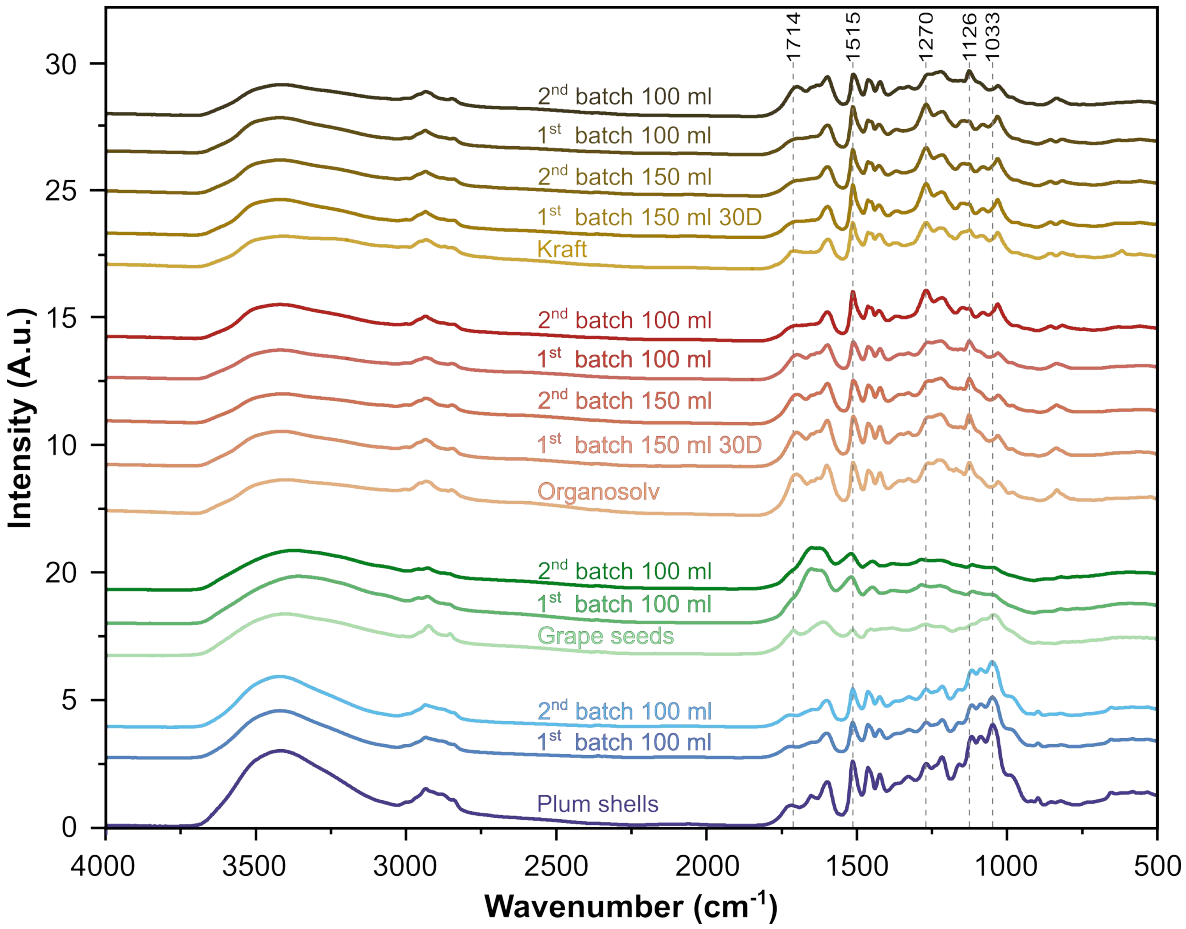

Figure 50 FT-IR DRIFT spectrum of modified lignin samples.

Given the challenges associated with biotechnological modification using white rot fungi, it was determined that the obstacles outweighed the potential benefits. Therefore, further experiments were conducted using unmodified lignin samples.

5.6 Application of lignin as ultrathin films

Lignin nanoparticles derived from grape seeds were used for surface modification, and their adsorption process was analysed. A LBL deposition technique was employed, involving the sequential and controlled assembly of oppositely charged polymers. Four positively charged polyelectrolytes (PAH, PLL, PDM, and PEI) were used as anchor layers, while negatively charged LNP were deposited as the functional layer.

The main advantage of this approach is its ability to overcome the challenge of lignin's low adhesion to most surfaces. Unlike lignin, polyelectrolytes exhibit strong adsorption capacity on a wide range of substrates, facilitating stable LNP deposition. The formation of multilayers was studied using QCM-D, providing real-time insights into adsorption kinetics, mass accumulation, stability, and particle swelling. LNP to the anchoring polymer surface until reaching saturation, after which excess LNP were removed during the rinsing cycle.

The formation of lignin nanoparticles resulted in an energetically favourable orientation of hydrophobic functional groups within the nanoparticle core, primarily stabilized via π-π and hydrophobic interactions. Conversely, the nanoparticle surface was enriched with hydrophilic functional groups (-OH and -COOH) which facilitated interaction with water and carry the overall negative charge of lignin [383].

Initially, LNP adsorption on gold crystal surfaces was verified. As shown in Figure 51, all LNP were removed during the rinsing step, confirming the necessity of an anchor layer. Subsequently, the four polyelectrolytes were evaluated as anchoring layers for LNP deposition.

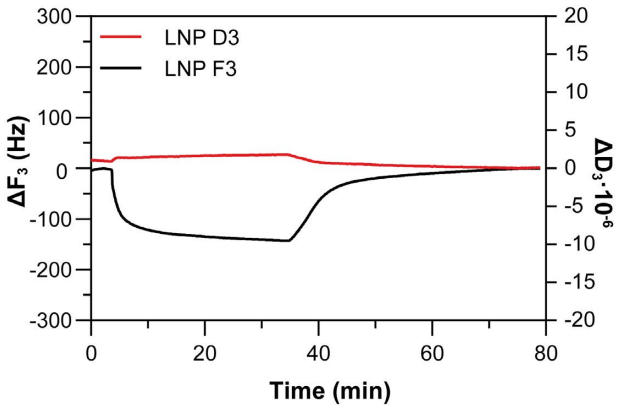

Figure 51 QCM-D measurement of grape seeds LNP deposition on gold crystals.

The adsorption of LNP on PEs was analysed over a pH range of 4.6 to 10.0 to assess how pH variations influenced the system. The QCM-D profile of the LBL assembly using PEs at their native pH is presented in Figure 52. During each deposition cycle, the oscillation frequency (*f*) decreased, indicating mass accumulation, while the dissipation (*D*) increased, suggesting a more viscoelastic film. However, the rinsing step led to a rise in frequency and a drop in dissipation, as loosely bound material was removed. Notably, during the rinsing of PEs with water, energy dissipation initially spiked, particularly for PDM, PAH and PLL (Figure 52A, B, C), due to the system swelling upon solvent exchange.

Kinetically, all PEs adsorbed rapidly, reaching equilibrium within a short time. In contrast, LNP adsorption was significantly slower, attributed to their larger size and slower diffusion toward the surface. As the surface approached saturation, electrostatic repulsion increased, reducing the available space for additional adsorption. This led to a gradual decline in the adsorption rate, indicating that the surface is becoming saturated with the adsorbed particles, leading to repulsion and rearrangement of the molecules on the surface.

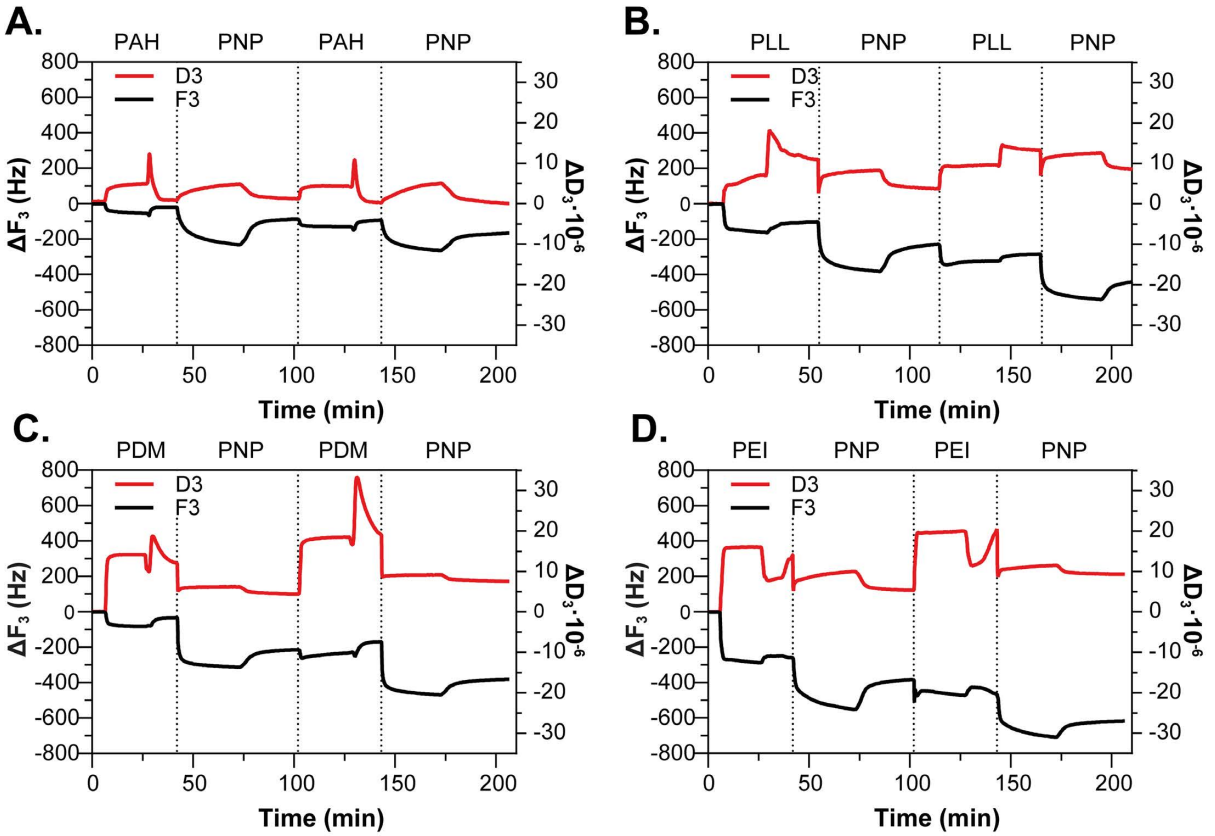

Figure 52 QCM-D measurements for LBL assembly of specific polyelectrolytes at unmodified pH and lignin nanoparticles: PAH pH 4.6 (A), PLL pH 8.0 (B), PDM pH 5.4 (C), and PEI pH 10.0 (D). The graph shows changes in oscillation frequency (black line, left axis) and energy dissipation (red line, right axis) over time, recorded from the 3rd overtone during the deposition of two bilayers for each system.

Among the investigated PEs, PLL at pH 10 exhibited the highest adsorption onto the gold substrate, causing an average frequency shift of 229 ± 29 Hz at the third overtone (Figure 53). In contrast, PAH showed the lowest affinity to the gold surface, with a frequency shift of 52 ± 1 Hz. However, after the rinsing step, the frequency shift (Δf) for PLL decreased to 204 ± 25 Hz, corresponding to 12 ± 1 mg·m^{-1} of adsorbed PLL, as calculated using the Sauerbrey equation (6).

The QCM-D experiment revealed that LBL systems prepared from PAH and PLL were pH-dependent, whereas those prepared with PEI and PDM were not. Each PEs solution had a different native (unmodified) pH value (Figure 54). The increased adsorption of PLL and PAH at higher pH levels was likely due to the pH approaching or exceeding their respective pKa values (pKa for PLL = 10.5, pKa for PAH = 8.5). As the pH increased, the proportion of protonated R-NH^{3+} groups decreased, reducing the overall charge of the PEs and enhancing their adsorption onto the gold surface. The highest adsorption was observed at pH 10, consistent with previous findings for PAH [384] and PLL [385]. The increased layer thickness and charge density of these PEs subsequently enhanced their interaction with lignin LNP, leading to the formation of a thicker lignin layer.

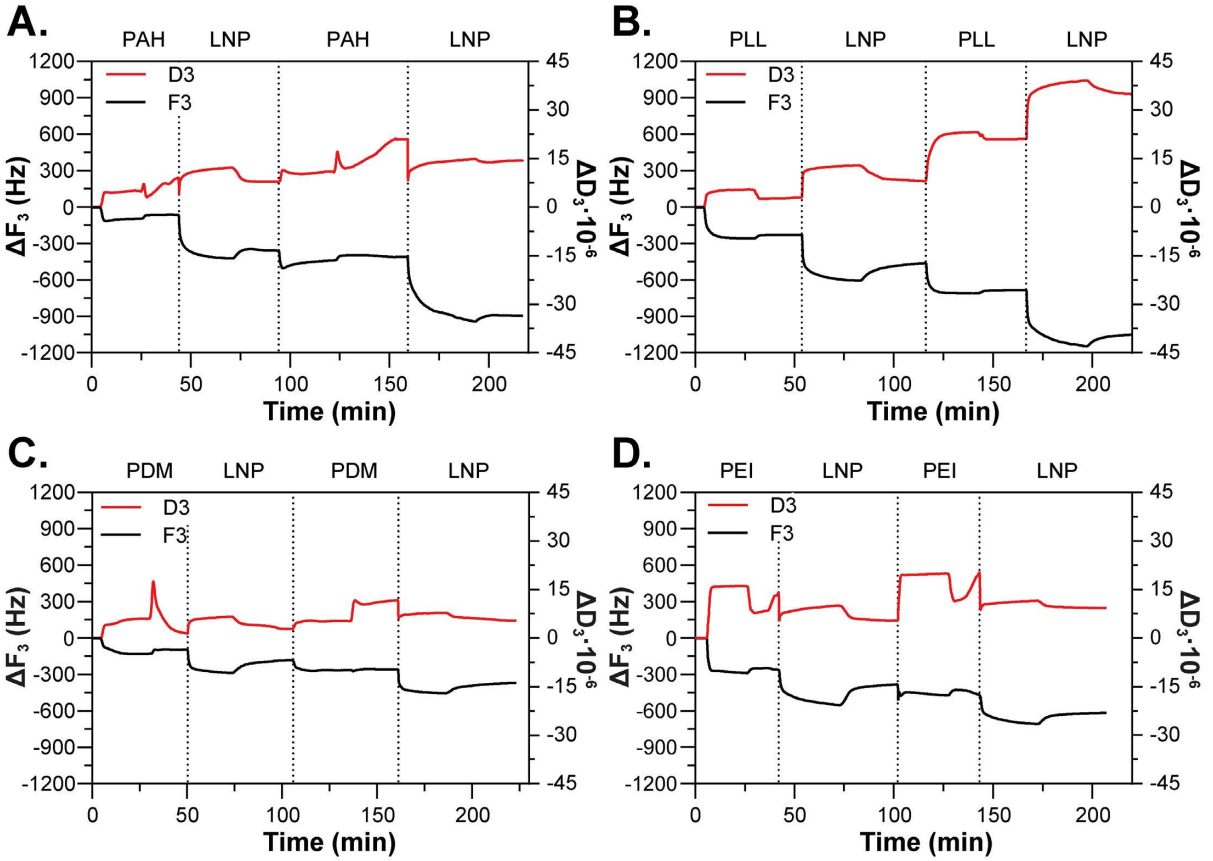

Figure 53 QCM-D measurements for LBL assembly of specific polyelectrolytes at pH 10.0 and lignin nanoparticles: PAH (A), PLL (B), PDM (C), and PEI (D). The graph shows changes in oscillation frequency (black line, left axis) and energy dissipation (red line, right axis) over time, recorded from the 3rd overtone during the deposition of two bilayers for each system.

As shown in Figure 54, the highest LNP adsorption occurred in LBL assemblies prepared from PAH and PLL at pH 10. At the second layer, 13.5 ± 3.2 and 13.1 ± 0.6 mmol·g^{-1} of LNP were adsorbed for PAH and PLL, respectively, while at the fourth layer, adsorption increased to 24.7 ± 3.7 and 20.0 ± 1.6 mmol·g^{-1} for PAH and PLL, respectively.

In contrast, the LBL system formed using PDM and PEI exhibited no significant pH dependence. This is because PDM, a permanently charged polyelectrolyte with no detectable pKa value, does not undergo further protonation. PEI, with a native pH around 10, showed slightly lower lignin adsorption at lower pH levels. However, a strong pH-dependent effect was not expected due to PEI's branched structure, which contains primary, secondary, and tertiary amine groups, resulting in a high charge density [386]. Consequently, PEI functioned as a weak base with broad buffering capacity, maintaining its effectiveness across a wide pH range from acidic to basic. Its buffering capacity peaks between pH 8 and 10, corresponding to the pKa values of its secondary and tertiary amines [387–389]. These findings align with a previous study [390], which analysed LBL assemblies prepared from PEI and a lignin-based polymer at pH 5 and 8, reporting no significant differences in adsorbed mass under these conditions, that is consistent with the observations in this study.

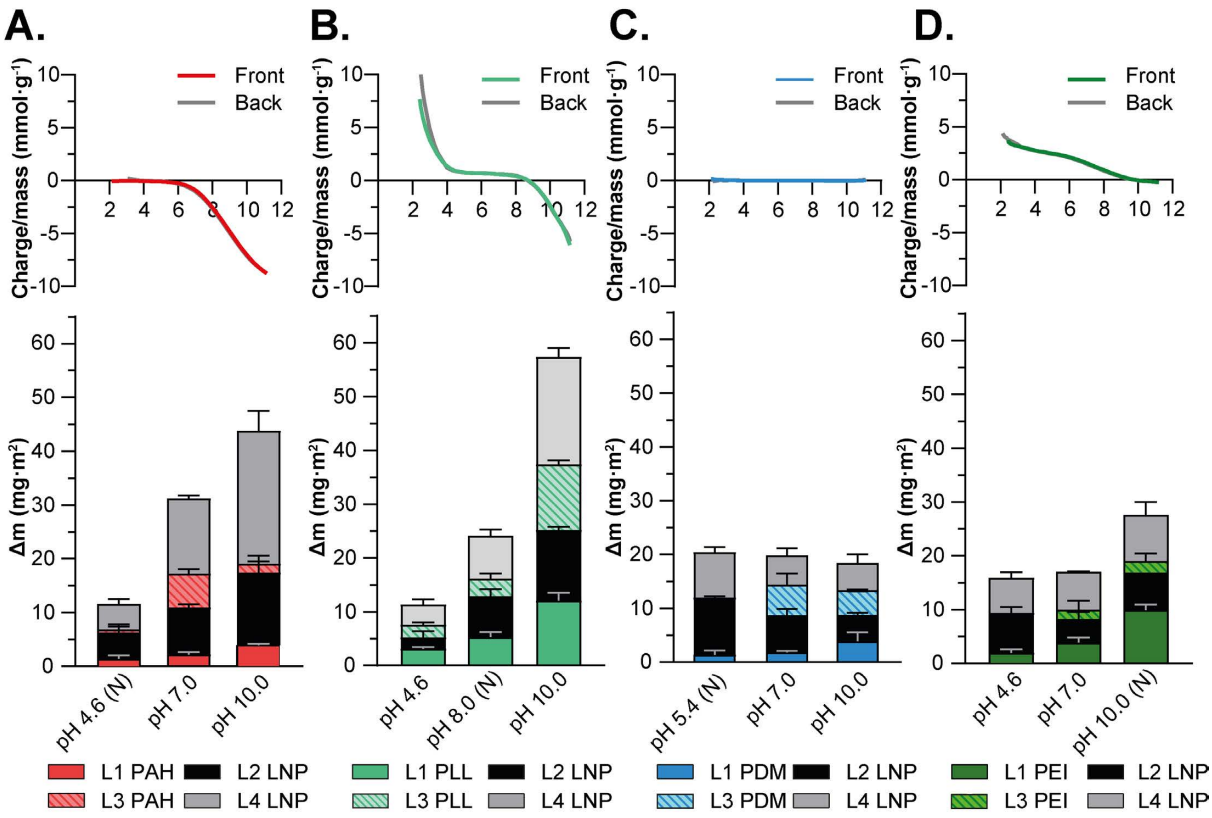

Figure 54 Adsorption of grape seeds LNP on specific PEs. In the upper part, the titration curves for specific polyelectrolytes PAH (A), PLL (B), PDM (C), and PEI (D) are shown. In the lower part, the adsorbed mass of LNP and PEs after rinsing, calculated according to the Sauerbrey equation, is presented for these specific polyelectrolytes under various pH conditions. The adsorbed masses are shown layer by layer (L). (N) indicates natural pH value of polyelectrolyte solution.

5.6.1 Morphology of LBL assemblies

The topography and phase images of LBL assemblies prepared using the investigated PEs at pH 10 and LNP were collected via AFM and are shown at Figure 55. The AFM micrographs revealed spherical lignin particles in all types of LBL thin films, with variations in surface roughness. The observed roughness is partly attributable to the QCM-D technique used for ultrathin film preparation. Smoother, more uniform thin films could be achieved through spin coating [383, 391, 392].

Spherical lignin particles were most prominent and abundant in the LBL thin films formed using PLL and LNP, resulting in the highest root-mean-square (RMS) roughness of 13.1 ± 0.2 nm, corresponding to the highest amount of adsorbed lignin. Other LBL assemblies exhibited lower roughness (Figure 55), although some clusters formed on the surface, likely due to aggregation upon drying [393].

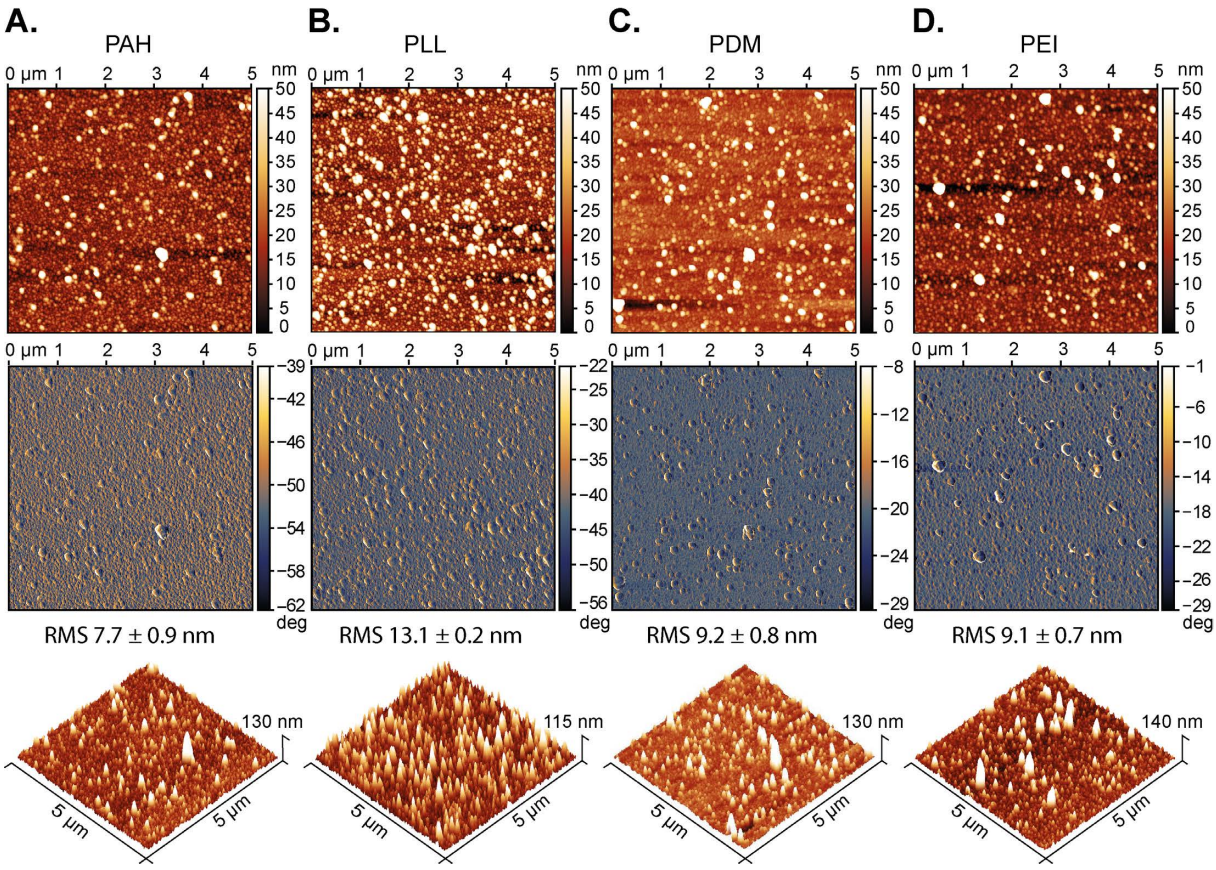

Figure 55 Atomic force microscopy images of LbL assembled polyelectrolytes and LNP at a pH value of 10: PAH (A), PLL (B), PDM (C), and PEI (D). The upper row displays topography images, while the middle row presents phase images. Both covering an area of 5 µm × 5 µm. The root-mean-square (RMS) roughness is indicated for each image. In the lower row are 3D visualization of topography.

The ultrathin films prepared using PLL at pH 10 and LNP were identified as the most promising and were further analysed. The surface wettability of these thin films exhibited a hydrophilic character, with a water contact angle (WCA) of 42.5 ± 3.1°. This WCA is slightly higher than that reported in a previous study [394], which may be attributed to the lower RMS roughness of the LBL assembly. Surface roughness plays a crucial role in determining wettability [395].

5.6.2 Radical scavenging and antimicrobial activity of LNP/PEs thin films

Since LNP prepared from GSL demonstrated antioxidant activity (chapter 5.2.35.4.2), I hypothesized that multilayer thin films composed of PEs and LNP would also exhibit high scavenging radical activity. Figure 56 shows the antioxidant activities of multilayer LBL thin films ranging from 40 µg to 71 µg Trolox·cm^{-2}. The data indicate that the antioxidant activity of ultra-thin films was higher in LBL assemblies prepared under alkaline conditions than in those prepared under acidic conditions. This could be due to the pH-dependent nature of antioxidant properties, as changes in pKa values influence the ionization of hydroxyl groups [396].

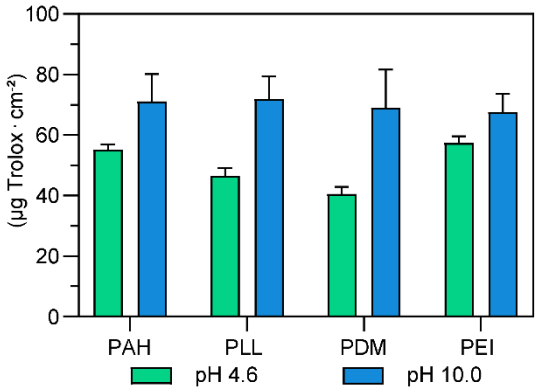

Figure 56 Antioxidant activity of multilayer films composed of PEs and LNP.

After confirming the antioxidant activity of LBL assembly, a system prepared from PLL at pH 10 and LNP was selected to evaluate antimicrobial properties. Growth inhibition was recorded at 50.7 ± 0.6% against *M. luteus* and 12.1 ± 0.6% against *E. coli.*

These results indicate that the antimicrobial activity of the LBL assemblies is primarily determined by the nature of the top layer, in this case, LNP. The findings suggest that simple adsorption-based coatings using grape seed LNP can create functional surfaces with both antioxidant and antimicrobial properties, making them promising for high-tech applications.

While the investigated grape seed lignin nanoparticles exhibit antioxidant and antimicrobial properties, their poor adhesion to gold and other surfaces presents a challenge for forming stable films. However, incorporating LNP into LBL assemblies with polyelectrolytes, particularly PLL, significantly enhances film stability. This approach enables the development of multifunctional coatings applicable to various surfaces. Nevertheless, the successful formation of LBL assemblies requires careful control of pH and processing conditions to ensure proper layering and stability.

6. CONCLUSION

Lignin, the second most abundant biopolymer, possesses a complex structure that presents significant challenges in its processing. This PhD thesis evaluated various strategies for extracting lignin from different agricultural sources, compared their properties, and assessed its potential applications.

In the first part of the work, lignin was extracted from agricultural wastes, specifically grape and rose hip seeds, as well as plum and cherry shells, using the soda pulping method, which effectively prevented sulfur contamination. The solubility of lignin, a critical parameter, was systematically analyzed, and it was confirmed that DMSO is the optimal solvent for most samples. Hansen solubility parameters were used for qualitative assessments, and a spreadsheet tool was developed to model ideal solvent mixtures for lignin recovery. Emphasis was placed on antioxidant activity, with grape seed lignin demonstrating the highest capacity, outperforming commercial lignin samples. Consequently, grape seeds lignin was selected for further studies.

The next section focused on the development of porous materials based on PHA without the use of halogenated solvents. The material was modified by incorporating bacterial cellulose and by blending with grape seed lignin. Porous cryogels were successfully fabricated, and blending with GSL enhanced thermal properties by shifting degradation to higher temperatures. BET analysis confirmed that P3HB cryogels exhibit a high specific surface area, although the addition of BC reduced the surface area in PHA blend cryogels. BC also effectively lowered the density of all cryogel types and modified their hydrophobicity, while cryogels containing GSL exhibited antioxidant activity.

Another strategy involved preparing lignin nanoparticles using an antisolvent precipitation method. Various organic solvent systems were compared, and LNP prepared from nearly all sample types using aqueous THF achieved sizes below 100 nm and demonstrated excellent long-term stability. As expected, these LNP exhibited antioxidant activity, and those derived from GSL also showed antimicrobial activity against both gram-positive and gram-negative bacteria.

Lignin was further modified through biotechnological methods using white-rot fungi that produce ligninolytic enzymes. Based on enzyme activity screening, *Lenzites betulina* was selected as the most promising candidate. However, this biotechnological modification unexpectedly increased the molecular weight of lignin, likely due to radical coupling reactions inherent to its complex structure. Although the modification enhanced antioxidant properties, it led to a reduction in antimicrobial activity.

Finally, the preparation of ultrathin films by adsorption of LNP (from GSL) was investigated using QCM-D with four different polyelectrolytes. Among these, PLL demonstrated the best adsorption properties, resulting in the highest uptake of LNP. The resulting ultrathin films exhibited both antioxidant and antimicrobial properties.

Overall, the applications explored in this thesis contribute to a deeper understanding of lignin and demonstrate its potential for developing high-tech materials.

7. REFERENCES

[1] Novo-Uzal, E., Pomar, F., Gómez Ros, L. V., Espiñeira, J. M., Ros Barceló, A. (2012). Evolutionary History of Lignins, *Advances in Botanical Research*, Vol. 61, 309–350. Doi:10.1016/B978-0-12-416023-1.00009-4

[2] Zhong, R., Ye, Z.-H. (2009). Transcriptional regulation of lignin biosynthesis, *Plant Signaling & Behavior*, Vol. 4, No. 11, 1028–1034. Doi:10.4161/psb.4.11.9875

[3] Lourenço, A., Rencoret, J., Chemetova, C., Gominho, J., Gutiérrez, A., del Río, J. C., Pereira, H. (2016). Lignin Composition and Structure Differs between Xylem, Phloem and Phellem in Quercus suber L., *Frontiers in Plant Science*, Vol. 7, No. OCTOBER2016, 218455. Doi:10.3389/fpls.2016.01612

[4] Sankaran, R., Markandan, K., Khoo, K. S., Cheng, C. K., Ashokkumar, V., Deepanraj, B., Show, P. L. (2021). The Expansion of Lignocellulose Biomass Conversion Into Bioenergy via Nanobiotechnology, *Frontiers in Nanotechnology*, Vol. 3, 793528. Doi:10.3389/fnano.2021.793528

[5] Henriksson, G. (2017). What are the biological functions of lignin and its complexation with carbohydrates?, *Nordic Pulp and Paper Research Journal*, Vol. 32, No. 4, 527–541. Doi:10.3183/NPPRJ-2017-32-04-p527-541

[6] Cazacu, G., Capraru, M., Popa, V. I. (2013). Advances Concerning Lignin Utilization in New Materials, S. Thomas; P. M. Visakh; Aji. P. Mathew (Eds.), *Advances in Natural Polymers* (Vol. 18), Springer Berlin Heidelberg, 255–312. Doi:10.1007/978-3-642-20940-6

[7] Huang, J., Shiyu, F., Lian, G. (2019). Structure and Characteristics of Lignin, *Lignin Chemistry and Applications*, 25–50. Doi:10.1016/b978-0-12-813941-7.00002-3

[8] Erdtman, H. (1957). Outstanding Problems in Lignin Chemistry, *Industrial and Engineering Chemistry*, Vol. 49, No. 9, 1385–1386. Doi:10.1021/ie50573a033

[9] Freudenberg, K. (1959). Biosynthesis and constitution of lignin, *Nature*, Vol. 183, No. 4669, 1152–1155. Doi:10.1038/1831152a0

[10] Li, Y., Meng, X., Meng, R., Cai, T., Pu, Y., Zhao, Z. M., Ragauskas, A. J. (2023). Valorization of homogeneous linear catechyl lignin: opportunities and challenges, *RSC Advances*, Vol. 13, No. 19, 12750–12759. Doi:10.1039/D3RA01546G

[11] Wang, P., Wang, S., Su, S., Zhang, D., Liao, Y., Song, G., Wang, L. (2025). A techno-economically feasible and sustainable C-lignin biorefinery, *Green Chemistry*, Vol. 27, No. 12, 3207–3216. Doi:10.1039/D4GC06090C

[12] Lundquist, K. (1987). On the Occurrence of β-1 Structures in Lignins, *Journal of Wood Chemistry and Technology*, Vol. 7, No. 2, 179–185. Doi:10.1080/02773818708085260

[13] Heitner, C., Dimmel, D. R., Schmidt, J. A. (2010). *Lignin and Lignans Advanced in Chemistry*, *Methods in Enzymology* (Vol. 161), Taylor and Francis Group, LLC

[14] van Erven, G., Nayan, N., Sonnenberg, A. S. M., Hendriks, W. H., Cone, J. W., Kabel, M. A. (2018). Mechanistic insight in the selective delignification of wheat straw by three white-rot fungal species through quantitative13c-is py-gc–ms and whole cell wall hsqc nmr, *Biotechnology for Biofuels*, Vol. 11, No. 1, 1–16. Doi:10.1186/s13068-018-1259-9

[15] Argyropoulos, D. S. (1999). *Advances in Lignocellulosics Characterization*, TAPPI Press

[16] Süss, R., Kamm, B., Arnezeder, D., Zeilerbauer, L., Paulik, C. (2022). Homogeneously catalyzed depolymerization of lignin from organosolv medium: Characterization, optimization, and minimization of coke formation, *The Canadian Journal of Chemical Engineering*, Vol. 100, No. S1. Doi:10.1002/cjce.24055

[17] Serrano, L., Esakkimuthu, E. S., Marlin, N., Brochier-Salon, M.-C., Mortha, G., Bertaud, F. (2018). Fast, Easy, and Economical Quantification of Lignin Phenolic Hydroxyl Groups: Comparison with Classical Techniques, *Energy & Fuels*, Vol. 32, No. 5, 5969–5977. Doi:10.1021/acs.energyfuels.8b00383

[18] Gosselink, R. J. A., Abächerli, A., Semke, H., Malherbe, R., Käuper, P., Nadif, A., van Dam, J. E. G. (2004). Analytical protocols for characterisation of sulphur-free lignin, *Industrial Crops and Products*, Vol. 19, No. 3, 271–281. Doi:10.1016/j.indcrop.2003.10.008

[19] Capanema, E. A., Balakshin, M. Y., Kadla, J. F. (2004). A Comprehensive Approach for Quantitative Lignin Characterization by NMR Spectroscopy, *Journal of Agricultural and Food Chemistry*, Vol. 52, No. 7, 1850–1860. Doi:10.1021/jf035282b

[20] Giummarella, N., Lawoko, M. (2016). Structural Basis for the Formation and Regulation of Lignin-Xylan Bonds in Birch, *ACS Sustainable Chemistry and Engineering*, Vol. 4, No. 10, 5319–5326. Doi:10.1021/acssuschemeng.6b00911

[21] Zhao, Y., Shakeel, U., Rehman, M. S. U., Li, H., Xu, X., Xu, J. (2020). Lignin-carbohydrate complexes (LCCs) and its role in biorefinery, *Journal of Cleaner Production*, Vol. 253, 120076. Doi:10.1016/j.jclepro.2020.120076

[22] Tao, J., Li, S., Ye, F., Zhou, Y., Lei, L., Zhao, G. (2020). Lignin–An underutilized, renewable and valuable material for food industry, *Critical Reviews in Food Science and Nutrition*, Vol. 60, No. 12, 2011–2033. Doi:10.1080/10408398.2019.1625025

[23] Tribot, A., Amer, G., Alio, M. A., de Baynast, H., Delattre, C., Pons, A., Mathias, J. D., Callois, J. M., Vial, C., Michaud, P., Dussap, C. G. (2019). Wood-lignin: Supply, extraction processes and use as bio-based material, *European Polymer Journal*, Vol. 112, No. October 2018, 228–240. Doi:10.1016/j.eurpolymj.2019.01.007

[24] Collins, M. N., Nechifor, M., Tanasă, F., Zănoagă, M., McLoughlin, A., Stróżyk, M. A., Culebras, M., Teacă, C. A. (2019). Valorization of lignin in polymer and composite systems for advanced engineering applications, *International Journal of Biological Macromolecules*, Vol. 131, 828–849. Doi:10.1016/j.ijbiomac.2019.03.069

[25] Asina, F., Brzonova, I., Voeller, K., Kozliak, E., Kubátová, A., Yao, B., Ji, Y. (2016). Biodegradation of lignin by fungi, bacteria and laccases, *Bioresource Technology*, Vol. 220, 414–424. Doi:10.1016/j.biortech.2016.08.016

[26] Janusz, G., Pawlik, A., Sulej, J., Świderska-Burek, U., Jarosz-Wilkołazka, A., Paszczyński, A. (2017). Lignin degradation: microorganisms, enzymes involved, genomes analysis and evolution, *FEMS Microbiology Reviews*, Vol. 41, No. 6, 941–962. Doi:10.1093/femsre/fux049

[27] Pandey, M. P., Kim, C. S. (2011). Lignin Depolymerization and Conversion: A Review of Thermochemical Methods, *Chemical Engineering and Technology*, Vol. 34, No. 1, 29–41. Doi:10.1002/ceat.201000270

[28] Schwanninger, M., Hinterstoisser, B. (2002). Klason lignin: Modifications to improve the precision of the standardized determination, *Holzforschung*, Vol. 56, No. 2, 161–166. Doi:10.1515/HF.2002.027

[29] Mandlekar, N., Cayla, A., Rault, F., Giraud, S., Salaün, F., Malucelli, G., Guan, J.-P. (2018). An Overview on the Use of Lignin and Its Derivatives in Fire Retardant Polymer Systems, *Lignin - Trends and Applications*, No. April. Doi:10.5772/intechopen.72963

[30] Dessbesell, L., Paleologou, M., Leitch, M., Pulkki, R., Xu, C. (Charles). (2020). Global lignin supply overview and kraft lignin potential as an alternative for petroleum-based polymers, *Renewable and Sustainable Energy Reviews*, Vol. 123, No. February 2019, 109768. Doi:10.1016/j.rser.2020.109768

[31] Schutyser, W., Renders, T., Van Den Bosch, S., Koelewijn, S. F., Beckham, G. T., Sels, B. F. (2018). Chemicals from lignin: An interplay of lignocellulose fractionation, depolymerisation, and upgrading, *Chemical Society Reviews*, Vol. 47, No. 3, 852–908. Doi:10.1039/c7cs00566k

[32] Arapova, O. V., Chistyakov, A. V., Tsodikov, M. V., Moiseev, I. I. (2020). Lignin as a Renewable Resource of Hydrocarbon Products and Energy Carriers (A Review), *Petroleum Chemistry*, Vol. 60, No. 3, 227–243. Doi:10.1134/S0965544120030044

[33] José Borges Gomes, F., de Souza, R. E., Brito, E. O., Costa Lelis, R. C. (2020). A review on lignin sources and uses, *Journal of Applied Biotechnology & Bioengineering*, Vol. 7, No. C, 100–105. Doi:10.15406/jabb.2020.07.00222

[34] Kienberger, M., Maitz, S., Pichler, T., Demmelmayer, P. (2021). Systematic review on isolation processes for technical lignin, *Processes*, Vol. 9, No. 5. Doi:10.3390/pr9050804

[35] Liao, J. J., Latif, N. H. A., Trache, D., Brosse, N., Hussin, M. H. (2020). Current advancement on the isolation, characterization and application of lignin, *International Journal of Biological Macromolecules*, Vol. 162, 985–1024. Doi:10.1016/j.ijbiomac.2020.06.168

[36] Yu, O., Kim, K. H. (2020). Lignin to materials: A focused review on recent novel lignin applications, *Applied Sciences (Switzerland)*, Vol. 10, No. 13. Doi:10.3390/app10134626

[37] Gonçalves, S., Ferra, J., Paiva, N., Martins, J., Carvalho, L. H., Magalhães, F. D. (2021). Lignosulphonates as an alternative to non-renewable binders in wood-based materials, *Polymers*, Vol. 13, No. 23, 1–29. Doi:10.3390/polym13234196

[38] Gonçalves, S., Ferra, J., Paiva, N., Martins, J., Carvalho, L. H., Magalhães, F. D. (2021). Lignosulphonates as an alternative to non-renewable binders in wood-based materials, *Polymers*, Vol. 13, No. 23, 1–29. Doi:10.3390/polym13234196

[39] Lalman, J. A., Shewa, W. A., Gallagher, J. (2016). *Quality Living Through Chemurgy and Green Chemistry*, (P. C.K. Lau, Ed.), Springer Berlin Heidelberg, Berlin, Heidelberg. Doi:10.1007/978-3-662-53704-6

[40] Liao, J. J., Latif, N. H. A., Trache, D., Brosse, N., Hussin, M. H. (2020). Current advancement on the isolation, characterization and application of lignin, *International Journal of Biological Macromolecules*, Vol. 162, 985–1024. Doi:10.1016/j.ijbiomac.2020.06.168

[41] Tao, J., Li, S., Ye, F., Zhou, Y., Lei, L., Zhao, G. (2020). Lignin–An underutilized, renewable and valuable material for food industry, *Critical Reviews in Food Science and Nutrition*, Vol. 60, No. 12, 2011–2033. Doi:10.1080/10408398.2019.1625025

[42] Liu, B., Abu-Omar, M. M. (2021). Lignin extraction and valorization using heterogeneous transition metal catalysts, *Advances in Inorganic Chemistry*, 137–174. Doi:10.1016/bs.adioch.2021.02.001

[43] Heitner, C., Dimmel, D. R., Schmidt, J. A. (2010). *Lignin and Lignans Advanced in Chemistry*, *Methods in Enzymology* (Vol. 161), Taylor and Francis Group, LLC, Boca Raton

[44] Liu, Z., Wang, H., Hui, L. (2018). Pulping and Papermaking of Non-Wood Fibers, *Pulp and Paper Processing*, 3–32. Doi:10.5772/intechopen.79017

[45] Brosse, N., Hussin, M. H., Rahim, A. A. (2017). Organosolv Processes, *Biorefineries*, Springer Nature Switzerland AG, Cham, 153–176. Doi:10.1007/10_2016_61

[46] Fialová, A., Kotlík, P. (2019). Parametry rozpustnosti a jejich využití pro výběr vhodného rozpouštědla nejen v restaurátorské praxi, *Chemické Listy*, Vol. 113, 10–15

[47] Rinaldi, R., Jastrzebski, R., Clough, M. T., Ralph, J., Kennema, M., Bruijnincx, P. C. A., Weckhuysen, B. M. (2016). Paving the Way for Lignin Valorisation: Recent Advances in Bioengineering, Biorefining and Catalysis, *Angewandte Chemie - International Edition*, Vol. 55, No. 29, 8164–8215. Doi:10.1002/anie.201510351

[48] Chung, H., Washburn, N. R. (2013). Chemistry of lignin-based materials, *Green Materials*, Vol. 1, No. 3, 137–160. Doi:10.1680/gmat.12.00009

[49] Mandlekar, N., Cayla, A., Rault, F., Giraud, S., Salaün, F., Malucelli, G., Guan, J.-P. (2018). An Overview on the Use of Lignin and Its Derivatives in Fire Retardant

Polymer Systems, *Lignin - Trends and Applications*, InTech, Rijeka. Doi:10.5772/intechopen.72963

[50] Ponomarenko, J., Dizhbite, T., Lauberts, M., Viksna, A., Dobele, G., Bikovens, O., Telysheva, G. (2014). Characterization of softwood and hardwood lignoboost kraft lignins with emphasis on their antioxidant activity, *BioResources*, Vol. 9, No. 2, 2051–2068. Doi:10.15376/biores.9.2.2051-2068

[51] Nsimba, R. Y., West, N., Boateng, A. A. (2012). Structure and radical scavenging activity relationships of pyrolytic lignins, *Journal of Agricultural and Food Chemistry*, Vol. 60, No. 51, 12525–12530. Doi:10.1021/jf3037787

[52] Ponomarenko, J., Lauberts, M., Dizhbite, T., Lauberte, L., Jurkjane, V., Telysheva, G. (2015). Antioxidant activity of various lignins and lignin-related phenylpropanoid units with high and low molecular weight, *Holzforschung*, Vol. 69, No. 6, 795–805. Doi:10.1515/hf-2014-0280

[53] Ponomarenko, J., Dizhbite, T., Lauberts, M., Volperts, A., Dobele, G., Telysheva, G. (2015). Analytical pyrolysis - A tool for revealing of lignin structure-antioxidant activity relationship, *Journal of Analytical and Applied Pyrolysis*, Vol. 113, 360–369. Doi:10.1016/j.jaap.2015.02.027

[54] Barclay, L. R. C., Xi, F., Norris, J. Q. (1997). Antioxidant properties of phenolic lignin model compounds, *Journal of Wood Chemistry and Technology*, Vol. 17, Nos. 1–2, 73–90. Doi:10.1080/02773819708003119

[55] García, A., González Alriols, M., Spigno, G., Labidi, J. (2012). Lignin as natural radical scavenger. Effect of the obtaining and purification processes on the antioxidant behaviour of lignin, *Biochemical Engineering Journal*, Vol. 67, 173–185. Doi:10.1016/j.bej.2012.06.013

[56] Arshanitsa, A., Ponomarenko, J., Dizhbite, T., Andersone, A., Gosselink, R. J. A., Van Der Putten, J., Lauberts, M., Telysheva, G. (2013). Fractionation of technical lignins as a tool for improvement of their antioxidant properties, *Journal of Analytical and Applied Pyrolysis*, Vol. 103, 78–85. Doi:10.1016/j.jaap.2012.12.023

[57] Domenek, S., Louaifi, A., Guinault, A., Baumberger, S. (2013). Potential of Lignins as Antioxidant Additive in Active Biodegradable Packaging Materials, *Journal of Polymers and the Environment*, Vol. 21, No. 3, 692–701. Doi:10.1007/s10924-013-0570-6

[58] An, L., Wang, G., Jia, H., Liu, C., Sui, W., Si, C. (2017). Fractionation of enzymatic hydrolysis lignin by sequential extraction for enhancing antioxidant performance, *International Journal of Biological Macromolecules*, Vol. 99, 674–681. Doi:10.1016/j.ijbiomac.2017.03.015

[59] Jiang, B., Zhang, Y., Gu, L., Wu, W., Zhao, H., Jin, Y. (2018). Structural elucidation and antioxidant activity of lignin isolated from rice straw and alkali-oxygen black liquor, *International Journal of Biological Macromolecules*, Vol. 116, 513–519. Doi:10.1016/j.ijbiomac.2018.05.063

[60] Espinoza-Acosta, J. L., Torres-Chaves, P. I., Ramirez-Wong, B., Lope-Saiz, C. M., Montario-Leyva, B. (2016). Antioxidant, Antimicrobial, and Antimutagenic Properties of Technical Lignins and Their Applications, *BioResources*, Vol. 11, No. 2, 1–14

[61] Sheng, Y., Ma, Z., Wang, X., Han, Y. (2022). Ethanol organosolv lignin from different agricultural residues: Toward basic structural units and antioxidant activity, *Food Chemistry*, Vol. 376, No. December 2021, 131895. Doi:10.1016/j.foodchem.2021.131895

[62] Faustino, H., Gil, N., Baptista, C., Duarte, A. P. (2010). Antioxidant activity of lignin phenolic compounds extracted from kraft and sulphite black liquors, *Molecules*, Vol. 15, No. 12, 9308–9322. Doi:10.3390/molecules15129308

[63] Aguié-Béghin, V., Foulon, L., Soto, P., Croînier, D., Corti, E., Legée, F., Cézard, L., Chabbert, B., Maillard, M. N., Huijgen, W. J. J., Baumberger, S. (2015). Use of Food and Packaging Model Matrices to Investigate the Antioxidant Properties of Biorefinery Grass Lignins, *Journal of Agricultural and Food Chemistry*, Vol. 63, No. 45, 10022–10031. Doi:10.1021/acs.jafc.5b03686

[64] Gregorová, A., Cibulková, Z., Košíková, B., Šimon, P. (2005). Stabilization effect of lignin in polypropylene and recycled polypropylene, *Polymer Degradation and Stability*, Vol. 89, No. 3, 553–558. Doi:10.1016/j.polymdegradstab.2005.02.007

[65] Pouteau, C., Dole, P., Cathala, B., Averous, L., Boquillon, N. (2003). Antioxidant properties of lignin in polypropylene, *Polymer Degradation and Stability*, Vol. 81, No. 1, 9–18. Doi:10.1016/S0141-3910(03)00057-0

[66] Espinoza Acosta, J. L., Torres Chávez, P. I., Ramírez-Wong, B., Bello-Pérez, L. A., Vega Ríos, A., Carvajal Millán, E., Plascencia Jatomea, M., Ledesma Osuna, A. I. (2015). Mechanical, thermal, and antioxidant properties of composite films prepared from durum wheat starch and lignin, *Starch/Staerke*, Vol. 67, Nos. 5–6, 502–511. Doi:10.1002/star.201500009

[67] Kai, D., Zhang, K., Liow, S. S., Loh, X. J. (2019). New Dual Functional PHB-Grafted Lignin Copolymer: Synthesis, Mechanical Properties, and Biocompatibility Studies, *ACS Applied Bio Materials*, Vol. 2, No. 1, 127–134, research-article. Doi:10.1021/acsabm.8b00445

[68] Vostrejs, P., Adamcová, D., Vaverková, M. D., Enev, V., Kalina, M., Machovsky, M., Šourková, M., Marova, I., Kovalcik, A. (2020). Active biodegradable packaging films modified with grape seeds lignin, *RSC Advances*, Vol. 10, No. 49, 29202–29213. Doi:10.1039/d0ra04074f

[69] Kai, D., Ren, W., Tian, L., Chee, P. L., Liu, Y., Ramakrishna, S., Loh, X. J. (2016). Engineering Poly(lactide)–Lignin Nanofibers with Antioxidant Activity for Biomedical Application, *ACS Sustainable Chemistry & Engineering*, Vol. 4, No. 10, 5268–5276. Doi:10.1021/acssuschemeng.6b00478

[70] Košíková, B., Lábaj, J., Gregorová, A., Slameňová, D. (2006). Lignin antioxidants for preventing oxidation damage of DNA and for stabilizing polymeric composites, *Holzforschung*, Vol. 60, No. 2, 166–170. Doi:10.1515/HF.2006.027

[71] Kai, D., Tan, M. J., Chee, P. L., Chua, Y. K., Yap, Y. L., Loh, X. J. (2016). Towards lignin-based functional materials in a sustainable world, *Green Chemistry*, Vol. 18, No. 5, 1175–1200. Doi:10.1039/c5gc02616d

[72] Klein, S. E., Alzagameem, A., Rumpf, J., Korte, I., Kreyenschmidt, J., Schulze, M. (2019). Antimicrobial activity of lignin-derived polyurethane coatings prepared from unmodified and demethylated lignins, *Coatings*, Vol. 9, No. 8. Doi:10.3390/coatings9080494

[73] Spiridon, I. (2018). Biological and pharmaceutical applications of lignin and its derivatives: A mini-review, *Cellulose Chemistry and Technology*, Vol. 52, Nos. 7–8, 543–550

[74] Ndaba, B., Roopnarain, A., Daramola, M. O., Adeleke, R. (2020). Influence of extraction methods on antimicrobial activities of lignin-based materials: A review, *Sustainable Chemistry and Pharmacy*, Vol. 18, No. April, 100342. Doi:10.1016/j.scp.2020.100342

[75] Dong, X., Dong, M., Lu, Y., Turley, A., Jin, T., Wu, C. (2011). Antimicrobial and antioxidant activities of lignin from residue of corn stover to ethanol production, *Industrial Crops and Products*, Vol. 34, No. 3, 1629–1634. Doi:10.1016/j.indcrop.2011.06.002

[76] Sunthornvarabhas, J., Liengprayoon, S., Suwonsichon, T. (2017). Antimicrobial kinetic activities of lignin from sugarcane bagasse for textile product, *Industrial Crops and Products*, Vol. 109, No. October, 857–861. Doi:10.1016/j.indcrop.2017.09.059

[77] Medina, J. D. C., Woiciechowski, A. L., Filho, A. Z., Bissoqui, L., Noseda, M. D., de Souza Vandenberghe, L. P., Zawadzki, S. F., Soccol, C. R. (2016). Biological activities and thermal behavior of lignin from oil palm empty fruit bunches as potential source of chemicals of added value, *Industrial Crops and Products*, Vol. 94, 630–637. Doi:10.1016/j.indcrop.2016.09.046

[78] García, A., Spigno, G., Labidi, J. (2017). Antioxidant and biocide behaviour of lignin fractions from apple tree pruning residues, *Industrial Crops and Products*, Vol. 104, No. January, 242–252. Doi:10.1016/j.indcrop.2017.04.063

[79] Shu, F., Jiang, B., Yuan, Y., Li, M., Wu, W., Jin, Y., Xiao, H. (2021). Biological Activities and Emerging Roles of Lignin and Lignin-Based Products-A Review, *Biomacromolecules*, Vol. 22, No. 12, 4905–4918. Doi:10.1021/acs.biomac.1c00805

[80] Li, M., Jiang, X., Wang, D., Xu, Z., Yang, M. (2019). In situ reduction of silver nanoparticles in the lignin based hydrogel for enhanced antibacterial application, *Colloids and Surfaces B: Biointerfaces*, Vol. 177, No. February, 370–376. Doi:10.1016/j.colsurfb.2019.02.029

[81] Aadil, K. R., Pandey, N., Mussatto, S. I., Jha, H. (2019). Green synthesis of silver nanoparticles using acacia lignin, their cytotoxicity, catalytic, metal ion sensing capability and antibacterial activity, *Journal of Environmental Chemical Engineering*, Vol. 7, No. 5, 103296. Doi:10.1016/j.jece.2019.103296

[82] Chen, J., An, L., Bae, J. H., Heo, J. W., Han, S. Y., Kim, Y. S. (2021). Green and facile synthesis of aminated lignin-silver complex and its antibacterial activity, *Industrial Crops and Products*, Vol. 173, No. October, 114102. Doi:10.1016/j.indcrop.2021.114102

[83] Dessbesell, L., Paleologou, M., Leitch, M., Pulkki, R., Xu, C. (Charles). (2020). Global lignin supply overview and kraft lignin potential as an alternative for petroleum-based polymers, *Renewable and Sustainable Energy Reviews*, Vol. 123, No. February 2019, 109768. Doi:10.1016/j.rser.2020.109768

[84] Gregorová, A., Cibulková, Z., Košíková, B., Šimon, P. (2005). Stabilization effect of lignin in polypropylene and recycled polypropylene, *Polymer Degradation and Stability*, Vol. 89, No. 3, 553–558. Doi:10.1016/j.polymdegradstab.2005.02.007

[85] Sadeghifar, H., Argyropoulos, D. S. (2015). Correlations of the Antioxidant Properties of Softwood Kraft Lignin Fractions with the Thermal Stability of Its Blends with Polyethylene, *ACS Sustainable Chemistry & Engineering*, Vol. 3, No. 2, 349–356. Doi:10.1021/sc500756n

[86] Barzegari, M. R., Alemdar, A., Zhang, Y., Rodrigue, D. (2012). Mechanical and rheological behavior of highly filled polystyrene with lignin, *Polymer Composites*, Vol. 33, No. 3, 353–361. Doi:10.1002/pc.22154

[87] Gadhave, R. V, Kasbe, P. S., Mahanwar, P. A., Gadekar, P. T. (2019). Synthesis and characterization of lignin-polyurethane based wood adhesive, *International Journal of Adhesion and Adhesives*, Vol. 95, No. August, 102427. Doi:10.1016/j.ijadhadh.2019.102427

[88] Nguyen, N. A., Bowland, C. C., Naskar, A. K. (2018). A general method to improve 3D-printability and inter-layer adhesion in lignin-based composites, *Applied Materials Today*, Vol. 12, 138–152. Doi:10.1016/j.apmt.2018.03.009

[89] Acosta, J. L. E., Chávez, P. I. T., Ramírez-Wong, B., Bello-Pérez, L. A., Ríos, A. V., Millán, E. C., Jatomea, M. P., Osuna, A. I. L. (2015). Mechanical, thermal, and antioxidant properties of composite films prepared from durum wheat starch and lignin, *Starch/Staerke*, Vol. 67, Nos. 5–6, 502–511. Doi:10.1002/star.201500009

[90] Vostrejs, P., Adamcová, D., Vaverková, M. D., Enev, V., Kalina, M., Machovsky, M., Šourková, M., Marova, I., Kovalcik, A. (2020). Active biodegradable packaging films modified with grape seeds lignin, *RSC Advances*, Vol. 10, No. 49, 29202–29213. Doi:10.1039/d0ra04074f

[91] Vaidya, A. A., Collet, C., Gaugler, M., Lloyd-Jones, G. (2019). Integrating softwood biorefinery lignin into polyhydroxybutyrate composites and application in 3D printing,

Materials Today Communications, Vol. 19, No. February, 286–296. Doi:10.1016/j.mtcomm.2019.02.008

[92] Kai, D., Chong, H. M., Chow, L. P., Jiang, L., Lin, Q., Zhang, K., Zhang, H., Zhang, Z., Loh, X. J. (2018). Strong and biocompatible lignin /poly (3-hydroxybutyrate) composite nanofibers, *Composites Science and Technology*, Vol. 158, 26–33. Doi:10.1016/j.compscitech.2018.01.046

[93] Kovalcik, A., Machovsky, M., Kozakova, Z., Koller, M. (2015). Designing packaging materials with viscoelastic and gas barrier properties by optimized processing of poly(3-hydroxybutyrate-co-3-hydroxyvalerate) with lignin, *Reactive and Functional Polymers*, Vol. 94, 25–34. Doi:10.1016/j.reactfunctpolym.2015.07.001

[94] Tanase-Opedal, M., Espinosa, E., Rodríguez, A., Chinga-Carrasco, G. (2019). Lignin: A Biopolymer from Forestry Biomass for Biocomposites and 3D Printing, *Materials*, Vol. 12, No. 18, 3006. Doi:10.3390/ma12183006

[95] Kovalcik, A., Pérez-Camargo, R. A., Fürst, C., Kucharczyk, P., Müller, A. J. (2017). Nucleating efficiency and thermal stability of industrial non-purified lignins and ultrafine talc in poly(lactic acid) (PLA), *Polymer Degradation and Stability*, Vol. 142, 244–254. Doi:10.1016/j.polymdegradstab.2017.07.009

[96] Sarika, P. R., Nancarrow, P., Khansaheb, A., Ibrahim, T. (2020). Bio-based alternatives to phenol and formaldehyde for the production of resins, *Polymers*, Vol. 12, No. 10, 1–24. Doi:10.3390/polym12102237

[97] Xu, C., Ferdosian, F. (2017). *Conversion of Lignin into Bio-Based Chemicals and Materials*, Springer Berlin Heidelberg. Doi:10.1007/978-3-662-54959-9

[98] Suota, M. J., Kochepka, D. M., Ganter Moura, M. G., Pirich, C. L., Matos, M., Magalhães, W. L. E., Ramos, L. P. (2021). Lignin functionalization strategies and the potential applications of its derivatives – A Review, *BioResources*, Vol. 16, No. 3, 6471–6511. Doi:10.15376/biores.16.3.Suota

[99] Sun, Z., Fridrich, B., Santi, A. De, Elangovan, S., Barta, K. (2018). Bright Side of Lignin Depolymerization: Toward New Platform Chemicals, *Chemical Reviews*, Vol. 118, No. 2, 614–678. Doi:10.1021/acs.chemrev.7b00588

[100] Marinović, M., Nousiainen, P., Dilokpimol, A., Kontro, J., Moore, R., Sipilä, J., de Vries, R. P., Mäkelä, M. R., Hildén, K. (2018). Selective Cleavage of Lignin β- O -4 Aryl Ether Bond by β-Etherase of the White-Rot Fungus Dichomitus squalens, *ACS Sustainable Chemistry & Engineering*, Vol. 6, No. 3, 2878–2882. Doi:10.1021/acssuschemeng.7b03619

[101] Schutyser, W., Renders, T., Bosch, S. Van Den, Koelewijn, S. F., Beckham, G. T., Sels, B. F. (2018). Chemicals from lignin: An interplay of lignocellulose fractionation, depolymerisation, and upgrading, *Chemical Society Reviews*, Vol. 47, No. 3, 852–908. Doi:10.1039/c7cs00566k

[102] Paone, E., Tabanelli, T., Mauriello, F. (2020). The rise of lignin biorefinery, *Current Opinion in Green and Sustainable Chemistry*, Vol. 24, No. Figure 1, 1–6. Doi:10.1016/j.cogsc.2019.11.004

[103] Jiang, L., Wang, C.-G., Chee, P. L., Qu, C., Fok, A. Z., Yong, F. H., Ong, Z. L., Kai, D. (2023). Strategies for lignin depolymerization and reconstruction towards functional polymers, *Sustainable Energy & Fuels*, Vol. 7, No. 13, 2953–2973. Doi:10.1039/D3SE00173C

[104] Bugg, T. D., Ahmad, M., Hardiman, E. M., Singh, R. (2011). The emerging role for bacteria in lignin degradation and bio-product formation, *Current Opinion in Biotechnology*, Vol. 22, No. 3, 394–400. Doi:10.1016/j.copbio.2010.10.009

[105] Li, C., Chen, C., Wu, X., Tsang, C. W., Mou, J., Yan, J., Liu, Y., Lin, C. S. K. (2019). Recent advancement in lignin biorefinery: With special focus on enzymatic degradation and valorization, *Bioresource Technology*, Vol. 291, No. May, 121898. Doi:10.1016/j.biortech.2019.121898

[106] Yang, C., Qin, J., Sun, S., Gao, D., Fang, Y., Chen, G., Tian, C., Bao, C., Zhang, S. (2024). Progress in developing methods for lignin depolymerization and elucidating the associated mechanisms, *European Polymer Journal*, Vol. 210, 112995. Doi:10.1016/j.eurpolymj.2024.112995

[107] Dashtban, M., Schraft, H., Syed, T. A., Qin, W. (2010). Fungal biodegradation and enzymatic modification of lignin., *International Journal of Biochemistry and Molecular Biology*, Vol. 1, No. 1, 36–50

[108] Wong, D. W. S. (2009). Structure and Action Mechanism of Ligninolytic Enzymes, *Applied Biochemistry and Biotechnology*, Vol. 157, No. 2, 174–209. Doi:10.1007/s12010-008-8279-z

[109] Šušla, M., Svobodová, K. (2006). Lignolytické enzymy jako účinné nástroje pro biodegradaci obtížně rozložitelných organopolutantů, *Chemické Listy*, Vol. 100, No. 100, 889–895

[110] Piontek, K., Antorini, M., Choinowski, T. (2002). Crystal Structure of a Laccase from the FungusTrametes versicolor at 1.90-Å Resolution Containing a Full Complement of Coppers, *Journal of Biological Chemistry*, Vol. 277, No. 40, 37663–37669. Doi:10.1074/jbc.M204571200

[111] Pollegioni, L., Tonin, F., Rosini, E. (2015). Lignin-degrading enzymes, *The FEBS Journal*, Vol. 282, No. 7, 1190–1213. Doi:10.1111/febs.13224

[112] Leynaud Kieffer Curran, L. M. C., Pham, L. T. M., Sale, K. L., Simmons, B. A. (2022). Review of advances in the development of laccases for the valorization of lignin to enable the production of lignocellulosic biofuels and bioproducts, *Biotechnology Advances*, Vol. 54, 107809. Doi:10.1016/j.biotechadv.2021.107809

[113] Bourbonnais, R., Paice, M. G. (1990). Oxidation of non-phenolic substrates, *FEBS Letters*, Vol. 267, No. 1, 99–102. Doi:10.1016/0014-5793(90)80298-W

[114] Weng, C., Peng, X., Han, Y. (2021). Depolymerization and conversion of lignin to value-added bioproducts by microbial and enzymatic catalysis, *Biotechnology for Biofuels*, Vol. 14, No. 1, 84. Doi:10.1186/s13068-021-01934-w

[115] Chan, J. C., Paice, M., Zhang, X. (2020). Enzymatic Oxidation of Lignin: Challenges and Barriers Toward Practical Applications, *ChemCatChem*, Vol. 12, No. 2, 401–425. Doi:10.1002/cctc.201901480

[116] Atiwesh, G., Parrish, C. C., Banoub, J., Le, T. T. (2022). Lignin degradation by microorganisms: A review, *Biotechnology Progress*, Vol. 38, No. 2, e3226. Doi:10.1002/btpr.3226

[117] Falade, A. O., Nwodo, U. U., Iweriebor, B. C., Green, E., Mabinya, L. V., Okoh, A. I. (2017). Lignin peroxidase functionalities and prospective applications, *MicrobiologyOpen*, Vol. 6, No. 1, e00394. Doi:10.1002/mbo3.394

[118] Abdel-Hamid, A. M., Solbiati, J. O., Cann, I. K. O. (2013). Insights into Lignin Degradation and its Potential Industrial Applications, *Advances in Applied Microbiology* (Vol. 82), Academic Press, 1–28. Doi:10.1016/B978-0-12-407679-2.00001-6

[119] Wariishi, H., Gold, M. H. (1989). Lignin peroxidase compound III, *FEBS Letters*, Vol. 243, No. 2, 165–168. Doi:10.1016/0014-5793(89)80122-X

[120] Bilal, M., Zdarta, J., Jesionowski, T., Iqbal, H. M. N. (2023). Manganese peroxidases as robust biocatalytic tool — An overview of sources, immobilization, and biotechnological applications, *International Journal of Biological Macromolecules*, Vol. 234, 123531. Doi:10.1016/j.ijbiomac.2023.123531

[121] Hofrichter, M. (2002). Review: lignin conversion by manganese peroxidase (MnP), *Enzyme and Microbial Technology*, Vol. 30, No. 4, 454–466. Doi:10.1016/S0141-0229(01)00528-2

[122] Reshmy, R., Athiyaman Balakumaran, P., Divakar, K., Philip, E., Madhavan, A., Pugazhendhi, A., Sirohi, R., Binod, P., Kumar Awasthi, M., Sindhu, R. (2022). Microbial valorization of lignin: Prospects and challenges, *Bioresource Technology*, Vol. 344, 126240. Doi:10.1016/j.biortech.2021.126240

[123] Ji, T., Liaqat, F., Khazi, M. I., Liaqat, N., Nawaz, M. Z., Zhu, D. (2024). Lignin biotransformation: Advances in enzymatic valorization and bioproduction strategies, *Industrial Crops and Products*, Vol. 216, 118759. Doi:10.1016/j.indcrop.2024.118759

[124] D'Arrigo, P., Rossato, L. A. M., Strini, A., Serra, S. (2024). From Waste to Value: Recent Insights into Producing Vanillin from Lignin, *Molecules*, Vol. 29, No. 2, 442. Doi:10.3390/molecules29020442

[125] Zulkarnain, A., Bahrin, E. K., Ramli, N., Phang, L. Y., Abd-Aziz, S. (2018). Alkaline Hydrolysate of Oil Palm Empty Fruit Bunch as Potential Substrate for Biovanillin Production via Two-Step Bioconversion, *Waste and Biomass Valorization*, Vol. 9, No. 1, 13–23. Doi:10.1007/s12649-016-9745-4

[126] Wu, W., Dutta, T., Varman, A. M., Eudes, A., Manalansan, B., Loqué, D., Singh, S. (2017). Lignin Valorization: Two Hybrid Biochemical Routes for the Conversion of Polymeric Lignin into Value-added Chemicals, *Scientific Reports*, Vol. 7, No. 1, 8420. Doi:10.1038/s41598-017-07895-1

[127] Barton, N., Horbal, L., Starck, S., Kohlstedt, M., Luzhetskyy, A., Wittmann, C. (2018). Enabling the valorization of guaiacol-based lignin: Integrated chemical and biochemical production of cis,cis-muconic acid using metabolically engineered Amycolatopsis sp ATCC 39116, *Metabolic Engineering*, Vol. 45, 200–210. Doi:10.1016/j.ymben.2017.12.001

[128] Rivaldi, J. D., Carvalho, A. K. F., da Conceição, L. R. V., de Castro, H. F. (2017). Assessing the potential of fatty acids produced by filamentous fungi as feedstock for biodiesel production, *Preparative Biochemistry & Biotechnology*, Vol. 47, No. 10, 970–976. Doi:10.1080/10826068.2017.1365246

[129] Kitcha, S., Cheirsilp, B. (2014). Bioconversion of lignocellulosic palm byproducts into enzymes and lipid by newly isolated oleaginous fungi, *Biochemical Engineering Journal*, Vol. 88, 95–100. Doi:10.1016/j.bej.2014.04.006

[130] Cheirsilp, B., Kitcha, S. (2015). Solid state fermentation by cellulolytic oleaginous fungi for direct conversion of lignocellulosic biomass into lipids: Fed-batch and repeated-batch fermentations, *Industrial Crops and Products*, Vol. 66, 73–80. Doi:10.1016/j.indcrop.2014.12.035

[131] Wang, Z., Li, N., Pan, X. (2019). Transformation of Ammonia Fiber Expansion (AFEX) corn stover lignin into microbial lipids by Rhodococcus opacus, *Fuel*, Vol. 240, 119–125. Doi:10.1016/j.fuel.2018.11.081

[132] Kosa, M., Ragauskas, A. J. (2012). Bioconversion of lignin model compounds with oleaginous Rhodococci, *Applied Microbiology and Biotechnology*, Vol. 93, No. 2, 891–900. Doi:10.1007/s00253-011-3743-z

[133] Zhang, K., Xu, R., Abomohra, A. E.-F., Xie, S., Yu, Z., Guo, Q., Liu, P., Peng, L., Li, X. (2019). A sustainable approach for efficient conversion of lignin into biodiesel accompanied by biological pretreatment of corn straw, *Energy Conversion and Management*, Vol. 199, 111928. Doi:10.1016/j.enconman.2019.111928

[134] Zhao, Z.-M., Meng, X., Pu, Y., Li, M., Li, Y., Zhang, Y., Chen, F., Ragauskas, A. J. (2023). Bioconversion of Homogeneous Linear C-Lignin to Polyhydroxyalkanoates, *Biomacromolecules*, Vol. 24, No. 9, 3996–4004. Doi:10.1021/acs.biomac.3c00288

[135] Wang, X., Lin, L., Dong, J., Ling, J., Wang, W., Wang, H., Zhang, Z., Yu, X. (2018). Simultaneous Improvements of Pseudomonas Cell Growth and Polyhydroxyalkanoate Production from a Lignin Derivative for Lignin-Consolidated Bioprocessing, *Applied and Environmental Microbiology*, Vol. 84, No. 18. Doi:10.1128/AEM.01469-18

[136] Mori, T., Kako, H., Sumiya, T., Kawagishi, H., Hirai, H. (2016). Direct lactic acid production from beech wood by transgenic white-rot fungus Phanerochaete sordida

YK-624, *Journal of Biotechnology*, Vol. 239, 83–89. Doi:10.1016/j.jbiotec.2016.10.014

[137] Rodríguez-Couto, S. (2017). Industrial and environmental applications of white-rot fungi, *Mycosphere*, Vol. 8, No. 3, 456–466. Doi:10.5943/mycosphere/8/3/7

[138] Chai, Y., Bai, M., Chen, A., Peng, L., Shao, J., Luo, S., Deng, Y., Yan, B., Peng, C. (2022). Valorization of waste biomass through fungal technology: Advances, challenges, and prospects, *Industrial Crops and Products*, Vol. 188, 115608. Doi:10.1016/j.indcrop.2022.115608

[139] Lan, W., Luterbacher, J. S. (2019). A Road to Profitability from Lignin via the Production of Bioactive Molecules, *ACS Central Science*, Vol. 5, No. 10, 1642–1644. Doi:10.1021/acscentsci.9b00954

[140] Saurabh Bidwai. (2025, January 16). Styrene Market Size to Hit USD 108.35 Billion by 2034, from https://www.precedenceresearch.com/styrene-market, accessed 19-3-2025

[141] Deng, J., Sun, S. F., Zhu, E. Q., Yang, J., Yang, H. Y., Wang, D. W., Ma, M. G., Shi, Z. J. (2021). Sub-micro and nano-lignin materials: Small size and rapid progress, *Industrial Crops and Products*, Vol. 164, No. December 2020, 113412. Doi:10.1016/j.indcrop.2021.113412

[142] Österberg, M., Sipponen, M. H., Mattos, B. D., Rojas, O. J. (2020). Spherical lignin particles: A review on their sustainability and applications, *Green Chemistry*, Vol. 22, No. 9, 2712–2733. Doi:10.1039/d0gc00096e

[143] Figueiredo, P., Lintinen, K., Kiriazis, A., Hynninen, V., Liu, Z., Bauleth-Ramos, T., Rahikkala, A., Correia, A., Kohout, T., Sarmento, B., Yli-Kauhaluoma, J., Hirvonen, J., Ikkala, O., Kostiainen, M. A., Santos, H. A. (2017). In vitro evaluation of biodegradable lignin-based nanoparticles for drug delivery and enhanced antiproliferation effect in cancer cells, *Biomaterials*, Vol. 121, 97–108. Doi:10.1016/j.biomaterials.2016.12.034

[144] Dai, L., Liu, R., Hu, L.-Q., Zou, Z.-F., Si, C.-L. (2017). Lignin Nanoparticle as a Novel Green Carrier for the Efficient Delivery of Resveratrol, *ACS Sustainable Chemistry & Engineering*, Vol. 5, No. 9, 8241–8249. Doi:10.1021/acssuschemeng.7b01903

[145] Schneider, W. D. H., Dillon, A. J. P., Camassola, M. (2021). Lignin nanoparticles enter the scene: A promising versatile green tool for multiple applications, *Biotechnology Advances*, Vol. 47, No. December 2020. Doi:10.1016/j.biotechadv.2020.107685

[146] Ago, M., Huan, S., Borghei, M., Raula, J., Kauppinen, E. I., Rojas, O. J. (2016). High-Throughput Synthesis of Lignin Particles (∼30 nm to ∼2 μm) via Aerosol Flow Reactor: Size Fractionation and Utilization in Pickering Emulsions, *ACS Applied Materials & Interfaces*, Vol. 8, No. 35, 23302–23310. Doi:10.1021/acsami.6b07900

[147] Lourencon, T. V., Greca, L. G., Tarasov, D., Borrega, M., Tamminen, T., Rojas, O. J., Balakshin, M. Y. (2020). Lignin-First Integrated Hydrothermal Treatment (HTT) and

Synthesis of Low-Cost Biorefinery Particles, *ACS Sustainable Chemistry & Engineering*, Vol. 8, No. 2, 1230–1239. Doi:10.1021/acssuschemeng.9b06511

[148] Lintinen, K., Xiao, Y., Bangalore Ashok, R., Leskinen, T., Sakarinen, E., Sipponen, M., Muhammad, F., Oinas, P., Österberg, M., Kostiainen, M. (2018). Closed cycle production of concentrated and dry redispersible colloidal lignin particles with a three solvent polarity exchange method, *Green Chemistry*, Vol. 20, No. 4, 843–850. Doi:10.1039/C7GC03465B

[149] Sipponen, M. H., Smyth, M., Leskinen, T., Johansson, L. S., Österberg, M. (2017). All-lignin approach to prepare cationic colloidal lignin particles: Stabilization of durable Pickering emulsions, *Green Chemistry*, Vol. 19, No. 24, 5831–5840. Doi:10.1039/c7gc02900d

[150] Tian, D., Hu, J., Chandra, R. P., Saddler, J. N., Lu, C. (2017). Valorizing Recalcitrant Cellulolytic Enzyme Lignin via Lignin Nanoparticles Fabrication in an Integrated Biorefinery, *ACS Sustainable Chemistry and Engineering*, Vol. 5, No. 3, 2702–2710. Doi:10.1021/acssuschemeng.6b03043

[151] Dai, L., Li, Y., Liu, R., Si, C., Ni, Y. (2019). Green mussel-inspired lignin magnetic nanoparticles with high adsorptive capacity and environmental friendliness for chromium(III) removal, *International Journal of Biological Macromolecules*, Vol. 132, 478–486. Doi:10.1016/j.ijbiomac.2019.03.222

[152] Schneider, W. D. H., Dillon, A. J. P., Camassola, M. (2021). Lignin nanoparticles enter the scene: A promising versatile green tool for multiple applications, *Biotechnology Advances*, Vol. 47, No. December 2020. Doi:10.1016/j.biotechadv.2020.107685

[153] Lee, J. H., Park, S. Y., Choi, I. G., Choi, J. W. (2020). Investigation of molecular size effect on the formation of lignin nanoparticles by nanoprecipitation, *Applied Sciences (Switzerland)*, Vol. 10, No. 14. Doi:10.3390/app10144910

[154] Hussin, M. H., Appaturi, J. N., Poh, N. E., Latif, N. H. A., Brosse, N., Ziegler-Devin, I., Vahabi, H., Syamani, F. A., Fatriasari, W., Solihat, N. N., Karimah, A., Iswanto, A. H., Sekeri, S. H., Ibrahim, M. N. M. (2022). A recent advancement on preparation, characterization and application of nanolignin, *International Journal of Biological Macromolecules*, Vol. 200, No. November 2021, 303–326. Doi:10.1016/j.ijbiomac.2022.01.007

[155] Leskinen, T., Smyth, M., Xiao, Y., Lintinen, K., Mattinen, M. L., Kostiainen, M. A., Oinas, P., Österberg, M. (2017). Scaling Up Production of Colloidal Lignin Particles, *Nordic Pulp and Paper Research Journal*, Vol. 32, No. 4, 586–596. Doi:10.3183/npprj-2017-32-04_p586-596_leskinen

[156] Lievonen, M., Valle-Delgado, J. J., Mattinen, M. L., Hult, E. L., Lintinen, K., Kostiainen, M. A., Paananen, A., Szilvay, G. R., Setälä, H., Österberg, M. (2016). A simple process for lignin nanoparticle preparation, *Green Chemistry*, Vol. 18, No. 5, 1416–1422. Doi:10.1039/c5gc01436k

[157] Yin, H., Liu, L., Wang, X., Wang, T., Zhou, Y., Liu, B., Shan, Y., Wang, L., Lü, X. (2018). A novel flocculant prepared by lignin nanoparticles-gelatin complex from switchgrass for the capture of Staphylococcus aureus and Escherichia coli, *Colloids and Surfaces A: Physicochemical and Engineering Aspects*, Vol. 545, No. February, 51–59. Doi:10.1016/j.colsurfa.2018.02.033

[158] Wang, B., Sun, D., Wang, H. M., Yuan, T. Q., Sun, R. C. (2019). Green and Facile Preparation of Regular Lignin Nanoparticles with High Yield and Their Natural Broad-Spectrum Sunscreens, *ACS Sustainable Chemistry and Engineering*, Vol. 7, No. 2, 2658–2666. Doi:10.1021/acssuschemeng.8b05735

[159] Pang, Y., Sun, Y., Luo, Y., Zhou, M., Qiu, X., Yi, C., Lou, H. (2021). Preparation of novel all-lignin microcapsules via interfacial cross-linking of pickering emulsion, *Industrial Crops and Products*, Vol. 167, No. March, 113468. Doi:10.1016/j.indcrop.2021.113468

[160] Gao, F., Qi, Q., Wu, X., Yu, J., Yao, J., Cao, Z., Mi, Y., Cui, Q. (2021). Multifunctional poly(quaternary ammonium)/Fe3O4 composite nanogels for integration of antibacterial and degradable magnetic redox-responsive properties, *Colloids and Surfaces A: Physicochemical and Engineering Aspects*, Vol. 615, 126235. Doi:10.1016/j.colsurfa.2021.126235

[161] Kai, D., Jiang, S., Low, Z. W., Loh, X. J. (2015). Engineering highly stretchable lignin-based electrospun nanofibers for potential biomedical applications, *Journal of Materials Chemistry B*, Vol. 3, No. 30, 6194–6204. Doi:10.1039/c5tb00765h

[162] Rangan, A., Manchiganti, M. V., Thilaividankan, R. M., Kestur, S. G., Menon, R. (2017). Novel method for the preparation of lignin-rich nanoparticles from lignocellulosic fibers, *Industrial Crops and Products*, Vol. 103, 152–160. Doi:10.1016/j.indcrop.2017.03.037

[163] Juikar, S. J., Vigneshwaran, N. (2017). Extraction of nanolignin from coconut fibers by controlled microbial hydrolysis, *Industrial Crops and Products*, Vol. 109, No. August, 420–425. Doi:10.1016/j.indcrop.2017.08.067

[164] Zhang, Z., Terrasson, V., Guénin, E. (2021). Lignin Nanoparticles and Their Nanocomposites, *Nanomaterials*, Vol. 11, No. 5, 1336. Doi:10.3390/nano11051336

[165] Liu, K., Zhuang, Y., Chen, J., Yang, G., Dai, L. (2022). Research Progress on the Preparation and High-Value Utilization of Lignin Nanoparticles, *International Journal of Molecular Sciences 2022, Vol. 23, Page 7254*, Vol. 23, No. 13, 7254. Doi:10.3390/ijms23137254

[166] Yadav, V. K., Gupta, N., Kumar, P., Dashti, M. G., Tirth, V., Khan, S. H., Yadav, K. K., Islam, S., Choudhary, N., Algahtani, A., Bera, S. P., Kim, D. H., Jeon, B. H. (2022). Recent Advances in Synthesis and Degradation of Lignin and Lignin Nanoparticles and Their Emerging Applications in Nanotechnology, *Materials 2022, Vol. 15, Page 953*, Vol. 15, No. 3, 953. Doi:10.3390/ma15030953

[167] Behera, S., Mohapatra, S., Behera, B. C., Thatoi, H. (2024). Recent updates on green synthesis of lignin nanoparticle and its potential applications in modern biotechnology, *Critical Reviews in Biotechnology*, Vol. 44, No. 5, 774–794. Doi:10.1080/07388551.2023.2229512

[168] Zhu, B., Xu, Y., Xu, H. (2022). Preparation and application of lignin nanoparticles: a review, *Nano Futures*, Vol. 6, No. 3, 032004. Doi:10.1088/2399-1984/ac8400

[169] Siddiqui, L., Bag, J., Seetha, Mittal, D., Leekha, A., Mishra, H., Mishra, M., Verma, A. K., Mishra, P. K., Ekielski, A., Iqbal, Z., Talegaonkar, S. (2020). Assessing the potential of lignin nanoparticles as drug carrier: Synthesis, cytotoxicity and genotoxicity studies, *International Journal of Biological Macromolecules*, Vol. 152, 786–802. Doi:10.1016/j.ijbiomac.2020.02.311

[170] Zhou, Y., Han, Y., Li, G., Yang, S., Xiong, F., Chu, F. (2019). Preparation of Targeted Lignin–Based Hollow Nanoparticles for the Delivery of Doxorubicin, *Nanomaterials*, Vol. 9, No. 2, 188. Doi:10.3390/nano9020188

[171] Pathania, K., Sah, S. P., Salunke, D. B., Jain, M., Yadav, A. K., Yadav, V. G., Pawar, S. V. (2023). Green synthesis of lignin-based nanoparticles as a bio-carrier for targeted delivery in cancer therapy, *International Journal of Biological Macromolecules*, Vol. 229, 684–695. Doi:10.1016/j.ijbiomac.2022.12.323

[172] Lu, F., Ni, S., Meng, X., Si, C., Qin, M., Wang, Y., Fu, Y., Chen, X. (2023). Preparation of pH-sensitive lignin nanoparticles and its application in hydrophobic drug delivery, *Industrial Crops and Products*, Vol. 202, 117012. Doi:10.1016/j.indcrop.2023.117012

[173] Lee, J. H., Im, J. S., Jin, X., Kim, T. M., Choi, J. W. (2022). In Vitro and In Vivo Evaluation of Drug-Encapsulated Lignin Nanoparticles for Release Control, *ACS Sustainable Chemistry & Engineering*, Vol. 10, No. 18, 5792–5802. Doi:10.1021/acssuschemeng.1c08529

[174] Gao, H., Sun, M., Duan, Y., Cai, Y., Dai, H., Xu, T. (2023). Controllable synthesis of lignin nanoparticles with antibacterial activity and analysis of its antibacterial mechanism, *International Journal of Biological Macromolecules*, Vol. 246, 125596. Doi:10.1016/j.ijbiomac.2023.125596

[175] Ali, M. A. S., Abdel-Moein, N. M., Owis, A. S., Ahmed, S. E., Hanafy, E. A. (2024). Eco-friendly lignin nanoparticles as antioxidant and antimicrobial material for enhanced textile production, *Scientific Reports 2024 14:1*, Vol. 14, No. 1, 1–13. Doi:10.1038/s41598-024-67449-0

[176] Bragato, C., Persico, A., Ferreres, G., Tzanov, T., Mantecca, P. (2024). Exploring the Effects of Lignin Nanoparticles in Different Zebrafish Inflammatory Models, *International Journal of Nanomedicine*, Vol. Volume 19, 7731–7750. Doi:10.2147/IJN.S469813

[177] Du, B., Li, W., Bai, Y., Pan, Z., Wang, Q., Wang, X., Ding, H., Lv, G., Zhou, J. (2022). Fabrication of uniform lignin nanoparticles with tunable size for potential

wound healing application, *International Journal of Biological Macromolecules*, Vol. 214, 170–180. Doi:10.1016/j.ijbiomac.2022.06.066

[178] Chaudhary, M., Sinha, V. R. (2023). Lignin-based carriers for drug delivery applications: From an industrial waste to a pharmaceutical aid, *European Polymer Journal*, Vol. 195, 112206. Doi:10.1016/j.eurpolymj.2023.112206

[179] Mukheja, Y., Kethavath, S. N., Banoth, L., Pawar, S. V. (2024). Lignin: The green powerhouse for enzyme immobilization in biocatalysis and biosensing, *International Journal of Biological Macromolecules*, Vol. 280, 135940. Doi:10.1016/j.ijbiomac.2024.135940

[180] Stanisz, M., Bachosz, K., Siwińska-Ciesielczyk, K., Klapiszewski, Ł., Zdarta, J., Jesionowski, T. (2022). Tailoring Lignin-Based Spherical Particles as a Support for Lipase Immobilization, *Catalysts*, Vol. 12, No. 9, 1031. Doi:10.3390/catal12091031

[181] Gorish, B. M. T., Abdelmula, W. I. Y., Sethupathy, S., Robele, A. B., Zhu, D. (2024). Harnessing Lignin Nanoparticles for Sustainable Enzyme Immobilization: Current Paradigms and Future Innovations, *Applied Biochemistry and Biotechnology*, 1–26. Doi:10.1007/S12010-024-05133-9/METRICS

[182] Sipponen, M. H., Farooq, M., Koivisto, J., Pellis, A., Seitsonen, J., Österberg, M. (2018). Spatially confined lignin nanospheres for biocatalytic ester synthesis in aqueous media, *Nature Communications 2018 9:1*, Vol. 9, No. 1, 1–7. Doi:10.1038/s41467-018-04715-6

[183] Tomaino, E., Capecchi, E., Piccinino, D., Saladino, R. (2022). Lignin Nanoparticles Support Lipase-Tyrosinase Enzymatic Cascade in the Synthesis of Lipophilic Hydroxytyrosol Ester Derivatives, *ChemCatChem*, Vol. 14, No. 18, e202200380. Doi:10.1002/cctc.202200380

[184] Rossato, L. A. M., Morsali, M., Ruffini, E., Bertuzzi, P., Serra, S., D'Arrigo, P., Sipponen, M. (2024). Phospholipase D Immobilization on Lignin Nanoparticles for Enzymatic Transformation of Phospholipids, *ChemSusChem*, Vol. 17, No. 3, e202300803. Doi:10.1002/cssc.202300803

[185] Capecchi, E., Piccinino, D., Delfino, I., Bollella, P., Antiochia, R., Saladino, R. (2018). Functionalized Tyrosinase-Lignin Nanoparticles as Sustainable Catalysts for the Oxidation of Phenols, *Nanomaterials 2018, Vol. 8, Page 438*, Vol. 8, No. 6, 438. Doi:10.3390/nano8060438

[186] Piccinino, D., Capecchi, E., Botta, L., Bollella, P., Antiochia, R., Crucianelli, M., Saladino, R. (2019). Layer by layer supported laccase on lignin nanoparticles catalyzes the selective oxidation of alcohols to aldehydes, *Catalysis Science & Technology*, Vol. 9, No. 15, 4125–4134. Doi:10.1039/C9CY00962K

[187] Capecchi, E., Piccinino, D., Tomaino, E., Bizzarri, B. M., Polli, F., Antiochia, R., Mazzei, F., Saladino, R. (2020). Lignin nanoparticles are renewable and functional platforms for the concanavalin a oriented immobilization of glucose oxidase–

peroxidase in cascade bio-sensing, *RSC Advances*, Vol. 10, No. 48, 29031–29042. Doi:10.1039/D0RA04485G

[188] Pereira, A. do E. S., Luiz de Oliveira, J., Maira Savassa, S., Barbara Rogério, C., Araujo de Medeiros, G., Fraceto, L. F. (2022). Lignin nanoparticles: New insights for a sustainable agriculture, *Journal of Cleaner Production*, Vol. 345, 131145. Doi:10.1016/j.jclepro.2022.131145

[189] Li, T., Lü, S., Wang, Z., Huang, M., Yan, J., Liu, M. (2021). Lignin-based nanoparticles for recovery and separation of phosphate and reused as renewable magnetic fertilizers, *Science of The Total Environment*, Vol. 765, 142745. Doi:10.1016/j.scitotenv.2020.142745

[190] Zikeli, F., Vinciguerra, V., Sennato, S., Scarascia Mugnozza, G., Romagnoli, M. (2020). Preparation of Lignin Nanoparticles with Entrapped Essential Oil as a Bio-Based Biocide Delivery System, *ACS Omega*, Vol. 5, No. 1, 358–368. Doi:10.1021/acsomega.9b02793

[191] Xiao, D., Ding, W., Zhang, J., Ge, Y., Wu, Z., Li, Z. (2019). Fabrication of a versatile lignin-based nano-trap for heavy metal ion capture and bacterial inhibition, *Chemical Engineering Journal*, Vol. 358, 310–320. Doi:10.1016/j.cej.2018.10.037

[192] Dai, L., Li, Y., Liu, R., Si, C., Ni, Y. (2019). Green mussel-inspired lignin magnetic nanoparticles with high adsorptive capacity and environmental friendliness for chromium(III) removal, *International Journal of Biological Macromolecules*, Vol. 132, 478–486. Doi:10.1016/j.ijbiomac.2019.03.222

[193] Pourbaba, R., Abdulkhani, A., Rashidi, A., Ashori, A. (2024). Lignin nanoparticles as a highly efficient adsorbent for the removal of methylene blue from aqueous media, *Scientific Reports 2024 14:1*, Vol. 14, No. 1, 1–13. Doi:10.1038/s41598-024-59612-4

[194] Sohni, S., Hassan, T., Khan, S. B., Akhtar, K., Bakhsh, E. M., Hashim, R., Nidaullah, H., Khan, M., Khan, S. A. (2023). Lignin nanoparticles-reduced graphene oxide based hydrogel: A novel strategy for environmental applications, *International Journal of Biological Macromolecules*, Vol. 225, 1426–1436. Doi:10.1016/j.ijbiomac.2022.11.200

[195] Obruča, S., Dvořák, P., Sedláček, P., Koller, M., Sedlář, K., Pernicová, I., Šafránek, D. (2022). Polyhydroxyalkanoates synthesis by halophiles and thermophiles: towards sustainable production of microbial bioplastics, *Biotechnology Advances*, Vol. 58, 107906. Doi:10.1016/j.biotechadv.2022.107906

[196] Tan, D., Wang, Y., Tong, Y., Chen, G.-Q. (2021). Grand Challenges for Industrializing Polyhydroxyalkanoates (PHAs), *Trends in Biotechnology*, Vol. 39, No. 9, 953–963. Doi:10.1016/j.tibtech.2020.11.010

[197] Diniz, M. S. da F., Mourão, M. M., Xavier, L. P., Santos, A. V. (2023). Recent Biotechnological Applications of Polyhydroxyalkanoates (PHA) in the Biomedical Sector—A Review, *Polymers*, Vol. 15, No. 22, 4405. Doi:10.3390/polym15224405

[198] Yang, X., Clénet, J., Xu, H., Odelius, K., Hakkarainen, M. (2015). Two Step Extrusion Process: From Thermal Recycling of PHB to Plasticized PLA by Reactive Extrusion Grafting of PHB Degradation Products onto PLA Chains, *Macromolecules*, Vol. 48, No. 8, 2509–2518. Doi:10.1021/acs.macromol.5b00235

[199] Zainal Abidin, A., Zango, Z. U., Akhdar, H., Aldaghri, O., Ibnaouf, K. H., Sulieman, A., Lim, J. W., Ng, H. S., Khoo, K. S. (2023). Sustainable grafting of poly(3-hydroxybutyrate-co-3-hydroxyhexanoate) and natural rubber into a new thermoplastic elastomer film, *Polymer*, Vol. 289, 126476. Doi:10.1016/j.polymer.2023.126476

[200] Kai, D., Zhang, K., Liow, S. S., Loh, X. J. (2019). New Dual Functional PHB-Grafted Lignin Copolymer: Synthesis, Mechanical Properties, and Biocompatibility Studies, *ACS Applied Bio Materials*, Vol. 2, No. 1, 127–134. Doi:10.1021/acsabm.8b00445

[201] Michalak, M., Kawalec, M., Kurcok, P. (2012). Reactive mono- and di-epoxy-functionalized poly(3-hydroxybutyrate)s. Synthesis and characterization, *Polymer Degradation and Stability*, Vol. 97, No. 10, 1861–1870. Doi:10.1016/j.polymdegradstab.2012.05.007

[202] Yang, J.-C., Yang, J., Zhang, T.-Y., Li, X.-J., Lu, X.-B., Liu, Y. (2023). Toughening Poly(3-hydroxybutyrate) by Using Catalytic Carbonylative Terpolymerization of Epoxides, *Macromolecules*, Vol. 56, No. 2, 510–517. Doi:10.1021/acs.macromol.2c02438

[203] Antonio, G. P., Fabbricino, P. M., Policastro, G., Fabbricino, Á. M., Fabbricino, M., Panico, A. (2021). Improving biological production of poly(3-hydroxybutyrate-co-3-hydroxyvalerate) (PHBV) co-polymer: a critical review, *Reviews in Environmental Science and Bio/Technology 2021 20:2*, Vol. 20, No. 2, 479–513. Doi:10.1007/S11157-021-09575-Z

[204] Ferre-Guell, A., Winterburn, J. (2018). Biosynthesis and Characterization of Polyhydroxyalkanoates with Controlled Composition and Microstructure, *Biomacromolecules*, Vol. 19, No. 3, 996–1005. Doi:10.1021/acs.biomac.7b01788

[205] McGregor, C., Minton, N. P., Kovács, K. (2021). Biosynthesis of Poly(3HB-co-3HP) with Variable Monomer Composition in Recombinant Cupriavidus necator H16, *ACS Synthetic Biology*, Vol. 10, No. 12, 3343–3352. Doi:10.1021/acssynbio.1c00283

[206] Sato, S., Maruyama, H., Fujiki, T., Matsumoto, K. (2015). Regulation of 3-hydroxyhexanoate composition in PHBH synthesized by recombinant Cupriavidus necator H16 from plant oil by using butyrate as a co-substrate, *Journal of Bioscience and Bioengineering*, Vol. 120, No. 3, 246–251. Doi:10.1016/j.jbiosc.2015.01.016

[207] Eraslan, K., Aversa, C., Nofar, M., Barletta, M., Gisario, A., Salehiyan, R., Goksu, Y. A. (2022). Poly(3-hydroxybutyrate-co-3-hydroxyhexanoate) (PHBH): Synthesis, properties, and applications - A review, *European Polymer Journal*, Vol. 167, 111044. Doi:10.1016/j.eurpolymj.2022.111044

[208] Huong, K. H., Sevakumaran, V., Amirul, A. A. (2021). P(3HB-co-4HB) as high value polyhydroxyalkanoate: its development over recent decades and current advances,

Critical Reviews in Biotechnology, Vol. 41, No. 4, 474–490. Doi:10.1080/07388551.2020.1869685

[209] Chen, J., Li, W., Zhang, Z.-Z., Tan, T.-W., Li, Z.-J. (2018). Metabolic engineering of Escherichia coli for the synthesis of polyhydroxyalkanoates using acetate as a main carbon source, *Microbial Cell Factories*, Vol. 17, No. 1, 102. Doi:10.1186/s12934-018-0949-0

[210] Sharma, V., Sehgal, R., Gupta, R. (2021). Polyhydroxyalkanoate (PHA): Properties and Modifications, *Polymer*, Vol. 212, 123161. Doi:10.1016/j.polymer.2020.123161

[211] Mariana, M., Alfatah, T., Abdul Khalil, H. P. S., Yahya, E. B., Olaiya, N. G., Nuryawan, A., Mistar, E. M., Abdullah, C. K., Abdulmadjid, S. N., Ismail, H. (2021). A current advancement on the role of lignin as sustainable reinforcement material in biopolymeric blends, *Journal of Materials Research and Technology*, Vol. 15, 2287–2316. Doi:10.1016/j.jmrt.2021.08.139

[212] Mousavioun, P., Doherty, W. O. S., George, G. (2010). Thermal stability and miscibility of poly(hydroxybutyrate) and soda lignin blends, *Industrial Crops and Products*, Vol. 32, No. 3, 656–661. Doi:10.1016/j.indcrop.2010.08.001

[213] Mousavioun, P., George, G. A., Doherty, W. O. S. (2012). Environmental degradation of lignin/poly(hydroxybutyrate) blends, *Polymer Degradation and Stability*, Vol. 97, No. 7, 1114–1122. Doi:10.1016/j.polymdegradstab.2012.04.004

[214] Vaidya, A. A., Collet, C., Gaugler, M., Lloyd-Jones, G. (2019). Integrating softwood biorefinery lignin into polyhydroxybutyrate composites and application in 3D printing, *Materials Today Communications*, Vol. 19, 286–296. Doi:10.1016/j.mtcomm.2019.02.008

[215] Luo, S., Cao, J., McDonald, A. G. (2017). Esterification of industrial lignin and its effect on the resulting poly(3-hydroxybutyrate-co-3-hydroxyvalerate) or polypropylene blends, *Industrial Crops and Products*, Vol. 97, 281–291. Doi:10.1016/j.indcrop.2016.12.024

[216] Camargos, C. H. M., Rezende, C. A. (2021). Antisolvent versus ultrasonication: Bottom-up and top-down approaches to produce lignin nanoparticles (LNPs) with tailored properties, *International Journal of Biological Macromolecules*, Vol. 193, 647–660. Doi:10.1016/J.IJBIOMAC.2021.10.094

[217] Camargo, F. A., Innocentini-Mei, L. H., Lemes, A. P., Moraes, S. G., Durán, N. (2012). Processing and characterization of composites of poly(3-hydroxybutyrate-co-hydroxyvalerate) and lignin from sugar cane bagasse, *Journal of Composite Materials*, Vol. 46, No. 4, 417–425. Doi:10.1177/0021998311418389

[218] Dong, J., Su, Y., Jiang, T., Li, D., Ma, X. (2022). Insight into the complex coupling agents on thermal, mechanical, and barrier properties of lignin-poly(3-hydroxybutyrate-co-3-hydroxyhexanoate) biocomposites, *Polymer Composites*, Vol. 43, No. 4, 2431–2439. Doi:10.1002/PC.26552

[219] Li, X., Jiang, T., Dong, J., Ma, X. (2022). Fabrication of high-performance lignin/PHBH biocomposites with excellent thermal, barrier and UV-shielding properties, *Journal of Polymer Research*, Vol. 29, No. 12, 517. Doi:10.1007/s10965-022-03378-8

[220] Weihua, K., He, Y., Asakawa, N., Inoue, Y. (2004). Effect of lignin particles as a nucleating agent on crystallization of poly(3-hydroxybutyrate), *Journal of Applied Polymer Science*, Vol. 94, No. 6, 2466–2474. Doi:10.1002/app.21204

[221] Lugoloobi, I., Li, X., Zhang, Y., Mao, Z., Wang, B., Sui, X., Feng, X. (2020). Fabrication of lignin/poly(3-hydroxybutyrate) nanocomposites with enhanced properties via a Pickering emulsion approach, *International Journal of Biological Macromolecules*, Vol. 165, 3078–3087. Doi:10.1016/j.ijbiomac.2020.10.156

[222] Kovalcik, A., Pernicova, I., Obruca, S., Szotkowski, M., Enev, V., Kalina, M., Marova, I. (2020). Grape winery waste as a promising feedstock for the production of polyhydroxyalkanoates and other value-added products, *Food and Bioproducts Processing*, Vol. 124, 1–10. Doi:10.1016/j.fbp.2020.08.003

[223] Svärd, A., Moriana, R., Brännvall, E., Edlund, U. (2019). Rapeseed Straw Biorefinery Process, *ACS Sustainable Chemistry and Engineering*, Vol. 7, No. 1, 790–801. Doi:10.1021/acssuschemeng.8b04420

[224] Schwanninger, M., Hinterstoisser, B. (2002). Klason lignin: Modifications to improve the precision of the standardized determination, *Holzforschung*, Vol. 56, No. 2, 161–166. Doi:10.1515/HF.2002.027

[225] Pérez, M., Dominguez-López, I., Lamuela-Raventós, R. M. (2023). The Chemistry Behind the Folin-Ciocalteu Method for the Estimation of (Poly)phenol Content in Food: Total Phenolic Intake in a Mediterranean Dietary Pattern, *Journal of Agricultural and Food Chemistry*, Vol. 71, No. 46, 17543–17553. Doi:10.1021/acs.jafc.3c04022

[226] Cleaver, G. (2015). *Artifact Free Analysis of Lignins by GPC using Agilent PolarGel-M*. Doi:5991-5765EN

[227] Hansen, C. M. (2007). *Hansen Solubility Parameters: A User's Handbook: Second Edition*, *Hansen Solubility Parameters: A Users Handbook, Second Edition*. Doi:10.1201/9781420006834

[228] Díaz de los Ríos, M., Hernández Ramos, E. (2020). Determination of the Hansen solubility parameters and the Hansen sphere radius with the aid of the solver add-in of Microsoft Excel, *SN Applied Sciences*, Vol. 2, No. 4, 1–7. Doi:10.1007/s42452-020-2512-y

[229] Żywicka, A., Ciecholewska-Juśko, D., Charęza, M., Drozd, R., Sobolewski, P., Junka, A., Gorgieva, S., El Fray, M., Fijałkowski, K. (2023). Argon plasma-modified bacterial cellulose filters for protection against respiratory pathogens, *Carbohydrate Polymers*, Vol. 302, No. July 2022. Doi:10.1016/j.carbpol.2022.120322

[230] Basics of Dynamic Mechanical Analysis (DMA). (n.d.), from https://wiki.anton-paar.com/en/basics-of-dynamic-mechanical-analysis-dma/

[231] Kucera, D., Pernicová, I., Kovalcik, A., Koller, M., Mullerova, L., Sedlacek, P., Mravec, F., Nebesarova, J., Kalina, M., Marova, I., Krzyzanek, V., Obruca, S. (2018). Characterization of the promising poly(3-hydroxybutyrate) producing halophilic bacterium Halomonas halophila, *Bioresource Technology*, Vol. 256, No. December 2017, 552–556. Doi:10.1016/j.biortech.2018.02.062

[232] Xiong, Z., Zhang, X., Wang, H., Ma, F., Li, L., Li, W. (2007). Application of Brown-Rot Basidiomycete Fomitopsis sp. IMER2 for Biological Treatment of Black Liquor, *Journal of Bioscience and Bioengineering*, Vol. 104, No. 6, 446–450. Doi:10.1263/jbb.104.446

[233] Peroxidase, L., Tien, M., Kirk, T. K., Morgan, M. A., Maytield, M. B., Kuwahara, M., Gold, M. H., Kirk, T. K., Croan, S. C., Tien, M., Murtagh, K. E., Farrell, R., Kirk, T. K., Kirk, T. K., Bull, C., Fee, J. A., Tien, M., Fee, J. A., Ondrias, M. R., Renganathan, V., Chiu, A. A., Loehr, T. M., Gold, M. H., Tien, M., Kalyanaraman, B., Kirk, T. K. (1988). Tien and Kirk, *Lignin*, Vol. 161, No. 1985, 238–249

[234] Mei, J., Shen, X., Gang, L., Xu, H., Wu, F., Sheng, L. (2020). A novel lignin degradation bacteria-Bacillus amyloliquefaciens SL-7 used to degrade straw lignin efficiently, *Bioresource Technology*, Vol. 310, No. 100, 123445. Doi:10.1016/j.biortech.2020.123445

[235] Bourbonnais, R., Paice, M. G. (1990). Oxidation of non-phenolic substrates, *FEBS Letters*, Vol. 267, No. 1, 99–102. Doi:10.1016/0014-5793(90)80298-w

[236] Linko, S., Haapala, R. (1993). A critical study of lignin peroxidase activity assay by veratryl alcohol oxidation, *Biotechnology Techniques*, Vol. 7, No. 1, 75–80. Doi:10.1007/BF00151094

[237] Kapich, A. N., Prior, B. A., Botha, A., Galkin, S., Lundell, T., Hatakka, A. (2004). Effect of lignocellulose-containing substrates on production of ligninolytic peroxidases in submerged cultures of Phanerochaete chrysosporium ME-446, *Enzyme and Microbial Technology*, Vol. 34, No. 2, 187–195. Doi:10.1016/j.enzmictec.2003.10.004

[238] Martínez, M. J., Ruiz-Dueñas, F. J., Guillén, F., Martínez, Á. T. (1996). Purification and catalytic properties of two manganese peroxidase isoenzymes from Pleurotus eryngii, *European Journal of Biochemistry*, Vol. 237, No. 2, 424–432. Doi:10.1111/j.1432-1033.1996.0424k.x

[239] Sampl, C., Schaubeder, J., Hirn, U., Spirk, S. (2023). Interplay of electrolyte concentration and molecular weight of polyDADMAC on cellulose surface adsorption, *International Journal of Biological Macromolecules*, Vol. 239, No. April, 124286. Doi:10.1016/j.ijbiomac.2023.124286

[240] Sauerbrey, G. (1959). Verwendung von Schwingquarzen zur Wägung dünner Schichten und zur Mikrowägung, *Zeitschrift Für Physik*, Vol. 155, No. 2, 206–222. Doi:10.1007/BF01337937

[241] Dardick, C. D., Callahan, A. M., Chiozzotto, R., Schaffer, R. J., Piagnani, M. C., Scorza, R. (2010). Stone formation in peach fruit exhibits spatial coordination of the lignin and flavonoid pathways and similarity to Arabidopsisdehiscence, *BMC Biology*, Vol. 8, No. 1, 13. Doi:10.1186/1741-7007-8-13

[242] Li, W., Amos, K., Li, M., Pu, Y., Debolt, S., Ragauskas, A. J., Shi, J. (2018). Fractionation and characterization of lignin streams from unique high-lignin content endocarp feedstocks, *Biotechnology for Biofuels*, Vol. 11, No. 1, 304. Doi:10.1186/s13068-018-1305-7

[243] García, A., Spigno, G., Labidi, J. (2017). Antioxidant and biocide behaviour of lignin fractions from apple tree pruning residues, *Industrial Crops and Products*, Vol. 104, No. May, 242–252. Doi:10.1016/j.indcrop.2017.04.063

[244] Yan, B., Lu, G., Wang, R., Kang, S., Huang, C., Wu, H., Yong, Q. (2023). Protective effects of lignin fractions obtained from grape seeds against bisphenol AF neurotoxicity via antioxidative effects mediated by the Nrf2 pathway, *Frontiers of Chemical Science and Engineering*, Vol. 17, No. 7, 976–989. Doi:10.1007/s11705-022-2237-0

[245] Górnaś, P., Rudzińska, M., Soliven, A. (2017). Industrial by-products of plum Prunus domestica L. and Prunus cerasifera Ehrh. as potential biodiesel feedstock: Impact of variety, *Industrial Crops and Products*, Vol. 100, 77–84. Doi:10.1016/j.indcrop.2017.02.014

[246] Spychaj, R., Kucharska, A. Z., Szumny, A., Przybylska, D., Pejcz, E., Piórecki, N. (2021). Potential valorization of Cornelian cherry (Cornus mas L.) stones: Roasting and extraction of bioactive and volatile compounds, *Food Chemistry*, Vol. 358, No. April. Doi:10.1016/j.foodchem.2021.129802

[247] Navarro Villa, P. (2025). Fruit: world production by type 2023 | Statista, from https://www.statista.com/statistics/264001/worldwide-production-of-fruit-by-variety/, accessed 10-3-2025

[248] Saini, A., Kaur, R., Kumar, S., Kumar, R., Kashyap, B., Kumar, V. (2024). New horizon of rosehip seed oil : Extraction , characterization for its potential applications as a functional ingredient, *Food Chemistry*, Vol. 437, No. P1, 137568. Doi:10.1016/j.foodchem.2023.137568

[249] Elkatry, H. O., Ahmed, A. R., El-Beltagi, H. S., Mohamed, H. I., Eshak, N. S. (2022). Biological Activities of Grape Seed By-Products and Their Potential Use as Natural Sources of Food Additives in the Production of Balady Bread, *Foods*, Vol. 11, No. 13. Doi:10.3390/foods11131948

[250] IOV. (2024). International Organization of Vine and Wine, *7.10.2024*, from https://www.oiv.int/what-we-do/global-report?oiv

[251] Dávila, I., Robles, E., Egüés, I., Labidi, J., Gullón, P. (2017). *The Biorefinery Concept for the Industrial Valorization of Grape Processing By-Products*, *Handbook of Grape*

Processing By-Products: Sustainable Solutions, Elsevier Inc. Doi:10.1016/B978-0-12-809870-7.00002-8

[252] Maroun, R. G., Rajha, H. N., Vorobiev, E., Louka, N. (2017). Emerging Technologies for the Recovery of Valuable Compounds From Grape Processing By-Products, *Handbook of Grape Processing By-Products*, Elsevier, 155–181. Doi:10.1016/B978-0-12-809870-7.00007-7

[253] Tangolar, S. G., Tangolar, P. S., Torun, A. (2009). Evaluation of fatty acid profiles and mineral content of grape seed oil of some grape genotypes, Vol. 7486. Doi:10.1080/09637480701581551

[254] Milic, S. M., Kostic, M. D., Milic, P. S., Vuc, V. M., Veljkovic, V. B., Stamenkovic, O. S. (2020). Extraction of Oil from Rosehip Seed : Kinetics , Thermodynamics , and Optimization, No. 12, 2373–2381. Doi:10.1002/ceat.201900689

[255] Abdelraof, M., Hasanin, M. S., El-Saied, H. (2019). Ecofriendly green conversion of potato peel wastes to high productivity bacterial cellulose, *Carbohydrate Polymers*, Vol. 211, No. January, 75–83. Doi:10.1016/j.carbpol.2019.01.095

[256] Blanco Parte, F. G., Santoso, S. P., Chou, C. C., Verma, V., Wang, H. T., Ismadji, S., Cheng, K. C. (2020). Current progress on the production, modification, and applications of bacterial cellulose, *Critical Reviews in Biotechnology*, Vol. 40, No. 3, 397–414. Doi:10.1080/07388551.2020.1713721

[257] Kovalcik, A., Pernicova, I., Obruca, S., Szotkowski, M., Enev, V., Kalina, M., Marova, I. (2020). Grape winery waste as a promising feedstock for the production of polyhydroxyalkanoates and other value-added products, *Food and Bioproducts Processing*, Vol. 124, 1–10. Doi:10.1016/j.fbp.2020.08.003

[258] Espinoza-Acosta, J. L., Torres-Chaves, P. I., Ramirez-Wong, B., Lope-Saiz, C. M., Montario-Leyva, B. (2016). Antioxidant, Antimicrobial, and Antimutagenic Properties of Technical Lignins and Their Applications, *BioResources*, Vol. 11, No. 2, 1–14

[259] Younesi-Kordkheili, H., Pizzi, A. (2023). Lignin-based wood adhesives: A comparison between the influence of soda and Kraft lignin, *International Journal of Adhesion and Adhesives*, Vol. 121, 103312. Doi:10.1016/j.ijadhadh.2022.103312

[260] Bueren, J. B. de, Héroguel, F., Wegmann, C., Dick, G. R., Buser, R., Luterbacher, J. S. (2020). Aldehyde-Assisted Fractionation Enhances Lignin Valorization in Endocarp Waste Biomass´, *ACS Sustainable Chemistry & Engineering*, Vol. 8, No. 45, 16737−16745. Doi:10.1021/acssuschemeng.0c03360

[261] Barbara H. Stuart. (2004). *INFRARED SPECTROSCOPY: FUNDAMENTALS AND APPLICATIONS* (1st editio.), John Wiley & Sons Ltd, Hoboken, NJ, USA

[262] Harman-Ware, A. E., Crocker, M., Pace, R. B., Placido, A., Morton, S., DeBolt, S. (2015). Characterization of Endocarp Biomass and Extracted Lignin Using Pyrolysis and Spectroscopic Methods, *Bioenergy Research*, Vol. 8, No. 1, 350–368. Doi:10.1007/s12155-014-9526-5

[263] Vin-nnajiofor, M. C., Li, W., Debolt, S., Cheng, Y., Shi, J. (2022). F u e l c - s n a m i l -i b, Vol. 38, No. 3, 509–516

[264] Reddy, I. A. K., Ghatak, H. R. (2018). Low-temperature thermal degradation behaviour of non-wood soda lignins and spectroscopic analysis of residues, *Journal of Thermal Analysis and Calorimetry*, Vol. 132, No. 1, 407–423. Doi:10.1007/s10973-017-6912-1

[265] Li, W., Amos, K., Li, M., Pu, Y., DeBolt, S., Ragauskas, A. J., Shi, J. (2018). Fractionation and characterization of lignin streams from unique high-lignin content endocarp feedstocks, *Biotechnology for Biofuels*, Vol. 11, No. 1, 1–14. Doi:10.1186/s13068-018-1305-7

[266] Kumar, N., Vijayshankar, S., Pasupathi, P., Nirmal Kumar, S., Elangovan, P., Rajesh, M., Tamilarasan, K. (2018). Optimal extraction, sequential fractionation and structural characterization of soda lignin, *Research on Chemical Intermediates*, Vol. 44, No. 9, 5403–5417. Doi:10.1007/s11164-018-3430-0

[267] Alekhina, M., Ershova, O., Ebert, A., Heikkinen, S., Sixta, H. (2015). Softwood kraft lignin for value-added applications: Fractionation and structural characterization, *Industrial Crops and Products*, Vol. 66, 220–228. Doi:10.1016/j.indcrop.2014.12.021

[268] Horikawa, Y., Hirano, S., Mihashi, A., Kobayashi, Y., Zhai, S., Sugiyama, J. (2019). Prediction of Lignin Contents from Infrared Spectroscopy: Chemical Digestion and Lignin/Biomass Ratios of Cryptomeria japonica, *Applied Biochemistry and Biotechnology*, Vol. 188, No. 4, 1066–1076. Doi:10.1007/s12010-019-02965-8

[269] Argyropoulos, D. D. S., Crestini, C., Dahlstrand, C., Furusjö, E., Gioia, C., Jedvert, K., Henriksson, G., Hulteberg, C., Lawoko, M., Pierrou, C., Samec, J. S. M., Subbotina, E., Wallmo, H., Wimby, M. (2023). Kraft Lignin: A Valuable, Sustainable Resource, Opportunities and Challenges, *ChemSusChem*, Vol. 16, No. 23. Doi:10.1002/cssc.202300492

[270] Sun, Y. C., Wang, M., Sun, R. C. (2015). Toward an understanding of inhomogeneities in structure of lignin in green solvents biorefinery. Part 1: Fractionation and characterization of lignin, *ACS Sustainable Chemistry and Engineering*, Vol. 3, No. 10, 2443–2451. Doi:10.1021/acssuschemeng.5b00809

[271] Mousavioun, P., Doherty, W. O. S. (2010). Chemical and thermal properties of fractionated bagasse soda lignin, *Industrial Crops and Products*, Vol. 31, No. 1, 52–58. Doi:10.1016/j.indcrop.2009.09.001

[272] Köhnke, J., Gierlinger, N., Mateu, B. P., Unterweger, C., Solt, P., Mahler, A. K., Schwaiger, E., Liebner, F., Gindl-Altmutter, W. (2019). Comparison of four technical lignins as a resource for electrically conductive carbon particles, *BioResources*, Vol. 14, No. 1, 1091–1109. Doi:10.15376/biores.14.1.1091-1109

[273] Li, K., Zhong, W., Li, P., Ren, J., Jiang, K., Wu, W. (2023). Recent advances in lignin antioxidant: Antioxidant mechanism, evaluation methods, influence factors and various applications, *International Journal of Biological Macromolecules*, Vol. 251, No. July, 125992. Doi:10.1016/j.ijbiomac.2023.125992

[274] Gordobil, O., Herrera, R., Yahyaoui, M., Ilk, S., Kaya, M., Labidi, J. (2018). Potential use of kraft and organosolv lignins as a natural additive for healthcare products, *RSC Advances*, Vol. 8, No. 43, 24525–24533. Doi:10.1039/c8ra02255k

[275] Eugenio, M. E., García-Fuentevilla, L., Martín-Sampedro, R., Santos, J. I., Wicklein, B., ibarra, D. (2025). Tuning the antioxidant and antibacterial properties of lignin by physicochemical modification during sequential acid precipitation from Kraft black liquor, *Wood Science and Technology*, Vol. 59, No. 1, 1–23. Doi:10.1007/s00226-024-01612-8

[276] Diment, D., Tkachenko, O., Schlee, P., Kohlhuber, N., Potthast, A., Budnyak, T. M., Rigo, D., Balakshin, M. (2024). Study toward a More Reliable Approach to Elucidate the Lignin Structure-Property-Performance Correlation, *Biomacromolecules*, Vol. 25, No. 1, 200–212. Doi:10.1021/acs.biomac.3c00906

[277] Rumpf, J., Burger, R., Schulze, M. (2023). Statistical evaluation of DPPH, ABTS, FRAP, and Folin-Ciocalteu assays to assess the antioxidant capacity of lignins, *International Journal of Biological Macromolecules*, Vol. 233, No. January. Doi:10.1016/j.ijbiomac.2023.123470

[278] Kozmelj, T. R., Voinov, M. A., Grilc, M., Smirnov, A. I., Jasiukaitytė-Grojzdek, E., Lucia, L., Likozar, B. (2024). Lignin Structural Characterization and Its Antioxidant Potential: A Comparative Evaluation by EPR, UV-Vis Spectroscopy, and DPPH Assays, *International Journal of Molecular Sciences*, Vol. 25, No. 16. Doi:10.3390/ijms25169044

[279] García, A., Spigno, G., Labidi, J. (2017). Antioxidant and biocide behaviour of lignin fractions from apple tree pruning residues, *Industrial Crops and Products*, Vol. 104, No. May, 242–252. Doi:10.1016/j.indcrop.2017.04.063

[280] Aadil, K. R., Barapatre, A., Sahu, S., Jha, H., Tiwary, B. N. (2014). Free radical scavenging activity and reducing power of Acacia nilotica wood lignin, *International Journal of Biological Macromolecules*, Vol. 67, 220–227. Doi:10.1016/j.ijbiomac.2014.03.040

[281] Majira, A., Godon, B., Foulon, L., van der Putten, J. C., Cézard, L., Thierry, M., Pion, F., Bado-Nilles, A., Pandard, P., Jayabalan, T., Aguié-Béghin, V., Ducrot, P. H., Lapierre, C., Marlair, G., Gosselink, R. J. A., Baumberger, S., Cottyn, B. (2019). Enhancing the Antioxidant Activity of Technical Lignins by Combining Solvent Fractionation and Ionic-Liquid Treatment, *ChemSusChem*, Vol. 12, No. 21, 4799–4809. Doi:10.1002/cssc.201901916

[282] María E. Eugenio , Raquel Martín-Sampedro , José I. Santos, B. W. and D. I. (2021). Chemical , Thermal and Antioxidant Properties of Lignins Pruning Residues, *Molecules*, Vol. 26

[283] Ivanova, D., Nikolova, G., Karamalakova, Y., Semkova, S., Marutsova, V., Yaneva, Z. (2023). Water-Soluble Alkali Lignin as a Natural Radical Scavenger and Anticancer

Alternative, *International Journal of Molecular Sciences*, Vol. 24, No. 16. Doi:10.3390/ijms241612705

[284] Shi, J., Yu, J., Pohorly, J. E., Kakuda, Y. (2003). Polyphenolics in Grape Seeds - Biochemistry and Functionality, *Journal of Medicinal Food*, Vol. 6, No. 4, 291–299. Doi:10.1089/109662003772519831

[285] Velíšek, J., Hajšlová, J. (2009). *Chemie Potravin 2* (3th editio.), OSSIS, Havlíčkův Brod

[286] Zinovyev, G., Sulaeva, I., Podzimek, S., Rössner, D., Kilpeläinen, I., Sumerskii, I., Rosenau, T., Potthast, A. (2018). Getting Closer to Absolute Molar Masses of Technical Lignins, *ChemSusChem*, Vol. 11, No. 18, 3259–3268. Doi:10.1002/cssc.201801177

[287] Rumpf, J., Burger, R., Schulze, M. (2023). Statistical evaluation of DPPH, ABTS, FRAP, and Folin-Ciocalteu assays to assess the antioxidant capacity of lignins, *International Journal of Biological Macromolecules*, Vol. 233, No. January. Doi:10.1016/j.ijbiomac.2023.123470

[288] Aufischer, G., Süss, R., Kamm, B., Paulik, C. (2022). Depolymerisation of kraft lignin to obtain high value-added products : antioxidants and UV absorbers, *Holzforschung*, Vol. 76, No. 9, 845–852. Doi:10.1515/hf-2022-0023

[289] Gaugler, E. C., Radke, W., Vogt, A. P., Smith, D. A. (2021). Molar mass determination of lignins and characterization of their polymeric structures by multi-detector gel permeation chromatography, *Journal of Analytical Science and Technology*, Vol. 12, No. 1. Doi:10.1186/s40543-021-00283-5

[290] An, L., Si, C., Wang, G., Sui, W., Tao, Z. (2019). Enhancing the solubility and antioxidant activity of high-molecular-weight lignin by moderate depolymerization via in situ ethanol/acid catalysis, *Industrial Crops and Products*, Vol. 128, 177–185. Doi:10.1016/J.INDCROP.2018.11.009

[291] Pylypchuk, I. V, Riazanova, A., Lindström, M. E., Sevastyanova, O. (2021). Structural and molecular-weight-dependency in the formation of lignin nanoparticles from fractionated soft- and hardwood lignins, *Green Chemistry*, Vol. 23, No. 8, 3061–3072. Doi:10.1039/D0GC04058D

[292] Abbott, S. (n.d.). Hansen Solubility Parameters, from https://www.hansen-solubility.com/

[293] van Leuken, S. H. M., van Osch, D. J. G. P., Kouris, P. D., Yao, Y., Jedrzejczyk, M. A., Cremers, G. J. W., Bernaerts, K. V., van Benthem, R. A. T. M., Tuinier, R., Boot, M. D., Hensen, E. J. M., Vis, M. (2023). Quantitative prediction of the solvent fractionation of lignin, *Green Chemistry*, Vol. 25, No. 19, 7534–7540. Doi:10.1039/d3gc00948c

[294] Ma, Q., Yu, C., Zhou, Y., Hu, D., Chen, J., Zhang, X. (2024). A review on the calculation and application of lignin Hansen solubility parameters, *International*

Journal of Biological Macromolecules, Vol. 256, No. P2, 128506. Doi:10.1016/j.ijbiomac.2023.128506

[295] Dastpak, A., Lourençon, T. V, Balakshin, M., Hashmi, S. F., Lundström, M., Wilson, B. P. (2020). Solubility study of lignin in industrial organic solvents and investigation of electrochemical properties of spray-coated solutions, *Industrial Crops and Products*, Vol. 148, 112310. Doi:10.1016/j.indcrop.2020.112310

[296] Volova, T. G., Shumilova, A. A., Nikolaeva, E. D., Kirichenko, A. K., Shishatskaya, E. I. (2019). Biotechnological wound dressings based on bacterial cellulose and degradable copolymer P(3HB/4HB), *International Journal of Biological Macromolecules*, Vol. 131, 230–240. Doi:10.1016/J.IJBIOMAC.2019.03.068

[297] Barud, H. S., Souza, J. L., Santos, D. B., Crespi, M. S., Ribeiro, C. A., Messaddeq, Y., Ribeiro, S. J. L. (2011). Bacterial cellulose/poly(3-hydroxybutyrate) composite membranes, *Carbohydrate Polymers*, Vol. 83, No. 3, 1279–1284. Doi:10.1016/J.CARBPOL.2010.09.049

[298] Zhijiang, C., Guang, Y., Kim, J. (2011). Biocompatible nanocomposites prepared by impregnating bacterial cellulose nanofibrils into poly(3-hydroxybutyrate), *Current Applied Physics*, Vol. 11, No. 2, 247–249. Doi:10.1016/J.CAP.2010.07.016

[299] Chiulan, I., Mihaela Panaitescu, D., Nicoleta Frone, A., Teodorescu, M., Andi Nicolae, C., Căşărică, A., Tofan, V., Sălăgeanu, A. (2016). Biocompatible polyhydroxyalkanoates/bacterial cellulose composites: Preparation, characterization, and in vitro evaluation, *Journal of Biomedical Materials Research Part A*, Vol. 104, No. 10, 2576–2584. Doi:10.1002/JBM.A.35800

[300] Víctor-Román, S., Simón-Herrero, C., Romero, A., Gracia, I., Valverde, J. L., Sánchez-Silva, L. (2015). CNF-reinforced polymer aerogels: Influence of the synthesis variables and economic evaluation, *Chemical Engineering Journal*, Vol. 262, 691–701. Doi:10.1016/J.CEJ.2014.10.026

[301] Nissilä, T., Hietala, M., Oksman, K. (2019). A method for preparing epoxy-cellulose nanofiber composites with an oriented structure, *Composites Part A: Applied Science and Manufacturing*, Vol. 125, 105515. Doi:10.1016/J.COMPOSITESA.2019.105515

[302] Geng, L., Li, L., Mi, H., Chen, B., Sharma, P., Ma, H., Hsiao, B. S., Peng, X., Kuang, T. (2017). Superior Impact Toughness and Excellent Storage Modulus of Poly(lactic acid) Foams Reinforced by Shish-Kebab Nanoporous Structure, *ACS Applied Materials & Interfaces*, Vol. 9, No. 25, 21071–21076. Doi:10.1021/acsami.7b05127

[303] Jahan, Z., Niazi, M. B. K., Gregersen, Ø. W. (2018). Mechanical, thermal and swelling properties of cellulose nanocrystals/PVA nanocomposites membranes, *Journal of Industrial and Engineering Chemistry*, Vol. 57, 113–124. Doi:10.1016/j.jiec.2017.08.014

[304] Falireas, P. G., Wróblewska, A. A., Servaes, K., Jedrzejczyk, M. A., Kouris, P. D., Boot, M. D., Hensen, E. J. M., Vanbroekhoven, K., Vendamme, R. (2023). Hemicellulosic Sugars and Lignin: A Synergistic Combination for the Synthesis of

High-Performance Bioresins, *ACS Sustainable Chemistry & Engineering*, Vol. 11, No. 51, 17896–17906. Doi:10.1021/acssuschemeng.3c02931

[305] Tomaszewska, J., Wieczorek, M., Skórczewska, K., Klapiszewska, I., Lewandowski, K., Klapiszewski, Ł. (2022). Preparation, Characterization and Tailoring Properties of Poly(Vinyl Chloride) Composites with the Addition of Functional Halloysite–Lignin Hybrid Materials, *Materials 2022, Vol. 15, Page 8102*, Vol. 15, No. 22, 8102. Doi:10.3390/MA15228102

[306] Luo, S., Cao, J., McDonald, A. G. (2016). Interfacial Improvements in a Green Biopolymer Alloy of Poly(3-hydroxybutyrate-co-3-hydroxyvalerate) and Lignin via in Situ Reactive Extrusion, *ACS Sustainable Chemistry and Engineering*, Vol. 4, No. 6, 3465–3476. Doi:10.1021/acssuschemeng.6b00495

[307] Kai, D., Zhang, K., Liow, S. S., Loh, X. J. (2019). New Dual Functional PHB-Grafted Lignin Copolymer: Synthesis, Mechanical Properties, and Biocompatibility Studies, *ACS Applied Bio Materials*, Vol. 2, No. 1, 127–134. Doi:10.1021/acsabm.8b00445

[308] Kovalcik, A., Obruca, S., Kalina, M., Machovsky, M., Enev, V., Jakesova, M., Sobkova, M., Marova, I. (2020). Enzymatic Hydrolysis of Poly(3-Hydroxybutyrate-co-3-Hydroxyvalerate) Scaffolds, *Materials 2020, Vol. 13, Page 2992*, Vol. 13, No. 13, 2992. Doi:10.3390/MA13132992

[309] Tsujimoto, T., Hosoda, N., Uyama, H. (2016). Fabrication of Porous Poly(3-hydroxybutyrate-co-3-hydroxyhexanoate) Monoliths via Thermally Induced Phase Separation, *Polymers 2016, Vol. 8, Page 66*, Vol. 8, No. 3, 66. Doi:10.3390/POLYM8030066

[310] Kovalcik, A., Sangroniz, L., Kalina, M., Skopalova, K., Humpolíček, P., Omastova, M., Mundigler, N., Müller, A. J. (2020). Properties of scaffolds prepared by fused deposition modeling of poly(hydroxyalkanoates), *International Journal of Biological Macromolecules*, Vol. 161, 364–376. Doi:10.1016/j.ijbiomac.2020.06.022

[311] Weihua, K., He, Y., Asakawa, N., Inoue, Y. (2004). Effect of lignin particles as a nucleating agent on crystallization of poly(3-hydroxybutyrate), *Journal of Applied Polymer Science*, Vol. 94, No. 6, 2466–2474. Doi:10.1002/app.21204

[312] Banpean, A., Hararak, B., Winotapun, C., Wijaranakul, P., Kitchaicharoenporn, S., Naimlang, S. (2023). Lignin nanoparticles as sustainable biobased nucleating agents of poly(L-lactic acid): crystallization behavior and effect of particle sizes, *Journal of Materials Science*, Vol. 58, No. 15, 6823–6838. Doi:10.1007/s10853-023-08418-2

[313] Aversa, C., Barletta, M., Koca, N. (2023). Processing PLA/P(3HB)(4HB) blends for the manufacture of highly transparent, gas barrier and fully bio-based films for compostable packaging applications, *Journal of Applied Polymer Science*, Vol. 140, No. 13, e53669. Doi:10.1002/APP.53669

[314] Fazeli, M., Mukherjee, S., Baniasadi, H., Abidnejad, R., Mujtaba, M., Lipponen, J., Seppälä, J., Rojas, O. J., Rojas, O. J. (2024). Lignin beyond the status quo : recent and

emerging composite applications, *Green Chemistry*, Vol. 26, No. 2, 593–630. Doi:10.1039/D3GC03154C

[315] Sen, S., Patil, S., Argyropoulos, D. S. (2015). Thermal properties of lignin in copolymers, blends, and composites: a review, *Green Chemistry*, Vol. 17, No. 11, 4862–4887. Doi:10.1039/C5GC01066G

[316] Shaw, A., Zhang, X., Jia, S., Fu, J., Lang, L., Brown, R. C. (2023). Mechanistic investigation of char growth from lignin monomers during biomass utilisation, *Fuel Processing Technology*, Vol. 239, 107556. Doi:10.1016/J.FUPROC.2022.107556

[317] Bertini, F., Canetti, M., Cacciamani, A., Elegir, G., Orlandi, M., Zoia, L. (2012). Effect of ligno-derivatives on thermal properties and degradation behavior of poly(3-hydroxybutyrate)-based biocomposites, *Polymer Degradation and Stability*, Vol. 97, No. 10, 1979–1987. Doi:10.1016/J.POLYMDEGRADSTAB.2012.03.009

[318] Yue, Y., Wang, Y., Li, J., Cheng, W., Han, G., Lu, T., Huang, C., Wu, Q., Jiang, J. (2022). High strength and ultralight lignin-mediated fire-resistant aerogel for repeated oil/water separation, *Carbon*, Vol. 193, 285–297. Doi:10.1016/J.CARBON.2022.03.015

[319] Wei, D., Wu, C., Jiang, G., Sheng, X., Xie, Y. (2021). Lignin-assisted construction of well-defined 3D graphene aerogel/PEG form-stable phase change composites towards efficient solar thermal energy storage, *Solar Energy Materials and Solar Cells*, Vol. 224, 111013. Doi:10.1016/J.SOLMAT.2021.111013

[320] Striz, R., Minisy, I. M., Bober, P., Taboubi, O., Smilek, J., Kovalcik, A. (2024). Free-Standing Bacterial Cellulose/Polypyrrole Composites for Eco-Friendly Remediation of Hexavalent Chromium Ions, *ACS Applied Polymer Materials*, Vol. 6, No. 11, 6383–6392. Doi:10.1021/acsapm.4c00579

[321] Dhania, S., Bernela, M., Rani, R., Parsad, M., Kumar, R., Thakur, R. (2023). Polyhydroxybutyrate (PHB) in nanoparticulate form improves physical and biological performance of scaffolds, *International Journal of Biological Macromolecules*, Vol. 236, 123875. Doi:10.1016/J.IJBIOMAC.2023.123875

[322] Ren, J., Feng, J., Wang, L., Chen, G., Zhou, Z., Li, Q. (2021). High specific surface area hybrid silica aerogel containing POSS, *Microporous and Mesoporous Materials*, Vol. 310, 110456. Doi:10.1016/J.MICROMESO.2020.110456

[323] Wang, Y., Chen, Y., Zhao, H., Li, L., Ju, D., Wang, C., An, B. (2022). Biomass-Derived Porous Carbon with a Good Balance between High Specific Surface Area and Mesopore Volume for Supercapacitors, *Nanomaterials 2022, Vol. 12, Page 3804*, Vol. 12, No. 21, 3804. Doi:10.3390/NANO12213804

[324] Elsehsah, K. A. A. A., Noorden, Z. A., Saman, N. M. (2024). Graphene aerogel electrodes: A review of synthesis methods for high-performance supercapacitors, *Journal of Energy Storage*, Vol. 97, 112788. Doi:10.1016/J.EST.2024.112788

[325] Deng, J., Sun, S. F., Zhu, E. Q., Yang, J., Yang, H. Y., Wang, D. W., Ma, M. G., Shi, Z. J. (2021). Sub-micro and nano-lignin materials: Small size and rapid progress,

Industrial Crops and Products, Vol. 164, 113412. Doi:10.1016/J.INDCROP.2021.113412

[326] Figueiredo, P., Lahtinen, M. H., Agustin, M. B., de Carvalho, D. M., Hirvonen, S., Penttilä, P. A., Mikkonen, K. S. (2021). Green Fabrication Approaches of Lignin Nanoparticles from Different Technical Lignins: A Comparison Study, *ChemSusChem*, Vol. 14, No. 21, 4718–4730. Doi:10.1002/cssc.202101356

[327] Lee, J. H., Park, S. Y., Choi, I. G., Choi, J. W. (2020). Investigation of molecular size effect on the formation of lignin nanoparticles by nanoprecipitation, *Applied Sciences (Switzerland)*, Vol. 10, No. 14. Doi:10.3390/app10144910

[328] Lievonen, M., Valle-Delgado, J. J., Mattinen, M. L., Hult, E. L., Lintinen, K., Kostiainen, M. A., Paananen, A., Szilvay, G. R., Setälä, H., Österberg, M. (2016). A simple process for lignin nanoparticle preparation, *Green Chemistry*, Vol. 18, No. 5, 1416–1422. Doi:10.1039/c5gc01436k

[329] Ortega-Sanhueza, I., Girard, V., Ziegler-Devin, I., Chapuis, H., Brosse, N., Valenzuela, F., Banerjee, A., Fuentealba, C., Cabrera-Barjas, G., Torres, C., Méndez, A., Segovia, C., Pereira, M. (2024). Preparation and Characterization of Lignin Nanoparticles from Different Plant Sources, *Polymers*, Vol. 16, No. 11, 1610. Doi:10.3390/polym16111610

[330] Sipponen, M. H., Lange, H., Ago, M., Crestini, C. (2018). Understanding Lignin Aggregation Processes. A Case Study: Budesonide Entrapment and Stimuli Controlled Release from Lignin Nanoparticles, *ACS Sustainable Chemistry & Engineering*, Vol. 6, No. 7, 9342–9351. Doi:10.1021/acssuschemeng.8b01652

[331] Ltd, M. I. (n.d.). Zeta Potential An Introduction in 30 Minutes, *Malvern Instruments Ltd*, from https://www.materials-talks.com/wp-content/uploads/2017/09/mrk654-01_an_introduction_to_zeta_potential_v3.pdf

[332] Evstigneyev, E. I., Shevchenko, S. M. (2019). Structure, chemical reactivity and solubility of lignin: a fresh look, *Wood Science and Technology*, Vol. 53, No. 1, 7–47. Doi:10.1007/s00226-018-1059-1

[333] Österberg, M., Sipponen, M. H., Mattos, B. D., Rojas, O. J. (2020). Spherical lignin particles: A review on their sustainability and applications, *Green Chemistry*, Vol. 22, No. 9, 2712–2733. Doi:10.1039/d0gc00096e

[334] Richter, A. P., Bharti, B., Armstrong, H. B., Brown, J. S., Plemmons, D., Paunov, V. N., Stoyanov, S. D., Velev, O. D. (2016). Synthesis and Characterization of Biodegradable Lignin Nanoparticles with Tunable Surface Properties, *Langmuir*, Vol. 32, No. 25, 6468–6477. Doi:10.1021/acs.langmuir.6b01088

[335] Tian, D., Hu, J., Chandra, R. P., Saddler, J. N., Lu, C. (2017). Valorizing Recalcitrant Cellulolytic Enzyme Lignin via Lignin Nanoparticles Fabrication in an Integrated Biorefinery, *ACS Sustainable Chemistry and Engineering*, Vol. 5, No. 3, 2702–2710. Doi:10.1021/acssuschemeng.6b03043

[336] Alipoormazandarani, N., Benselfelt, T., Wang, L., Wang, X., Xu, C., Wågberg, L., Willför, S., Fatehi, P. (2021). Functional Lignin Nanoparticles with Tunable Size and Surface Properties: Fabrication, Characterization, and Use in Layer-by-Layer Assembly, *ACS Applied Materials & Interfaces*, Vol. 13, No. 22, 26308–26317. Doi:10.1021/acsami.1c03496

[337] Ragnar, M., Lindgren, C. T., Nilvebrant, N.-O., Kungliga, M. R., Hogskolan, T., Hogskolan, K. T. (2000). pKa-Values of Guaiacyl and Syringyl Phenols Related to Lignin, *Journal of Wood Chemistry and Technology*, Vol. 20, No. 3, 277–305. Doi:10.1080/02773810009349637

[338] Sipponen, M. H., Lange, H., Ago, M., Crestini, C. (2018). Understanding Lignin Aggregation Processes. A Case Study: Budesonide Entrapment and Stimuli Controlled Release from Lignin Nanoparticles, *ACS Sustainable Chemistry & Engineering*, Vol. 6, No. 7, 9342–9351. Doi:10.1021/acssuschemeng.8b01652

[339] Ortega-Sanhueza, I., Girard, V., Ziegler-Devin, I., Chapuis, H., Brosse, N., Valenzuela, F., Banerjee, A., Fuentealba, C., Cabrera-Barjas, G., Torres, C., Méndez, A., Segovia, C., Pereira, M. (2024). Preparation and Characterization of Lignin Nanoparticles from Different Plant Sources, *Polymers*, Vol. 16, No. 11, 1610. Doi:10.3390/polym16111610

[340] Trevisan, H., Rezende, C. A. (2020). Pure, stable and highly antioxidant lignin nanoparticles from elephant grass, *Industrial Crops and Products*, Vol. 145, 112105. Doi:10.1016/j.indcrop.2020.112105

[341] Zhang, X., Yang, M., Yuan, Q., Cheng, G. (2019). Controlled Preparation of Corncob Lignin Nanoparticles and their Size-Dependent Antioxidant Properties: Toward High Value Utilization of Lignin, *ACS Sustainable Chemistry & Engineering*, Vol. 7, No. 20, 17166–17174. Doi:10.1021/acssuschemeng.9b03535

[342] Manisekaran, A., Grysan, P., Duez, B., Schmidt, D. F., Lenoble, D., Thomann, J.-S. (2022). Solvents drive self-assembly mechanisms and inherent properties of Kraft lignin nanoparticles (<50 nm), *Journal of Colloid and Interface Science*, Vol. 626, 178–192. Doi:10.1016/j.jcis.2022.06.089

[343] Alzagameem, A., Klein, S. E., Bergs, M., Do, X. T., Korte, I., Dohlen, S., Hüwe, C., Kreyenschmidt, J., Kamm, B., Larkins, M., Schulze, M. (2019). Antimicrobial Activity of Lignin and Lignin-Derived Cellulose and Chitosan Composites against Selected Pathogenic and Spoilage Microorganisms, *Polymers*, Vol. 11, No. 4, 670. Doi:10.3390/polym11040670

[344] Yang, W., Fortunati, E., Dominici, F., Giovanale, G., Mazzaglia, A., Balestra, G. M., Kenny, J. M., Puglia, D. (2016). Effect of cellulose and lignin on disintegration, antimicrobial and antioxidant properties of PLA active films, *International Journal of Biological Macromolecules*, Vol. 89, 360–368. Doi:10.1016/j.ijbiomac.2016.04.068

[345] Deng, L. L., Alexander, A. A., Lei, S., Anderson, J. S. (2010). The Cell Wall Teichuronic Acid Synthetase (TUAS) Is an Enzyme Complex Located in the

Cytoplasmic Membrane of Micrococcus luteus, *Biochemistry Research International*, Vol. 2010, No. 1, 1–8. Doi:10.1155/2010/395758

[346] Goodsell, D. S. (2012). Putting Proteins in Context: Scientific illustrations bring together information from diverse sources to provide an integrative view of the molecular biology of cells, *BioEssays : News and Reviews in Molecular, Cellular and Developmental Biology*, Vol. 34, No. 9, 718. Doi:10.1002/BIES.201200072

[347] Efenberger-Szmechtyk, M., Nowak, A., Czyzowska, A. (2021). Plant extracts rich in polyphenols: antibacterial agents and natural preservatives for meat and meat products, *Critical Reviews in Food Science and Nutrition*, Vol. 61, No. 1, 149–178. Doi:10.1080/10408398.2020.1722060

[348] Rauf, A., Imran, M., Abu-Izneid, T., Iahtisham-Ul-Haq, Patel, S., Pan, X., Naz, S., Sanches Silva, A., Saeed, F., Rasul Suleria, H. A. (2019). Proanthocyanidins: A comprehensive review, *Biomedicine & Pharmacotherapy*, Vol. 116, 108999. Doi:10.1016/J.BIOPHA.2019.108999

[349] Krasteva, D., Ivanov, Y., Chengolova, Z., Godjevargova, T. (2023). Antimicrobial Potential, Antioxidant Activity, and Phenolic Content of Grape Seed Extracts from Four Grape Varieties, *Microorganisms*, Vol. 11, No. 2, 395. Doi:10.3390/microorganisms11020395

[350] Mattinen, M.-L., Valle-Delgado, J. J., Leskinen, T., Anttila, T., Riviere, G., Sipponen, M., Paananen, A., Lintinen, K., Kostiainen, M., Österberg, M. (2018). Enzymatically and chemically oxidized lignin nanoparticles for biomaterial applications, *Enzyme and Microbial Technology*, Vol. 111, 48–56. Doi:10.1016/j.enzmictec.2018.01.005

[351] Adamovic, T., Tarasov, D., Demirkaya, E., Balakshin, M., Cocero, M. J. (2021). A feasibility study on green biorefinery of high lignin content agro-food industry waste through supercritical water treatment, *Journal of Cleaner Production*, Vol. 323, 129110. Doi:10.1016/J.JCLEPRO.2021.129110

[352] Yan, B., Lu, G., Wang, R., Kang, S., Huang, C., Wu, H., Yong, Q. (2023). Protective effects of lignin fractions obtained from grape seeds against bisphenol AF neurotoxicity via antioxidative effects mediated by the Nrf2 pathway, *Frontiers of Chemical Science and Engineering*, Vol. 17, No. 7, 976–989. Doi:10.1007/s11705-022-2237-0

[353] Tian, D., Hu, J., Chandra, R. P., Saddler, J. N., Lu, C. (2017). Valorizing Recalcitrant Cellulolytic Enzyme Lignin via Lignin Nanoparticles Fabrication in an Integrated Biorefinery, *ACS Sustainable Chemistry and Engineering*, Vol. 5, No. 3, 2702–2710. Doi:10.1021/ACSSUSCHEMENG.6B03043/ASSET/IMAGES/LARGE/SC-2016-03043W_0006.JPEG

[354] Figueiredo, P., Lahtinen, M. H., Agustin, M. B., de Carvalho, D. M., Hirvonen, S. P., Penttilä, P. A., Mikkonen, K. S. (2021). Green Fabrication Approaches of Lignin Nanoparticles from Different Technical Lignins: A Comparison Study, *ChemSusChem*, Vol. 14, No. 21, 4718–4730. Doi:10.1002/CSSC.202101356

[355] Zikeli, F., Vinciguerra, V., Taddei, A. R., D'Annibale, A., Romagnoli, M., Scarascia Mugnozza, G. (2018). Isolation and characterization of lignin from beech wood and chestnut sawdust for the preparation of lignin nanoparticles (LNPs) from wood industry side-streams, *Holzforschung*, Vol. 72, No. 11, 961–972. Doi:10.1515/hf-2017-0208

[356] Steck, J., Junker, F., Eichhöfer, H., Bunzel, M. (2022). Chemically Different but Often Mistaken Phenolic Polymers of Food Plants: Proanthocyanidins and Lignin in Seeds, *Journal of Agricultural and Food Chemistry*, Vol. 70, No. 37, 11704–11714. Doi:10.1021/acs.jafc.2c03782

[357] Giummarella, N., Pu, Y., Ragauskas, A. J., Lawoko, M. (2019). A critical review on the analysis of lignin carbohydrate bonds, *Green Chemistry*, Vol. 21, No. 7, 1573–1595. Doi:10.1039/C8GC03606C

[358] Wen, J.-L., Sun, S.-L., Xue, B.-L., Sun, R.-C. (2013). Quantitative structural characterization of the lignins from the stem and pith of bamboo (Phyllostachys pubescens), *Hfsg*, Vol. 67, No. 6, 613–627. Doi:10.1515/hf-2012-0162

[359] Kumar, A., Chandra, R. (2020). Ligninolytic enzymes and its mechanisms for degradation of lignocellulosic waste in environment, *Heliyon*, Vol. 6, No. 2, e03170. Doi:10.1016/j.heliyon.2020.e03170

[360] Daou, M., Farfan Soto, C., Majira, A., Cézard, L., Cottyn, B., Pion, F., Navarro, D., Oliveira Correia, L., Drula, E., Record, E., Raouche, S., Baumberger, S., Faulds, C. B. (2021). Fungal Treatment for the Valorization of Technical Soda Lignin, *Journal of Fungi*, Vol. 7, No. 1, 39. Doi:10.3390/jof7010039

[361] Cui, T., Yuan, B., Guo, H., Tian, H., Wang, W., Ma, Y., Li, C., Fei, Q. (2021). Enhanced lignin biodegradation by consortium of white rot fungi: microbial synergistic effects and product mapping, *Biotechnology for Biofuels*, Vol. 14, No. 1, 162. Doi:10.1186/s13068-021-02011-y

[362] Knežević, A., Milovanović, I., Stajić, M., Lončar, N., Brčeski, I., Vukojević, J., Ćilerdžić, J. (2013). Lignin degradation by selected fungal species, *Bioresource Technology*, Vol. 138, 117–123. Doi:10.1016/j.biortech.2013.03.182

[363] Goud, J. V. S., Bindu, N. S. V. S. S. S. L. H., Samatha, B., Prasad, M. R., Charya, M. A. S. (2011). Lignolytic enzyme activities of wood decaying fungi from Andhra Pradesh, *Journal of the Indian Academy of Wood Science*, Vol. 8, No. 1, 26–31. Doi:10.1007/s13196-011-0019-2

[364] Jaouani, A., Sayadi, S., Vanthournhout, M., Penninckx, M. J. (2003). Potent fungi for decolourisation of olive oil mill wastewaters, *Enzyme and Microbial Technology*, Vol. 33, No. 6, 802–809. Doi:10.1016/S0141-0229(03)00210-2

[365] Li, Z., Zhang, J., Qin, L., Ge, Y. (2018). Enhancing Antioxidant Performance of Lignin by Enzymatic Treatment with Laccase, *ACS Sustainable Chemistry & Engineering*, Vol. 6, No. 2, 2591–2595. Doi:10.1021/acssuschemeng.7b04070

[366] Filley, T. R., Cody, G. D., Goodell, B., Jellison, J., Noser, C., Ostrofsky, A. (2002). Lignin demethylation and polysaccharide decomposition in spruce sapwood degraded by brown rot fungi, *Organic Geochemistry*, Vol. 33, No. 2, 111–124. Doi:10.1016/S0146-6380(01)00144-9

[367] Bugg, T. D. H. (2024). The chemical logic of enzymatic lignin degradation, *Chemical Communications*, Vol. 60, No. 7, 804–814. Doi:10.1039/D3CC05298B

[368] Roth, S., Spiess, A. C. (2015). Laccases for biorefinery applications: a critical review on challenges and perspectives, *Bioprocess and Biosystems Engineering*, Vol. 38, No. 12, 2285–2313. Doi:10.1007/s00449-015-1475-7

[369] Kim, K. H., Kim, C. S. (2018). Recent Efforts to Prevent Undesirable Reactions From Fractionation to Depolymerization of Lignin: Toward Maximizing the Value From Lignin, *Frontiers in Energy Research*, Vol. 6, No. SEP, 413496. Doi:10.3389/fenrg.2018.00092

[370] Agarwal, A., Rana, M., Park, J.-H. (2018). Advancement in technologies for the depolymerization of lignin, *Fuel Processing Technology*, Vol. 181, 115–132. Doi:10.1016/j.fuproc.2018.09.017

[371] Hahn, V., Mikolasch, A., Schauer, F. (2014). Cleavage and synthesis function of high and low redox potential laccases towards 4-morpholinoaniline and aminated as well as chlorinated phenols, *Applied Microbiology and Biotechnology*, Vol. 98, No. 4, 1609–1620. Doi:10.1007/s00253-013-4984-9

[372] Hämäläinen, V., Grönroos, T., Suonpää, A., Heikkilä, M. W., Romein, B., Ihalainen, P., Malandra, S., Birikh, K. R. (2018). Enzymatic Processes to Unlock the Lignin Value, *Frontiers in Bioengineering and Biotechnology*, Vol. 6, No. MAR, 326539. Doi:10.1007/s00253-013-4984-9

[373] Choolaei, Z., Flick, R., Khusnutdinova, A. N., Edwards, E. A., Yakunin, A. F. (2021). Lignin-oxidizing activity of bacterial laccases characterized using soluble substrates and polymeric lignin, *Journal of Biotechnology*, Vol. 325, 128–137. Doi:10.1016/j.jbiotec.2020.11.007

[374] Bugg, T. D. H. (2024). The chemical logic of enzymatic lignin degradation, *Chemical Communications*, Vol. 60, No. 7, 804–814. Doi:10.1039/D3CC05298B

[375] Rahmanpour, R., King, L. D. W., Bugg, T. D. H. (2017). Identification of an extracellular bacterial flavoenzyme that can prevent re-polymerisation of lignin fragments, *Biochemical and Biophysical Research Communications*, Vol. 482, No. 1, 57–61. Doi:10.1016/j.bbrc.2016.10.144

[376] Pajer, N., Gigli, M., Crestini, C. (2024). The Laccase Catalysed Tandem Lignin Depolymerisation/Polymerisation, *ChemSusChem*, Vol. 17, No. 15, e202301646. Doi:10.1002/cssc.202301646

[377] Cameron, M. D., Aust, S. D. (2001). Cellobiose dehydrogenase–an extracellular fungal flavocytochrome, *Enzyme and Microbial Technology*, Vol. 28, Nos. 2–3, 129–138. Doi:10.1016/S0141-0229(00)00307-0

[378] Huang, F., Fang, J., Lu, X., Gao, P., Chen, J. (2001). Synergistic effects of cellobiose dehydrogenase and manganese-dependent peroxidases during lignin degradation, *Chinese Science Bulletin*, Vol. 46, No. 23, 1956–1961. Doi:10.1007/BF02901905

[379] Steinmetz, V., Villain-gambier, M., Klem, A., Ziegler, I., Dumarcay, S., Trebouet, D. (2020). In-situ extraction of depolymerization products by membrane filtration against lignin condensation, *Bioresource Technology*, Vol. 311, 123530. Doi:10.1016/j.biortech.2020.123530

[380] Rodríguez-Escribano, D., de Salas, F., Pliego, R., Marques, G., Levée, T., Suonpää, A., Gutiérrez, A., Martínez, Á. T., Ihalainen, P., Rencoret, J., Camarero, S. (2023). Depolymerisation of Kraft Lignin by Tailor-Made Alkaliphilic Fungal Laccases, *Polymers*, Vol. 15, No. 22, 4433. Doi:10.3390/polym15224433

[381] Pajer, N., Gigli, M., Crestini, C. (2024). The Laccase Catalysed Tandem Lignin Depolymerisation/Polymerisation, *ChemSusChem*, Vol. 17, No. 15, e202301646. Doi:10.1002/cssc.202301646

[382] Lu, X., Gu, X., Shi, Y. (2022). A review on lignin antioxidants: Their sources, isolations, antioxidant activities and various applications, *International Journal of Biological Macromolecules*, Vol. 210, 716–741. Doi:10.1016/j.ijbiomac.2022.04.228

[383] Farooq, M., Tao, Z., Valle-Delgado, J. J., Sipponen, M. H., Morits, M., Österberg, M. (2020). Well-Defined Lignin Model Films from Colloidal Lignin Particles, *Langmuir*, Vol. 36, No. 51, 15592–15602. Doi:10.1021/acs.langmuir.0c02970

[384] Garg, A., Heflin, J. R., Gibson, H. W., Davis, R. M. (2008). Study of Film Structure and Adsorption Kinetics of Polyelectrolyte Multilayer Films: Effect of pH and Polymer Concentration, *Langmuir*, Vol. 24, No. 19, 10887–10894. Doi:10.1021/la8005053

[385] Barrantes, A., Santos, O., Sotres, J., Arnebrant, T. (2012). Influence of pH on the build-up of poly-L-lysine/heparin multilayers, *Journal of Colloid and Interface Science*, Vol. 388, No. 1, 191–200. Doi:10.1016/j.jcis.2012.08.008

[386] Bus, T., Traeger, A., Schubert, U. S. (2018). The great escape: How cationic polyplexes overcome the endosomal barrier, *Journal of Materials Chemistry B*, Vol. 6, No. 43, 6904–6918. Doi:10.1039/c8tb00967h

[387] Benjaminsen, R. V., Mattebjerg, M. A., Henriksen, J. R., Moghimi, S. M., Andresen, T. L. (2013). The possible "proton sponge " effect of polyethylenimine (PEI) does not include change in lysosomal pH, *Molecular Therapy*, Vol. 21, No. 1, 149–157. Doi:10.1038/mt.2012.185

[388] Curtis, K. A., Miller, D., Millard, P., Basu, S., Horkay, F., Chandran, P. L. (2016). Unusual salt and pH induced changes in polyethylenimine solutions, *PLoS ONE*, Vol. 11, No. 9, 1–20. Doi:10.1371/journal.pone.0158147

[389] Jain, M., Seth, J. R., Hegde, L. R., Sharma, K. P. (2020). Unprecedented self-assembly in dilute aqueous solution of polyethyleneimine: Formation of fibrillar network, *Macromolecules*, Vol. 53, No. 20, 8974–8981. Doi:10.1021/acs.macromol.0c01501

[390] Abbadessa, A., Dogaris, I., Kishani Farahani, S., Reid, M. S., Rautkoski, H., Holopainen-Mantila, U., Oinonen, P., Henriksson, G. (2023). Layer-by-layer assembly of sustainable lignin-based coatings for food packaging applications, *Progress in Organic Coatings*, Vol. 182, No. February, 107676. Doi:10.1016/j.porgcoat.2023.107676

[391] Borrega, M., Päärnilä, S., Greca, L. G., Jääskeläinen, A. S., Ohra-Aho, T., Rojas, O. J., Tamminen, T. (2020). Morphological and wettability properties of thin coating films produced from technical lignins, *Langmuir*, Vol. 36, No. 33, 9675–9684. Doi:10.1021/acs.langmuir.0c00826

[392] Cui, M., Duan, Y., Ma, Y., Al-Shwafy, K. W. A., Liu, Y., Zhao, X., Huang, R., Qi, W., He, Z., Su, R. (2020). Real-Time QCM-D Monitoring of the Adsorption-Desorption of Expansin on Lignin, *Langmuir*, Vol. 36, No. 16, 4503–4510. Doi:10.1021/acs.langmuir.0c00104

[393] Alipoormazandarani, N., Benselfelt, T., Wang, L., Wang, X., Xu, C., Wågberg, L., Willför, S., Fatehi, P. (2021). Functional Lignin Nanoparticles with Tunable Size and Surface Properties: Fabrication, Characterization, and Use in Layer-by-Layer Assembly, *ACS Applied Materials and Interfaces*, Vol. 13, No. 22, 26308–26317. Doi:10.1021/acsami.1c03496

[394] Farooq, M., Tao, Z., Valle-Delgado, J. J., Sipponen, M. H., Morits, M., Österberg, M. (2020). Well-Defined Lignin Model Films from Colloidal Lignin Particles, *Langmuir*, Vol. 36, No. 51, 15592–15602. Doi:10.1021/acs.langmuir.0c02970

[395] Wolansky, G., Marmur, A. (1999). Apparent contact angles on rough surfaces: the Wenzel equation revisited, *Colloids and Surfaces A: Physicochemical and Engineering Aspects*, Vol. 156, Nos. 1–3, 381–388. Doi:10.1016/S0927-7757(99)00098-9

[396] Amorati, R., Franco Pedulli, G., Cabrini, L., Zambonin, L., Landi, L. (2006). Solvent and pH Effects on the Antioxidant Activity of Caffeic and Other Phenolic Acids, *Journal of Agricultural and Food Chemistry*, Vol. 54, No. 8, 2932–2937. Doi:10.1021/jf053159+

8. LIST OF ABBREVIATIONS

AcOH	Acetone
AFM	Atomic force microscopy
BC	Bacterial cellulose
BET	Brunauer–Emmett–Teller
***Cis, cis*-MA**	*Cis, cis*-muconic acid
CNF	Cellulose nanofibers
DMA	Dynamic mechanical analysis
DRIFT	Diffuse Reflectance Infrared Fourier Transform Spectroscopy
DSC	Differential scanning calorimetry
E′	Storage modulus
EDTA	Ethylenediaminetetraacetic acid
EtOH	Ethanol
FESEM	Field-Emission Scanning Electron Microscope
FT-IR	Infra-red spectroscopy
GAE	Gallic acid equivalent
GSL	Grape seeds lignin
HSP	Hansen solubility parameters
LBL	Layer-by-Layer
LiP	Lignin peroxidase
LNP	Lignin nanoparticles
LVE range	Linear viscoelastic range
MALLS	Multiangle laser light scattering detection
MeOH	Methanol
MIC	Minimum inhibitory concentration
$\mathbf{m_{rest}}$	Residual mass at 400 °C
Mn	Number-average molecular weight
MnP	Manganese-dependent peroxidase
Mw	Weight-average molecular weight
$\mathbf{M_{w_{app}}}$	Apparent molecular weight
PAH	Poly(allylamine hydrochloride)

PEI	Polyethyleneimine
PEs	Polyelectrolytes
PDI	Polydispersity index
PDM	Poly(diallyldimethylammonium chloride)
PHA	Polyhydroxyalkanoates
P3HB	Poly-3hydroxybutyrate
P3HB-*co*-4HB	Poly-3hydroxy-*co*-4-hydroxybutyrate
PHBV	Poly-3-hydroxybutyrate-*co*-3-hydroxyvalerate
PHBH	Poly-3-hydroxybutyrate-*co*-3-hydroxyhexanoate
PLA	Polylactic acid
PLL	Poly-L-lysine
PVA	Polyvinyl alcohol
QCM-D	Quartz crystal microbalance with dissipation monitoring
RHL	Rose hips lignin
RMS	Root mean square
SEC	Size exclusion chromatography
SEM	Scanning Electron Microscopy
TEAC	Trolox Equivalent Antioxidant Capacity
$\mathbf{T_{onset}}$	The onset temperature of thermal degradation
$\mathbf{T_{max}}$	Temperature of maximal degradation
$\mathbf{T_g}$	Glass transition temperature
TGA	Thermogravimetric analysis
TPC	Total Phenolic Content
WCA	Water contact angle

9. APPENDIX

Table A1 Comparison of lignin samples solubility in organic solvents and their aqueous mixtures for HSP spheres generation

Solvent	Alkali	Kraft	Organosolv	Grape seeds Soda	Plum stone Soda
Acetone	**0**	**0**	**0**	**0**	**0**
Acetonitrile	**0**	**0**	**0**	**0**	**0**
Aceton - water 3:1	**0**	**1**	**1**	**0**	**0**
Diethylether	**0**	**0**	**0**	**0**	**0**
Diethyltriamine	**0**	**1**	**1**	**0**	**1**
Dichloromethane (DCM)	**0**	**0**	**0**	**0**	**0**
DCM - methanol 1:1	**0**	**1**	**1**	**0**	**0**
Dimethylformamide	**0**	**1**	**1**	**0**	**0**
1.4-dioxane	**0**	**0**	**0**	**0**	**0**
1.4-dioxane - water 9:1	**0**	**1**	**1**	**0**	**0**
DMSO	**1**	**1**	**1**	**1**	**1**
Ethylmethylketon	**0**	**0**	**0**	**0**	**0**
Ethanol	**0**	**0**	**0**	**0**	**0**
Ethanol - water 3:1	**1**	**0**	**0**	**0**	**0**
Ethyl acetate	**0**	**0**	**0**	**0**	**0**
Ethylene glycol	**1**	**1**	**1**	**0**	**1**
n-hexane	**0**	**0**	**0**	**0**	**0**
Chloroform	**0**	**0**	**0**	**0**	**0**
Isooktane	**0**	**0**	**0**	**0**	**0**
Isopropanol	**0**	**0**	**0**	**0**	**0**
Isoamyl alcohol	**0**	**0**	**0**	**0**	**0**
Methanol - water 3:1	**0**	**0**	**0**	**0**	**0**
Methanol	**0**	**0**	**0**	**0**	**0**
1.3-propandiol	**1**	**1**	**1**	**0**	**0**
Pyridine	**0**	**1**	**1**	**0**	**0**
Tetrahydrofuran (THF)	**0**	**0**	**1**	**0**	**0**
THF - water 3:1	**0**	**1**	**1**	**1**	**0**
Toluene	**0**	**0**	**0**	**0**	**0**
Water	**1**	**0**	**0**	**0**	**0**

1 – soluble, 0 – insoluble

9.1 Curiculum vitae

PERSONAL DATA:

Title, Name, Surname:	Ing. Pavel Vostrejš
Place and date of birth:	Brno, 03.03.1993
Nationality:	Czech
E-mail:	pavel.vostrejs@vutbr.cz
ORCID:	0000-0002-9383-7293

EDUCATION AND QUALIFICATION:

from 2020	**Doctoral's study programme:** Biophysical Chemistry Brno University of Technology Doctoral Thesis: **Preparation and characterisation of lignin nanoparticles**
09/2018–06/2020	**Master's study programme**: Chemistry and technology of foodstuff Brno University of Technology Branch: Food Science and Biotechnology Final state examination: Grade A Summary grade average: 1.1*, Awarded with honours* Diploma Thesis: **Isolation of lignin from grape seeds and its application as filler for polyhydroxyalkanoates (PHA)** Diploma Thesis: Grade A
09/2014–06/2018	**Bachelor's study programme**: Chemistry and technology of foodstuff Brno University of Technology Branch: Food Science Final state examination: Grade A Summary grade average: 1.59 Bachelor Thesis: Impact of nitrogen fertilization and drought on glutenins content in winter wheat Bachelor Thesis: Grade A

RESEARCH EXPERIENCE

Internships:

1/2025-2/2025	**Erasmus+ Traineeship**
Organization	Stockholm University, Department of Materials and Environmental Chemistry, Sweden,
Type of work	Poly(3-hydroxybutyrate) - lignin composite extrusion
9/2021-12/2021	**Erasmus+ Traineeship**
Organization	Graz University of Technology, Institute of Bioproducts and Paper Technology, Austria,
Type of work	Preparation and characterization of ultrathin lignin films
7/2019-10/2019	**Erasmus+ Traineeship**
Organization	University of Natural Resources and Life Sciences Vienna (Department of Chemistry, Institute for Chemistry of Renewable Resources), Austria
Type of work	preparation of hydrogels and cryogels based on bacterial cellulose and poly(3-hydroxybutyrate) Research under the project 8J19AT030, Multifunctional biocomposites based on spent coffee grounds

***Academic awards*:**

Award of the Dean of the Faculty of Chemistry for the excellent study results, 12/2020

Ing. Degree in Food Science and Biotechnology (with honour) 09/2020, Brno University of Technology, Faculty of Chemistry.

Nomination for Josef Hlavek Prise for excellent students, 07/2020, Brno University of Technology, Faculty of Chemistry, Institute of Food Chemistry and Biotechnology.

9.2 Scientific papers:

Vostrejs P., Kovalcik A, Schaubeder J.B., Spirk S., Hricovini M., Nypelö T., Kalina M., Cernekova N., Brezina M., Kargl R. (2025). Biobased Antimicrobial Coatings: Layer-by-Layer Assemblies Based on Natural Polyphenols. ACS Applied Polymer Materials doi: 10.1021/acsapm.4c03681

Cernekova N., Hricovini M., Vostrejs P., Kovalcik A. (2025). Innovative antimicrobial lignins: Extraction and characterization for advanced hydrogel applications. International Journal of Biological Macromolecules, 307. doi:10.1016/j.ijbiomac.2025.141959.

Vostrejs, P., Adamcová, D., Vaverková, M. D., Enev, V., Kalina, M., Machovsky, M., Kovalcik, A. (2020). Active biodegradable packaging films modified with grape seeds lignin. RSC Advances, 10(49), 29202-29213. doi:10.1039/d0ra04074f

9.3 Conference Abstracts:

Vostrejs P, Hruskova L, Kovalcik A. Systematic assesment of lignin solubility for nanoparticle preparation from various sources. 11th International Conference on Chemical Technology. Mikulov, Czech Republic, 15.4.2024. ISBN: 978-80-88214-48-9.

Vostrejs P, Hruskova L, Kovalcik A. Isolation and analysis of grape seeds lignin for potential application in polymeric blends. 10th International Conference on Chemical Technology., 2023. s. 179-179. ISBN: 978-80-88214-40-3.

Hruskova L, Vostrejs P, Kovalcik A. *Antioxidační aktivita ligninových nanočástic.* Chemistry is life, 2022, Brno university of technology, Faculty of chemistry, Brno, Czech republic, ISBN: 978-80-214-6117-8.

Cernekova N, Vostrejs P, Kovalcik A. *GRAPE LIGNIN BASED HYDROGELS.* Chémia a technológie pre život, 24. celoslovenská študentská vedecká konferencia s medzinárodnou účasťou. 2022. SLOVENSKÁ TECHNICKÁ UNIVERZITA V BRATISLAVE. ISBN: 978-80-8208-083-7.

Chovanec M, Vostrejš P, Kovalčík A. *Má lignín antibakteriálne vlastnosti?* Chemistry is life, 2021. Brno university of technology, Faculty of chemistry, Brno, Czech Republic, ISBN: 978-80-214-6002-7.

Vostrejs P, Kovalcik A. Utilization of lignin in polyhydroxyalakanoate blends. Chemistry is life, 27.11.2020, Brno university of technology, Faculty of chemistry, Brno, Czech Republic, ISBN: 978-80-214-5920-0.

9.4 Teaching and thesis co-supervision:

9.4.1 Teaching

Praktikum z technologie zpracování biopolymerů – LS 2021/2022

9.4.2 Bachelor thesis co-supervision

Kateřina Jahnová – Extrakce a aplikace keratinu z ovčí vlny (2023)

Lucie Hrušková – Analýza rozpustnosti antioxidačních lignocelulózových látek (2022)

Šárka Borová – Stanovení účinku plodů šípkové růže (*Rosa canina L.*) na oxidační stabilitu čerstvých šťáv (2021)

9.4.3 Master thesis co-supervision

Tereza Fialová – Studium vlivu mikrobiální degradace ligninu na jeho výslednou molekulovou hmotnost (2023)

Bianka Péčiová – Produkce lignin-degradujících enzymů za pomocí plísně *Phanerochaete chrysosporium* (2023)

Zuzana Červinková – Návrh receptury potravinového doplňku na bázi bioaktivních látek izolovaných z plodů trnky obecné (*Prunus spinosa*) (2023)